Modeling the land-use legacy effect of agricultural practices on the water quality of streams from forest watersheds of Puerto Rico

By:

Gabriel Román Valentín

Thesis submitted in partial fulfillment of the requirements for the degree of

MASTER OF SCIENCE
in
CIVIL ENGINEERING

UNIVERSITY OF PUERTO RICO
MAYAGÜEZ CAMPUS

2018

Approved by:

________________________ ____________
Luis R. Pérez-Alegría, Ph.D. Date
President, Graduate Committee

________________________ ____________
Sangchul Hwang, Ph.D. Date
Member, Graduate Committee

________________________ ____________
Rafael Segarra, Ph.D. Date
Member, Graduate Committee

________________________ ____________
Felix R. Román Velazquez, Ph.D. Date
Representative of Graduate School

________________________ ____________
Ismael Pagán Trinidad, M.S.C.E. Date
Chair, Department of Civil Engineering and Surveying

Abstract

In order to aid in the establishment of "reference" criteria the nutrient status and dynamics of soils, water and stream sediments of a secondary forested watershed is being compared with the dynamics of an "historically" forested watershed in Puerto Rico. Additionally an empirical framework was developed for both watersheds using the Soil and Water Assessment Tool (SWAT) to account for the land use legacy effect on the present nutrient status of the waters. Results show that the hydrogeology of these watersheds is partially responsible for the discrepancies shown above. Calibrated model simulations show that agricultural succession tropical forests can have twice the annual phosphorous discharge of primary forests in the tropical island of Puerto Rico. Also a version of SWAT 2009 developed for the tropics by M. Strauch, M. Volk, (2013) resulted in a difference of up to 35.6% of annual dissolved phosphorous loads in simulation results.

Resumen

Con el fin de ayudar en el establecimiento de criterios de "referencia" de nutrientes la dinámica de precipitación, suelos, sedimentos y descargas de una cuenca boscosa secundaria se va a comparar con la dinámica de una cuenca hidrográfica "históricamente" boscosa en Puerto Rico. Un marco empírico fue desarrollado para ambas cuencas utilizando el modelo de simulación hidrológica SWAT para cuantificar el efecto del legado de uso de terrenos sobre la situación actual de nutrientes de las aguas. Los resultados muestran que la hidrogeología de estas cuencas es parcialmente responsable de las discrepancias entre estas cuencas. Según las simulaciones de los modelos calibrados un bosque tropical de sucesión agrícola puede tener dos veces la descarga de fósforo anual de bosques primarios en la isla sub-tropical de Puerto Rico. Ademas, las simulaciones utilizando la version ajustada de SWAT para el tropico muestran diferencias de hasta 35.6% en descargas de fósforo anual disuelto.

© Gabriel Román Valentín, 2018

To God for Life and the Universe within it…

To my wife and kids, Veronica, Antara and Matias

Acknowledgements

I would like to thank Dr. Luis Perez Alegria for his guidance, knowledge, ideas, opportunities, trust, support, assistance and friendship. I have gained invaluable experience through this and other research opportunities under his guidance. I would also like to thank Dr. Sangchul Hwang for his friendship, guidance and advise. For believing in me and giving me the opportunity to do research. I'm thankful for the support, knowledge and guidance of Dr. Rafael Segarra it was an honor to have him in my graduate committee.

I would like to thank my wife Veronica for all the sacrifices she has made for us to achieve this goal, this work is hers also. To my kids Antara and Matias for their light, happiness and making me focus on what matters most.

Everybody that has been directly or indirectly related to my academic career. My mother, Mayra for her advice, unconditional support and love, my aunt, Jeannette for her advice, love and for being there for me always and to my grandma, Gloria for all her love and advise (she would've been even prouder now). To my father, Gabriel and my grandma Nilda for their genes, advise, support and love and to the rest of my family and friends that always believed in me and motivated me since the beginning.

I'm also thankful to professor Carlos Otero (SEA) for his friendship, support and advise. For his help in investigating the watershed's history, coffee phenology and connecting me with Dr. Miguel Monroig. To Dr. Monroig for his advice and valuable information. To Gustavo Castro for his help in field instrumentation and sampling and his good friendship. To Victoria Viggiano for her support in BF samlpling, processing and friendship. To Dr. Gustavo Martinez for lab analyses, advise and support. To Dr. David Sotomayor for his advice and guidance. To Casa Pueblo in Adjuntas and Mr. Luis Velez for allowing us access through their lands for watershed instrumentation and to everybody that made this possible in any way.

Table of Contents

List of Figures

List of Tables

List of Appendix

1. Introduction

In the island of Puerto Rico while precipitation is abundant, given our location and the humidity brought by trade winds, the reservoirs that provide water for civilian use and consumption have been declining rapidly in terms of quantity and quality. This is mainly attributed to excess sediments and nutrients (specifically phosphorous and nitrogen) transported by draining waters from lands within the reservoir's watershed. Also excess sediments and nutrients discharges caused by anthropogenic modifications to watersheds have been proven to damage coral reef health as in the case of the Guanica bay in southwestern region of the island (Sotomayor et al., 2012; Yuan et al., 2016). Both problems are effects of cultural eutrophication. Eutrophication is the process by which water is enriched with excess nutrients boosting the growth of aquatic plant life. This process has been accelerated by anthropogenic activities thus the term cultural eutrophication, which in turn causes oxygen depletion in water through the decomposition process of biomass. Decomposed vegetation turns into sediment, reducing the storage capacity of reservoirs. Eutrophication is nowadays a problem globally witnessed by developed and under developed countries alike and poses direct threats to wildlife and humans. "The detrimental impacts of eutrophication range from the decline of aquatic resources (wild and cultured) that support coastal, riverine and lacustrine communities, to the degradation of water for human consumption and recreation, to the expansion of acutely toxic algal blooms that can directly impact human health" (Kleinman et al., 2011). Eutrophication is mainly attributed to nonpoint source pollution, which comes from many diffuse sources and is caused by rainfall moving over and through the soil. As the runoff moves, it picks up and carries away natural and human-made pollutants, finally depositing them into lakes, rivers, wetlands, coastal waters and ground waters. Furthermore non-point source pollution from agricultural fields is believed to be the leading cause of eutrophication and impairment on waters draining the lands under the EPA jurisdiction (USEPA, 2007).

The USEPA has recognized that phosphorous over enrichment in water bodies from non-point sources (NPS) poses a serious environmental issue, for which the National Nutrient Strategy Program was created in 1994 establishing that in order to protect the Nation's water an eco-region stream nutrient based criteria must be developed. Today, in the tropical island of Puerto Rico, primary forests (which are the ideal for establishing said stream nutrient-based criteria) are scarce while secondary forests (most of them with past agricultural practices) constitute about 80% of the island's forests. However in the 1930's only 6% of the total landscape of Puerto Rico was forested and agriculture land cover (including pasture lands) extended over 70% of the island (Kennaway et al., 2007). In the 1940's industrialization policies in the island caused the agriculture industry to experience a sharp cutback. The exodus of the people living in the mountains to the city resulted in the abandonment of agricultural practices and these lands, left to the natural growth of native and introduced plant species, turned into secondary tropical forests. As a result in a 50yr lapse agricultural land use declined in 95% and forest cover increased from 17.8% to 45% (Kennaway et al., 2007). In 2010 in a study published by Martinez et al., 2010 statistical analyses of the nutrient status of waters draining six reference watersheds of Puerto Rico showed that phosphorous levels draining former agricultural watersheds (succession forests) are at least 10 times higher than streams draining lands that have been under forest cover for more than 100 years (historical forests). In said study four of these watersheds where historical while the other two (succession forests) used to be under coffee production approximately until the mid 80's.

This work aims to evaluate and elucidate, using comprehensive semi-distributed hydrologic modeling software and statistical analyses, the possible long-term effects of intensive farming in the island of Puerto Rico to the nutrient status (in terms of TP) of the waters draining the lands of secondary agricultural succession forests in the island. To do this the Soil and Water Assessment Tool (SWAT) was used to construct and calibrate watershed models and simulate long term hydrologic and nutrient dynamics in an agricultural succession forested watershed versus an historical forest watershed. The assessment of long term P dynamics will help in the establishment of reference nutrient criteria for stream water in the tropical climate eco-region. Also, it will provide a methodology for determining the long-term effects of agricultural practices on nutrient loadings to streams. Characteristic physical, chemical and hydrologic parameters for these watersheds were developed, a database including sampled weather, discharge and nutrient loading data was created and the effects of incorporating a modified plant growth module for the tropics in the SWAT long-term simulations was evaluated. The latter will improve our ability to predict the impacts of management decisions regarding biomass production in the tropics and its temporal-spatial dynamics with soil and water.

As part of the 1998 EPA National Nutrient Criteria program the EPA Office of Water has established that states which are further from developing numeric criteria, such as Puerto Rico, should be aided in developing modeling tools that allow states to evaluate a causative approach for developing criteria and assessing the likelihood of criteria for being attained (USEPA, 2007). The development of assessment tools that aid in the understanding and conservation of our natural resources and regional ecology is a topic of great civil, federal and scientific importance. Many environmental national policies were created thanks to the insight that modeling tools provide to scientists. Additionally the calibration, validation and improvement of models that simulate natural processes occurring in forested, agricultural or urbanized watersheds will increase our ability to properly manage, protect and remediate the environment. Consequently it will aid all the elements and living organisms, which make part of who we are, what we need and what we love.

The general objective of this study is:

Evaluate the agricultural land use legacy effect on the long-term P loading dynamics of secondary tropical forests using SWAT, a continuous semi-distributed hydrologic simulation model, to perform long-term hydrologic simulation of NPS phosphorous loadings to waters.

The specific objectives are:

a) Develop discharge and nutrient loading data and compare dynamics of these in a primary sub-tropical forest watershed and a secondary sub-tropical forest watershed with previous agricultural practices in Puerto Rico.
b) Construct and calibrate SWAT models in order to compare actual phosphorous loading dynamics to receiving waters of a primary forest watershed (the Cupeyes River watershed) with the one of a secondary forest watershed (the Bosque la Olimpia watershed). This will aid to identify physical and hydrological characteristics leading to discrepancies in phosphorous loadings between the latter.
c) Determine the magnitude of contribution of antecedent agricultural practices on phosphorous loadings to streams draining a secondary sub-tropical forested watershed in Puerto Rico by using the Soil and Water Assessment Tool (SWAT).
d) Assess the effects of using the SWAT 2009 version with the plant growth module modified by Strauch et al., (2013) for the long-term simulation of nutrient (phosphorous) loadings to waters draining a secondary sub-tropical forest watershed in Puerto Rico with and without previous agricultural practices that applied organic and inorganic fertilizers in the soil and that after several decades still continue to leach nutrients to runoff.

2. Literature Review

2.1. Eutrophication and Stream Nutrient Criteria

Excessive nutrients (nitrogen and phosphorus) can cause negative ecological impacts to water bodies on a national scale by stimulating harmful algal blooms (USEPA, 2007). This process by which lakes and streams are enriched by nutrients that leads to excessive plant growth is called eutrophication. Although this is a natural process by which lakes and ponds become more productive and shallower, human impact accelerates it by contributing different sources of pollution; thereby the term cultural eutrophication, which damages directly human and ecological health. Algal blooms block sunlight and results in the destruction of submerged aquatic vegetation, which serves as food and habitat for many organisms. Algal blooms eventually die off and consume dissolved oxygen (DO) due to biological decomposition. Low DO leads to die off of aquatic organisms and as a result a decreased biological diversity and population of fish occurs. Human health problems include taste and odor problems in drinking water, neurological and respiratory problems in swimmers and blue baby syndrome from excessive nitrates in groundwater caused by leaching of nitrate generated from fertilizer used in agricultural lands and waste dumps in rural and urban areas (USEPA, 2007; Majumdar, 2003). Limited studies are available on the economic costs of eutrophication however the mitigation programs that have been developed to combat the causes of eutrophication suggest a magnitude of cost equivalent to a big fraction of national economies. For example at the Chesapeake Bay the mitigation of eutrophication problems has required a tremendous amount of money, time and legislation.

As part of the 1977 Clean Water Act (CWA) as amended the USEPA set the goal of establishing national water quality goals. This gave way for the National Nutrient Criteria Program in 1994, which major focus is the development of waterbody-type technical guidance and region-specific nutrient criteria. This was done in order to address the issue of nutrient over enrichment in the nation’s waters by means of establishing a numeric estimate of the nutrient status of minimally impacted waters for a particular eco region; these minimally impacted waters are considered as reference streams or rivers. In places such as Puerto Rico few scarce areas remain that can be considered primary forestlands, which is the ideal for establishing such criteria (Martínez et al., 2010). By 1930’s only 6% of the total landscape of Puerto Rico was forested and agriculture land cover (including pasture lands) extended over 70% of the island (Kennaway et. al., 2007) as cited by Martínez et al. (2010). In the 1940’s industrialization policies in the island caused the agriculture industry to experience a sharp cutback. The exodus of the people living in the mountains to the city resulted in the abandonment of agricultural fields, which left to the natural development of native and introduced plant species turned into secondary tropical forests. Figure 2.1 displays a GIS map showing the age of forests in Puerto Rico (Kennaway, 2007). As a result in a 50yr lapse agricultural land use declined in 95% and forest cover increased from 17.8% to 45% (Martínez et al., 2010). These secondary succession forests constitute nowadays 86% of the forest cover in the island making them essential in the establishment of nutrient reference criteria for the island. In 2010 statistical analyses of the nutrient status of waters draining six reference watersheds of Puerto Rico showed that phosphorous levels draining former agricultural watersheds are at least 10 times higher than streams that have never been impacted by human activities (Martínez et al., 2010). In said study four watersheds have been under forest cover over a century (historical watersheds) while the other two (succession watersheds) used to be under coffee production approximately until the mid 80's. Table 2.1 shows the results obtained for these six reference watersheds under study. Dupouey, 2002 states that: "the concept of land use legacy has received increase attention in recent years as scientists have recognized that effects of historical human interventions in natural ecosystems might last for centuries", according to Martínez et al. (2010) the effects of land use legacy on the nutrient status of streams and stream ecology in general have been less well characterized.

Table 2. 1 Statistical summary of nutrient status of waters from reference reaches in PR (Martinez et al. 2010).

TP (mg/L)	Historical watersheds	Succession Watersheds	TN (mg/L)	Historical watersheds	Succession Watersheds
Average	0.004	0.033	Average	0.20	0.28
Media	0.003	0.032	Media	0.16	0.24
25th percentile	0.002	0.031	25th percentile	0.12	0.14
75th percentile	0.007	0.034	75th percentile	0.29	0.35

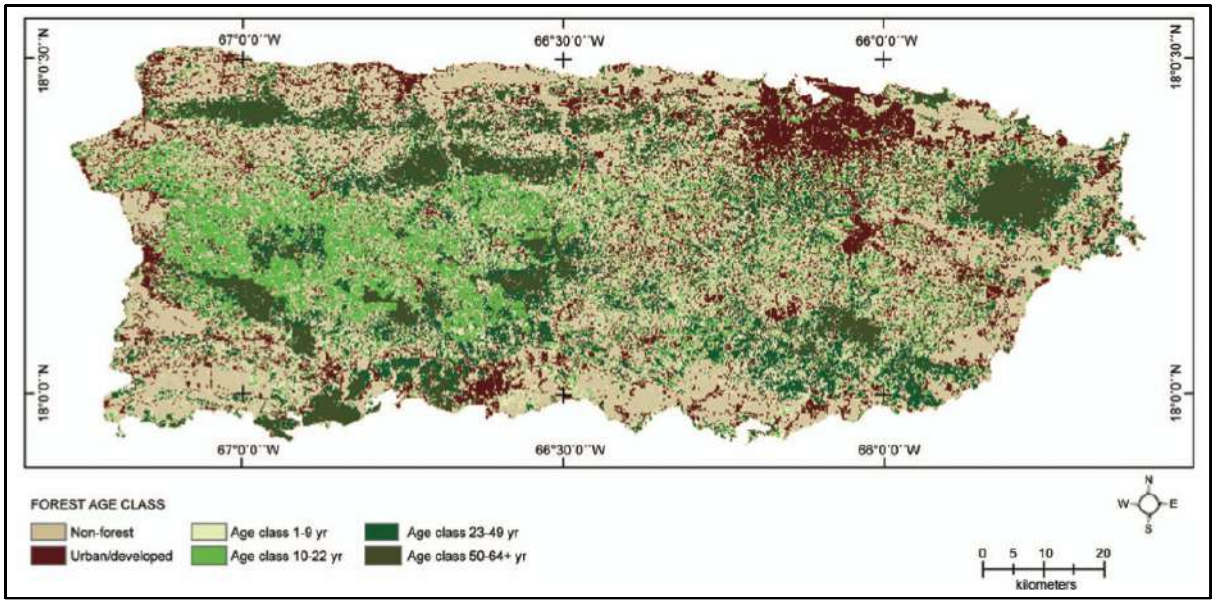

Figure 2. 1 Forest cover classification by age where to the year 2000, 55% of the forest were between 1-13 yrs. old (Kennaway, 2007).

The assessment of the impact of past land uses on the nutrient status of receiving waters is a subject of interest among the scientific communities and government agencies since it will help to establish reference conditions which will maintain and improve the ecological integrity of sub-tropical secondary forest watersheds. Puerto Rico represents the future status of many developing countries that are currently undergoing industrialization after their lands have been under intensive crop farming conditions (Martínez et al., 2010). By estimating the effect that crop fertilizers can have on the long term in the phosphorous levels of soil and waters draining tropical forests this study will provide insight into the long-term effects that conventional agricultural watershed management has on water quality. Additionally several countries are changing conventional agricultural practices where chemical fertilizers were replaced by organic agriculture yet the effects that past management practices had on the actual phosphorous loadings to streams and soil P concentrations is still being explored.

In 2013 Evans-White et al. published a paper in where the EPA suggested nutrient criteria is evaluated in terms of several independent studies that determined nutrient criteria based on percentile analysis of streams grouped into aggregate nutrient eco-regions in the US. Their main objectives in the study as stated by (Evans-White, et al., 2013) was to determine whether the 75th percentiles of reference streams were equal to or more conservative than the 25th percentile estimates of a general population of streams and to compare the individual study percentile estimates with USEPA percentile estimates in 2000 in order to determine whether more focused regional studies resulted in more or less conservative estimates than those originally proposed by the USEPA. In this study they found that even though the USEPA assumed that the 25th percentile of a general population will be approximately equal to the 75th percentile of a reference population, the 75th percentile of the reference population of streams resulted in higher nutrient conditions where the mean 75th to 25th percentile ratio was 3.9+/-0.66 and 1.6 +/- 0.1 in Total Phosphorous and Total Nitrogen respectively. Yet for region II (western forested mountains) TP values for the 75^{th} percentile of a reference stream was more conservative than the 25^{th} percentile of the general population of streams. The authors point to the fact that the possibility of the 25^{th} percentile of the general population being more conservative in the majority of the regions could be due to the inclusion of human impacted streams in the reference site pool which happens if relatively un-impacted reference sites are rare causing managers to use sites in moderately developed watersheds (Dodds et al,, 2004) as cited by (Evans-White et al., 2013). This paper suggests that the establishment of nutrient criteria for specific ecoregions as in Puerto Rico and similar tropical climates is necessary since the regional criteria established by EPA generally differ to the values obtained by independent studies in several ecoregions. Additionally it recommends a basin approach to setting nutrient criteria since it may be more appropriate than an ecoregion approach in some lotic ecosystems. Evans-White et al. (2013) mentioned that studies by Smith et al. (2003) have found that as much as one order of magnitude of variation existed in background nutrient concentrations within aggregate nutrient eco-regions. In this study the basin approach will allow for the comparison of base flow and storm loadings for each watershed and to elucidate if these secondary forest watersheds exhibit higher loadings during storm events.

2.2. Soil Plant Phosphorous Dynamics

In order to successfully simulate P loadings into receiving waters the soil-plant phosphorous dynamics must be studied and understood. This will ensure that the processes being simulated are in agreement with the recent advances in the understanding of the P dynamics in the soil/rhizosphere-plant continuum. In soil (especially on clays with low pH) phosphorous is a highly fixated nutrient with slow diffusion rates. Often plants are not able to use applied inorganic phosphorous unless other necessary parameters such as proper soil pH are present to make it available (labile) in the soil solution pool. Due to its low solubility and mobility in soil, P can be rapidly depleted in the rhizosphere by root uptake, resulting in a gradient of P concentration in a radial direction away from the root surface (Shen et al., 2011). Metal phosphates become adhered to soil particles resulting in soil phosphorous over-enrichment, where the phosphorous will become available in the solution pool in the long term through the process of oxidation. When P is available for plant uptake is considered to be in the labile pool, in the other hand if it is adhered to a soil particle is considered to be in the active pool. The P dynamics in the soil/rhizosphere-plant continuum are shown in figure 2.2 as published by (Shen et al. 2011).

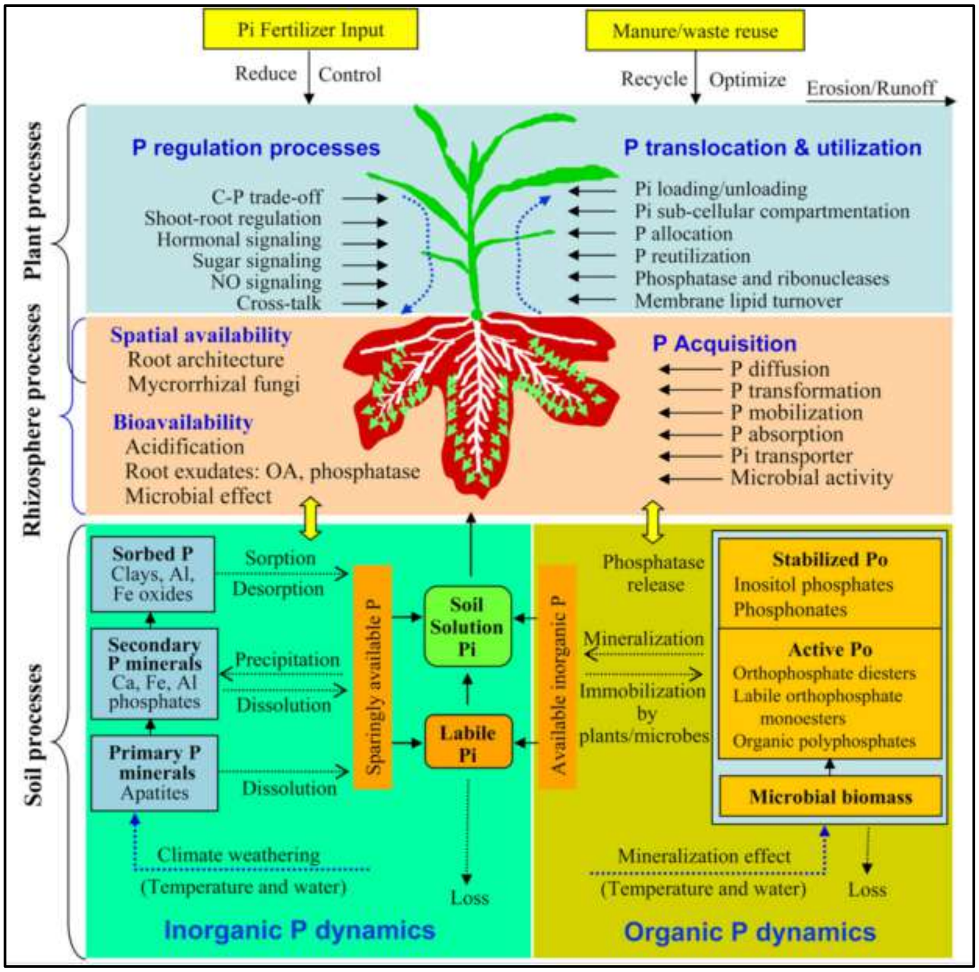

Figure 2. 2 Organic and inorganic P - soil dynamics (Shen et al., 2011)

When inorganic phosphorous is applied labile (plant available) phosphorous is rapidly transferred to the active P pool, this is the process of soil P sorption. After labile phosphorous is depleted by either runoff or plant uptake P slowly transfers by mineralization to the labile pool by the process of soil P buffering. Experiments have shown that soil inorganic P sorption usually slows down with time and computer models simulating dissolved and sediment phosphorous transfer from soil to runoff have been adjusted to simulate this. In such models as EPIC (nutrient dynamics module used by SWAT), where labile P is the main source for dissolved phosphorous in water and contributes to sediment phosphorous in runoff, labile P dynamics must accurately simulate short and long-term phosphorous dynamics (Vadas et al., 2006). Shen et al. on 2011 stated that the chemical and biological processes in the rhizosphere not only determine mobilization and acquisition of soil nutrients, but also control nutrient-use efficiency of crops (Shen et al., 2011). "Phosphorus in soils exists in a variety of forms, many of which are considered to be occluded or only sparingly soluble and thus not readily available to biota. However, these recalcitrant and occluded pools of P (sorbed to Al and Fe oxides, trapped within soil aggregates, or contained within clays or phosphate minerals) are slowly liberated and thus can be considered bioavailable when integrating over longer (e.g., decadal) timescales" Cumming et al., Richter et al. (1990, 2006 cited from Buss et al., 2010). Therefore soil P dynamics will affect water quality by soil erosion mechanisms and will also work as a catalyst in the short and long term for vegetation growth and biomass production. Shen et al. 2011 reported that organic soil P can be released through mineralization processes mediated by soil organisms and plant roots and that these processes are highly influenced by soil moisture, temperature, surface physical-chemical properties, and soil pH and Eh (for redox potential). As for inorganic P, solubility of Fe and Al phosphates increases with increasing soil pH except for values above 8 (Shen et al., 2011).

Given that the tropical forest under study is young (10-22 yrs.) the effect of these discussed processes on phosphorous cycling and transport and therefore on perennial vegetation could be accounted for by an array of physical and empirical equations incorporated into the hydrologic simulation model. In these processes water plays a main role as the solvent in which phosphorous dissolves and is made available to plants, it is also the main transporter of phosphorous loadings to streams through the process of water erosion. Furthermore, without moisture no mineralization or biological activity will be possible in the soil.

2.3. Watershed Models

Distributed watershed models are an important tool to support decisions about alternative management strategies, pollution control and river restoration projects among others. They are a reflection of our understanding of watershed systems and provide the ability to estimate impacts, compare levels of stress, prioritize areas or sources of pollution, examine trends, extrapolate monitored data and evaluate multiple systems. One of the most common uses of these models is simulating the effect of watershed processes and management on soil and water resources (Moriasi, et al., 2007). In 2005 Neitsch et al., noted that in order to properly simulate the long-term processes occurring in the watershed level a river, basin or watershed scale model that is also physically based should be used, rather than only incorporating regression equations to describe the relationship between input and output variables (Neitsch, et al., 2005).

2.3.1. Past Hydrologic Modeling Studies in Puerto Rico

In the island of Puerto Rico hydrologic models have been successfully implemented in simulation of discharges and sediment loadings of tropical forested watersheds. In 2005 Suarez Navarez employed the Hydrologic Simulation Program Fortran (HSPF) to successfully simulate discharges and sediment loadings in the Rio Grande de Arecibo watershed. Discharge data from 8 USGS stations within the watershed was used for a period of 3 to 8 years for precipitation, 2 to 5 years of discharge and 2 to 3 years of sediments. After sensitivity analysis and calibration, statistical correlation values for mean monthly flows of NSE and R^2 were 0.63 and 0.81 respectively. Average monthly sediment export calibration results were at an average of 0.29 and 0.61 for MSE and R^2 respectively. Using the calibrated model Suarez established sediment export coefficients for each land use in the watershed to simulate loading values per land use that could aid in the determination of total maximum daily loads (TMDLs) for the island.

Yuan (Yuan et al., 2016) used the SWAT model to simulate discharge and sediment loadings to the Guanica Bay watershed (~4,520 ha) using USGS gage data from the Yahuecas watershed (4,520 ha) in the upper watershed for a period of 5 years (1980 to 1985) and sediment loadings from the adjacent Adjuntas watershed for 5 years (2000 to 2005). Precipitation data used was obtained from NOAA gages at the Adjuntas watershed for the whole simulation. After calibration, values of NSE and R^2 for the mean monthly discharge validation period were 0.86 and 0.90 respectively. Sediment loadings calibration values of NSE and R^2 were 0.70 and 0.77. Using the calibrated model the study group identified critical land use areas and factors that impact sediment yields. This study proves the capacity of hydrologic models and SWAT to simulate hydrologic processes in mountainous tropical watersheds given continuous discharge data is available for calibration. Also, both authors calibrated small mountainous watersheds in order to extrapolate these values to large-scale watersheds.

2.3.2. Land Use Change Modeling Studies Using SWAT

SWAT has been successfully employed in multiple watershed modeling applications that involve dynamics between, soil, fertilization, vegetation and non-point source loadings to water bodies. The temporal spatial dynamics of land cover and non-point nutrient exports were analyzed for an upper stream of the Yellow River catchment using SWAT (Ouyang, et al., 2009). In order to assign the corresponding land cover data variance they used the normalized difference vegetation index (NDVI) calculated from MODIS satellite images. Based on the model results they determine that forestry and farmland are the main critical loss areas of NPS nitrogen. Farmland contributed sustainable soluble N, but the loading of soluble and organic N from grassland sub-basins was much lower; most P loading came from the areas covered with dense grassland and forestry (Ouyang et al., 2009). In this paper they prove that nutrient export loadings are sensitive to vegetation growth type and its spatial variation and that these dynamics can be successfully simulated using the SWAT model. Ouyang et al. (2009) writes as to the reason the SWAT model was chosen: "Most of the model systems can simulate the yield of total nitrogen and phosphorus based on the summation of modeling cells and discharge rate (Yuan et al., 2007; Gowda et al., 2008). However, the variation of land cover at the temporal-spatial scale cannot be considered." A year later (Ouyang et al., 2010) published a paper where they calibrated and validated non-point source nutrient loadings in the long term for several vegetation landscapes from 1977 to 2006. They found that landscape patterns of vegetative cover had a close effect on NPS nutrients pollution (Ouyang et al., 2010). Table 2.2 shows the correlations of the different land uses in the watershed with the nutrient loadings along with the coefficient of correlation (R^2) and results of a T-test. In 2015 (Gier, 2015) used SWAT to study the effects that changing of land use to coffee-based agroforestry in the upper basin of the Genale River Basin would have in hydrology. He concluded that in the long-term discharge could decrease up to 47,5000 cubic meters per day in a dry year. Meaning a possible increase in irrigation needs and a decrease in drinking water resources.

Table 2. 2 Correlation of vegetation area with nutrient loadings (Ouyang et al., 2010).

x (area)	Correlation model of N	R^2	F	Correlation model of P	R^2	F
Forest	$N_{Organic} = 0.024x - 0.966$	0.849	1.414	$P_{Organic} = 0.0106x - 0.5007$	0.560	1.862
	$N_{Nitrate} = 0.001x - 0.021$	0.035	0.091	$P_{Sediment} = 0.028x - 1.2825$	0.478	2.502
Farmland	$N_{Organic} = 0.016x - 0.4$	0.539	2.346	$P_{Organic} = -0.0042x + 0.9305$	0.478	1.301
	$N_{Nitrate} = -0.0016x + 0.105$	0.109	0.214	$P_{Sediment} = 0.0059x - 1.1071$	0.117	0.125
Grassland	$N_{Organic} = -0.0018x + 0.617$	0.028	0.057	$P_{Organic} = 0.0108x - 0.3981$	0.838	1.853
	$N_{Nitrate} = -0.002x - 0.39$	0.614	2.937	$P_{Sediment} = 0.0081x - 0.1859$	0.059	0.264

2.3.3. Model Comparisons

In 2005 Singh & Knapp compared the empirical, semi-distributed numerical model Soil and Water Assessment Tool (SWAT) to another popular continuous simulation model Hydrological Simulation Program- FORTRAN (HSPF). The main objective of their study was to compare and assess the suitability of these models for simulating the hydrology of one major tributary of the Upper Illinois River Basin. Both models were calibrated for a nine-year period and verified using an independent fifteen-year period by comparing simulated and observed daily, monthly and annual streamflow. In this study they found that SWAT predicted flows slightly better than HSPF with a NSE value of 0.84 for SWAT versus 0.82 for HSPF and the primary advantage being better simulation of low flows (Singh et al., 2005). One of the main reasons to which they attributed the overestimation of low flows in HSPF was the lack of specific parameters that represented the watershed's properties. Other study applied the SWAT models and another hydrologic model SMDR to a small headwater watershed (39.5 ha) in east central Pennsylvania (Srinivasan et al., 2005). The soil moisture distribution and routing (SMDR) model is a physically based fully distributed non-calibrated model used to simulate runoff generation of small watersheds developed by Cornell University by the Soil and Water Laboratory in collaboration with NRCS-USDA. The program uses grids as a distribution parameter and a 5X5 m grid was used for this study. Precipitation and discharge data was obtained for a 4-year lapse (1997-2000) and used for calibration of SWAT and evaluation of both models. Statistical parameters resulted in a better simulation of discharge for the SWAT with a NSE of 0.62 versus SMDR with 0.33. This watershed consisted of 20 percent pasture, 30 percent woodland and 50 percent cropland.

2.4. The SWAT Hydrologic Modeling Software

2.4.1. Model Description

The soil and water assessment tool (SWAT) is a computer watershed scale model developed by the Agricultural Research Service (ARS) to predict the impact of land management practices on water, sediment and agricultural chemical yields in large complex watersheds with varying soils, land use and management conditions over long periods of time (Neitsch et al., 2011). In the theoretical documentation it is described as a semi-distributed, partly physically based watershed model for continuous long term simulations of daily discharge as well as point and non-point sources of nutrient, pesticide, and sediment loads (Neitsch et al., 2011). The fundamental strengths of SWAT are flexibility in combining upland and channel processes and simulation of land management, however; as noted by Gassman et al. (2007), each process is a simplification of reality and could be improved (Arnold et al., 2012). Another main advantage of SWAT is that the temporal accounting routine allows users to introduce the adoption of different selected management practices or account for changes in land use part way through a SWAT simulation run (Arnold et al., 2012). Given that within one of the purposes of the study is to simulate the transition from agriculture to secondary forest in the Bosque Olimpia watershed this feature plays a key role in the land use temporal-spatial dynamics that is to be simulated. The climatic variables required by SWAT consist of daily precipitation, maximum/minimum air temperature, solar radiation, wind speed and relative humidity. The model allows values for daily precipitation, maximum/minimum air temperatures, solar radiation, wind speed and relative humidity to be input from records of observed data or generated during the simulation (Neitsch et al., 2011).

2.4.2. Hydrologic Components

SWAT divides the watershed into sub-basins of similar land use, soil and topography called hydrologic response units (HRU's) where land phase processes as vegetation growth, water flow, nutrient transformation and transport are simulated (Neitsch et al., 2011). All the equations and theory discussed in this section can be found in the SWAT theoretical documentation version (Neitsch et al., 2011). The user may also delineate the HRUs within each sub-basin, a maximum of 10 different HRUs per sub-basin is permitted. The land phase of the hydrologic cycle is based on the water balance equation (2.1) where all the different and specific components of the hydrologic cycle are calculated daily in mm of H_2O to obtain the soil water content fluctuation in mm of H_20.

$$S_w = S_{w_0} + \sum_{i=1}^{t}\left(R_{day} - Q_{surf} - E_a - w_{seep} - Q_{gw}\right) \tag{2.1}$$

where: S_w= final soil water content, S_{w_0}= initial soil water content, R_{day}= precipitation on day i, Q_{surf}= surface runoff on day i, E_a= evapotranspiration on day i, W_{seep}= amount of percolation and bypass flow exiting the soil profile on day i, Q_{gw}= amount of return flow on day i, t= time in days

2.4.2.1. Surface Runoff

Runoff will occur whenever the rate of water entering the soil profile exceeds the rate of infiltration of the soil. The rate of infiltration decreases as soil gets saturated, when this happens depressions will be filled first and afterwards runoff will start to occur. In our case runoff is calculated using the empirically based Soil Conservation Service Curve Number method or CN method (SCS 1972), which takes into account the land use, soil, topography and precipitation in each HRU to calculate runoff. SWAT also offers the option to use the Green & Ampt infiltration method.

The CN method is based on empirical data collected over 20 years in small rural watersheds of the U.S. Using this data, equations and CN values for rainfall runoff relations were developed for varying land uses and soils. The SCS CN method equation is shown in (2.2):

$$Q_{surf} = \frac{\left(R_{day} - I_a\right)^2}{\left(R_{day} - I_a + S\right)} \tag{2.2}$$

where: Q_{surf}- accumulated surface runoff (mm H_2O), R_{day}- rainfall depth of the day (mm H_2O), I_a- initial abstractions (mm H_2O), S- retention parameter (mm H_2O)

The retention parameter varies temporally according to soils, land uses, management, slope and soil water content and is calculated as in equation (2.3). This is because curve numbers (CN) are values developed to represent the soil permeability (in terms of hydrologic soil groups), land use and antecedent soil water conditions of an area. Generally a lower CN will produce lower runoff while larger CN values will produce higher runoff volumes.

$$S = 25.4\left(\frac{1000}{CN} - 10\right) \qquad (2.3)$$

where: CN is the Curve Number and S is the retention parameter.

Hydrologic soil groups (HSG) represent the rate of infiltration characteristics of the soil, which can be classified in 4 groups A, B, C or D or three dual classes A/D, B/D, C/D. In groups A to D infiltration characteristics vary from A having high infiltration capacity and low runoff potential to D having low infiltration capacity and high runoff potential. Dual classes are assigned only to wet soils that can be adequately drained. General characteristics used to establish HSG where depth to seasonal high water table, saturated hydraulic conductivity and depth to a very slowly permeable layer. Tables with curve numbers for different land uses, hydrologic soil groups and conditions can be found in the NRCS TR-55.

The SCS CN method equation mandates that runoff starts when Rday>I_a; by assuming I_a=0.2S equation (2.2) turns to equation (2.4).

$$Q_{surf} = \frac{\left(R_{day} - 0.2S\right)^2}{\left(R_{day} + 0.8S\right)} \qquad (2.4)$$

where: Q_{surf} is the accumulated surface runoff (mm H_2O), R_{day}, rainfall depth of the day (mm H_2O) and S, the retention parameter (mm H_2O)

In addition to precipitation SWAT varies runoff output by calculating the retention parameter for each day based on not only the land use and soil physical properties but in the deficit of available soil profile water content. This is done using equation (2.5):

$$S = S_{max}\cdot\left[1 - \frac{S_w}{(S_w + \exp\,[w_1 - w_2 * S_w])}\right] \qquad (2.5)$$

where: S is the retention parameter for a given day (mm), $S_{max,}$ the maximum value the retention parameter can achieve on any given day (mm), S_W - the soil water content of the entire profile excluding the amount of water held in the profile at wilting point (mm H2O), w_1 and w_2 - shape coefficients.

These coefficients (w1 and w2) are calculated assuming CNs at three different antecedent soil moisture conditions: wilting point (condition I), average (condition II) and field capacity (condition III) and solving equation (2.5) for conditions I and III simultaneously. S_{max} is calculated assuming the curve number value for condition I and solving equation (2.3).

2.4.2.2. Peak Runoff Rate

Peak runoff rate, obtained by using the rational method, is used to calculate sediment loss in the SWAT model. SWAT uses a modified rational method (2.6), which is incorporated into the model using certain assumptions discussed below.

$$q_{peak} = \frac{\propto_{tc} * Q_{surf} * Area}{3.6 * t_{conc}} \tag{2.6}$$

where: q_{peak} - the peak runoff rate (m3 s-1), $\propto_{tc}$ - the fraction of daily rainfall that occurs during t_{conc}, Q_{surf} - the surface runoff (mm H2O), Area is the subbasin area (km2), t_{conc} - the time of concentration for the subbasin (hr.), 3.6 - a unit conversion factor

First the rational method assumes that the peak runoff rate occurs at the time of concentration. The time of concentration is the time from the beginning of an event to the moment when all runoff is contributing to the flow at the outlet. The time of concentration (2.7) is the sum of the time it takes for a drop of water to flow overland from the farthest ridge across the slope to the river reach and the time it takes for this same drop to travel down the reach or channel to the watershed outlet.

$$t_{conc} = t_{ov} + t_{ch} \tag{2.7}$$

where: t_{conc}- time of concentration for a subbasin (hr.), t_{ov} – time of concentration for overland flow (hr.), t_{ch}- time of concentration for channel flow (hr.)

The following equation (2.8) is used for the overland flow time of concentration calculation. In order to obtain the overland travel time. Manning's equation for velocity is used assuming a 1 m wide strip along the sloping surface and an average flow rate of 6.35 mm/hr. converted into cubic meters per second to substitute into equation (2.8) and obtain overland travel time in terms of slope, length of slope and Manning's roughness coefficient.

$$t_{ov} = \frac{L_{slp}}{3600 * v_{ov}} \tag{2.8}$$

where: L_{slp} - the subbasin slope length (m), v_{ov} - the overland flow velocity ($m.s^{-1}$), 3600 - a unit conversion factor

For the channel flow time of concentration equation (2.9) was used. In order to calculate velocity the Manning equation was used assuming a trapezoidal channel with 2:1 side slopes and a 10:1 bottom width-depth ratio. Also to obtain the average channel flow length the watershed's centroid along the channel's length was assumed to be half (0.5L) of the total channel length.

$$t_{ch} = \frac{L_{ch}}{3.6 * V_c} \tag{2.9}$$

where: L_{ch} - the average flow channel length for the subbasin (km), v_c - the average channel velocity ($m.s^{-1}$), 3.6 - a unit conversion factor

2.4.2.3. Transmission Losses

Transmission losses or channel abstraction is calculated in SWAT using a procedure found in Chapter 19 of the SCS Hydrology Handbook. The procedure incorporates regression parameters defined by channel dimensions and effective hydraulic conductivity (K_{sat}) of the channel alluvium to calculate the volume of runoff after transmission losses.

2.4.2.4. Evapotranspiration

Evapotranspiration is considered in SWAT by several processes including evaporation from the plant canopy, transpiration and evaporation from the soil. It considers the canopy storage as a function of the leaf area index, meaning that the canopy storage will depend on the age and development of trees in the watershed. When precipitation starts the program fills the canopy first before any water is allowed to reach the soil.

The total potential evapotranspiration (E_0) is calculated using the Pennman-Monteith method (2.10), which requires solar radiation, air temperature, relative humidity and wind speed. These values are provided to the model through either the weather simulator or daily measured data.

$$\lambda E = \frac{\Delta \cdot (H_{net} - G) + \rho_{air} \cdot c_p \cdot [e_z^0 - e_z]/r_a}{\Delta + \gamma \cdot (1 + {}^{r_c}/_{r_a})} \tag{2.10}$$

where: λE is the latent heat flux density (MJ m^{-2} d^{-1}), E is the depth rate evaporation (mm d^{-1}), Δ is the slope of the saturation vapor pressure-temperature curve, de/dT (kPa °C^{-1}), H_{net} is the net radiation (MJ m^{-2} d^{-1}), G is the heat flux density to the ground (MJ m^{-2} d^{-1}), ρ_{air} is the air density (kg m^{-3}), c_p is the specific heat at constant pressure (MJ kg^{-1} °C^{-1}), e_z^0 is the saturation vapor pressure of air at height z (kPa), e_z is the water vapor pressure of air at height z (kPa), γ is the psychrometric constant (kPa °C^{-1}), r_c is the plant canopy resistance (s m^{-1}), and ra is the diffusion resistance of the air layer (aerodynamic resistance) (s m^{-1}).

To calculate the actual evapotranspiration SWAT starts by comparing the amount of free water stored in the canopy (R_{int}) with the total potential evapotranspiration (E_0). If E_0 is less than R_{int} the total amount of evaporated water from the canopy E_{can} is equal to E_0 and R_{int} is reduced. If E_0 is greater than R_{int} then E_{can}=R_{int} and E_0 is reduced by E_{can}. The remaining evaporative water demand (E'_0) is partitioned between vegetation and soil evaporation.

When the Pennman-Monteith method is used, transpiration is calculated using the same approach as for potential evapotranspiration. Assuming neutral atmospheric stability, logarithmic wind profiles and plant canopy resistance derived from plant leaf area index (LAI) the transpiration rate for a given canopy can be calculated. This allows transpiration values to change dynamically with LAI, which is simulated by SWAT in the plant growth module discussed later on. The remaining potential evaporation is then adjusted as a function of the above ground biomass and residue to calculate soil water evaporation (E_s). In order to account for periods of high plant water use, soil evaporation is adjusted by taking into account transpiration and choosing the lowest result between them (E_s and E'_s) as the maximum soil water evaporation in a given day.

This calculated value is then compared to the actual evaporative demand of the soil (if available) and assumes that 50% of the water will be evaporated in the top 10 mm of soil and 95% in the top 100 mm. SWAT incorporated a coefficient (esco), which allows user to modify the soil water depth distribution used to meet the evaporative water demand. As the value for esco is reduced, the model is able to extract more of the evaporative demand from lower levels of the soil profile.

2.4.2.5. Soil Water

SWAT simulates saturated soil flow only; unsaturated flow between layers is indirectly modeled with depth distribution of plant water uptake and depth distribution of soil water evaporation. Water is allowed to percolate if soil water content exceeds field capacity in a layer and underlying layer is not saturated. Field capacity is calculated as the permanent wilting point soil water content plus the available water capacity, which is provided by the user for each soil mapping unit in the catchment area. The program calculates wilting point by taking into account soil's clay percent and bulk density. The excess water will move to the next layer and the daily amount of percolation to the lower layers will depend on the travel time for percolation that is defined as the time in hours it takes a drop of water to move vertically from edge to edge of a soil layer.

Lateral flow is incorporated into SWAT using a kinematic storage model for subsurface flow developed by Sloan et al. (1983) (as cited by Neitsch et al., 2011). This model simulates subsurface flow in a two-dimensional cross-section along a flow path down a steep hillslope. This model is based on the mass continuity equation, or mass water balance, with the entire hillslope segment used as the control volume. The hillslope segment has a permeable soil surface layer of depth D_{perm} and length L_{hill} with an impermeable soil layer or boundary below. This model assumes the lines of flow in the saturated zone are parallel to the impermeable boundary and the hydraulic gradient equals the slope of the bed. The drainable volume of water stored in the saturated zone will be the difference between the soil water in a given soil layer and the field capacity of that layer. This calculated volume, the drainable porosity of the soil, the hillslope length, the average slope of the sub basin and the hydraulic conductivity are taken into account to determine the water discharged from the hillslope outlet in millimeters per hour.

2.4.2.6. Groundwater

SWAT simulates two aquifers in each subbasin: shallow and deep aquifers. The shallow aquifer is an unconfined aquifer that contributes to flow in the main channel or reach of the subbasin. The deep aquifer is a confined aquifer. Water that enters the deep aquifer is assumed to contribute to streamflow somewhere outside of the watershed. The water balance for the shallow aquifer is shown on equation (2.11):

$$aq_{sh,i} = aq_{sh,i-1} + W_{rchrg,sh} - Q_{gw} - w_{revap} - w_{pump,sh} \tag{2.11}$$

where: $aq_{sh,i}$ - the amount of water stored in the shallow aquifer on day i (mm H2O), $aq_{sh,i-1}$ is the amount of water stored in the shallow aquifer on day i-1 (mm H2O), $w_{rchrg,sh}$ is the amount of recharge entering the shallow aquifer on day i (mm H2O), Q_{gw} is the groundwater flow, or base flow, into the main channel on day i (mm H2O), w_{revap} is the amount of water moving into the soil zone in response to water deficiencies on day i (mm H2O), and $w_{pump,sh}$ is the amount of water removed from the shallow aquifer by pumping on day i (mm H2O).

The amount of recharge entering the shallow aquifer is the water that moves past the lowest depth of the soil profile by percolation and flows through the vadose zone. The delay time (δ_{gw}) this water takes to reach the shallow aquifer depends on the physical properties of the vadose and ground water zones. An exponential decay equation proposed by Ventis in 1969 is used in SWAT to calculate the aquifer recharge in mm of H_2O (Neitsch et al., 2011). The equation depends directly on the amount of water exiting the bottom soil profile and the delay time of overlying geologic formations. Although the delay time cannot be directly measured Sangrey et al., 1984 noted that once this value is defined for a geomorphic area similar delay times can be used for watersheds within the same geomorphic area (Neitsch et al., 2011). The amount of water percolating to the deep aquifer is estimated using an aquifer percolation coefficient.

Base flow from the shallow aquifer is allowed to enter the reach only if the amount of water stored in the shallow aquifer exceeds a threshold value specified by the user. In order to calculate the groundwater flow into the main channel for a given day in mm of H2O the model combines steady state equation for groundwater flow to recharge with equation for water table fluctuations due to non-steady-state response of groundwater flow to periodic recharge and assumes that variation in groundwater flow is linearly related to the rate of change in water table height (Neitsch et al., 2011). This equation is also used to determine and update the daily groundwater height or water table. Aquifer parameters considered for this are saturated hydraulic conductivity and the baseflow recession constant (α_{gw}). The latter (α_{gw}) is a direct response of the groundwater flow response to changes in recharge and it can be easily calculated if base flow data is available for a period long enough for the baseflow recession curve to decline through one log cycle by dividing 2.3 by the amount of days.

Other pathways water can be removed for the aquifer are revap, which accounts for the water diffused upward by capillarity after water from the overlying capillary fringe is evaporated and pumping where the model allows an amount of water up to the total volume of the shallow aquifer to be removed on any given day.

2.4.3. Nutrient Cycle

The model simulates the production of biomass through its land cover/plant growth module and then the movement and transformations in the macro nutrient (N, P) cycles. The land cover/plant growth model is used to assess removal of water and nutrients from the root zone, transpiration and biomass production. The model also estimates stresses to plants caused by water, nutrients and temperature (Neitsch et al., 2011). SWAT tracks the movement and transformation of several forms of nitrogen and phosphorus in the watershed. The transformation of phosphorus in the soil is controlled by the phosphorus cycle shown in figure 2.3 where nutrients may be introduced to the main channel and transported downstream through surface runoff and lateral subsurface flow (Neitsch et al., 2011). Instream nutrient processes are also simulated in SWAT taking into account algae death rate, mineralization of organic phosphorous to soluble phosphorous.

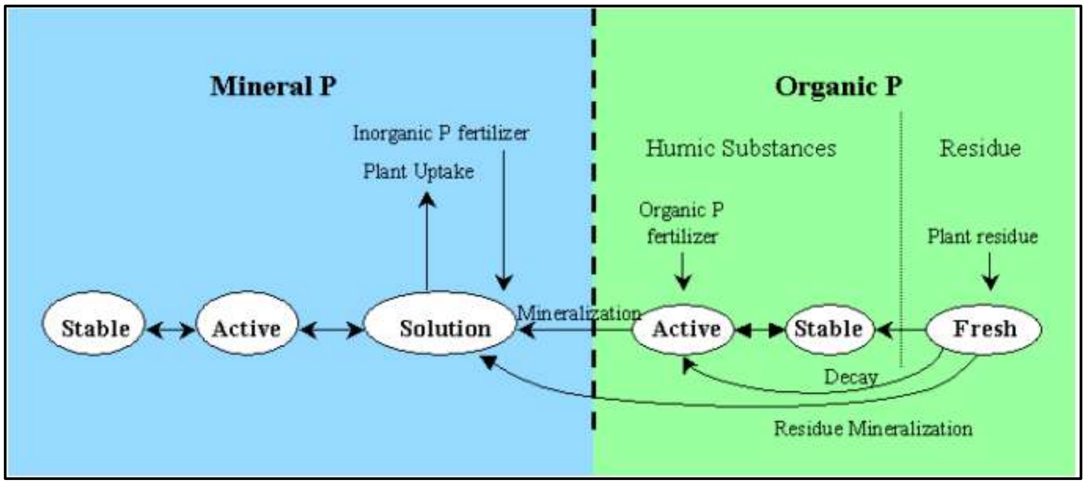

Figure 2. 3 Partitioning of phosphorous in SWAT (Neitsch et al., 2011).

In SWAT management practices taking place in each HRU can be defined. The user may define the beginning and the ending of the growing season, specify timing and amounts of fertilizer as well as to decide if the biomass will be placed on the surface as residue or removed as yield. As it can be seen in Figure 2.3 residue from biomass is transformed into nutrients by mineralization in where a part of these nutrients will be made available (labile) to the plants and others will be immobilized. Phosphorus mineralization algorithms developed by Jones et al. (1984) are used in SWAT considering two sources, the fresh organic pool containing crop residue and microbial biomass and active organic pool associated with soil humus. Two main factors are considered for mineralization to occur: temperature and soil water availability. SWAT simulates slow inorganic phosphorus sorption by assuming the active mineral phosphorus pool is in slow equilibrium with the stable mineral phosphorus pool. At equilibrium, the stable mineral pool is 4 times the size of the active mineral pool. If the stable pool is larger than this established ratio the difference is passed to the stable pool at the slow equilibrium rate constant, which is 0.0006/d.

The transfer from the solution to the active inorganic P pool is governed by equilibrium equations and the phosphorous availability index of the soil (pai), which is provided by the user. If phosphorous in solution is more than the possible phosphorous in solution in the soil layer after fertilization and incubation, then P moves from solution to the active mineral pool. If the phosphorous in solution is less, then P is transferred from the active mineral pool to solution. In this equilibrium equation the rate of sorption is 10 times the rate of mineralization. Leaching of P is considered in the top 10 mm of soil taking into account the low P mobility, the amount of water percolating to the first soil layer from the top 10 mm, the bulk density of soil and the phosphorous percolation coefficient.

In addition to plant use, soluble phosphorus and organic P may be removed from the soil via mass flow of water. Phosphorus is not a mobile nutrient and interaction between surface runoff with solution P in the top 10 mm of soil will be partial. The amount of soluble P removed in runoff is predicted using solution P concentration in the top 10 mm of soil, the runoff volume and a partitioning factor. P and Organic N transport with sediment is calculated with a loading function developed by McElroy et al. (1976) and modified by Williams et al., (1978) for application to individual runoff events (as cited from Neitsch et al., 2011).

Vadas et al., (2006) evaluated the capacity of SWAT in modeling phosphorous transfer between labile and non-labile soil pools. Here they stated that the effect of changing constant rate factors used in the model with dynamic ones could change the predictions in dissolved P load in runoff in 8% in the long terms vs. in the short term it could be up to a 30% difference. Given that the aim of this study is long-term simulation the margin of 8% will be considered appropriate and therefore it is assumed that SWAT simulates the sorption and desorption dynamics of phosphorous species in soil sufficiently well. The statement that processes included in the SWAT model has the capacity of properly modeling Soil P dynamics in tropical forest is to be explored in the thesis study along with the proper values of relevant parameters in each of the P cycling equations used in the model.

2.4.4. Sediment and Nutrient Transport

Erosion and sediment yield are estimated for each HRU using the modified universal soil loss equation (2.12) by (Williams 1995), which uses the amount of runoff to simulate erosion and sediment yield. The hydrology model supplies estimates of runoff volume and peak runoff rates which, with the sub-basin area, are used to calculate the runoff erosive energy variable (Neitsch et al., 2011).

$$sed=11.8(Q_{surf}*q_{peak}*area_{hru})^{0.56}\ K_{USLE} * C_{USLE}*P_{USLE}*LS_{USLE}*CFRG \qquad (2.12)$$

where: sed - the sediment yield on a given day (metric tons), Q_{surf} - the surface runoff volume (mm H2O/ha), q_{peak} - the peak runoff rate (m3/s), $area_{hru}$ is the area of the HRU (ha), K_{USLE} is the USLE soil erodibility factor, C_{USLE} - the USLE cover and management factor, P_{USLE} - the USLE support conservation practice factor, LS_{USLE} - the USLE topographic factor and CFRG - the coarse fragment factor.

Nutrient transport for phosphorous happens in two possible ways: dissolved into runoff by the process of diffusion or attached to sediment in surface runoff. Diffusion is defined as the migration of ions over small distances of approximately 2 mm in response to a concentration gradient. The amount of soluble P removed in runoff is predicted using solution P concentration in the top 10 mm of soil, the runoff volume and a partitioning factor. “P and Organic N transport with sediment is calculated with a loading function developed by McElroy et al. (1976) and modified by Williams et al., (1978) for application to individual runoff events” (as cited from Neitsch et al., 2011). The equation used to obtain the concentration of phosphorous attached to sediment in the soil surface layer takes into account the stable mineral P, humic organic P, organic P in the fresh organic pool and bulk density of soil; all in the top 10 mm of soil.

2.4.5. Channel Processes

Channel processes include streamflow, channel erosion and deposition, in-stream transformation and transport of nutrients (Neitsch et al., 2011; Strauch et al., 2013). The in-stream kinetics used in SWAT for nutrient routing is adapted from QUAL2E (Brown et al., 1987) as cited by Neitsh et al., (2011). The model tracks nutrients dissolved in the stream and nutrients adsorbed to the sediment. Dissolved nutrients are transported with the water while those sorbed to sediments are allowed to be deposited with the sediment on the bed of the channel (Neitsch et al., 2011).

Stream flow is calculated using Manning’s equation for uniform open channel flow in a reach segment for a given time step. The variable storage routing method is used by default in SWAT for water routing through the channel network. This method is based on the continuity equation and by adding the stored volume in a reach segment for a given time lapse and multiplying it by a storage coefficient provide final volume of water for a given time lapse. The program also allows choosing the Muskingum Routing Method; both methods are variations of the kinematic wave model. The final volume is calculated by the channel water balance, which takes into account transmission losses, evaporation losses, diversions and bank storage.

2.5. Plant Growth Module in SWAT

Given that the land use change and phosphorous dynamics in the soil and water depend on the vegetation growth, plant nutrient uptake and residue contribution to the WS and that key hydrological features as evapotranspiration (ET) and canopy water storage rely on the proper simulation of the leaf area index (LAI) of the land use, the proper simulation in SWAT of perennial vegetation growth is crucial to simulate the long term dynamics of NPS phosphorous loadings in tropical forest watersheds. The following limitations for the simulation of trees and perennial vegetation in SWAT were found by Strauch & Volk (2013): Dormancy, a fundamental feature of trees and perennials during which plants do not grow, is the only approach in SWAT to repeat growing cycles for perennials and trees each year. This occurs when the day length approaches its minimum for the year, then a fraction of biomass is converted to residue and the LAI is set to a plant specific minimum value. Dormancy also resets the specific fraction of potential heat units (FR_{PHU}) to zero, which allows the beginning of a new growing cycle once the day length exceeds a latitude-specific threshold. FR_{PHU} is calculated as in equation (2.13) where potential heat units (PHU) for trees and perennials refer to the number of days between budding and leaf senescence. However, in the tropics plants do not undergo dormancy. In that case, heat units and thus FR_{PHU} are accumulated continuously throughout the whole simulation period. The model will only simulate plant growth until the plant reaches maturity (at FR_{PHU} = 1), i.e. from that point on, plants will not transpire or take up nutrients and water (Neitsch et al., 2011).

$$FR_{PHU,i,j} = \frac{\sum_{k=1}^{i} HU_k}{PHU_j} \tag{2.13}$$

where: $FR_{PHU,i,j}$- is the fraction of potential heat units from day i to day j, PHU_j – potential heat units for a given plant or tree on day j, HU_k – heat units on a given day k.

Without dormancy, the model requires management operation "kill" for stopping a growing season and thus enabling a new one (by resetting FR_{PHU} to zero). Management operations such as the "kill" operation can be scheduled by FR_{PHU} or by date. Yet if the kill operation is used by FR_{PHU} (i.e. plant" operation at FR_{PHU}=0.1 and a "kill" operation at FR_{PHU}=0.925) the seasonality is represented insufficiently since LAI reaches its maximum in the driest months of the year and drops to zero during wet season (see Figure 2.4 graph b). Alternatively if the dates are used for the kill operation it is possible to match the simulated LAI to the end of the rainy season, however, the start of a growing season will be static (growing season will start all year's same date) and the LAI will drop down towards zero when FR_{PHU} approaches the value of one (figure 2.4 graph c). For trees and perennials SWAT considers a plant specific minimum LAI to ensure that LAI doesn't fall to zero yet LAI_{min} is only effective in the dormant period and, thus, not effective for the tropics (Strauch et al., 2013).

Strauch, M. and Volk, M. developed a modification to the plant growth module used in the SWAT model in order to improve the vegetation growth modeling for the tropics. Their main approach is that moisture – and not temperature – is the primary control for plant phenology in tropical regions, especially in those having distinct dry and wet seasons, and that in tropical regions there is no dormancy so that the nutrient and water plant uptake dynamics should be adjusted. Additionally that growing cycles should be initiated automatically without requiring management operations. They used the simulated plant available water in the upper soil layers as a trigger for new growing cycles. To ensure that short dry periods do not terminate growing seasons they implemented two parameters which define the first and the last month of a region specific transition period from dry to wet season. The actual plant growth follows the normal heat unit based LAI cycle until a new growing season is initiated. Figure 2.5 shows the implementation of soil moisture into the SWAT plant growth module; the figure was taken directly from Strauch and Volk (2013). The algorithm starts by verifying that the center geographic coordinates of the watershed are within the correct latitudes, that the simulation date is within the transition period and that there hasn't occurred a transition from one growing cycle to the next (Iseason=1). Then a threshold fraction FR_{AWC} similar to FR_{PHU} but in terms of available water content is compared with the actual soil water content in the upper two soil layers (SW_{UPPER2}). In the case that $SW_{UPPER2} > AWC_{UPPER2}FR_{AWC}$ then FR_{PHU} is set to zero, the LAI is set to minimum and plant residue decomposition and nutrient release are calculated as if dormancy will occur. If the soil water content remains below the threshold it is evaluated if the actual month is within the transition period then it will follow normal plant growth, if it's after the transition period, it goes to dormancy. The author also states that using the SWAT default version is not recommended for studies focused on cumulative biomass production of tropical perennials. Figures 2.4a and 2.6a shows the unmodified SWAT LAI and biomass production simulation respectively, Figure 2.6b shows the modified SWAT biomass production (right). It can be seen that the unmodified SWAT module does not properly simulate LAI since as stated before, when the kill operation takes place, in the absence of dormancy for tropical regions the LAI (2.4b and c) and with it the biomass (2.6a) defaults to zero. If it were a temperate zone it would've defaulted to dormancy and therefore it would've had a minimum leaf area index. However in Figure 2.6b the biomass production is cumulative and therefore representing realistic biomass dynamics for the tropics.

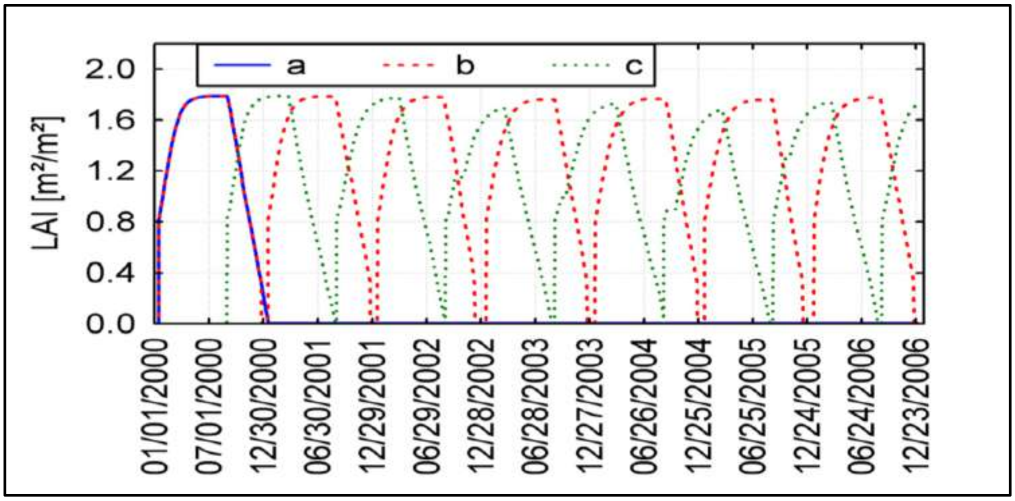

Figure 2. 4 LAI simulation for the tropics using the unmodified version of SWAT (a) using management option "vegetation is growing", (b) "plant & kill" operations using PHU fractions (c) "plant & kill" operations using dates. Taken from Strauch et al., (2013).

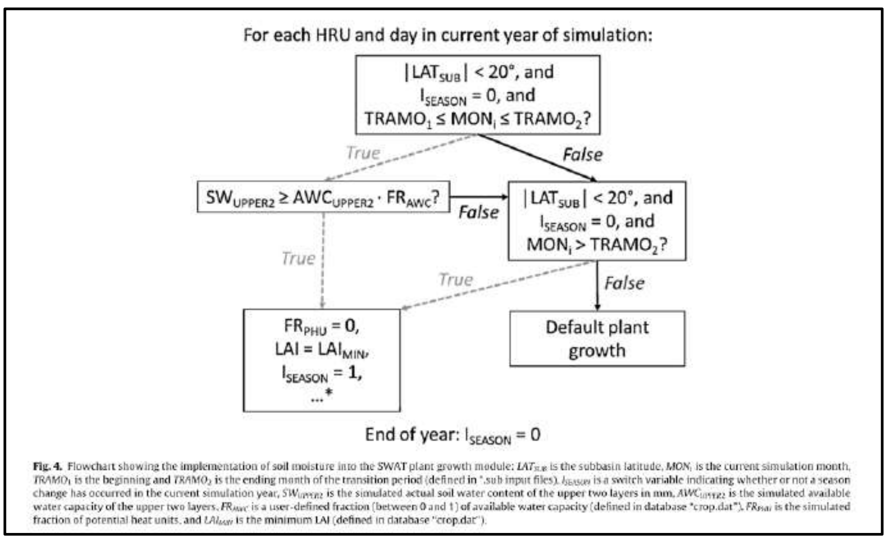

Figure 2. 5 Flowchart showing the implementation if soil moisture into the SWAT plant growth module. Taken from (Strauch et al., 2013).

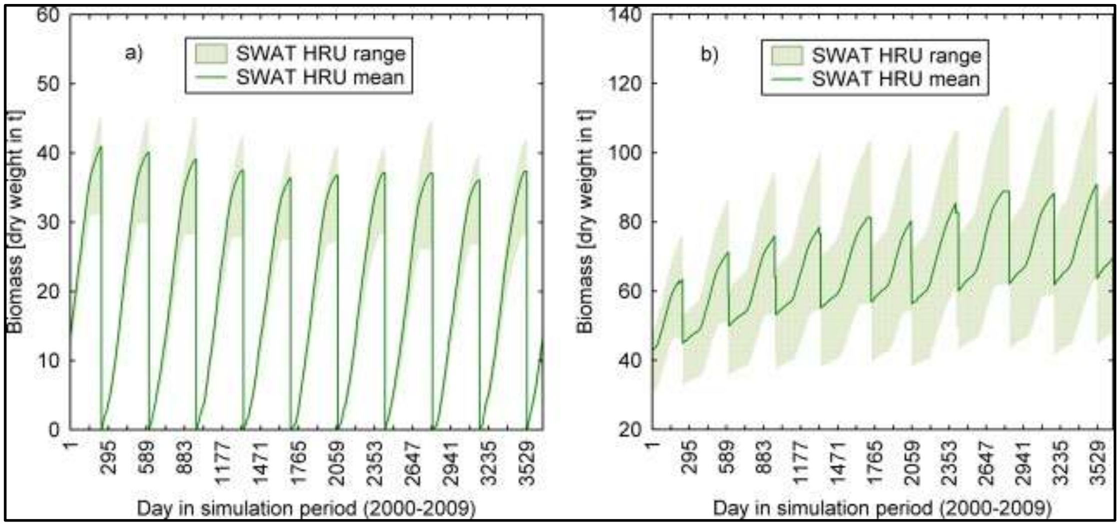

Figure 2. 6 Biomass production of unmodified SWAT 2009 (a) vs SWAT 2009 with modified plant growth module (b) (Strauch et al., 2013).

In their study Strauch M. and Volk, M. (2013) validated their model by comparing evapotranspiration and leaf area index data derived from the Moderate Resolution Imaging Spectoradiometer (MODIS) with the outputs obtained by the modified SWAT model of the Santa Maria/Torto watershed in Central Brazil. They also validated the model in terms of daily and monthly discharge, yet they did not test the model for non-point nutrient loadings since they concentrated on the vegetation growth dynamics. Strauch et al. (2013) writes: "The vast majority of SWAT studies for tropical regions did not critically reflect the model's suitability to simulate vegetation dynamics probably because model calibration and validation is usually based only on discharge and/or water quality outputs. However, successfully matching those outputs do not mean that internal catchment processes are simulated correctly." It is evident that one of the most important factors in this process is the proper simulation of hydrologic dynamics in the watershed and hence poses a question regarding the adequacy of SWAT for simulation hydrologic processes in tropical watersheds that should be studied by hydrologists and water resources engineers.

2.6. Land Use Dynamics

As mentioned above the temporal spatial dynamics of land cover is directly related to non-point nutrient pollution loadings. To obtain land cover data, researchers have used MODIS data as well as other approaches based on land cover reflectivity recorded by satellite images (Ouyang et al., 2009; Strauch et al., 2013). Even when this has proven to be an effective technique to obtain land cover data for long term simulations our basins under study are too small for satellite based data to reflect the variability of the tropical forests within; furthermore, cloud-free satellite imagery for Puerto Rico is scarce. Studies have been made to determine the optimal grid size for radar reflectivity using the SWAT model (Jeong, et al., 2013). By analyzing the variation in runoff an optimal grid size of radar reflectivity in the range of 4-8 km for the Soyanggangdam basin was obtained (Jeong et al., 2013); this exceeds the area of both watersheds under study. Additionally the normalized difference vegetation index (NDVI) used to describe forested lands in remote sensing (Ouyang et al., 2009) will not reflect the long term biomass dynamics in our watersheds. Thus, in order to simulate the land use temporal spatial dynamics appropriately we will rely on the plant growth module along with the historical management conditions gathered by the study group.

2.7. Calibration and SWAT-CUP

Model Calibration, in short terms, is the process of adjusting model parameters within the margin of uncertainties to obtain a model representation of the processes under study that satisfies a determined criterion. There are multiple ways to calibrate a model, yet they're all are oriented towards the optimization of parameters in order to obtain an acceptable performance defined in terms of single or multiple objective functions. Naumov (2005) used single and multi-criteria automated validation to successfully simulate and validate flows in a small (7.2 km^2) forested watershed. With his results he concluded that automated calibration be it single or multi criteria will achieve better model performance than traditional manual calibration. He also found that multi-criteria calibration achieves better results than single criteria calibration. As we will see below the second version of the Sequential Uncertainty Fitting (SUFI2) calibration routine within the SWAT Calibration and Uncertainty Programs (SWAT-CUP) developed by the Swiss Federal Institute of Aquatic Science and Technology (Abbaspour, 2014) provides the user the ability to calibrate with respect to more than one criteria while using manual and automated procedures for doing so.

In SWAT-CUP, all SWAT parameters can be included in the calibration process, including all water quality, crop, management and weather generator parameters. SWAT-CUP provides a decision-making framework using both manual and automatic calibration and incorporates sensitivity and uncertainty analysis. Users can manually adjust parameters and ranges between each iteration run and can also use output from sensitivity and uncertainty analysis to provide statistics for goodness of fit. This user interaction in the manual component forces users to obtain a better understanding of the overall hydrologic processes and of parameter sensitivity (Arnold et al., 2012).

The SUFI-2 routine starts by obtaining the objective function selected by the user. SUFI-2 can currently handle different objective functions (two types of root mean square error, Chi square, Nasch-Sutcliffe, R^2, and bR^2). We will be using the Nasch-Sutcliffe objective function defined in terms of discharge and TP. These objective functions will be defined and discussed in the calibration section of the methodology. The optimization routine is initially based on obtaining the parameter combination that minimizes the objective function (g). Parameter ranges that are as large as possible yet physically meaningful are established by the user. Next SUFI-2 uses Latin hypercube sampling (equivalent to Monte-Carlo Simulation) to generate *n* parameter combinations where each parameter oscillates within general user defined ranges. Then, in each round, previous parameter ranges are updated by calculating the sensitivity matrix (2.14), followed by the calculation of the covariance matrix (2.15), the estimated standard deviation (2.16) and the 95% confidence intervals of the parameters (2.17 & 2.18). Then the range is updated leaving out 5% percent of the very bad simulations, using equations (2.18) and (2.19), producing narrower parameter ranges for subsequent simulations and always centering on the best estimates (Abbaspour, 2014).

$$J_{ij} = \frac{\Delta g_i}{\Delta b_j} \tag{2.14}$$

Where: J_{ij} is the sensitivity matrix, i is the number of rows in the sensitivity matrix (equal to all possible combinations of two simulations), j is the number of parameters (also columns in the matrix), g is the objective function and b_j is the parameter j.

$$C = S_g^2 (J^T J)^{-1} \tag{2.15}$$

Where: C is the covariance matrix, S_g^2 is the variance of the objective function values resulting from n runs and J^T is the matrix transpose of J.

$$s_j = \sqrt{C_{jj}} \tag{2.16}$$

Where: s_j is the estimated standard deviation of C_{jj} which is the diagonal term of the covariance matrix.

$$b_{j,lower} = b_j^* - t_{v,0.025} s_j \tag{2.17}$$

$$b_{j,lupper} = b_j^* + t_{v,0.025} s_j \tag{2.18}$$

Where: $t_{v,0.025}$ is the t distribution value of v degrees of freedom (v = n-m) to the 2.5% and 97.5% values of the cumulative distribution of the output variable (b_j), b_j* are the parameters that returned the best objective function value and $b_{j,lower,upper}$ are the 95% cofindence intervals of the parameters.

$$b'_{j,min} = b_{j,lower} - MAX\left(\frac{(b_{j,lower} - b_{j,min})}{2}, \frac{(b_{j,max} - b_{j,upper})}{2}\right) \tag{2.19}$$

$$b'_{j,max} = b_{j,upper} + MAX\left(\frac{(b_{j,lower} - b_{j,min})}{2}, \frac{(b_{j,max} - b_{j,upper})}{2}\right) \quad (2.20)$$

Where: $b'_{j,min,max}$ indicates updated values a define the updated parameter range.

Global parameter sensitivity is calculated by a multiple regression system, see equation (2.21) which regresses the Latin hyper cube generated parameters against the objective function values. Then a *t test* is used to identify the significance of each parameter where the higher the absolute value the higher the sensitivity of the objective function to a certain parameter. The *t test* is defined as the probability of difference between two samples, in this case, the parameters generated by the optimization routine and the values of the objective function. The sensitivities given by the t-test of the multiple regression system regression are estimates of the average changes in the objective function resulting from changes in each parameter, while all other parameters are changing and due to the fact that is calculated from a linear approximation it only provides partial information on the sensitivity of the objective function to model parameters. Also the range of each parameter is changing along the optimization routine and since the t test depends on the deviation of the parameter the ranking of sensitive parameters may change in every iteration (Abbaspour, 2014). The p-value, which ranges from 0 to 1, is used to identify the significance of the sensitivity determined by the *t-test* and is defined as the level of marginal significance to null a hypothesis. If a high p-value (close to 1) is obtained this means the hypothesis should be null. In the other hand a smaller p value (close to 0) means the hypothesis has more probability of being correct and should be accepted.

$$g = \alpha + \sum_{i=1}^{m} \beta_i b_i \quad (2.21)$$

Where: g is the objective function and b_i represents a certain parameter. Alpha and beta are the constants to be determined by the regression.

For calibration the user will identify the most sensible parameters using the indicators discussed above and then minimize the parameter range (using the SUFI-2 routine as explained above) as much as possible to obtain the range of values for the identified variables that will produce the best possible value of the objective function. Validation consists on running the simulation for a different time period than the one used for calibration and confirming that an acceptable value of the objective function is generated.

3. Study Area

The study area covers two small watersheds located in central southwest Puerto Rico with reduced anthropogenic impact at least during the last 50 years. The Cupeyes River watershed has been chosen as the historical tropical forest watershed and is located in the southwestern region of the island at the Maricao Forest Reserve (Bosque del Estado) within the Municipalities of Sabana Grande and Maricao (Figure 3.1 left). This watershed has historically remained under forest cover for more than a century (Martinez, et al., 2010), it has center geographic coordinates at 18º06’38”N, 66º59’11”W and a catchment area of 4.81 km². For the secondary forest the Bosque Olimpia watershed in Adjuntas with center coordinates at 18º08‘‘15”N, 66º42‘‘41”W and a catchment area of 1.09 km² has been chosen (Figure 3.1 right). This watershed used to be under intensive sun coffee farming conditions where it produced up to 1,500 hundredweights (quintals) of coffee in 1945 (Vivoni, n.d.). In 1953 management conditions changed and the lands remained under shadow coffee cultivation up to the 1980’s. After this it was abandoned until a local community organization, Casa Pueblo, acquired the land to make it a conservation and educational forest. Forest and groves cover more than 97% of the land use in both watersheds; soil classification in Cupeyes shows saprolite with shallow soil horizons while in Bosque Olimpia the predominant soils are oxisols.

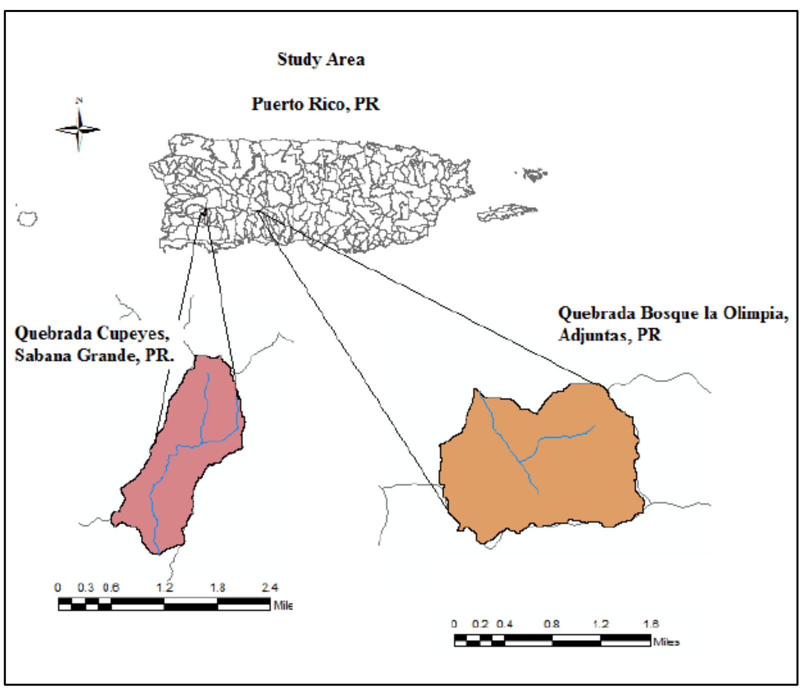

Figure 3. 1 Study Area showing the Cupeyes and La Olimpia watersheds.

3.1. Catchment Delineation

For watershed delineation a combination of tools over a 7 by 7 m resolution digital elevation model (DEM) provided by the Puerto Rico Planning Board (PRPB, 2011) was used. The ARC Info platform by ESRI was used in combination with the hydrology toolbox features within the ArcGIS interphase and ground data taken with Geographic Positioning System (GPS) equipment by Trimble to define watershed outlet and other key features within the watershed. All maps were developed in an Arc INFO platform by ESRI for Geographic Information System (GIS) support.

3.2. GIS Coverage

All GIS coverages were developed from existing geographic databases available in the Office of Management and Budget (OMB) of the Government of Puerto Rico, the U.S. Geological Survey (USGS) and the Planning Board of Puerto Rico. ArcGIS v 10.2 was used as the preferred platform for coverage development to support hydrologic-hydraulic modeling. Watershed outlets required to define the watershed closure were taken with a Trimble GPS, PRO-XR and a Trimble Geoexplorer XH.

3.3. Land Use Coverage

Land use was cropped from the Puerto Rico GAP Analysis Project (PRGAP, 2006), which uses the Natural Resources Conservation Service (NRCS) classification system to interpret and classify 2006 Landsat TM imagery. Three main classes were identified in these forested watersheds (Table 3.1; Figures 3.2 and 3.3):

1. Forest and Groves
2. Low density urban development
3. Grasses and Shrubs

Table 3. 1 Land use distribution in the study area, taken from PRPB (2011).

Land Use Class	**Cupeyes**		**Bosque Olimpia**	
	Area (ha)	**(%)**	**Area (ha)**	**(%)**
Forests and Groves	464.936	97.8	104.864	97.2
Low density urban development	2.816	0.59	0.0336	0.03
Grasses and Shrubs	7.52	1.58	2.972	2.75

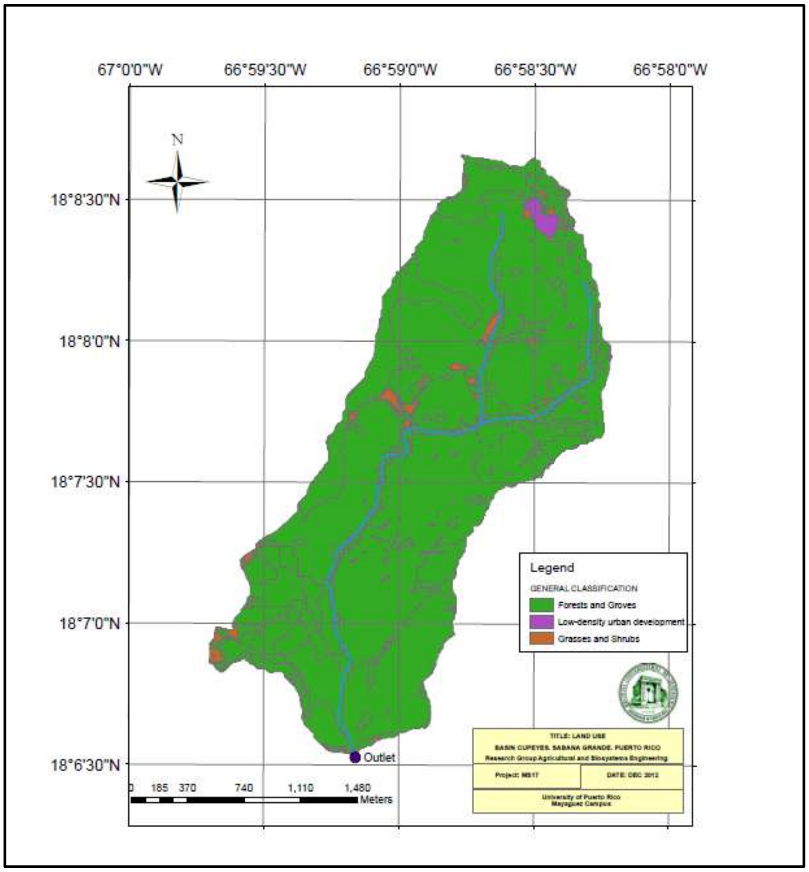

Figure 3. 2 Cupeyes land use coverage, PRPB (2011)

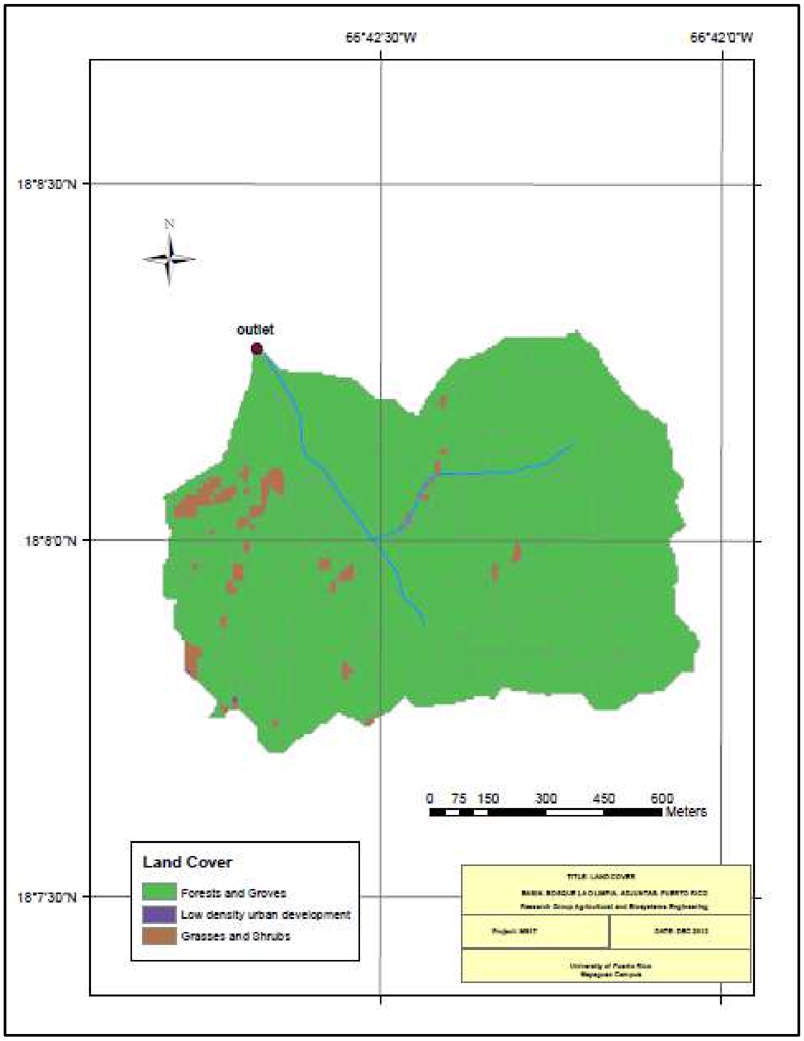

Figure 3. 3 Land use map for Bosque Olimpia watershed, PRPB (2011)

3.4. Soil Coverages

Soil series and soil mapping units for both watersheds in Tables 3.2 and 3.3 were taken from digital soil survey by the NRCS (2010). Figures 3.4 and 3.5 show maps of the soil series within each watershed.

Table 3. 2 Soil mapping unit and hydrologic soil group (HSG) in Cupeyes watershed.

Soil Mapping Unit	HSG	Area (ha)	%
CbF2	D	23.28	4.90
MuE2	D	14.16	2.98
NcD2	C	20.82	4.38
RsD2	C	16.54	3.48
So	D	400.50	84.26

Table 3. 3 Soil mapping units and hydrologic soil group (HSG) in BO watershed.

Soil Mapping Unit	HSG	Area (ha)	%
AnF2	B	4.12	9.55
CbF2	D	8.73	20.23
HmF2	D	16.12	37.36
LuE	C	1.53	3.55
LuF	C	8.23	19.07
MkF2	D	4.42	10.24

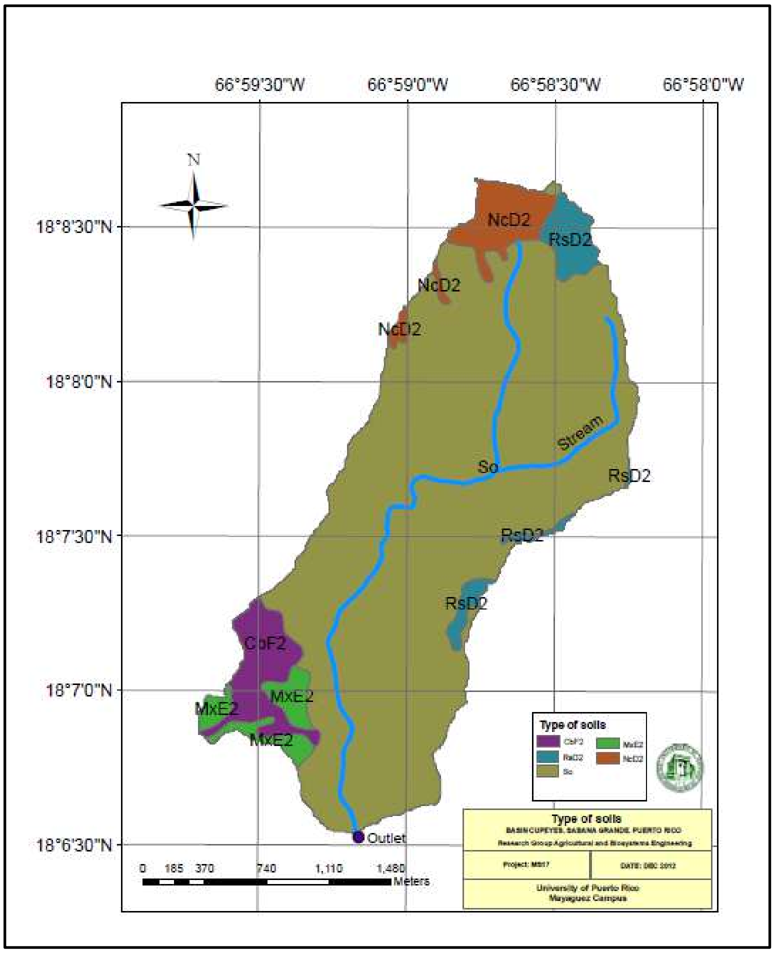

Figure 3. 4 Soil mapping units in Cupeyes watershed (NRCS, 2010).

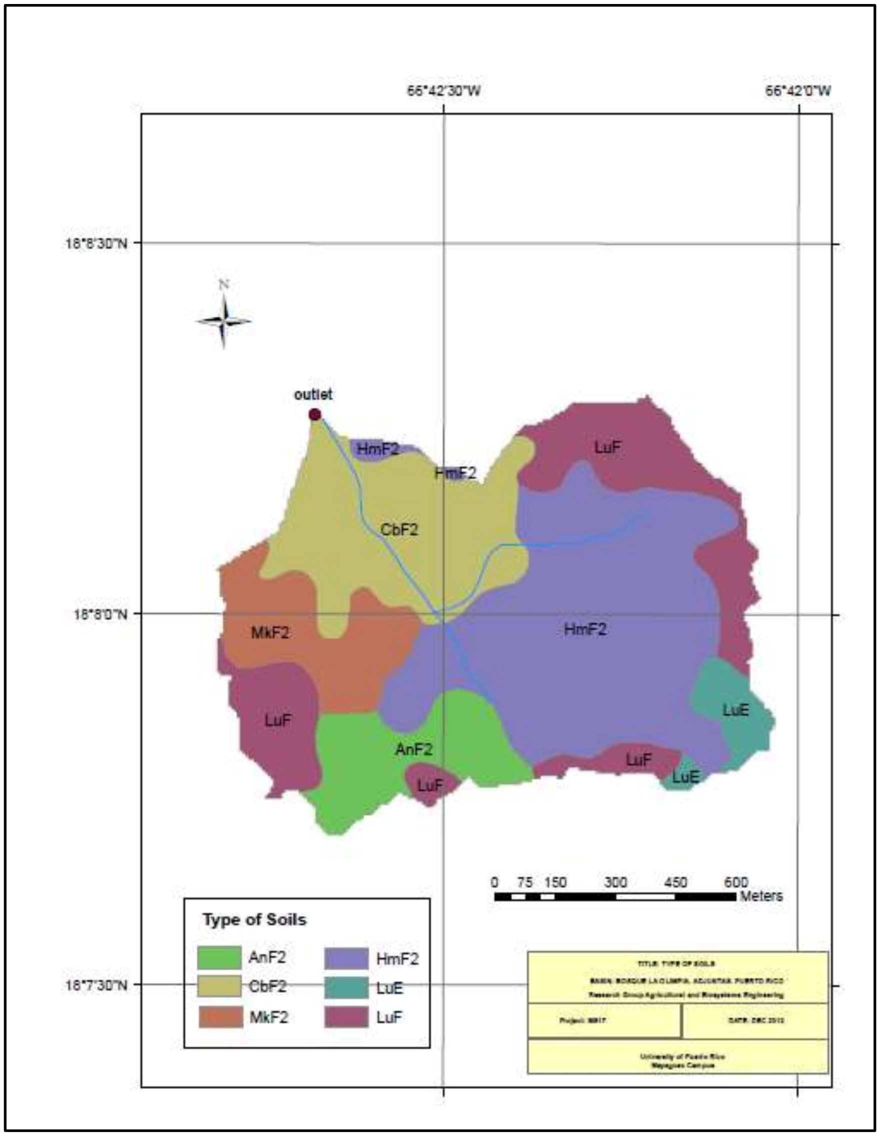

Figure 3. 5 Soil mapping units in Bosque Olimpia watershed (NRCS, 2010).

4. Methodology

4.1. Field Instrumentation

Storm event monitoring stations were installed at the outlet of each watershed and programmed in order to monitor storm events by taking samples at predetermined time lengths along a given storm event. The temporal sampling distribution allows for a proper representation of suspended sediment and nutrient concentrations of the sampled event. Pressure transducers were installed at the same cross section of the monitoring station to monitor water depth continuously, this will allow for the calculation of hydrologic discharge data for each watershed. Using these data, nutrient (TP and TN) loads for storm events were calculated by integrating the runoff hydrograph generated by the storm event and the product with the species concentration. Rain gages were installed at the upper and lower sections of each watershed in order to monitor precipitation, at least four years of precipitation data for each watershed is available. The data collected will be used to run the models for short-term simulation and calibration period.

4.1.1. Location of Storm Event Monitoring Stations

The Cupeyes monitoring station is located at Sabana Grande, Puerto Rico at plane coordinates 140,209.193 easting, 229,438.037 northing and 101.80 m msl (Figure 5.3) (State Plane NAD 1983, Puerto Rico and U.S. Virgin Island FIP 5200). Access to the monitoring location on the river is provided through a farm owned by Mr. Luis Velez. Figure 5.1 shows the view to the watershed from the farm where its predominating land cover can be seen. The Bosque Olimpia monitoring station is located at Adjuntas, Puerto Rico at coordinates 170,646 easting, 233,659 northing and 717 m msl. This is a protected forest managed by Casa Pueblo, an organization dedicated to the conservation of the island's natural resources; Figure 5.2 shows the main entrance to the forest.

Figure 4. 1 Cupeyes watershed view form the farm, which provides access to the WQ monitoring station.

Figure 4. 2 Bosque Olimpia's main entrance, which provides access to the WQ monitoring location.

4.1.2. Water Quality Monitoring Stations

The water quality monitoring station consists of an automatic water sampler (ISCO 3700) coupled to a flow meter (ISCO 4220) and located at a strategic point that was also the watershed outlet. The location of the outlet or WQ Stations (see table 4.1) was deliverable selected to avoid human activity intervention and warrant the security of the equipment. This set up has been used successfully by the study group to monitor water quality parameters during severe storm events (Sotomayor et. al. 2012). When a storm event occurs runoff rushes down the main channel of the watershed flushing sediments and nutrients and increasing water stage at the outlet. The instruments at the sampling station are programmed to begin sampling the runoff hydrograph when a threshold of the water elevation is reached; usually this threshold is set at 6 or 12 inches from normal water elevation at the monitoring site. Sampling of the event will continue as long as the condition is maintained. The instruments record water stage and the timing of all samples taken during the event. For sampling the ISCO station uses a 10-liter bottle and takes composite samples in a single bottle for the entire event.

Table 4. 1 Geographic location of the ISCO Monitoring Stations

	Latitude	Longitude
Bosque Olimpia	18°8'16.179"N	66°42'40.819"W
Cupeyes	18° 6' 31.579" N	66° 59' 9.517" W

Sampling started on December 23, 2010 in Cupeyes river and April 4, 2012 in Bosque Olimpia. The sampler on Cupeyes at first was set to take 24-bottles, 300 mL water samples (one sample per bottle) at non-uniform time intervals: the first five samples were taken at 5 minute intervals, samples from 6-10 at 15 minute intervals, samples from 11-20 at 30 minute intervals and 21-24 at 1 hour intervals. On August 28, 2012, we configured the sampler to take water samples as composite samples using a 10L container, each sample consists of 300-mL. At Bosque Olimpia all samples were taken as composite samples. The flow meter records the time at which the water samples were taken and prints a report out to a paper roll.

Figure 4. 3 The Cupeyes river monitoring station showing suction line and intake basket.

Figure 4. 4 Bosque Olimpia monitoring station taking samples during an intermediate storm event when the sampler was automatically enabled.

Water samples obtained from the ISCO automated water samplers were prepared with 1-3 drops of 0.2% sulfuric acid solution for preservation and sent to the UPR Agricultural Experimental Station Soil and Water Quality Laboratory for analysis. Performed analyses included dissolved and total reactive P (EPA method 365.4), total Kjeldha nitrogen (EPA method 351.2), ammonium (EPA method 350.1), and nitrate (EPA method 353.2). Event and annual loads of nutrients and sediments will be standardized by the precipitation recorded in the watershed for the event (in the case of event load).

4.1.3. Rain Gages

Two Onset RG3 data logging rain gages with a 0.01in precision tipping bucket were installed in each watershed; one rain gage was installed near the outlet in the lower part of the watershed and a second in the upper ridge or near the water divide (see geodetic location of each rain gage in Table 4.2 in State Plane NAD83 coordinates). Upper rain gages were used because in both cases they provided the most continuous, accurate and complete data.

Table 4. 2 Location of rain gages at Cupeyes and Bosque Olimpia watersheds

Rain Gage	Cupeyes			Bosque Olimpia		
	Easting (m)	Northing (m)	Elevation (msl)	Easting (m)	Northing (m)	Elevation (msl)
Low elevation	140,681	229,531	151	170,719	233,701	650
High elevation	142,804	233,947	824	170,940	233,336	868

4.1.4. Pressure Transducers

HOBO-Ware pressure transducers were installed in each river reach under analysis in order to obtain continuous water level data for each watershed which will then be transformed into hydrographs and mean daily flows (MDF). In order to do so, stilling wells were constructed for each pressure transducer (also known as water levels) so readings wouldn't be affected by water surface disruptions. In the Bosque Olimpia watershed the water level was installed 6.5 meters upstream from the sampling station and in Cupeyes the water level was installed in the same cross section as the sampling station. HOBO water levels were processed and corrected for atmospheric pressure using HOBOware PRO software, the same software used to retrieve the water depth data from these instruments. Installation dates were February 12, 2014 for Bosque Olimpia and April 4, 2014 on Cupeyes.

Figure 4. 5 Water level installation on Bosque Olimpia.

4.2. Discharge and Nutrient Load Calculations

By constructing a hydrologic model of each WS using US Army Corps of Engineers HEC-HMS and a hydraulic model of each transect at the monitoring station outlets using US Army Corps of Engineers HEC-RAS a rating (elevation vs. discharge) curve of the monitoring stations' cross sections at each river was constructed. Using results from the hydraulic model at the peak outflows generated from the hydrologic models, rating curves were developed for the Cupeyes and Bosque Olimpia watersheds. These rating curves relate a specific water depth at a given cross section to the runoff generated from the precipitation corresponding to each recurrence in each watershed and were used to convert observed water depth data at the water quality sampling station into discharges for any recorded event. These generated runoff hydrographs are taken as estimates of the observed event hydrographs and converted into volume of water generated by a given storm event by integrating the area under the curve. Hydrologic and Hydraulic models constructed for both watersheds are shown in appendix 1 and 2 respectively. Developed rating curves and their respective depth to discharge equations are shown in appendix 3. Event nutrient load calculation for each sampled storm event and corresponding results are shown in appendix 4. A total of nine events were analyzed for Bosque Olimpia and ten for Cupeyes.

4.2.1. Total Phosphorous Loading Analyses

Storm nutrient loadings analyzed were standardized with antecedent precipitation responsible for the runoff recorded at the watershed outlet by regression analysis. These are shown on figures 4.6 and 4.7 for the Bosque Olimpia and Cupeyes with a coefficient of determination (R^2) was 0.98 and 0.93 for the B.O. and Cupeyes watersheds respectively, these high correlations prove the data is statistically significant. Given these loads are expressed in kilograms per hectare it can be seen that Bosque Olimpia has higher TP loads than Cupeyes during storm events.

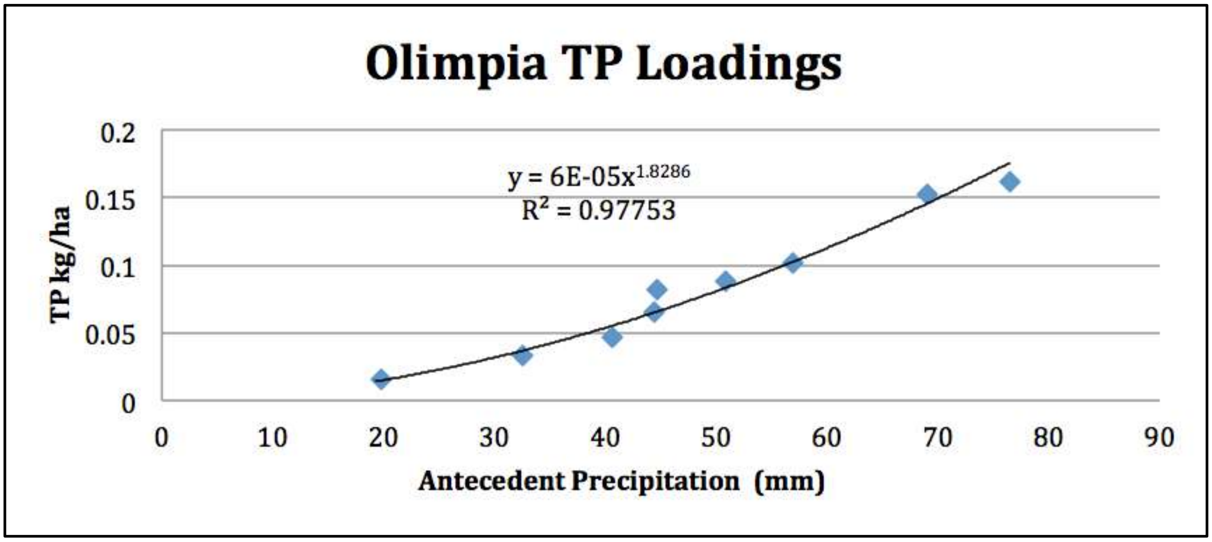

Figure 4. 6 TP storm loadings vs antecedent precipitation at Bosque Olimpia

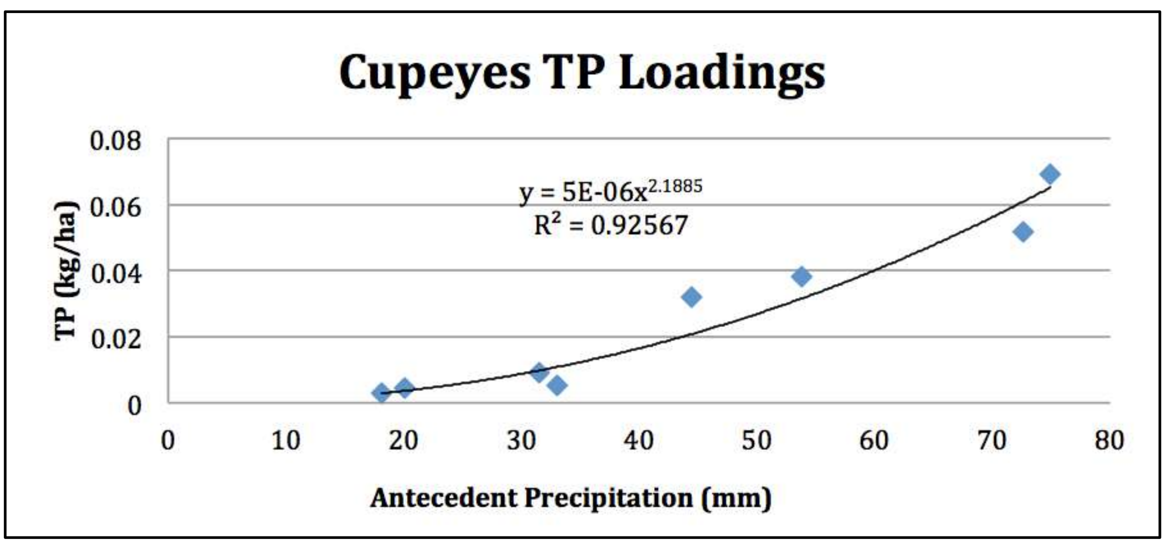

Figure 4. 7 TP storm loadings vs. antecedent precipitation at Cupeyes

The high correlation (R^2>0.90) shown in the regression curves for the power equations of loads vs. antecedent precipitation values allow us to use this method effectively to estimate loads as a function of precipitation. Additionally past studies have used this method to successfully estimate annual sediment and nutrient loads in the Guanica Bay Watershed (Sotomayor et al., 2012). The standardization of nutrient load per storm event was established by using the precipitation data recorded at the rain gages in each watershed corresponding to the sampled event. For this, daily precipitation was evaluated with respect to a determined threshold. This threshold corresponded to the required precipitation rate necessary for runoff to occur in each watershed. Moreover these thresholds will be the criteria that will separate storm loadings from baseflow loadings. In order to establish these, the HEC-HMS models of each watershed (discussed in appendix 1) were executed for different precipitations until a discharge higher than the average baseflow at each watershed was obtained. A threshold of 2.54 mm and 5.08 mm in 30 minutes was obtained for the Bosque Olimpia and Cupeyes watershed respectively. For days where this threshold was not met or where no precipitation was recorded a TP daily loading corresponding to the daily baseflow was assumed. If the threshold was met, then the precipitation was considered “effective precipitation” and considered for the storm loading calculation. Loading calculation procedures used for each watershed are further explained in the following sections.

4.2.2. Bosque la Olimpia Total P Loading Calculations

In order to calculate loads, daily precipitation (mm/day) values and the maximum 30-minute precipitation per day (0.5PCP) were obtained from the upper and lower precipitation gages installed in the B.O. watershed using the HOBOware Pro software. For days where precipitation values were not available from the installed rain gages, the average precipitation from USGS weather stations at Lago Garzas and Lago Adjuntas were used. The location of these weather stations with respect of our study watershed is shown on Appendix 6. For Bosque Olimpia the average daily precipitation (Figure 4.8) for the watershed and average 0.5PCP was used for the calculations. The series has precipitation data from January 1st 2012 to July 31st 2014 and 0.5PCP data from August 29, 2012 to July 31st 2014. Figure 4.9 shows the “effective precipitation” series for the BO watershed, defined as the daily rainfall that meets the established threshold (2.54mm in 30 min) and is therefore considered to produce runoff. Given the absence of 0.5PCP data for the beginning of 2012 (up to august 2012) the threshold used for effective precipitation (during missing data period only) was 5.08 mm/day.

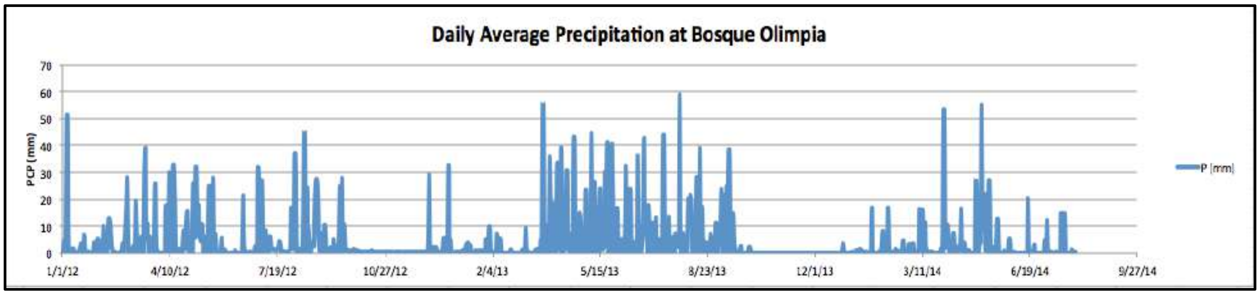

Figure 4. 8 Average daily precipitation retrieved from rain gages at the Bosque Olimpia watershed

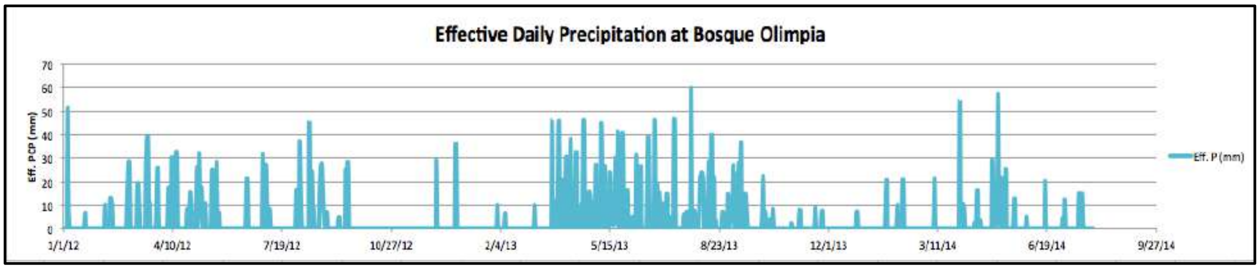

Figure 4. 9 Daily effective precipitation at the Bosque Olimpia watershed

Daily baseflow was computed at B.O. using the average value of measured baseflow data at the WS outlet. Baseflow was calculated following the United States Geological Survey (USGS) methodology (Nolan et al., 2000) by dividing the WS outlet cross section in equally spaced sections, measuring water depth and using a Sontek acoustic doppler velocimeter (ADV) to determine velocity values. See appendix 9 for average baseflow calculation and measured values. To calculate daily baseflow loadings the average baseflow was integrated with respect to time using the trapezoidal rule to obtain the daily volume and multiplying it by the average total phosphorous (TP) concentration obtained from lab analysis of grab samples (see Table 4.3). Baseflow nutrient concentration data is shown in Appendix 7. Average baseflow was verified by the hydrograph baseflow separation method shown in figure 4.10. In order to accurately estimate loadings corresponding to precipitation events equation 4.1 describing the storm TP loading vs antecedent precipitation relationship was used. This equation was obtained by extending the interpolation of the antecedent precipitation vs TP loading data from section 4.2.1 to include an additional data point corresponding to the daily baseflow load and effective precipitation for Bosque Olimpia. A power function regression was used with a correlation factor R^2 of 0.99 as seen in figure 4.11. By incorporating a logical condition (i.e. “IF:THEN statement”) the loading equation was applied only to days with effective precipitation, else the daily baseflow loading (calculated on table 4.5) was applied to the corresponding days. It is noted that a slight underestimation may be present given that baseflow loading was not added to days where the loading equation was applied yet it is considered negligible given that past studies in the island state that approximately 97% of the sediment loadings occur during storm events (Perez et al., 2012). Daily loadings for the Bosque Olimpia watershed are shown in Figure 4.12.

Table 4. 3 Bosque Olimpia daily baseflow TP loading calculation.

Avg. BF phosphorous concentration	0.035	mg/L
Average baseflow	0.029	m3/s
Daily Baseflow volume	2475.131	m3
Daily Baseflow Loading	87623.60	mg/d
Daily Baseflow Loading	0.0876236	kg/d

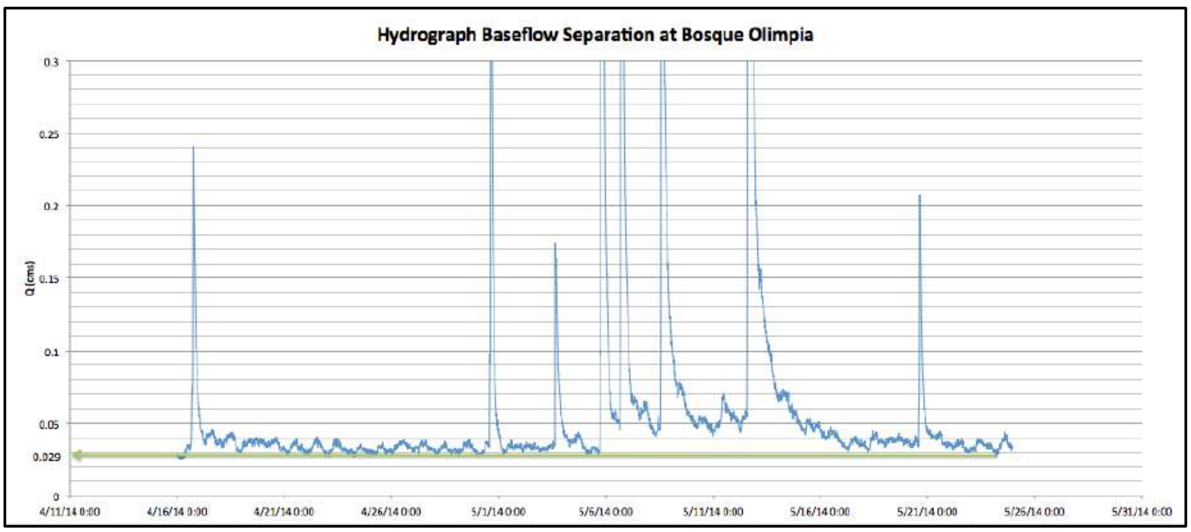

Figure 4. 10 Baseflow separation analysis for Bosque Olimpia stream flow data.

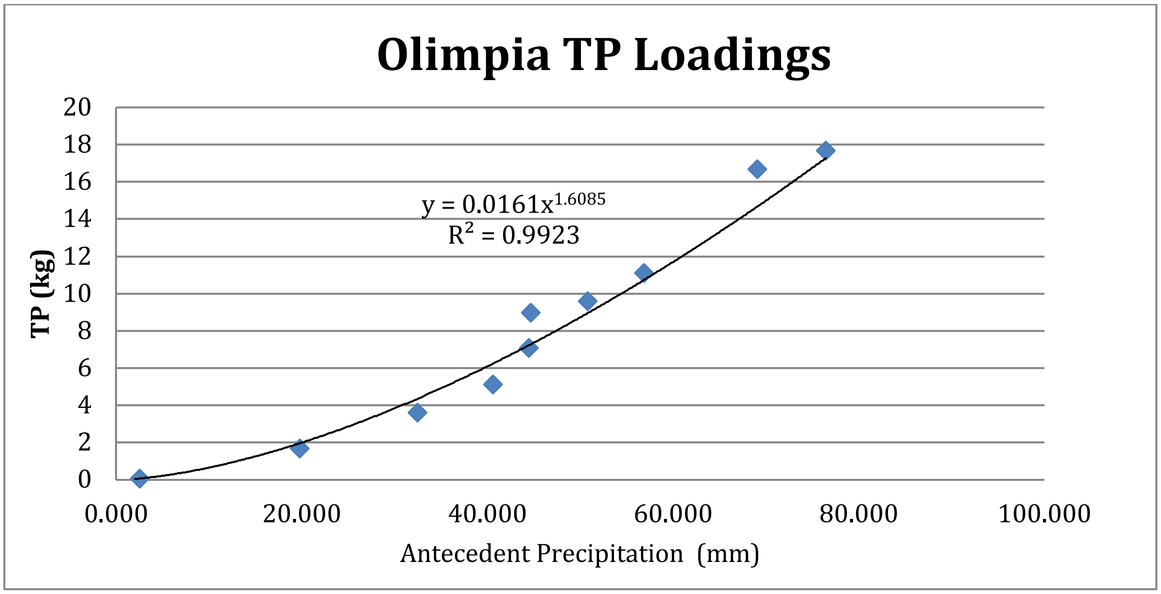

Figure 4. 11 Bosque Olimpia TP loads vs corresponding antecedent precipitation.

$$\text{TP Load (kg/ha)} = 0.0161PCP^{1.6085} \qquad \textbf{(4.1)}$$

Where: PCP is the effective daily precipitation in millimeters.

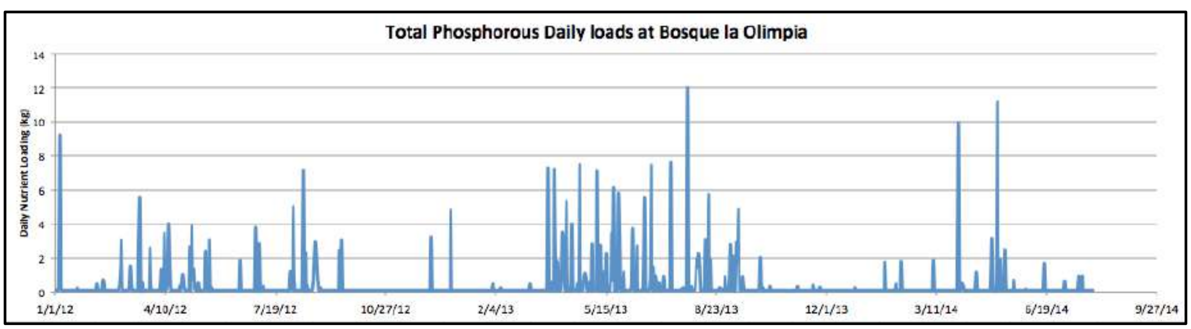

Figure 4. 12 Daily phosphorous loadings from the Bosque Olimpia watershed under study.

4.2.3. Cupeyes River Total P Loading Calculation

Cupeyes loadings were calculated the same way as loads for Bosque Olimpia watershed. Daily precipitation and effective daily precipitation (as defined on section 4.2.1) for Cupeyes watershed are shown in Figures 4.13 and 4.14, respectively. When precipitation data was not available from the installed rain gages data from rain gage at the DRNA Maricao Fish hatchery was used (see location on Appendix section 6). Specifically, data from this rain gage was used from January 1st to April 23, 2012 however, no precipitation data was available at these rain gages from 8/28/2012 to 10/31/2012.

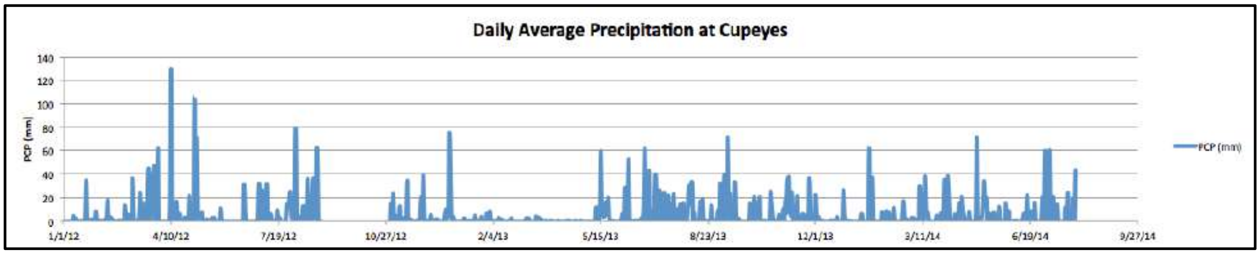

Figure 4. 13 Average daily precipitation in Cupeyes watershed.

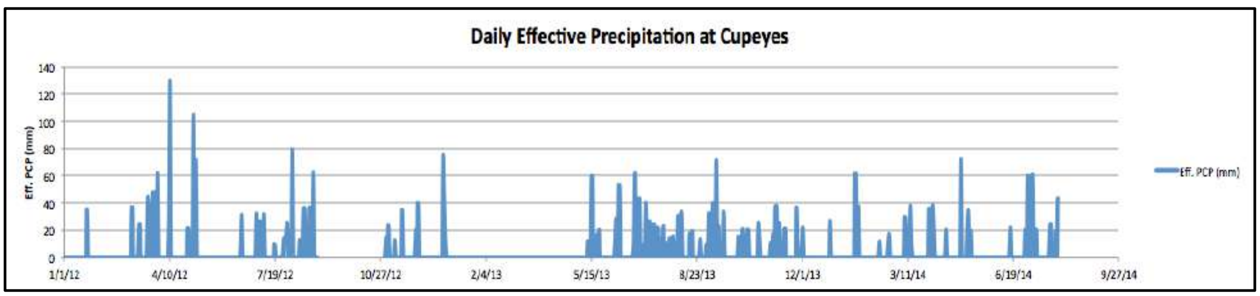

Figure 4. 14 Average daily effective precipitation at the Cupeyes river watershed.

Daily baseflow loading was calculated by integrating the average measured baseflow for a day and multiplying it by the average TP baseflow concentration; table 4.16 shows corresponding values and results. Average baseflow was obtained from measured baseflow and confirmed using the Cupeyes storm hydrograph separation method shown in Figure 4.29, due to its high variability an average of 0.04 m^3/s was used. This measurement coincides with the baseflow measured the second day at the cupeyes watershed outlet. Equation 4.7 shows the corresponding TP loading to antecedent precipitation equation used for daily loading calculations and Figure 4.30 shows the corresponding rating curve and power equation fit including its corresponding coefficient of determination of 0.92. Daily loading results for the

Cupeyes watershed are shown graphically in Figure 4.31. Note that loadings corresponding to baseflow are included in this graph.

Table 4. 4 Cupeyes daily baseflow loading calculation.

Baseflow phosphorous concentration	0.003	mg/L
Average baseflow	0.040	m^3/s
Daily Baseflow volume	3,456	m^3
Daily Baseflow Loading	10,368.00	mg/d
Daily Baseflow Loading	0.010368	kg/d

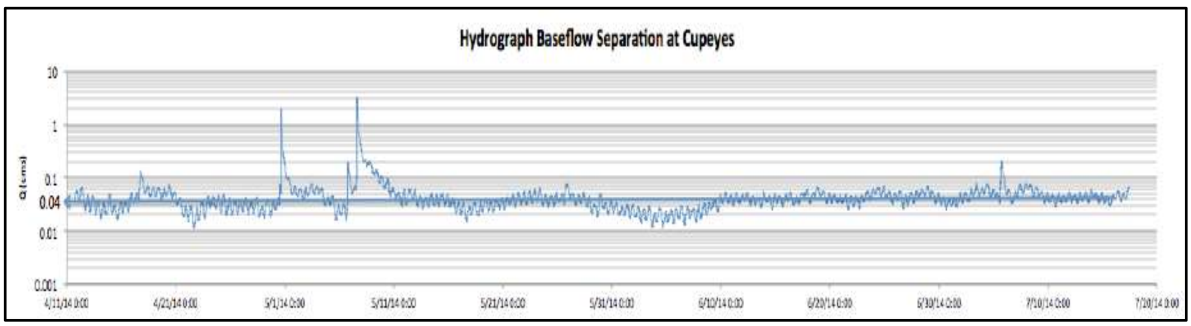

Figure 4. 15 Cupeyes storm hydrograph, average baseflow estimation.

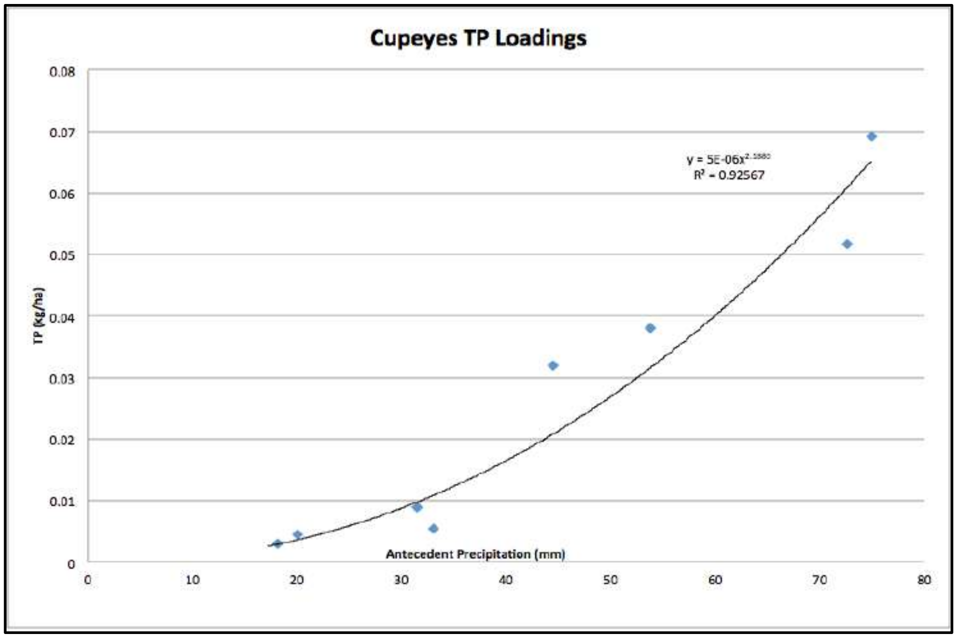

Figure 4. 16 Loading vs antecedent precipitation regression equation.

$$TP\ Load\ \left(\frac{kg}{ha}\right) = 5x10^{-6}PCP^{2.1885} \quad (4.2)$$

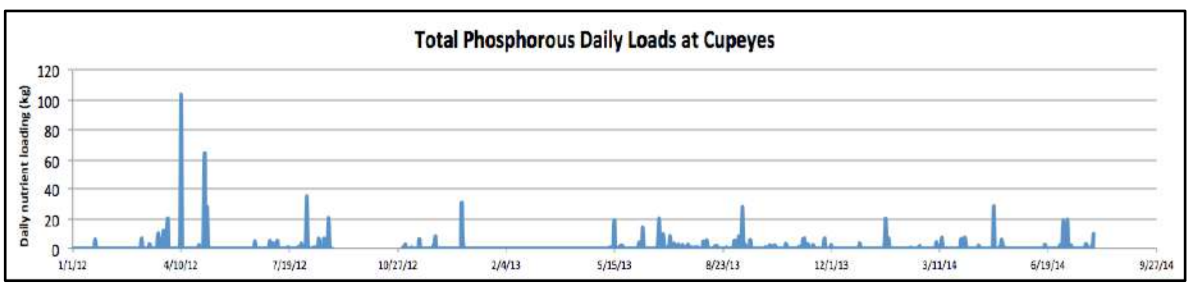

Figure 4. 17 Daily TP loads from the Cupeyes River watershed.

4.3. SWAT Model Construction

Using ArcSWAT (a ArcGIS compatible version of SWAT) each watershed will be delineated and divided into sub basins. The soil, land use and other geomorphologic data will be incorporated into each model by preparing a series of formatted input text files, which include all the necessary parameters for SWAT to simulate the natural processes occurring in the watersheds. The models will then be calibrated and validated using the weather data gathered from the installed weather stations along with the discharge and loading data gathered at the installed monitoring stations in each stream outlet. Instructions provided on the SWAT 2000 Arcview interface manual, the SWAT 2009 Input/Output File Documentation.

4.3.1. Watershed Delineation and Sub-basin Distribution

ArcSWAT uses the digital elevation model (DEM) and geographic location of the outlet in the watershed (pour point) to be modeled to delineate the basin divide. The sub basins, the main reach and sub reaches of the watershed as well as the longest raindrop path from the highest to the lowest point of a sub basin will also be determined using this tool. To do this the program performs various operations, which consists of filling sinks or filling empty spaces across the DEM, establishing flow direction to locate the streams or "low areas" and delineating each of the sub-basins corresponding to the selected watershed outlet. The DEM used has a 7x7 m spatial resolution that was obtained from the PR planning board data available in their web page. The figures 4.18 and 4.19 show the Bosque Olimpia and Cupeyes watershed delineation and the distribution of sub basins as well as the other mentioned parameters. The geographic location in WGS NAD 83 of each outlet is shown in table 4.5.

Table 4. 5 Geographic location the watershed's outlets

	Latitude	Longitude
Bosque Olimpia	18°8'16.179"N	66°42'40.819"W
Cupeyes	18° 6' 31.579" N	66° 59' 9.517" W

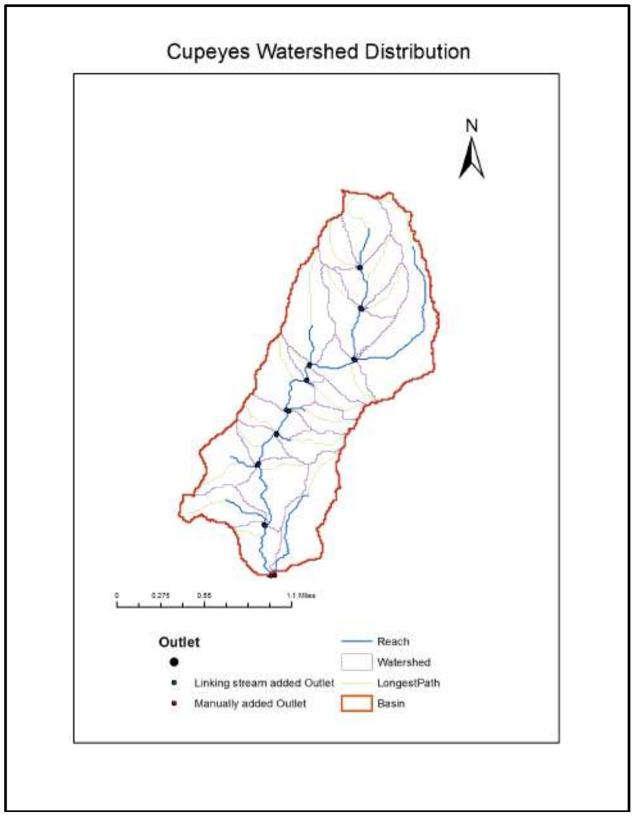

Figure 4. 18 Bosque Olimpia watershed distribution.

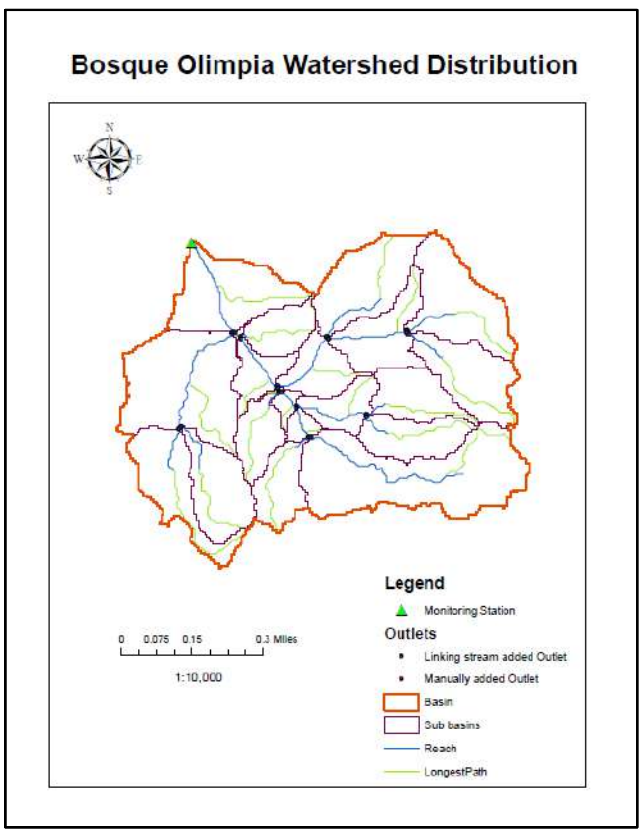

Figure 4. 19 Cupeyes Watershed Delineation

4.3.2. Soil Series Distribution

In order to assign soil series properties to the Bosque Olimpia model a “user soil database” was constructed including all the soil series in the watershed. The parameters used for the model were obtained from the web soil survey (NRCS, 2010). By projecting the delineated watershed into the web tool the necessary parameters for the soil input file (.sol) in the model were obtained and added to the user database by using the ArcSWAT tools. Appendix 13 shows the parameters used for the Bosque Olimpia model construction. Figure 4.20 shows the spatial distribution of each soil series in the watershed.

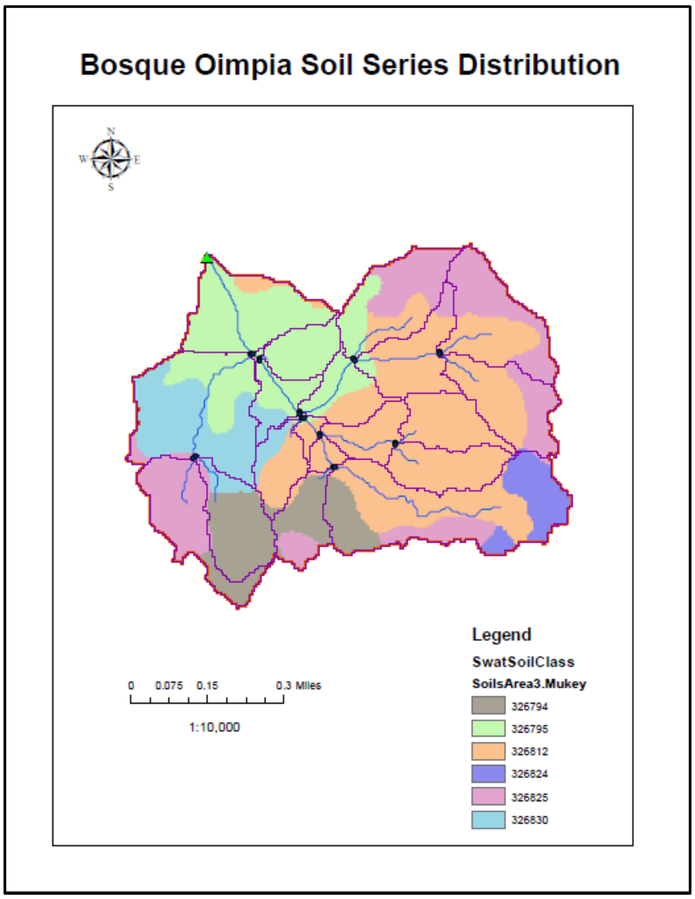

Figure 4. 20 Spatial distribution of soil series in the Bosque Olimpia watershed.

For the Cupeyes watershed the soil data was obtained from the SSURGO database which obtains the data from the National Cooperative Soil Survey (NASIS) the same database that the Web Soil Survey uses and can be downloaded from the SWAT web page. A shapefile containing polygons corresponding to the different soil series and their corresponding map unit key (MUKEY) was downloaded from the NRCS web page for the southwestern region (San German Region). The spatial distribution of the soil series in Cupeyes watershed is shown in Figure 4.21. The SSURGO database contains all the soil parameters necessary for SWAT including the different soil layers and their physical properties. A table with the series name and parameters corresponding to each series in the Cupeyes Watershed is shown in Appendix 13.

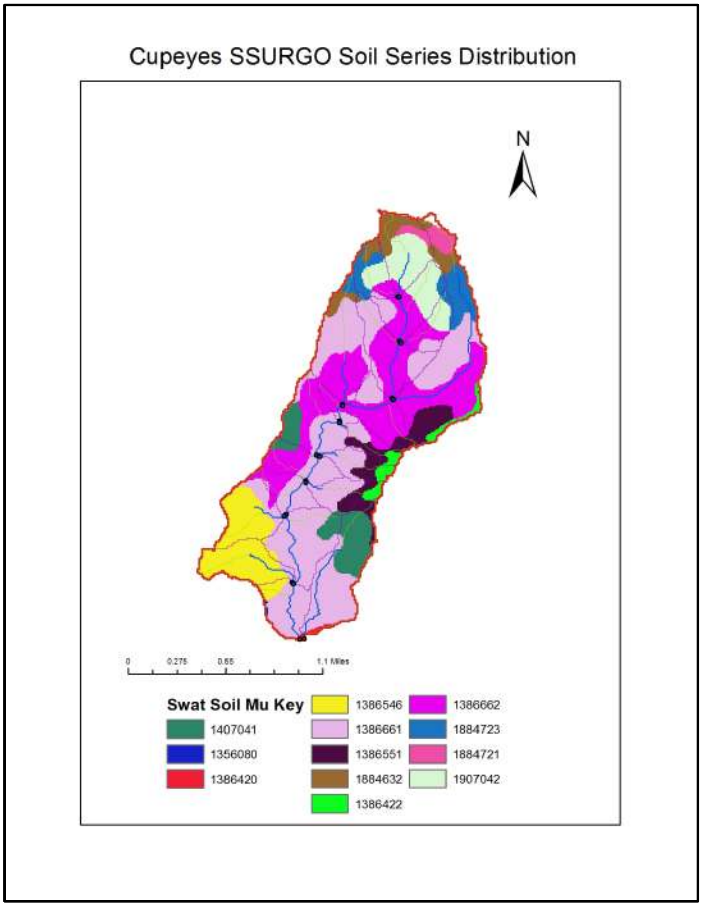

Figure 4. 21 Spatial distribution of soil series in the Cupeyes watershed.

4.3.3. Land Use Distribution

Land uses were assigned by choosing the corresponding land use provided by SWAT. Using the Puerto Rico Gap Analysis Project (Gould et al., 2008) land use cover data the distribution of land uses was summarized into four (4) land use classifications. Table 4.6 shows the PRGAP land use description and the SWAT land cover chosen (in terms of the PRGAP Analysis landcover description). Figure 4.22 and 4.23 show the final distribution of land use assignment in the Bosque Olimpia and Cupeyes watersheds respectively.

Table 4. 6 SWAT land cover classification chosen in terms of the PRGAP land cover descriptions.

Raster Value	Class name (Gould et. al., 2008)	General Class	SWAT Land Cover
14	Mature primary Elfin woodland and secondary montane wet non calcareous evergree cloud forest	Forest and Groves	Forest Mixed (FRST)
15	Mature primary colorado and secondary montane wet non calcareous evergree cloud forest	Forest and Groves	Forest Mixed (FRST)
16	Mature primary sierra palm and secondary montane wet non calcareous evergreen forest	Forest and Groves	Forest Mixed (FRST)
31	Montane wet non-calcareous evergreeen shoubland and woodland	Forest and Groves	Forest Mixed (FRST)
42	Young secondary montane wet non-calcareous evergreen forest	Forest and Groves	Forest Evergreen (FRSE)
49	Moist grasslands and pastures	Grasses and shrubs	Rangeland and bushes (RNGB)
66	Low density urban development	Urban development	Low density urban development (URLD)

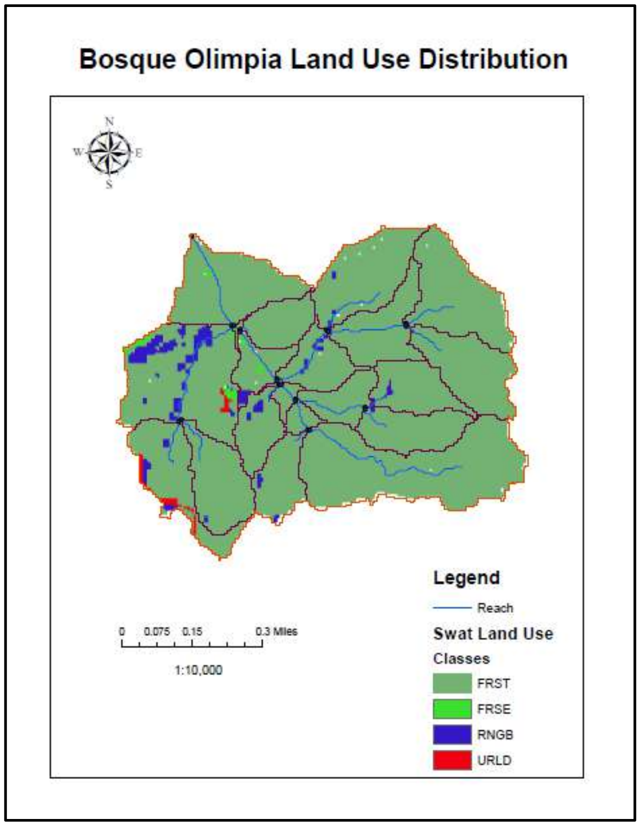

Figure 4. 22 Land cover distribution in the Bosque Olimpia SWAT model.

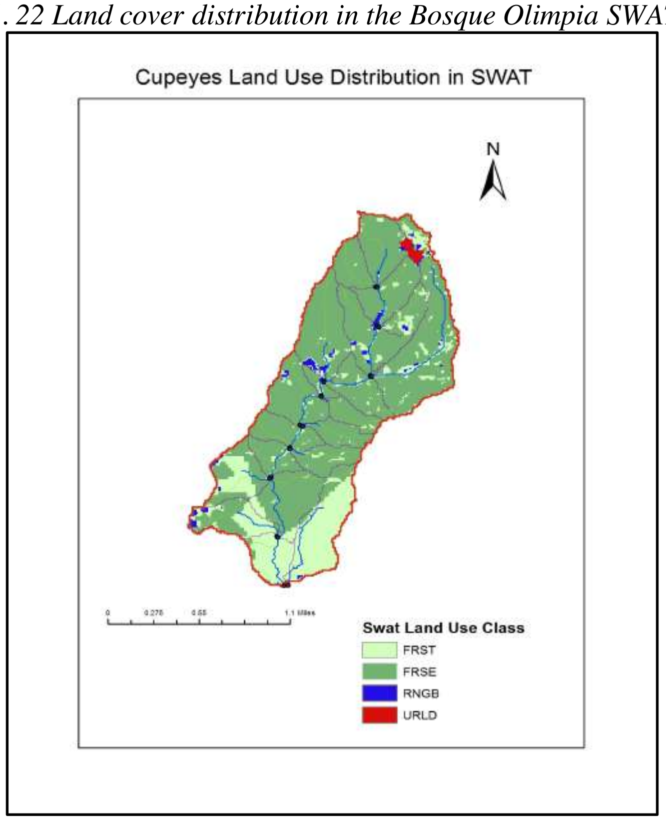

Figure 4. 23 Land cover distribution in the Cupeyes watershed.

4.3.4. Land Slope Distribution

In order to define HRU's the slope in the watershed was divided into three classifications. These were 0-20, 20-40, 40-60, and >60 percent (%) in Bosque Olimpia and 0-12, 12-20, 20-40, 40,60 and >60 in the Cupeyes Watershed. Using the provided "HRU definition tool" in ArcSWAT the DEM data was used to calculate and classify it into these slope % ranges. Figures 4.24 and 4.25 show the slope distribution in Bosque Olimpia and Cupeyes watershed respectively. These values are considered for HRU classification, for instance the values that are above 60% will be considered into their specific slope when the modified universal soil loss equation is applied. This makes the watershed model sensible to slope since areas with different slopes will react different in terms of hydrology, sediment transport, nutrient leaching and or enrichment.

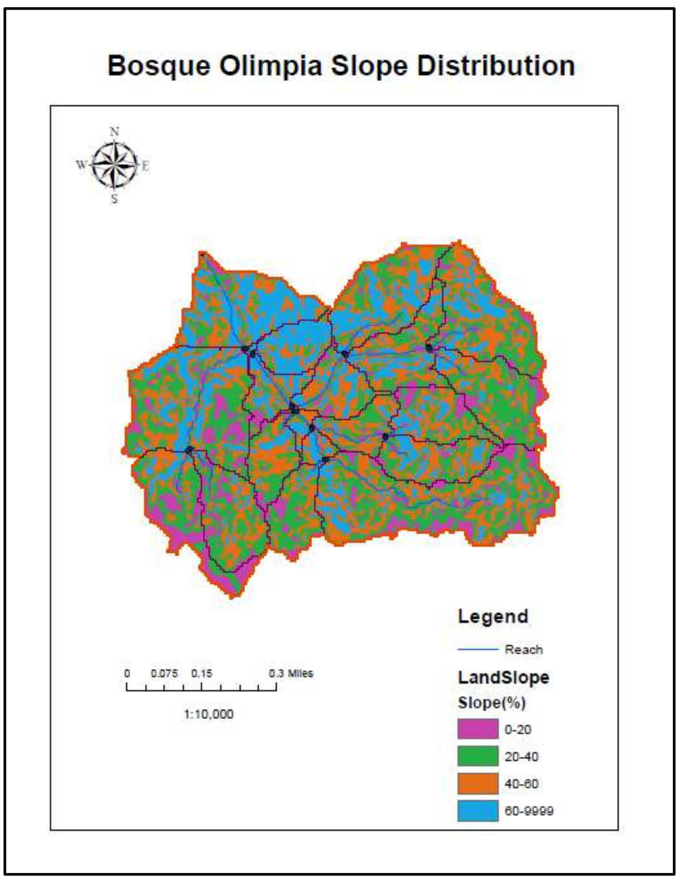

Figure 4. 24 Land slope distribution in the Bosque Olimpia SWAT model.

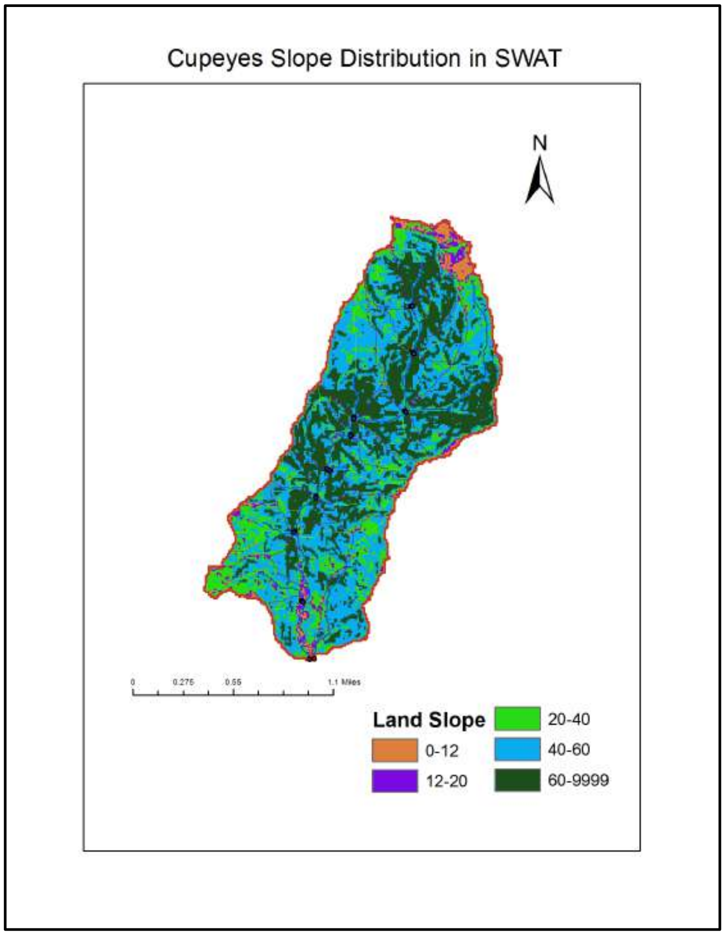

Figure 4. 25 Land slope distribution of the Cupeyes watershed.

4.3.5. HRU Definition and Distribution

After adding the soil, land use and slope data the ArcSWAT tool will divide the watershed into HRU's which will correspond to a certain soil, land use and slope range. The HRU is what makes this model a semi-distributed watershed model since each HRU will respond differently in terms of water yield and sediment exports. The combination of the parameters that create an HRU can be present in more than one sub basin, thus HRUs will be repeated in different sub basins and will respond the same hydrologically except in terms of the hydraulic routing, which will depend on the position of the HRU within the watershed. In the Bosque Olimpia and Cupeyes watersheds each combination of soil, land use and slope within each sub basin will correspond to a specific HRU. Figures 9.26 and 9.27 show the models division of HRUs in each watershed.

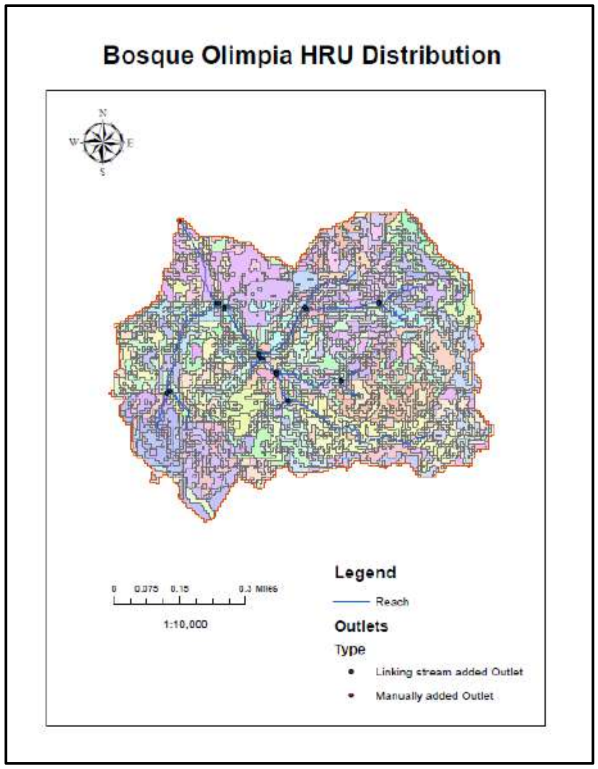

Figure 4. 26 HRU distribution in each of the 21 sub basins in the BO watershed SWAT model with each polygon being a different HRU.

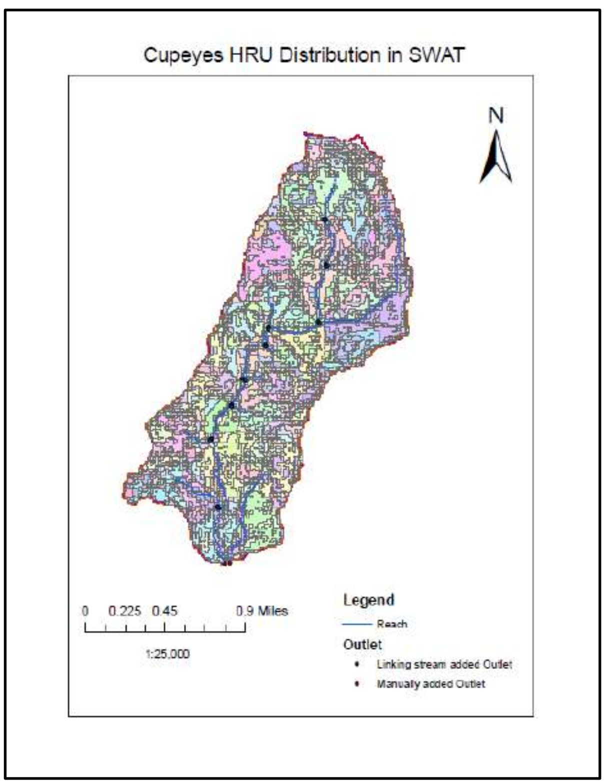

Figure 4. 27 HRU distribution within the 20 sub basins in the Cupeyes watershed SWAT model with each polygon being a different HRU.

4.3.6. Weather Generator Statistics

Spatial weather data statistics must be provided to the weather generator included in the SWAT model in order to perform long term simulations and allow for a necessary warm up period. The model will use the statistical data discussed in this section to simulate the weather parameters that drive the hydrologic cycle. This statistical data should include at least 10 years of continuous meteorological data. Global weather data is available at globalweather.tamu.edu from 1979 to 2014. The available data is obtained from the Climate Forecast System Reanalysis (CFSR), a global meteorological dataset that uses the forecasts generated by the National Centers for Environmental Prediction (NCEP) to produce a 30 km grid with continuous weather data. The CFSR has been effectively proven to render better hydrologic results than models constructed using data from nearby gages, especially when gages are 10 km apart or more than the modeled watershed (Fuka et al., 2014). This data, retrieved and formatted for SWAT from the nearest grid location available, must include at least 10 years of continuous daily maximum and minimum temperature (degC), precipitation (mm), wind (m/s), relative humidity and solar radiation (MJ/m^2). In our case compiling 10 years of this data for nearby gages would have been very time consuming and perhaps impossible, therefore it was decided to use this readily available data.

Weather data from 1979 to 2010 (31 yrs.) at Lares and Jayuya, PR (geographical coordinates shown in tables 4.7 and 4.8) was retrieved from the CFSR and used to calculate the monthly statistical data necessary for the weather generator. The Jayuya and Lares Stations were used for Bosque Olimpia and Cupeyes simulations respectively. Precipitation statistics were calculated using the program PCPstat (Liersch, 2003), a recommended program in the SWAT web page. The maximum 30 minute precipitation for the corresponding month (RAINHHMX) was calculated out of the precipitation data from the installed rain gages within the watershed. Rain YRS refer to the amount of years used to calculate RAINHHMX. Definition of all the monthly statistic variables introduced to the weather generator and shown in table 4.7 and 4.8 can be found in the SWAT User manual (Neitsch et al., 2011).

Table 4. 7 Monthly weather statistics for the SWAT weather generator at Lares, PR.

TITLE	LARES_WEATHER_STATS											
WLAT	18.265	WLON -66.875			RAIN_YRS 2.00			WELEV 394.00m				
Month	1	2	3	4	5	6	7	8	9	10	11	12
TMPMX	27.52	27.66	28.35	28.89	29.03	29.91	29.93	30.20	30.13	29.51	28.42	27.83
TMPMN	21.37	21.22	21.21	21.86	22.99	24.11	24.39	24.40	24.07	23.60	22.96	22.15
TMPSTDMX	01.80	01.87	02.13	01.99	02.14	01.79	01.75	01.86	02.22	02.00	01.89	01.72

TMPSTDMX	01.58	01.50	01.42	01.28	01.08	00.82	00.71	00.82	01.02	01.08	01.23	01.50
PCPMM	45.65	46.45	55.42	117.83	248.81	154.78	168.63	208.30	253.66	227.72	129.32	58.40
PCPSTD	02.65	02.87	02.83	07.64	16.51	05.93	06.18	08.24	13.30	07.95	07.10	02.95
PCPSKW	05.74	03.48	02.79	09.68	09.56	05.95	03.08	08.64	11.01	03.76	07.15	02.93
PR_W1_	00.59	00.51	00.55	00.64	00.55	00.68	00.72	00.90	00.81	00.82	00.70	00.71
PR_W2_	00.80	00.81	00.83	00.87	00.91	00.88	00.89	00.93	00.93	00.94	00.90	00.81
PCPD	24.13	21.47	24.66	26.22	27.91	26.59	27.84	29.72	28.69	29.97	27.22	25.47
RAINHHMX	00.77	00.91	02.20	01.94	01.68	01.98	01.92	01.82	01.70	00.94	00.47	02.11
SOLARAV	16.96	19.43	21.55	23.73	24.45	26.36	26.81	26.39	24.59	21.57	18.15	16.33
DEWPT	19.33	19.00	19.25	20.29	21.64	22.00	22.09	22.60	22.89	22.72	21.44	20.01
WNDAV	02.84	02.83	02.64	02.46	02.45	02.84	03.11	02.83	02.50	02.25	02.65	02.84

Table 4. 8 Monthly weather statistics for the SWAT weather generator at Jayuya, PR.

TITLE	JAYUYA_WEATHER_STATS											
WLAT	18.27	WLNG -66.56				WELEV 531.00			RAIN_YRS 2.00			
Month	1	2	3	4	5	6	7	8	9	10	11	12
TMPMX	26.73	26.92	27.56	28.08	28.19	29.01	28.96	29.22	29.19	28.57	27.53	27.01
TMPMN	20.86	20.69	20.76	21.40	22.50	23.50	23.70	23.76	23.51	23.08	22.37	21.57
TMPSTDMX	01.82	01.89	02.09	01.90	02.11	01.87	01.92	01.99	02.24	01.96	01.92	01.77
TMPSTDMN	01.54	01.56	01.42	01.26	01.06	00.86	00.79	00.83	00.98	01.05	01.23	01.52
PCPMM	71.31	65.53	71.79	142.03	310.55	240.36	289.23	324.54	353.49	308.81	196.53	93.68
PCPSTD	03.51	03.61	03.53	07.76	16.74	08.11	09.40	10.03	14.18	08.61	08.42	04.30
PCPSKW	03.67	02.62	02.46	07.36	07.98	02.78	01.74	02.75	08.09	02.00	04.55	02.20
PR_W1_	00.60	00.57	00.53	00.70	00.52	00.63	00.75	00.76	00.78	00.89	00.64	00.66
PR_W2_	00.85	00.83	00.83	00.88	00.92	00.89	00.91	00.93	00.93	00.94	00.91	00.86
PCPD	25.81	22.75	24.63	26.72	28.28	26.72	28.41	29.72	28.72	30.16	27.63	26.59
RAINHHMX	00.77	00.91	02.20	01.94	01.68	01.98	01.92	01.82	01.70	00.94	00.47	02.11
SOLARAV	16.78	19.16	21.42	23.55	24.49	26.44	26.85	26.42	24.59	21.54	17.98	16.12

DEWPT	19.28	18.92	19.13	20.16	21.61	22.05	22.19	22.65	22.88	22.64	21.40	19.97
WNDAV	02.83	02.83	02.66	02.45	02.43	02.84	03.11	02.81	02.45	02.20	02.56	02.79

4.3.7. Observed Weather Data, Model Setup and First Run

When available, observed precipitation and temperature data was used to run the simulations. This data corresponded to the data collected by the rain gages installed within the watershed and was available from January 2012 to May 2014 with certain gaps as discussed in sections 4.2.2. and 4.2.3. This same period of time was used for calibration and validation purposes. For periods where no data was available, data from the supplementary rain gages was used. Since the model requires a warm up period of 2 to 3 years the model was run from Jan 1, 2009 to Dec 31, 2014 and weather data before Jan 1, 2012 and after July 31, 2014 was simulated by the weather generator. Observed precipitation data used was from Jan 1, 2012 to July 31, 2014 for Bosque Olimpia and from Jan 1, 2012 to May 7, 2014 in Cupeyes. Available temperature data used for both models was obtained from their respective rain gages for the same period that precipitation data was available. Missing temperature data, wind, solar and dew point data were simulated by the weather generator using the statistics discussed in the past section. After setting up all these parameters SWAT was successfully run from 2009 to 2014 with a warm up period of 3 years.

4.4. Model Calibration

In order to calibrate the model, an objective function should be defined, and a physically meaningful global parameter range should be established. The Nasch-Sutcliffe model efficiency coefficient (Eq. 4.3) was used as the objective function in the development of these models due to its common use in hydrologic modeling and that it can easily provide the ability to compare results with other studies. Nash-Sutcliffe efficiencies can range from -∞ to 1 where an efficiency of 0 indicates that the model predictions are as accurate as the mean of the observed data and a value of 1 corresponds to a perfect match of the modeled and observed data (Nash et al., 1970).

$$NS = 1 - \frac{\sum_i (Q_m - Q_s)^2}{\sum_i (Q_{m,i} - \overline{Q}_m)^2} \tag{4.3}$$

where: Qm-observed discharges, $\overline{Q}_m$ -mean of observed samples, Qs-simulated discharges.

The semi-automated program SUFI2 included in the SWAT-CUP package was used for model calibration. Parameters and ranges can be manually adjusted between each iteration run and can also use output from sensitivity and uncertainty analysis to provide statistics for goodness of fit. It is recommended that an initial global analysis for all parameters is done at the beginning of the calibration process. This is done by varying multiple selected parameters within a realistic range established by the user.

Given the need for continuous discharge data an analysis of the data available from the HOBO water level was done. The available data had to be statistically representative, meaning it should include low and high discharge events. As a result the study group decided to calibrate the Bosque Olimpia model the water level data from the HOBO pressure transducers. This data provides the convenience that it is continuous whereas the data from the ISCO stations that was only available when the sampler was activated at high flows. This allowed the calculation of mean daily and monthly flows, which are compatible with the outputs provided by the constructed SWAT models, without having to assume baseflow. For Cupeyes the data from both sources (HOBO pressure transducers and ISCO stations) was analyzed and converted into MDF.

Rating curves were constructed to change the water level data obtained from the HOBO pressure transducers into discharge,. For Bosque Olimpia the cross section where the transducer was installed was upstream from the ISCO station. This cross section was already included into each of the hydraulic models constructed so the water level output from this cross section given the corresponding discharge obtained from the hydrologic models was used to build the rating curve in Figure 4.28. For Cupeyes the water level was installed in the same cross section as the ISCO station. Figures 4.28 and 4.29 shows the rating curve and equations used for the Bosque Olimpia and Cupeyes watersheds respectively. As it can be seen low flows were accounted for by adding a data point corresponding to the measured baseflow and the corresponding talweg depth during baseflow measured in the pressure transducer's cross section. For Cupeyes two baseflows & water depths were included in the rating curve.

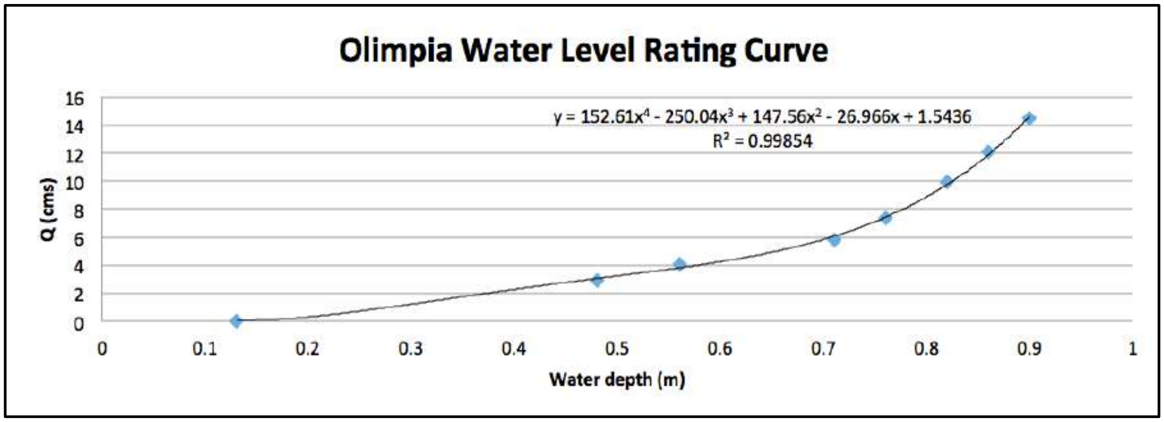

Figure 4. 28 Rating curve (water depth vs discharge) for the water level installed at Bosque Olimpia.

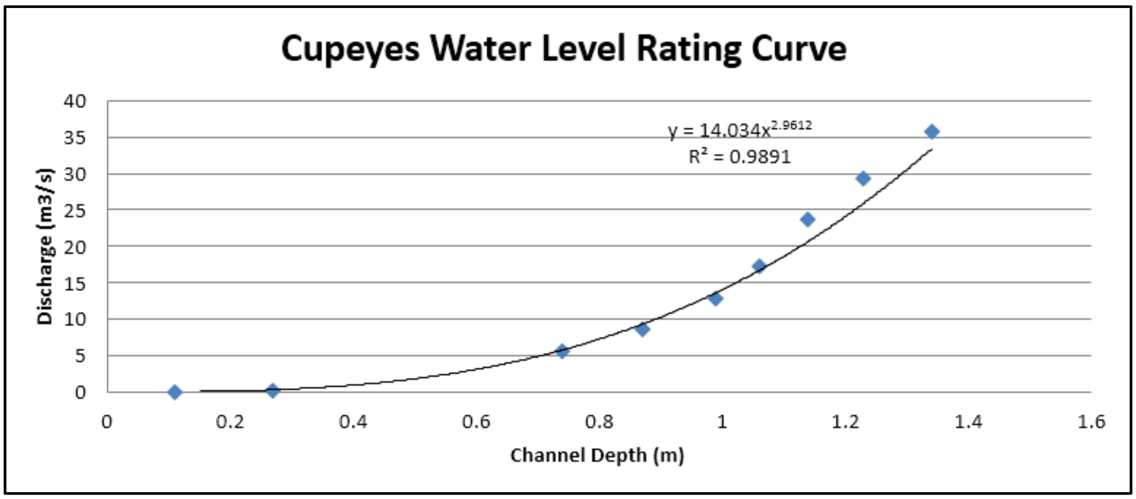

Figure 4. 29 Rating curve (water depth vs discharge) for the water level installed at Cupeyes.

4.4.1. Bosque Olimpia Calibration and Validation

As stated above, for Bosque Olimpia, the calibration period for observed streamflow data from the HOBO water level pressure transducers was used since it provided continuous data including baseflow and storm events. The calibration period was then chosen from February to July 2014 providing 6 months of average monthly flow calculated from the mean daily flow data at the Bosque Olimpia outlet. Figure 4.30 shows mean daily flow data used for the BO watershed model calibration. Monthly flow was used because its more useful to calibrate for a longer time lapse and then if necessary move to MDF for example. Table 4.9 shows calculated average monthly flow values used for calibration.

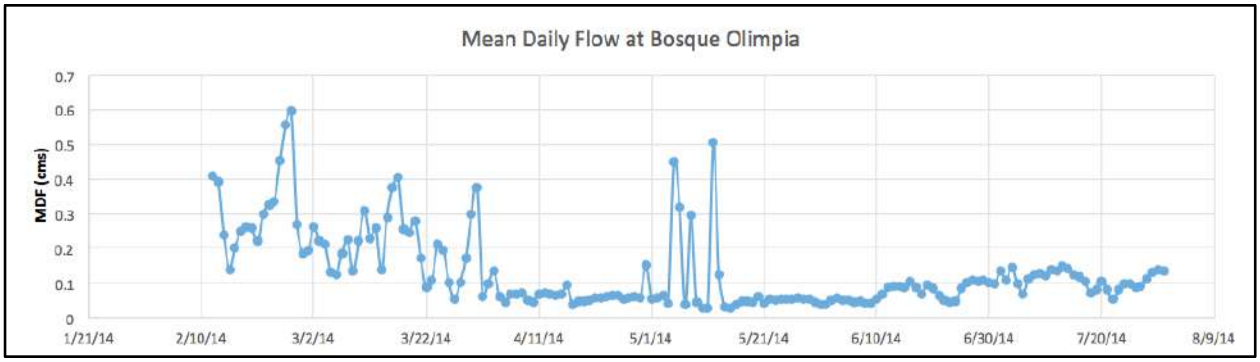

Figure 4. 30 Calculated MDF for Bosque Olimpia.

Table 4. 9 Calculated monthly average of mean daily flow

Bosque Olimpia Discharge Data		
Year	**Month**	**Monthly Avg. of MDF (cms)**
2014	2	0.31748204
2014	3	0.211985657
2014	4	0.066677498
2014	5	0.094041385
2014	6	0.071981032
2014	7	0.109804871

Global sensitivity shows the sensitivity of the output (variance) in terms of the change in variable values while other parameters are also changing. A low P value and a large T-stat value represents higher sensitivity. Global sensitivity was performed for all variables related to discharge where greater sensitivity for CN2 and soil available water capacity was found (see figure 4.31). Table 4.10 shows the parameters considered in the global sensitivity analysis and the variation range where the preceding letter will choose if the routine will multiply the existing value by 1+ the number given (r), add the given value to the existing number (a), or replace the value with the given one (v). In order to avoid losing spatial variability values that changed relative to the actual HRU like the curve number and bulk density were only “multiplied (r) or added (a)” not “replaced (v)”. Also the established initial ranges were chosen to be physically meaningful. The name and description of each of the varied parameters in Table 4.10 can be found in the SWAT Input Output Documentation (Arnold et al., 2011).

Table 4. 10 Parameters used for global sensitivity analysis.

v__GW_REVAP.gw	0.02	0.051449
v__GW_DELAY.gw	0	5
v__ALPHA_BNK.rte	0.4	0.8
v__ALPHA_BF.gw	0.1	0.8
v__GW_DELAY.gw	30	450
v__SOL_AWC(1).sol	0.38	0.62
r__SOL_BD(1).sol	-0.87	0.07
r__SOL_K(1).sol	0.47	0.83
r__CN2.mgt	-0.23	0.97
v__GW_REVAP.gw	0.01	0.051449
v__SHALLST.gw	500	2000
a__SOL_AWC(1).sol	0.5	0.6
v__ESCO.hru	0.9	1
v__GWQMN.gw	0	0.3
v__SOL_Z(1).sol	2000	2000

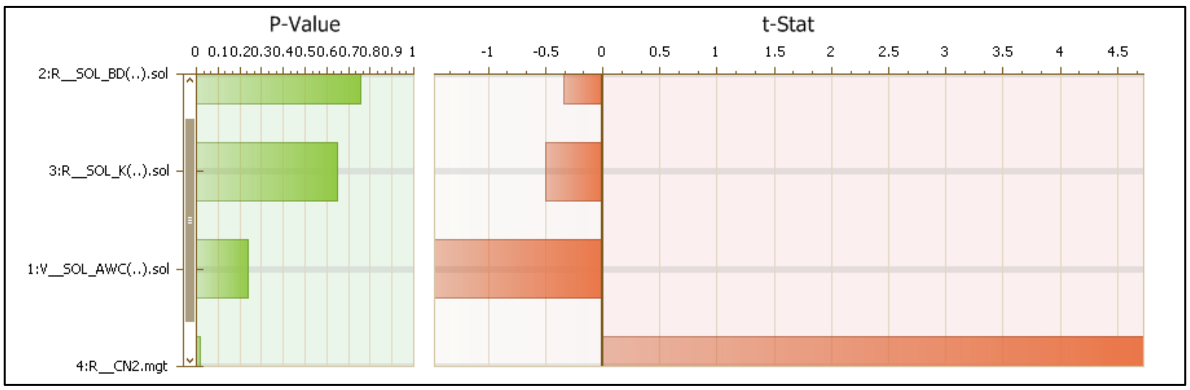

Figure 4. 31 Global sensitivity of the BO SWAT model in terms of monthly discharge.

Then local sensitivity analysis was done to find that the most sensible parameters to monthly discharge were the curve number (CN2), the Layer Saturated Hydraulic Conductivity (SOL_K), the moist bulk density of soil (SOL_BD) and the soil layer available water capacity (SOL_AWC). The model showed the same sensitivity to saturated hydraulic conductivity and CN variations. Figures 4.32 to 4.34 show the local sensitivity (or one at a time analysis) for these parameters, respectively. The simulated monthly flow did not show significant sensitivity for other variables including those pertinent to the base flow discharge. The dotted line represents the observed monthly average flow data.

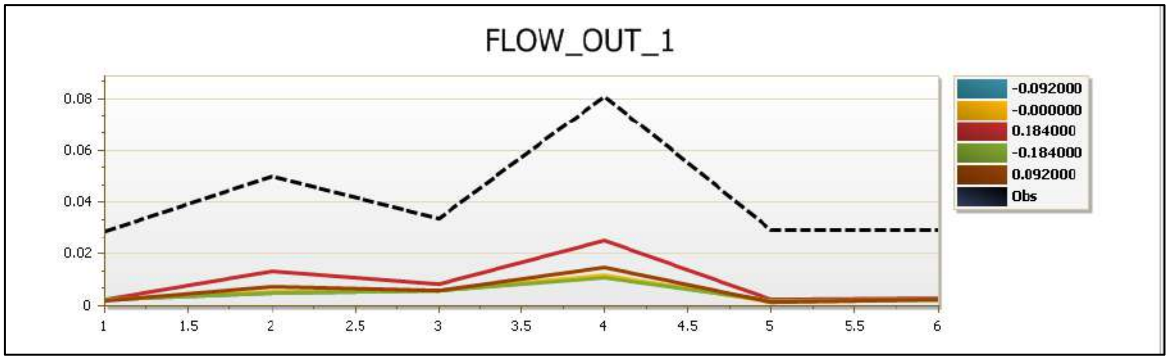

Figure 4. 32 Graph shows response in discharge (m³/s, monthly average of MDF) to different values of CN for the Bosque Olimpia SWAT Model. Note that values correspond to the variation (r) as explained above in this section.

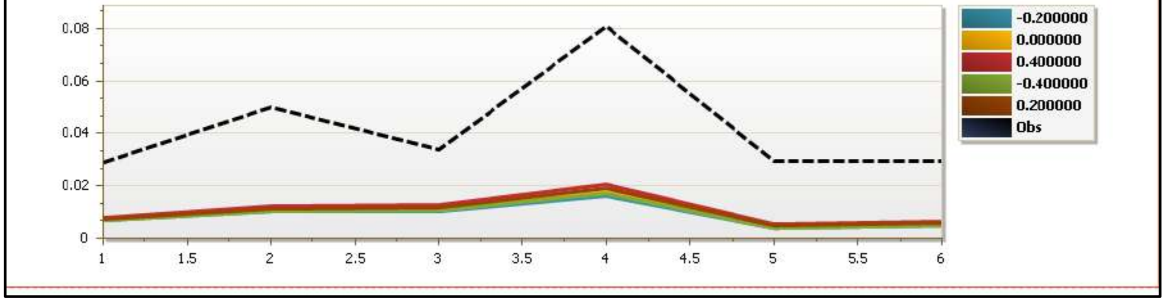

Figure 4. 33 Graph shows response in discharge (m³/s, monthly average of MDF) to different values of bulk density for the Bosque Olimpia SWAT Model. Note that values correspond to the variation (r) as explained above in this section.

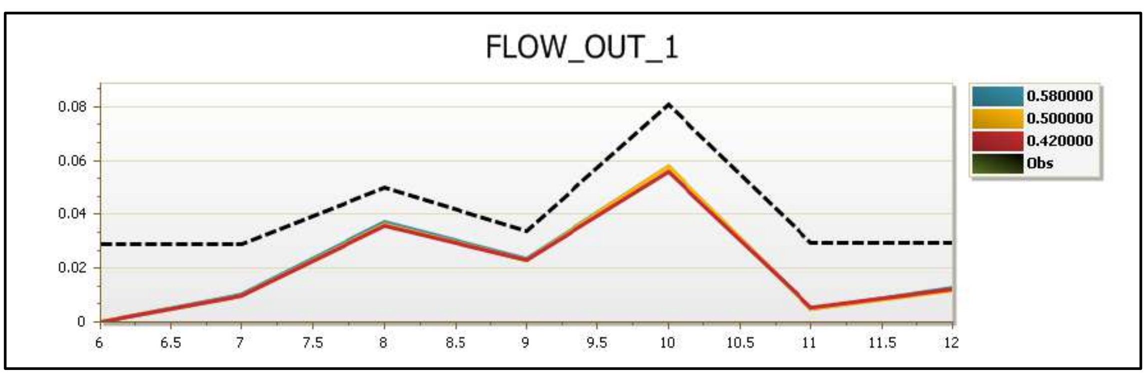

Figure 4. 34 Graph shows response in discharge (m³/s, monthly average of MDF) to different values of soil available water capacity for the Bosque Olimpia SWAT Model. Note that values correspond to the variation (v) as explained above in this section.

Calibration was performed by reducing the physically meaningful range for these sensible variables. To do this the SUFI-2 routine calibration tool was used which, as explained in the literature review, varied the chosen parameters simultaneously and chose the best solution in terms of the objective function (NSE), R-stat and T-stat. The routine will also provide the recommended parameter variation range for the next run thus allowing to reduce the variation ranges as much as possible. The best value for the objective function reached was NSE=0.07 (see Table 4.11) meaning that the average of observed and simulated values is equal, and that model prediction is acceptable. Figure 4.35 shows the simulated (red line) vs the observed (blue line) average monthly discharge values. In the figure it can be seen that the model variability is good and that even when simulation values are lower the average flow within 6 months is similar. The 95PPU can be observed showing the effect of parameterization and optimization.

Monthly total phosphorous loadings were used for model validation using the same period as for discharge calibration to obtain a Nasch-Sutcliffe model efficiency coefficient of NSE=0.63, which indicates good model performance. Figure 4.36 shows that lower loadings were slightly underestimated while higher loadings were over estimated. This, in terms of the 6 month total loading will result in similar loadings. Yet baseflow loadings are under estimated as so is the case in baseflow discharge. This issue is discussed below given it could be largely related to the reliability of the observed data used for calibration. Table 4.11 shows the statistical results including the arithmetic mean and standard deviation of the simulated and observed data, the objective function results (NS) and the coefficient of determination. Calibration was performed for the same period (January to July 2014) as validation, yet the model was validated using TP loadings not discharge.

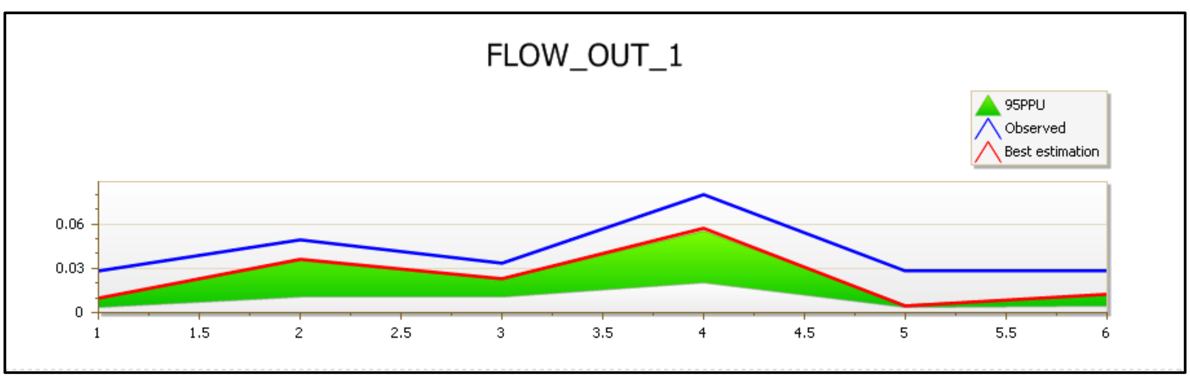

Figure 4. 35 Observed vs simulated monthly discharge values for the Bosque Olimpia SWAT model.

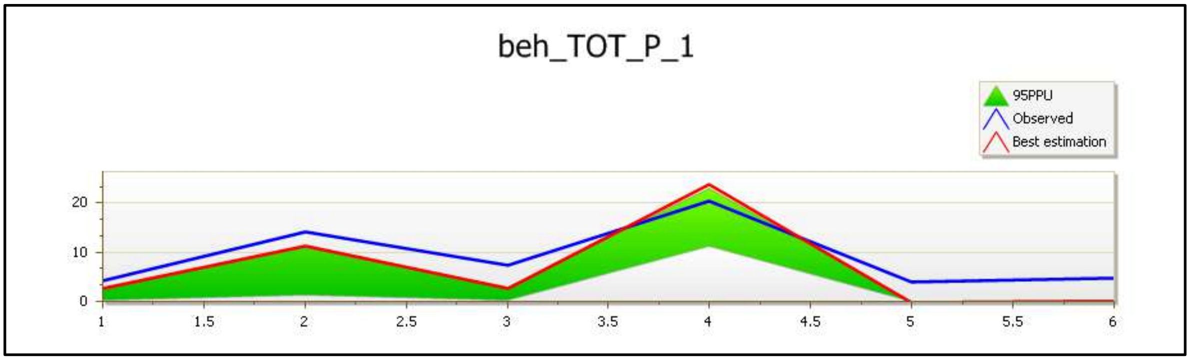

Figure 4. 36 Simulated (red line) vs observed (blue line) monthly total phosphorous loadings for Bosque Olimpia SWAT model.

Table 4. 11 Bosque Olimpia calibration and validation results

	Variable	R2	NS	Mean_sim(Mean_obs)	StdDev_sim(StdDev_obs)
Calibration	FLOW_OUT_1	0.93	0.07	0.02(0.04)	0.02(0.02)
Validation	TOT_P_1	0.96	0.63	6.95(9.36)	8.53(6.07)

4.4.2. Cupeyes Calibration and Validation

For Cupeyes the mean daily flow data was calculated for different periods using the data retrieved from the ISCO sampling station and the HOBO water level. The period used from the ISCO station was from June 5, 2013 to November 7, 2013 and the data used from the HOBO water level was from April 11, 2014 to July 17, 2014. Mean daily flow for each is shown in Figures 4.37 and 4.38. Data from the ISCO station was used for calibration because it provided a longer period of data and was more representative of the climate variability in the area. The monthly averaged flow used for calibration is shown in Table 4.12.

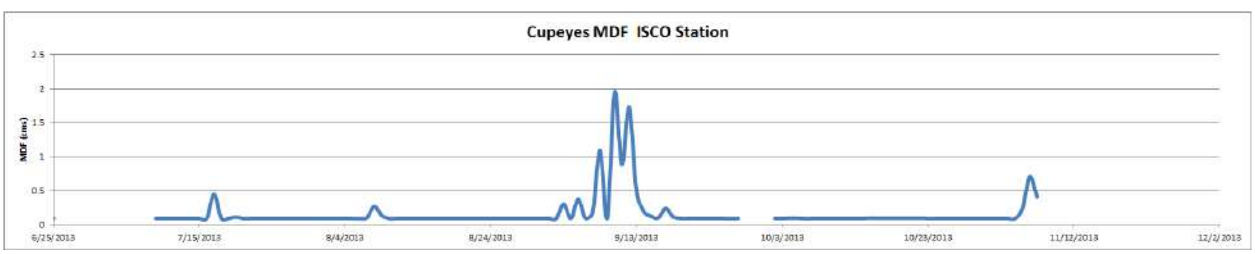

Figure 4. 37 Mean daily flow corresponding to Cupeyes ISCO sampling station.

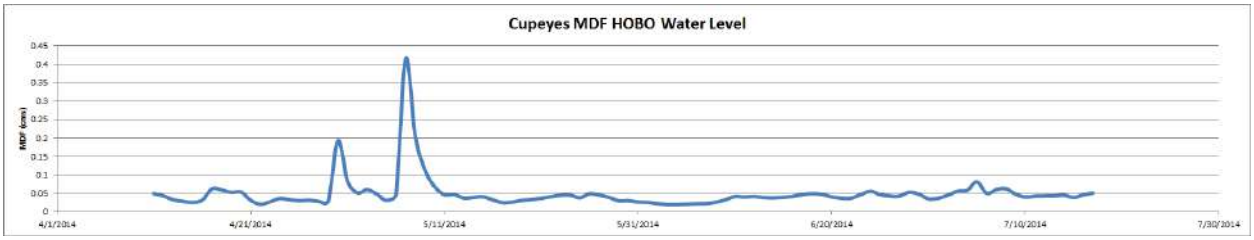

Figure 4. 38 Mean daily flow corresponding to Cupeyes installed water level.

Table 4. 12 Cupeyes observed monthly average of MDF.

Cupeyes Discharge Observed Data		
Year	**Month**	**Monthly Avg. of MDF (cms)**
2013	6	0.090042635
2013	7	0.106383129
2013	8	0.098168549
2013	9	0.334568095
2013	10	0.090944651
2013	11	0.244549067

The Cupeyes watershed was calibrated simultaneously for Discharge and Total Phosphorous (multiparameter). This, according to Abbaspour, 2014 and Naumov, 2005 will result in better calibration results when using SUFI-2. The idea is that the probability of obtaining the best combination of parameters is to have them fluctuating simultaneously in order to obtain results as close as possible to both observed discharge and nutrient loadings. Global sensitivity analysis, or parameterization, was performed to obtain the parameters to which the desired calibration outputs were sensible in the Cupeyes watershed SWAT model. Global sensitivity analysis for discharge is shown in Figure 4.39. Varied parameters are also shown in Figure 4.39. This shows that the most significant parameters when all other parameters are varying are the CN and GW_Delay. As in for the Bosque Olimpia watershed SWAT model, parameters that vary with HRU were adjusted relative to the actual value in order to avoid losing spatial variability.

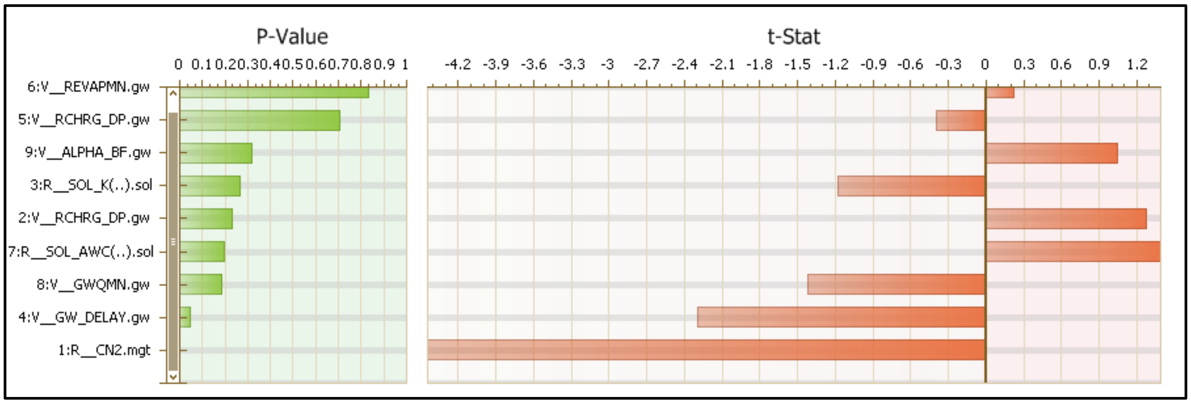

Figure 4. 39 Global sensivity analysis for the Cupeyes watershed model.

Figures 4.40 to 4.44 show the local sensitivity analysis for CN, SOL_K, GW_DELAY, RCHRG_DP and USLE_K. These were the most sensible parameters in the model, other parameters like the phosphorous percolation factor did not affect the output of either discharge and TP loadings. Global sensitivity analysis showed that CN and SOL_K where the most significant for discharge and USLE_K for TP loadings.

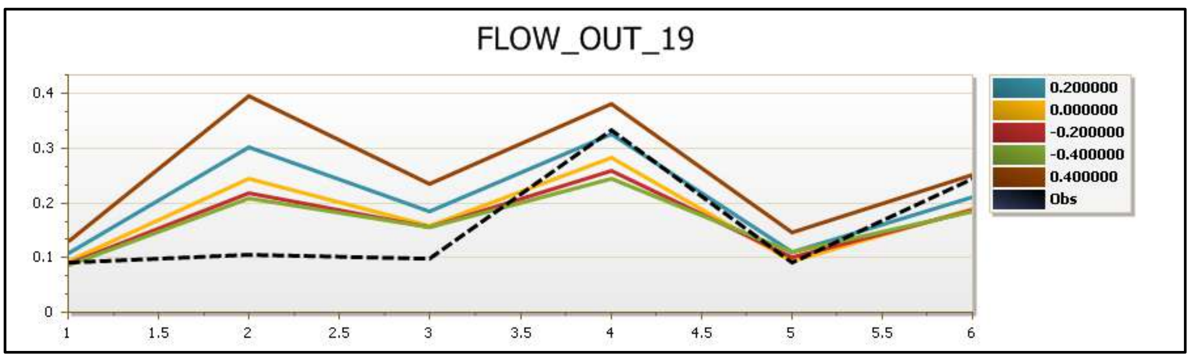

Figure 4. 40 Cupeyes watershed model discharge sensitivity to changes in CN parameter.

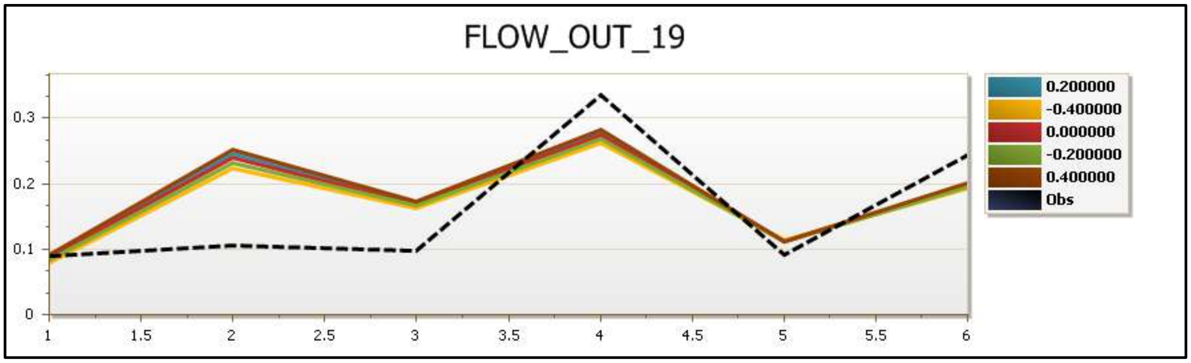

Figure 4. 41 Cupeyes watershed model discharge sensitivity to changes in soil hydraulic conductivity.

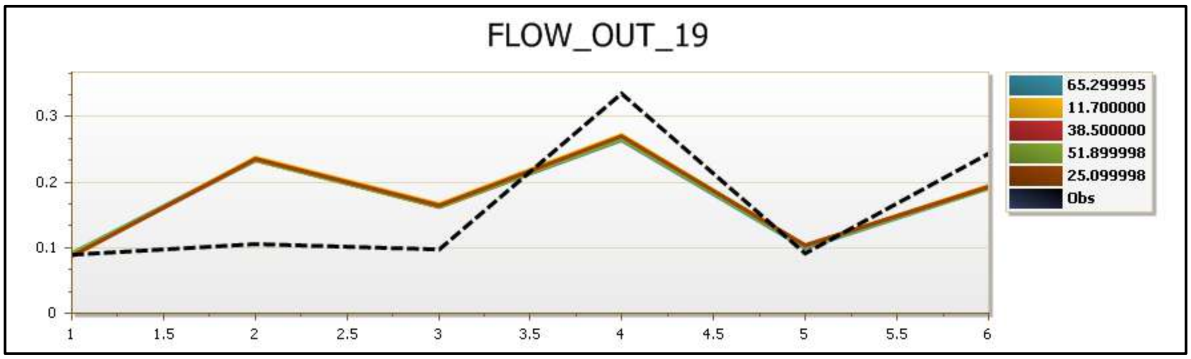

Figure 4. 42 Cupeyes watershed model discharge sensitivity to changes in GW delay.

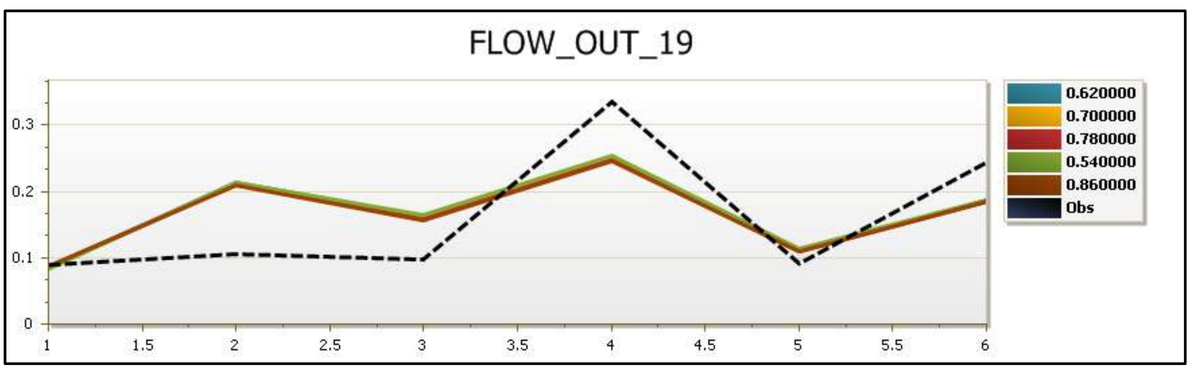

Figure 4. 43 Cupeyes watershed model discharge sensitivity to changes in deep aquifer recharge (RCHG_DEP).

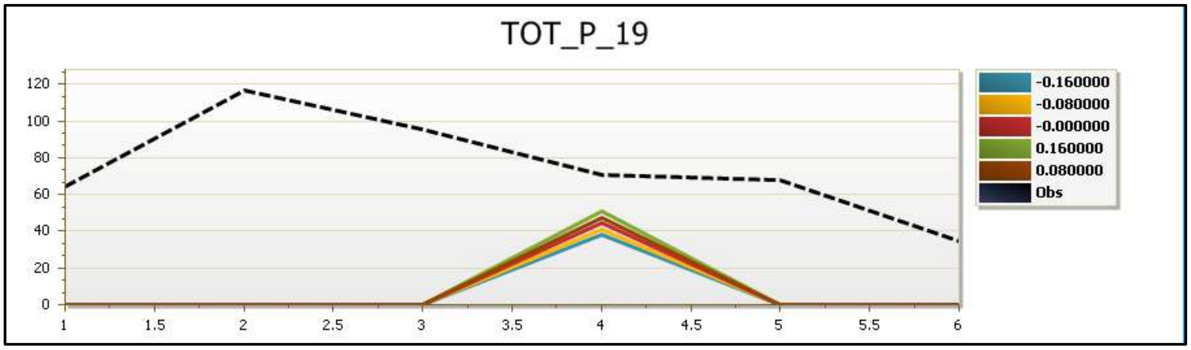

Figure 4. 44 Cupeyes watershed model discharge sensitivity to changes in the USLE_K parameter.

After these parameters were identified calibration was performed using mostly CN and USLE_K since it resulted in better objective function (NS) values. Also these were the most sensible parameters and the observed and simulated average values that resulted of these simulations were better obtaining an objective function value of NS= 0.68. Figures 4.45 and 4.46 show the simulated (red line) and observed (blue line) values of monthly average of MDF in cubic meters per second (cms) and monthly TP loads in (kg) respectively. Average monthly discharges (Figure 4.45) shown correspond to the months of May through November 2013, this period was used for calibration and as stated above it includes TP observed values. Monthly total phosphorous (Figure 4.46) was used for validation and corresponds to January through May 2014. Validation returned a NS=-1.1 where the model seems to be overestimating the loadings in the watershed. The reason to this overestimation could be due to the watershed's hydrogeological characteristics and will be discussed in the following sections.

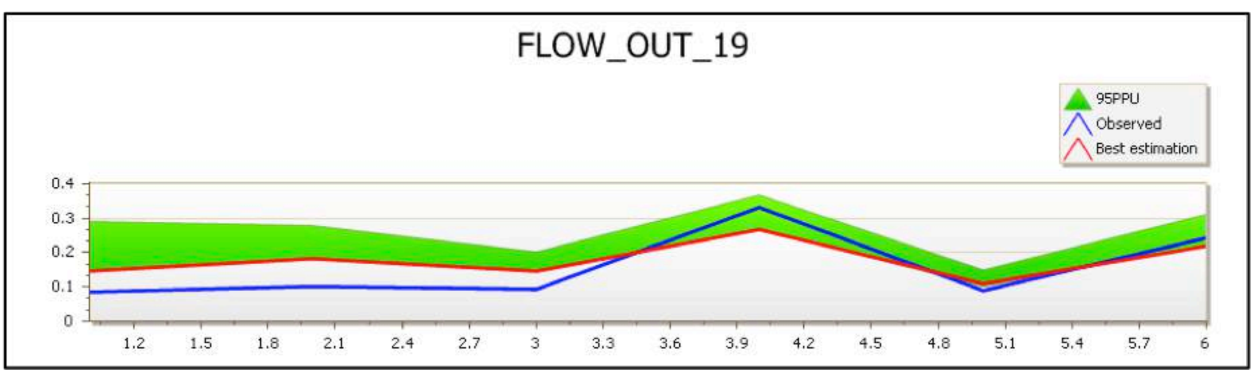

Figure 4. 45 Cupeyes watershed model calibration vertical axis is in average MDF (cms) for the given month.

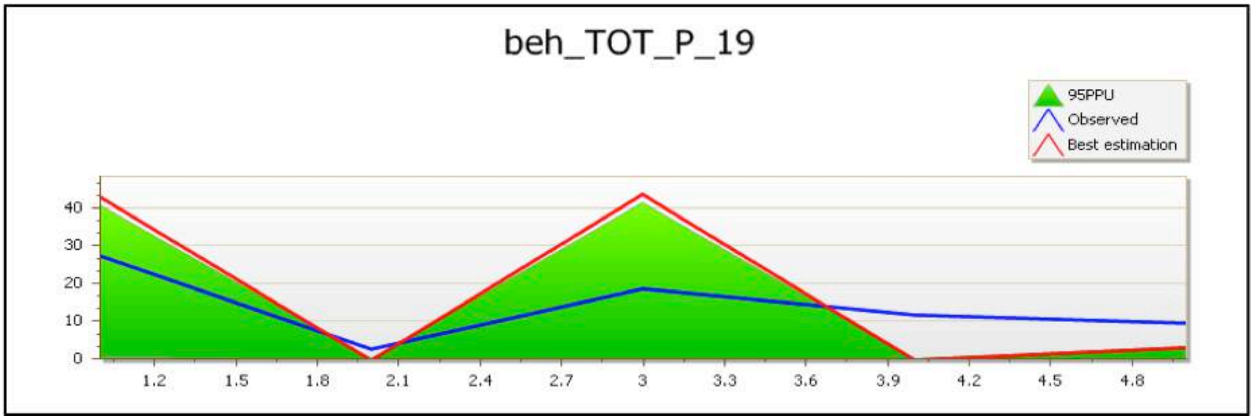

Figure 4. 46 Cupeyes WS model validation. Vertical axis is TP loading (kg) for the given month (horizontal axis).

Table 4. 13 Cupeyes WS calibration and validation results

	Variable	R2	NS	Mean_sim(Mean_obs)	StdDev_sim(StdDev_obs)
Calibration	FLOW_OUT_19	0.87	0.68	0.18(0.16)	0.05(0.09)
Validation	TOT_P_19	0.03	-1.1	12.97(18.62)	19.41(16.64)

4.4.3. Calibration Results

The calibration results shown above for each watershed are considered acceptable given that the observed values were gathered and processed by the study group, different equipment and methods were used which can reduce the reliability of the observed values. For example the TP loadings are based on daily precipitation and does not consider antecedent conditions, which could result in overestimation of loadings during intense storm events with dry antecedent conditions. So is the case for the fourth month (April) in the validation period of the Cupeyes watershed where a large daily precipitation value resulted in a TP load of approximately 24 kg on a single day. Additionally, calibration of hydrological models requires long and continuous data sets with dry and wet years which were not available given the restraints of field sampling, battery life and others. However both models resulted in similar mean observed and simulated values and in both cases the NS coefficient values were acceptable. In Bosque Olimpia TP loadings resulted in the best simulation with a NS coefficient of 0.63 and in Cupeyes average monthly discharge values resulted in a NS coefficient of 0.68. These are both very good results that can provide adequate simulations into the past or future using different land uses and evaluating their effect on water quality in terms of nutrients. Model calibration issues and parameterization will be further discussed in the results and analyses section.

4.5. Long Term Simulation of Agricultural Activities in B.O.

In order to evaluate the possible effects of past intensive agriculture in the Bosque Olimpia secondary forest and other secondary forests in the island the calibrated SWAT model for Bosque Olimpia was used. SWAT's ability to simulate land use changes and evaluate the effects in water quality was used. Two long term simulations will be performed. The first will include the past agricultural activities in the Bosque Olimpia watershed and continue its transition into a secondary subtropical forest. The second will assume a mixed forest for the same period that the long term simulation of the secondary forest was performed, all other parameters including weather will be identical in both simulations. Doing so will allow us to compare the temporal nutrient output of both simulations and assess any difference between the two. We hypothesize that there will be an effect in nutrient loading exports and that SWAT will be able to simulate these effects properly.

The first step was to establish a time line of the land use changes in the forest. To do so we interviewed historians and local entities like Casa Pueblo in Adjuntas to get estimates of approximate dates and the kind of agricultural activities in the watershed and the region. For instance Casa Pueblo provided us with "Historia Oral de la Olimpia" see timeline in Figure 4.47, gathered by E. E. Vivoni (see Appendix 14). Technical reports (ARS, 1997) and local coffee specialists like Prof. Miguel Monroig, former coffee specialist for the Agricultural Extension Service of UPRM, were consulted to assess information related to the amount of fertilizer and chemical formulation, amount of trees planted per acres, years to maturity, amount of shade and common shade species used in the study area. Other sources were also consulted which will be cited further below. The most relevant information obtained was that approximately 300 coffee trees per acre were generally planted at that time, in this case the farm was also planted with orange trees and plantains harvesting at a time up to 25,000 plantains weekly. We also learned that farmers used to apply 1-2 pound (0.45-0.90 kg) of 10-5-15 fertilizer formulation to each coffee tree per year. That a C. Arabica from the "typica" variety reached its peak height at 7 to 8 years in partial shade. It's important to consider that this was coffee shade trees, meaning at least 30% of the land use were trees with a DBH > 6" and provided shade to coffee plantation with its large canopy in the study area. Shade trees in the area at that time were typically Guama, Moca, Guaraguao, Bucare among others. Casa Pueblo provided us with a list of trees identified in the forest where trees like Guama (*Inga Cuarternata*) and other evergreens like Guaraguao (*Guarea Guidonia*) were found. In order to properly simulate the dynamics of the nutrient cycling processes between the soil and plants, plant growth dynamics, nutrient uptakes, fertilizer applications, soil erosion and nutrient export to receiving waters on the SWAT model, the following assumptions were made for parameterization.

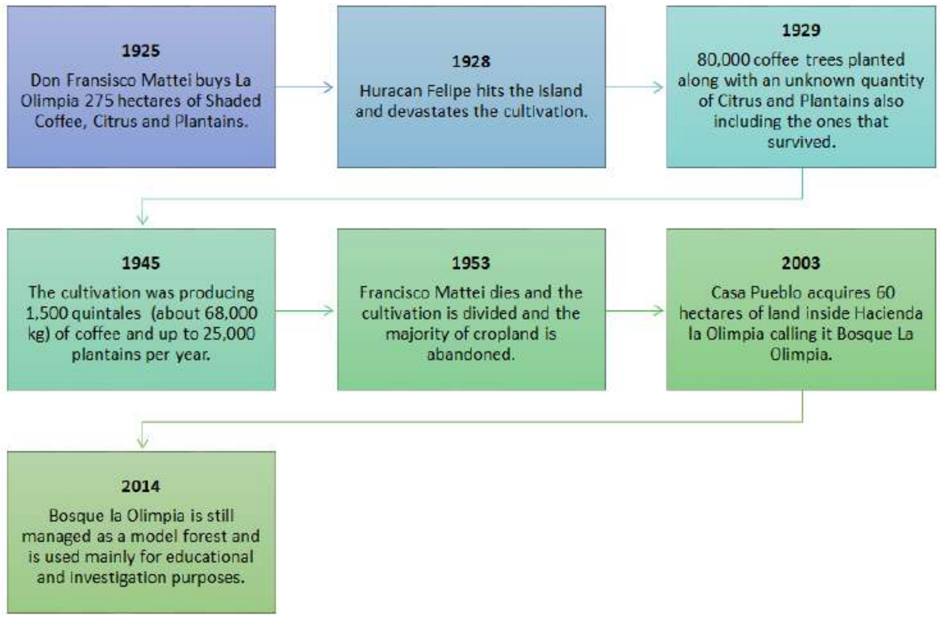

Figure 4. 47 Timeline of events for the transition of B.O. from plantation to secondary forest.

The plant growth database in SWAT already included crop type parameters for Coffee, however some values were adjusted to adapt this to typical values for Puerto Rico's coffee plantations. Changes to this database were based in the literature found and consisted in the number of years required for species to reach full development (MAT_YRS) and in the Maximum Leaf Area Index (BLAI). For coffee MAT_YRS was 10 years and for mixed forest (chosen for the secondary tropical forest transition) it was 50 yrs. The maximum leaf area index (BLAI) for coffee was chosen as 5.5 and for tropical forests 8.6. These values were taken from (Pereira et al., 2011) & (Asner et al., 2003) for coffee and tropical forests respectively. The rest of the parameters were included as established by the plant growth database. Appendix 15 shows the plant database information for each of the land covers chosen.

In order to simulate land use changes the management operations editor within SWAT was used. In here the different operations can be added including planting of new crops, clearing of land (kill operation), harvesting, fertilization and others. Table 4.15 shows the different operations included to simulate the land use changes in Bosque Olimpia and the corresponding parameter values used by the model to run each operation. For the planting operation the following parameters were provided to the model. Current age of trees, when planted (CURYR), assumed as 2 years for coffee and 25 for trees to assume they were already mature. This only will establish the amount of time until the program assumes death and replanting of that plant. Heat units to maturity (PHU_PLT) or also time from budding to maturity of fruit when it's a perennial that produces fruits. This was obtained from equation (4.4) assuming an average base temperature of 10° C (ARS, 1997). The initial leaf area index (LAI_INIT) for both, obtained from (Pereira et al., 2011) & (Asner et al., 2003) for coffee and tropical forests respectively is the LAI corresponding to when the seedling are transplanted. The initial dry weight biomass (BIO_INIT) is the biomass corresponding to the whole plant when this plant is transplanted. This was obtained from (Farfan et al., 2007). Using the information provided by Miguel Monroig the fertilizer applied was assumed to have a 10-5-15 formulation and to be applied at a rate of 0.45 kg/plant and 2,471 plants per ha. It was assumed that both plantains and citrus were fertilized. Instead of using the maximum suggested (2 Lb. per tree) assuming 0.45 kg/tree (approximately 1 Lb. per tree) will compensate for the shade and assuming such planting density. Other operations used were: kill/end of growing season, this operation stops all plant growth and converts all plant biomass to residue; harvest and kill operation: this operation harvests the portion of the plant designated as yield, removes the yield from the HRU and converts the remaining plant biomass to residue on the soil surface; harvest only operation: this operation harvests the portion of the plant designated as yield and removes the yield from the HRU, but allows the plant to continue growing. The last two were selected to have an 85% efficiency to account for fruits that fall to the floor or don't get picked. These management operations were applied to all the land with 60% percent slope or less excluding the low urban development area, see Figure 4.48. Appendix 16 shows the management operation parameters as entered to the program and Appendix 17 shows the management operation as entered in the operation manager interphase. Meteorological data was simulated with the same user provided statistical parameters discussed in section 4.3.6 for calibration in all years except from 2012 to 2014, for which the observed data from the installed rain gages discussed in section 4.3.7 was used. Finally model setup was performed for yearly outputs, from 1926 to 2014 and the transition (from plantation to secondary forest) simulation was successfully ran. For the forest simulation Mixed Forest was selected for the whole watershed and the exact same weather data from the transition simulation was copied into the *txtintxtout* folder where the program reads the data from. This ensured that the only variable was the land use change and that any difference in output was due to the past agricultural activities in the watershed. Results are shown in Chapter 5.

$$PHU = \sum_{d=1}^{n} HU \tag{4.4}$$

$$HU = T_{av} - T_{base} \tag{4.5}$$

Where: PHU are the potential heat units, n is the number of days, HU are the Heat Units, T_{av} is the average temperature of day n and T_{base} is the base temperature.

Table 4. 14 Management operations and necessary parameters for land use change routine.

Year #	Date	Operation	Plant/Land cover	Parameter	Decription	Value	Unit
1	1/1/1926	Beginning of simulation	Forest Mixed	N/A	Includes warming period 3 years.	1926	year
2	12/31/1927	Skip to end of year	FRST		Existing landuse is FRST		
3	9/13/1928	Kill operation	Forest mixed	Simulates Hurricane	70% of the land cover that used to be FRST	1928	year
4	3/1/1929	Plant/begin growing season	Coffee	Date	Starting date of the operation	1929	date
				CURYR_MAT	Current age of trees	2	yrs
				HU's to maturity	HU for plant to reach	2466.4	hu
				LAI_INIT	Initial leaf area index	1.82	index
				BIO_INIT	Initial dry weight biomass (0 to 200)	30	kg/ha
		Fertilization		FRT_KG	Fertilizer applied 10-5-15	1134	kg/ha
5	1930	Fertilization - March		FRT_KG	Fertilizer applied 10-5-15	1134	kg/ha
		Harvest only - December		HARVEFF	Grain harvest was selected	0.8	fraction
6...	1931	Fertilization		FRT_KG	Fertilizer applied 10-5-15	1134	kg/ha
		Harvest only		HARVEFF	Grain harvest was selected	0.8	fraction
...27	1952	Fertilization		FRT_KG	Fertilizer applied 10-5-15	1134	kg/ha
		Harvest only					
28	1953	Fertilization					
29	1/1/1954	Harvest and Kill					
	1/2/1954	Plant/begin growing season	Mixed Forest	CURYR_MAT	Current age of trees	25	yrs
				HU's to maturity	HU for plant to reach	4392	hu
				LAI_INIT	Initial leaf area index	5	index
				BIO_INIT	Initial dry weight biomass (0 to 200)	190	kg/ha
89	12/30/2014	End of Simulation					

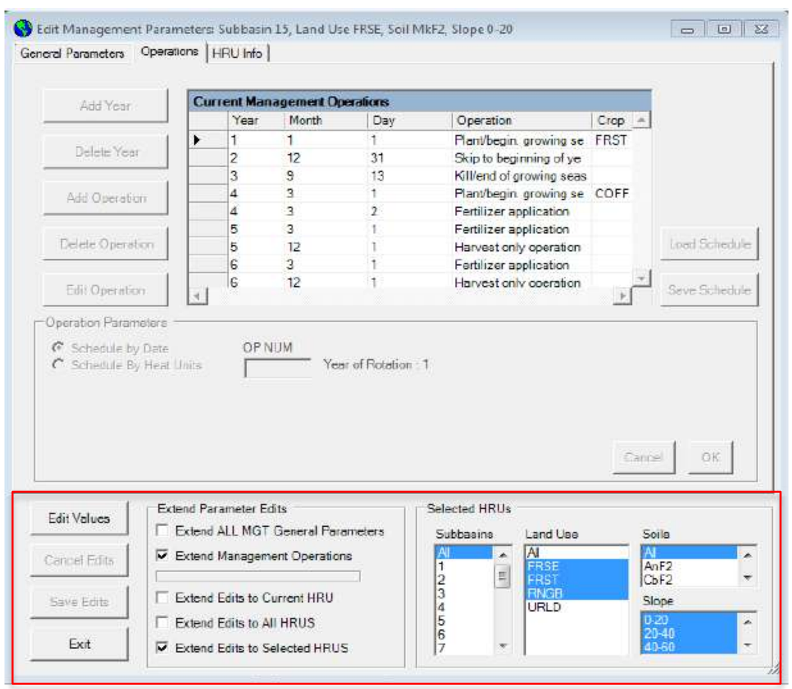

Figure 4. 48 Management parameters window and extend management operations boxed in red.

4.6. Modified Plant Growth Module for the Tropics

As discussed in section 2.5 the plant growth module in SWAT has some limitations in the simulation of vegetation growth in the tropics. In their study Strauch et. al. validates the model in terms of the evapotranspiration and leaf area index. In our case, we want to test if the long term simulation of sub-tropical secondary forests will be affected by using the modified plant growth module for the tropics. We hypothesize that nutrient loading outputs could be affected due to incorrect simulation of plant growth in the original SWAT program. This would be due to the incorrect contributions of litter fall and simulation of nutrient uptake caused by the long term simulation of plant growth based in potential heat units and not simulated soil water (moisture) in the model. Our approach to evaluate these effects is that since the long term simulations are not being calibrated to match observed values, changes in the nutrient export values should be due to the only factor changing between simulations and that is the modified plant growth module routine for the tropics that's being used. To do this we're using the calibrated Olimpia Model with the same land use transition changes and weather data as in the past section but with the modified SWAT2009 routine developed by (Strauch et al., 2013). We will run the simulation two times, one with the past agricultural activities and transition into secondary forest and another with the permanent primary forest. These will be compared with the results from the unmodified SWAT model from the past section (4.5).

This version of SWAT (Modified SWAT2009) is compatible with all the txt files developed for the unmodified SWAT. It only needs establishment of the following new parameters. $TRAMO_1$ and $TRAMO_2$ are the first and last month of a transition period from dry to wet season. The months of march and April are default for the northern hemisphere for $TRAMO_1$ and $TRAMO_2$ respectively. These values were added to each of the 21 sub basins (.sub) txt files. Figure 4.49 shows the modification for subbasin 1. This ensures that the routine doesn't initiate plant growth on the dry season due to a single rainfall event or stop plant growth during the wet season due to a short dry period. Another new parameter is the fraction of the available water capacity of the two upper layers (FR_{AWC}). This value can be defined in the crop.dat txt file and is a nondimensional parameter between 0 and 1 that works as a threshold. If the actual soil water content of the upper two layers is above this fraction the routine will initiate plant growth. If the soil water content remains below the threshold it is evaluated if the actual month is within the transition period then it will follow normal plant growth if it's after the transition period it goes to dormancy. The first two layers of soil in the BO watershed are a total of 0.48 meters deep. Considering the root depth of each plant the depth of the upper two layers a FR_{AWC} of 0.1 was selected for Coffee (see Figure 4.50) and of 0.02 for Forest (see section 2.5 for FR_{AWC} use in modified plant growth module). After all the files were copied to the "default" *txtintxtout* folder (the folder where the program reads all the user entered data from) the location of the SWAT executable, which is the actual SWAT program version that's going to be used, was changed to the location of the modified SWAT model for the tropics and model was run from 1926 to 2014.

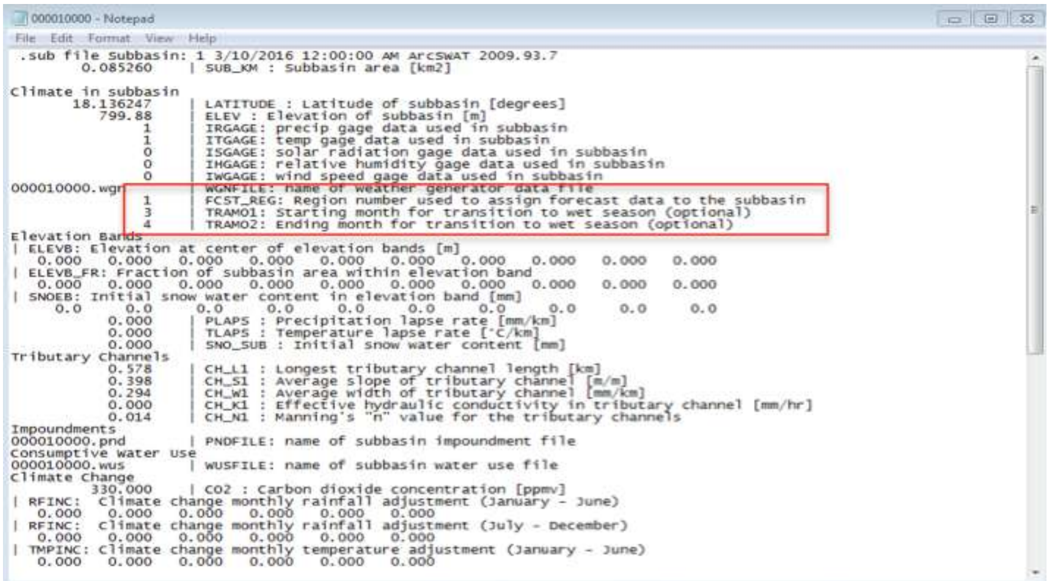


```
 .sub file Subbasin: 1 3/10/2016 12:00:00 AM ArcSWAT 2009.93.7
       0.085260    | SUB_KM : Subbasin area [km2]

Climate in subbasin
      18.136247    | LATITUDE : Latitude of subbasin [degrees]
         799.88    | ELEV : Elevation of subbasin [m]
              1    | IRGAGE: precip gage data used in subbasin
              1    | ITGAGE: temp gage data used in subbasin
              0    | ISGAGE: solar radiation gage data used in subbasin
              0    | IHGAGE: relative humidity gage data used in subbasin
              0    | IWGAGE: wind speed gage data used in subbasin
000010000.wgn      | WGNFILE: name of weather generator data file
              1    | FCST_REG: Region number used to assign forecast data to the subbasin
              3    | TRAMO1: Starting month for transition to wet season (optional)
              4    | TRAMO2: Ending month for transition to wet season (optional)
Elevation Bands
| ELEVB: Elevation at center of elevation bands [m]
  0.000   0.000   0.000   0.000   0.000   0.000   0.000   0.000   0.000   0.000
| ELEVB_FR: Fraction of subbasin area within elevation band
  0.000   0.000   0.000   0.000   0.000   0.000   0.000   0.000   0.000   0.000
| SNOEB: Initial snow water content in elevation band [mm]
    0.0     0.0     0.0     0.0     0.0     0.0     0.0     0.0     0.0     0.0
          0.000    | PLAPS : Precipitation lapse rate [mm/km]
          0.000    | TLAPS : Temperature lapse rate [°C/km]
          0.000    | SNO_SUB : Initial snow water content [mm]
Tributary Channels
          0.578    | CH_L1 : Longest tributary channel length [km]
          0.398    | CH_S1 : Average slope of tributary channel [m/m]
          0.294    | CH_W1 : Average width of tributary channel [mm/km]
          0.000    | CH_K1 : Effective hydraulic conductivity in tributary channel [mm/hr]
          0.014    | CH_N1 : Manning's "n" value for the tributary channels
Impoundments
000010000.pnd      | PNDFILE: name of subbasin impoundment file
Consumptive Water Use
000010000.wus      | WUSFILE: name of subbasin water use file
Climate Change
        330.000    | CO2 : Carbon dioxide concentration [ppmv]
| RFINC:  Climate change monthly rainfall adjustment (January - June)
  0.000   0.000   0.000   0.000   0.000   0.000
| RFINC:  Climate change monthly rainfall adjustment (July - December)
  0.000   0.000   0.000   0.000   0.000   0.000
| TMPINC: Climate change monthly temperature adjustment (January - June)
  0.000   0.000   0.000   0.000   0.000   0.000
```

Figure 4. 49 Modification of sub-basin 1 txt file to include TRAMO1 and TRAMO2

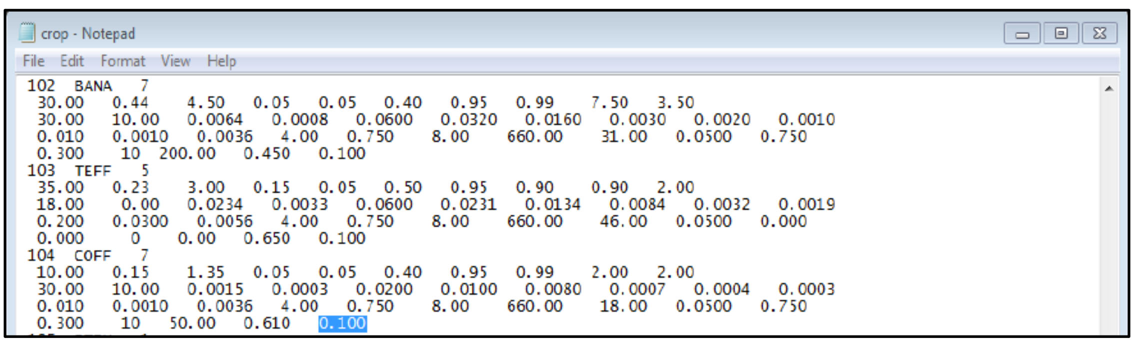


```
102  BANA   7
 30.00   0.44    4.50   0.05   0.05   0.40   0.95   0.99   7.50   3.50
 30.00   10.00   0.0064   0.0008   0.0600   0.0320   0.0160   0.0030   0.0020   0.0010
 0.010   0.0010   0.0036   4.00   0.750   8.00   660.00   31.00   0.0500   0.750
 0.300   10  200.00   0.450   0.100
103  TEFF   5
 35.00   0.23    3.00   0.15   0.05   0.50   0.95   0.90   0.90   2.00
 18.00   0.00   0.0234   0.0033   0.0600   0.0231   0.0134   0.0084   0.0032   0.0019
 0.200   0.0300   0.0056   4.00   0.750   8.00   660.00   46.00   0.0500   0.000
 0.000   0   0.00   0.650   0.100
104  COFF   7
 10.00   0.15    1.35   0.05   0.05   0.40   0.95   0.99   2.00   2.00
 30.00   10.00   0.0015   0.0003   0.0200   0.0100   0.0080   0.0007   0.0004   0.0003
 0.010   0.0010   0.0036   4.00   0.750   8.00   660.00   18.00   0.0500   0.750
 0.300   10   50.00   0.610   0.100
```

Figure 4. 50 Inclusion of the FR_{AWC} in the crop database

5. Analysis of results

5.1. Annual and Monthly Total Phosphorous Loadings

Annual and monthly TP loads were calculated using daily loadings, where the summation of daily loads is performed to obtain monthly and annual loads. This will provide insight into what is the net TP export by each watershed. Tables 5.1 and 5.2 show the annual total loadings for Bosque Olimpia and Cupeyes watersheds, respectively. Also, in such tables, the annual precipitation and the net base flow and storm TP load contributions are shown. These values show that Cupeyes watershed received 813 millimeters more of precipitation than Olimpia, also 78% of the precipitation in Cupeyes was considered for storm loading calculations while in Bosque Olimpia watershed 90.35% of the total precipitation produced storm loadings. These values are over the whole period considered for the study (2 years and 7 months). Baseflow phosphorous loadings constituted only 2% of the total loadings in Cupeyes while in Bosque Olimpia baseflow phosphorous loadings constituted 17% of the total loadings.

Table 5. 1 Annual TP loadings from the Bosque Olimpia watershed.

Olimpia					
Year	Annual P (mm)	Annual Eff. P (mm)	Annual TP load (kg)	Annual TP Base flow load (kg)	Annual TP Storm load (kg)
2012	1,376	1,112	136.032	26.988	109.044
2013	1,642	1,669	197.547	22.957	174.521
2014	526	421	60.548	16.386	44.162[1]

Table 5. 2 Annual TP loadings form the Cupeyes watershed.[2]

Cupeyes					
Year	Annual P (mm)	Annual Eff. P (mm)	Annual TP load (kg)	Annual TP Base flow load (kg)	Annual TP Storm load (kg)
2012	1,742	1,382	422.131	6.837	418.566
2013	1,593	1,289	210.083	8.023	202.060
2014	1,053	761	158.704	4.824	153.879

[1] Load estimates for 2014 are from January to July 2014
[2] No precipitation data was available for Sept and Oct 2012.

Loadings corresponding to the year 2014 were calculated up to July 31, 2014 at both watersheds and as stated above no precipitation data was available for September and October of 2012. Still, Cupeyes annual loadings were higher than loadings at Olimpia for the three years under analysis. This makes sense in that Cupeyes watershed is approximately 4 times the size of the Bosque Olimpia watershed. In order to make proper loading comparison TP loadings were standardized by area creating the loading coefficients shown in Tables 5.3 and 5.4 for the Bosque Olimpia and Cupeyes watersheds respectively. Here it is evident that Bosque Olimpia has higher loading rates yet baseflow loading contribution and storm contribution ratios between watersheds are quite different. Baseflow loadings at Olimpia (in average) are almost 20 times baseflow contributions at Cupeyes. However, storm-loading contributions are almost the same for the year 2012 (even when no precipitation data is available for almost two months –September and October- at Cupeyes). This can be accounted for by extreme precipitation events in the watershed, which resulted in higher TP loading values. These events took place in April 10 and May 3, 2012 with corresponding daily precipitation values of 129.54 and 104.14 millimeters respectively. The first was retrieved from the Maricao Fish Hatchery rain gage and the latter was retrieved from the rain gages installed by the study group. During high intensity and long duration precipitation events the effect of hydrograph attenuation is not present, and the soil profile becomes saturated thus resulting in high discharge (and loading) events. For 2013 (the only year with complete and continuous data at both watersheds) Olimpia's storm loading coefficient is 3.8 times Cupeyes loading coefficient. While in this year (2013) the Olimpia watershed received only 102 millimeters more of precipitation (see Tables 5.1 and 5.2).

Table 5. 3 Annual loading coefficients (kg/ha) for the Cupeyes river watershed.[3]

Cupeyes			
Year	Annual TP Load per area (kg/ha)	Annual TP Base flow load coeff. (kg/ha)	Annual TP Storm load coeff. (kg/ha)
2012	0.877	0.0074	0.870
2013	0.436	0.016	0.420
2014	0.329	0.010	0.319

[3] No precipitation data was available for Sept and Oct 2012.

Table 5. 4 Annual loading coefficients (kg/ha) for the Bosque Olimpia watershed.

Olimpia			
Year	Annual TP Load per area (kg/ha)	Annual TP Base flow load coeff. (kg/ha)	Annual TP Storm load coeff. (kg/ha)
2012	1.247	0.247	0.999
2013	1.811	0.210	1.600
2014	0.555	0.150	0.405

Figures 5.1 and 5.2 show the monthly total precipitation (right axis) compared to the monthly total phosphorous loads (left axis) for the Cupeyes and Olimpia watersheds respectively. Also plotted is the storm loading TP coefficient. By analysis it can be determined that monthly loadings in general are higher for the Olimpia watershed also that baseflow contribution is very low for the Cupeyes watershed and that Cupeyes has a lower response at months with high precipitation. Statistical analysis results show that Olimpia monthly TP loadings were higher than Cupeyes 21 out of 29 months (72.4% of the time), storm phosphorous loadings were higher at Olimpia 19 out of 29 months (65.5% of the time) and at baseflow TP loadings 100% of the time. This shows that Olimpia's loads are higher during baseflow and storm events yet to different extents since base flow loads are up to 20 times higher and storm loads up to 3 times higher. Calculation of these monthly loading statistics is shown on Appendix 6.

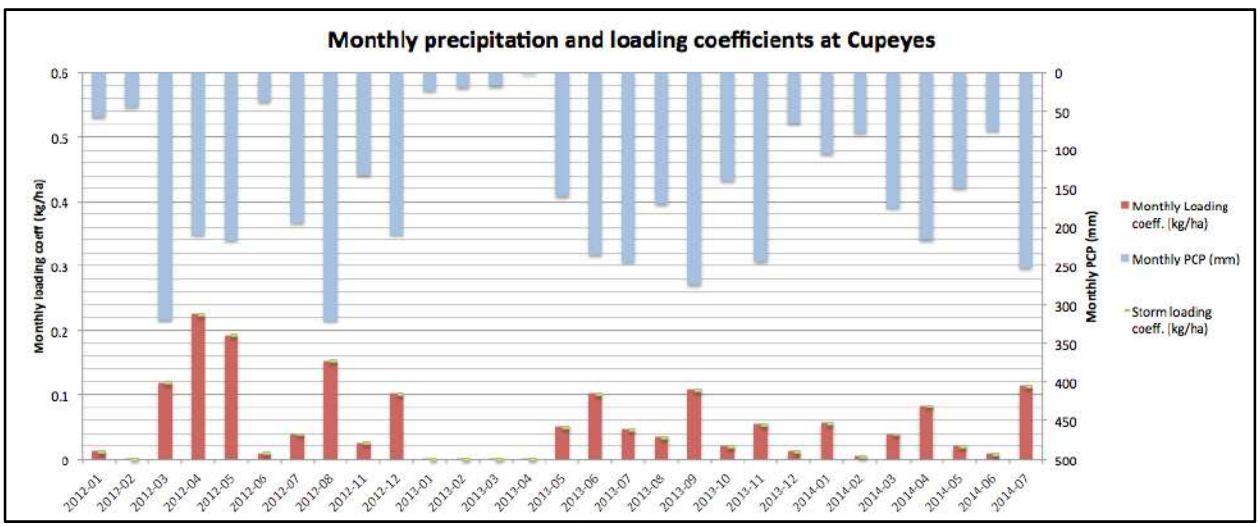

Figure 5. 1 Cupeyes monthly loading coefficients (kg/ha) in red and total monthly precipitation (mm) in blue.

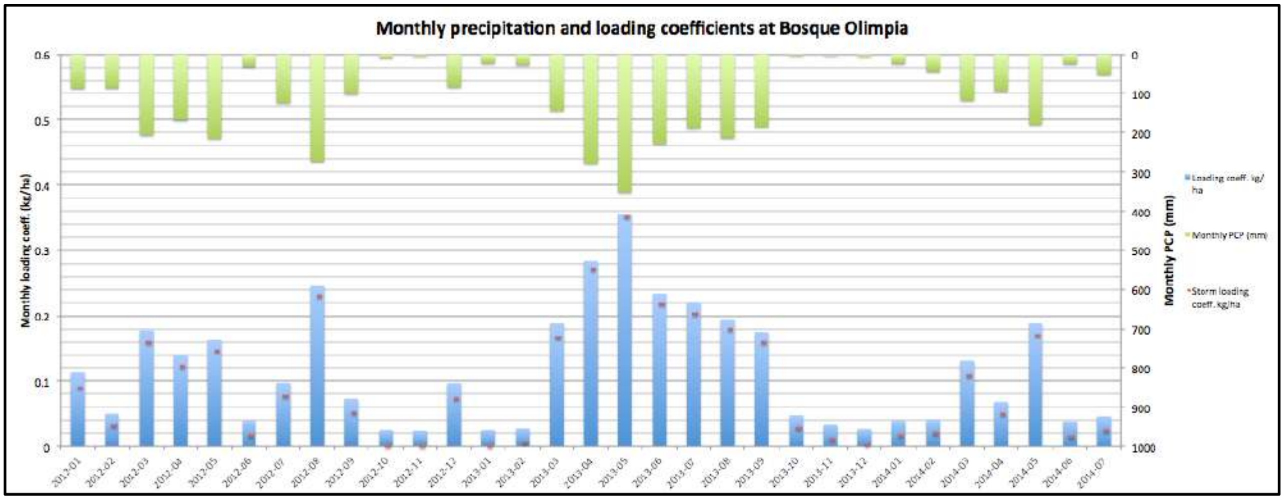

Figure 5. 2 Bosque Olimpia monthly loading coefficients (kg/ha) in blue and total monthly precipitation in green.

5.2. Loading Data Statistical Analyses

Statistical analyses were used to explore the relationship between TP loadings and driving variables of the hydrologic balance in the watershed. Given the discrepancies in loadings between these two watersheds it is imperative to assess if higher loadings in Bosque Olimpia correspond to a soil erosion, and or water quantity issue or if it is due to soil phosphorous concentrations acquired from past agricultural activities in the area. It is known that storm loadings are directly related to soil permeability and storm recharge into the river stream for which these and other relationships will be compared for these watersheds.

5.2.1. Antecedent Precipitation and Storm Phosphorous Concentration

Composite samples from sampled events were analyzed for total phosphorous (TP) concentration. Table 5.5 shows antecedent precipitation and storm TP concentration for sampled events. Table 8.2 shows the statistical data showing that storm TP concentrations are similar at both watersheds and that precipitation events are also similar which make this data sample statistically equivalent. Similar storm TP concentrations suggest that storm-loading discrepancies come from the storm volume produced and not from the soil P concentration.

Table 5. 5 Antecedent precipitation and Storm TP concentration from composite samples.

Bosque Olimpia			Cupeyes		
Date	Antecedent Precipitation (mm)	Mean TP (mg/L)	Storm Event Date	Antecedent Precipitation (mm)	Mean TP Conc. (mg/L)
24-Aug-12	74.93	0.24	24-Aug-12	40.64	0.100
25-Dec-12	74.17	0.16	15-Apr-13	56.90	0.39
26-Dec-12	43.18	0.16	17-Apr-13	19.81	0.39
16-Apr-13	53.85	0.62	29-Apr-13	44.70	0.36
29-Apr-13	31.50	0.10	30-Apr-13	53.59	0.36
7-May-13	20.10	0.20	15-May-13	76.45	0.25
10-May-13	72.64	0.20	8-Jun-13	69.10	0.240
17-Jul-13	44.45	0.501	12-Jun-13	50.8	0.240
20-Jul-13	18.29	0.501	29-Jun-13	32.51	0.08
8-Aug-13	33.02	0.131	28-Jul-13	75.18	0.378
			6-Aug-13	40.89	0.378

Table 5. 6 Precipitation and TP concentration statistics.

	Cupeyes	Olimpia
Mean Antecedent PCP (mm)	46.48	51.05
Std Dev	0.85	0.70
Mean TP (mg/L)	0.2181	0.2890
Std Dev	0.1858	0.1154

Figure 5.3 shows storm TP concentration vs antecedent precipitation. Here it is evident that Cupeyes is very variable with respect to P concentration values at different precipitation rates. Also in the majority of the cases the Cupeyes watershed has a higher concentration, this is true for the relatively lower precipitation values. The variability of Cupeyes could be due to high infiltration taking place in the watershed; at events where the antecedent soil water conditions were high, P concentration will be higher and caused by erosion processes. Conversely at low soil water antecedent conditions, much of the water will be infiltrated resulting in lower runoff volumes (less dilution) and higher concentration values. Another possibility in this scenario is that at high infiltration rates, less soil erosion is observed. For

precipitation values after 63.5 mm we can see that Cupeyes has lower P concentration values than Bosque Olimpia. These precipitation values represent long duration events which clearly after reaching its final infiltration capacity produce higher runoff volumes and therefore much more dilution in the Cupeyes watershed. Olimpia on the other side produces relatively predictable values where concentration vs precipitation values follow the expected dilution dynamics and therefore it suggests that this watershed has less infiltration and higher dilution at storm events.

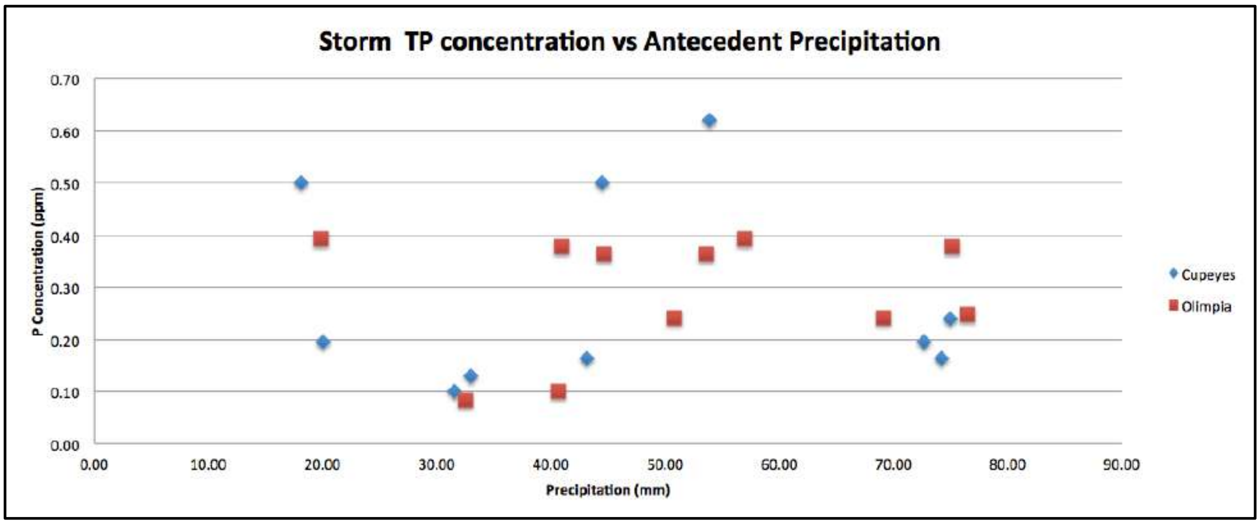

Figure 5. 3 Storm TP concentration (mg/l) vs antecedent precipitation (mm) at both watersheds under study.

5.2.2. Precipitation vs Runoff Volume

The relationship between precipitation events and their corresponding storm hydrograph volume is shown in Figure 5.4 where high correlation (R^2) shows consistency between storm volume and antecedent precipitation in Olimpia and lower correlation values in Cupeyes shows more variability in storm volume. Dividing volumes by the total watershed area standardized the total storm volume of each event. Figure 5.4 thus shows that similar precipitation events produce higher storm volumes in Olimpia. These analyses suggest that Cupeyes has higher infiltration rates, which recharge the unconfined aquifer and reduce the storm runoff volume. This directly impacts storm phosphorous loadings since lower runoff ratios mean less storm energy and suggest a lower rainfall erosion index (Wischmeier et al., 1978).

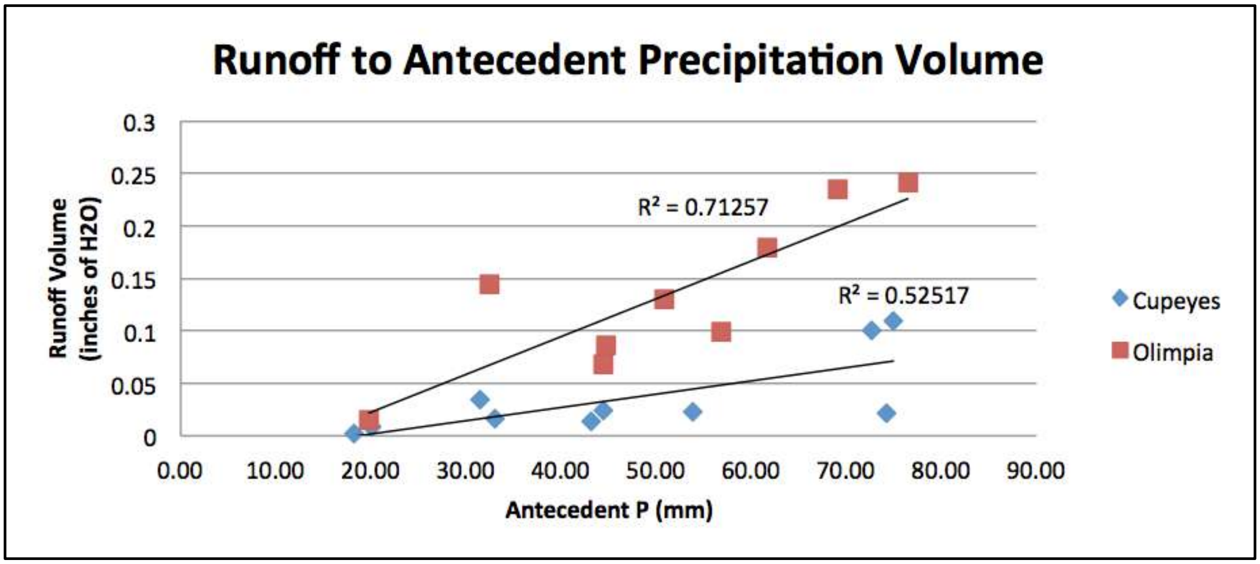

Figure 5. 4 Runoff volume (expressed as depth of H2O over the drainage basin) vs antecedent precipitation at both watersheds. (use runoff volume in the y axis label).

The runoff to precipitation (%) per event (Figure 5.5) was constructed in order to see which percentage of the rain falling in the watershed was actually flowing out during the corresponding storm volume. In order to do this, the runoff volume to antecedent precipitation volume ratio was calculated for each event by dividing the total storm volume by the volume of its corresponding antecedent precipitation event (vertical axis on Figure 5.5). Assuming rain falls homogeneously in the watershed precipitation depth can be converted into volume by multiplying it by the total catchment area. As it is seen in the chart, Bosque Olimpia storm events on average correspond to approximately 100% of the total antecedent precipitation in the basin. Yet for the Cupeyes River basin storm events discharge on average between 10% and 40% of the total precipitation in the basin. Considered that Cupeyes has a larger catchment area than Olimpia (4.81 km^2 vs 1.08 km^2), the calculated values suggest high infiltration and unconfined aquifer recharge at Cupeyes.

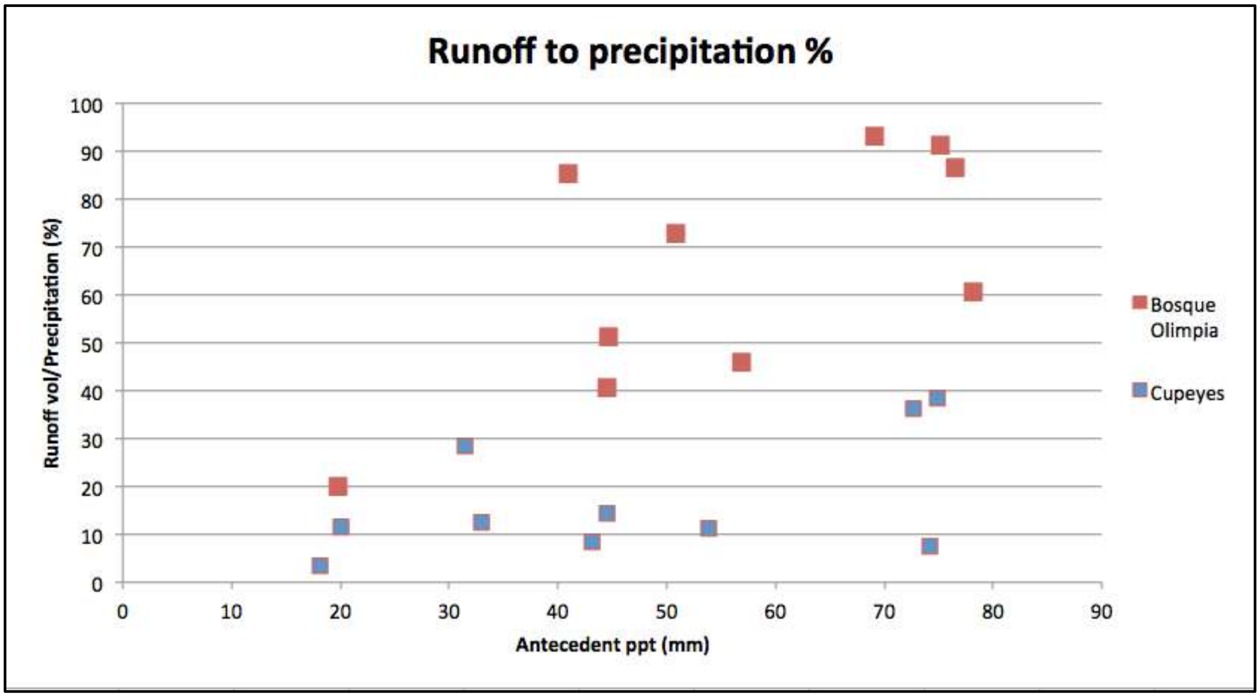

Figure 5. 5 Runoff to precipitation ratios vs their corresponding antecedent precipitation at each watershed.

5.2.3. Duration Curve Analysis

Duration curves are used to evaluate the percent of the time (statistically) a flow can be less or greater than a given value; in other words it describes the chance of exceedance of a given discharge. As suggested by (Fetter, 2001) the distribution of runoff provided by duration curves can be used in watersheds where annual precipitation and evapotranspiration rates are similar in order to compare their hydraulic conductivity in terms of their geological properties. Fetter compares three basins in the same region with different geology, Waupaca River having unconsolidated sand deposits and high permeability, resulting in intermediate flows and lower peaks; Embarrass having till and lake clay and having an intermediate hydraulic response and Rib River being mostly crystalline rock and with low permeability resulting in very low baseflow and high storm peaks. These different distributions of annual runoff (duration curves) are shown in Figure 5.6 along with their respective geology as described by Fetter (2001). Duration curves will be used in this study to compare hydraulic conductivity characteristics between the watersheds under study.

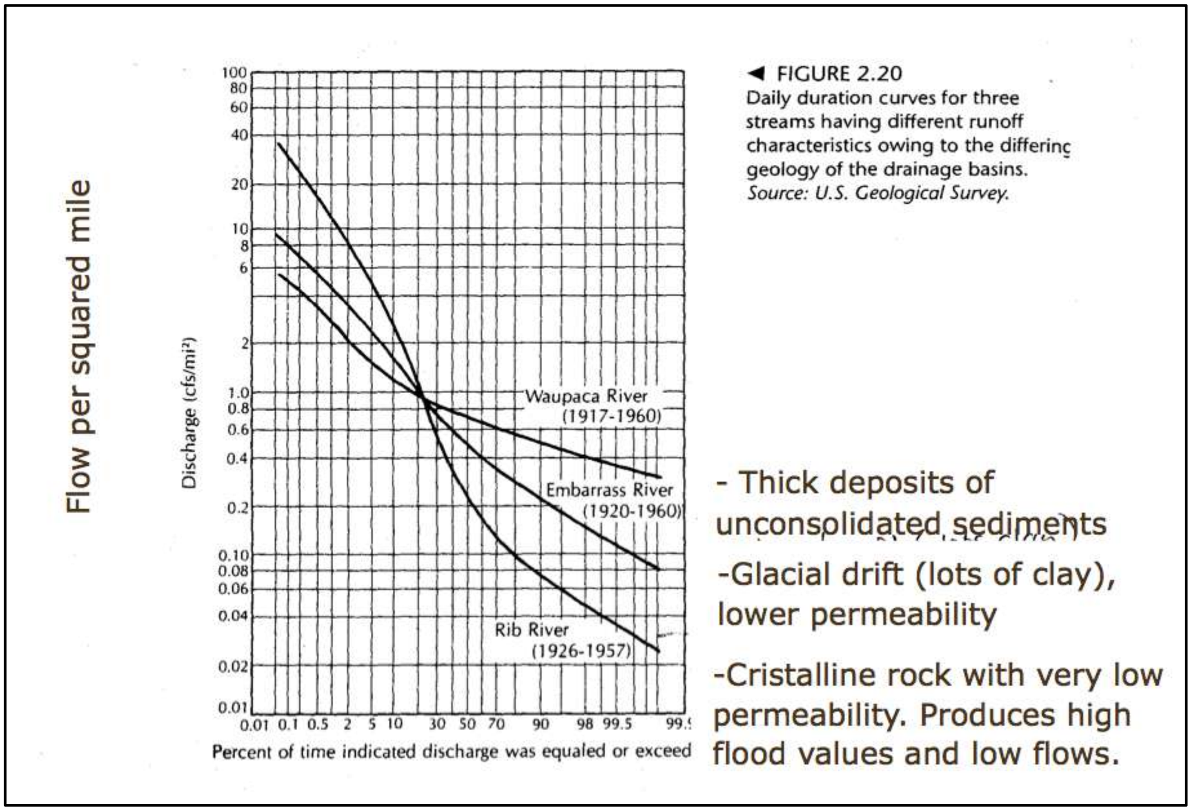

Figure 5. 6 Duration curves for streams with different runoff characteristics associated with the geology of their drainage basin (Fetter, 2001)

5.2.3.1. Mean Daily Flow Calculation

In order to construct duration curves for each watershed mean daily flow (MDF) was calculated using instantaneous flow data obtained by applying the corresponding rating curve to the water level data gathered by the pressure transducers installed at the corresponding storm monitoring stations. Data series is available at a fifteen (15) minute interval for storm events occurring in each watershed. Availability of this data depends on the battery life of the equipment and how often they are replaced (these stations work with 13 V rechargeable lithium ion batteries). Additionally pressure transducers were installed at both watersheds in order to monitor low flows for which additional data was available since February 2014 and April 2014 for Bosque Olimpia and Cupeyes watersheds, respectively. These pressure transducers were HOBO water levels and were processed and corrected for atmospheric pressure using HOBOware PRO software. Also since they were installed in order to monitor low flows, baseflow measurements from the ADV at each watershed were incorporated into the existing rating curves. Mean daily flows for each watershed were calculated using equation 5.1. Figures 8.5 and 8.6 show mean daily flows for the Cupeyes River and Bosque Olimpia watersheds, respectively. Water level rating curves and stream hydrographs are included in Appendix 8 and 9 respectively.

$$MDF = \frac{\sum_1^n Q_i * \Delta t}{n * \Delta t} \tag{5.1}$$

where Q is the average discharge in cms between t_i and t_{i+1}, Δt is t_{i+1}- t_i, n is the total amount of discharge measurements and MDF is mean daily flow in cms.

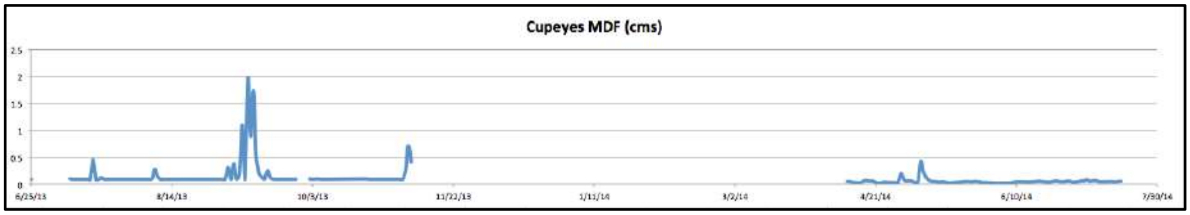

Figure 5. 7 Calculated mean daily flow for the Cupeyes River watershed from July 2013 to July 2014.

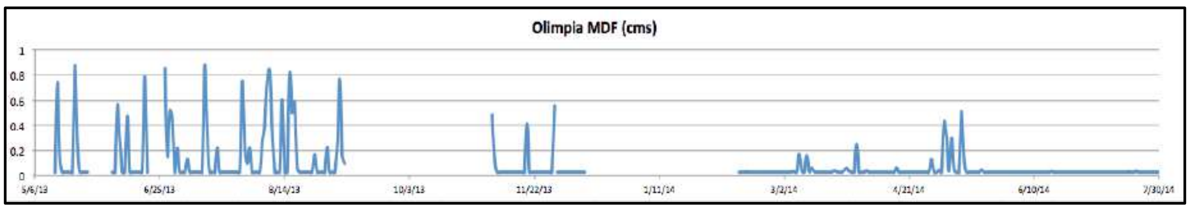

Figure 5. 8 Calculated mean daily flow for the Bosque Olimpia watershed from May 2013 to July 2014.

5.2.3.2. Duration Curves

Duration curves are usually constructed in mean daily flow and then a serial rank is applied starting with the number one for the greatest flow. MDF values are divided by the catchment area to obtain the standardized discharge coefficient (cms/km2). If two values are equal each should receive a different serial rank number (Fetter et al., 2001). The probability of exceedance in percent is calculated by equation 5.2. Figure 5.9 shows duration curves for the Cupeyes and Bosque Olimpia watersheds. By inspection of the duration curves it can be seen that at Olimpia flows exceeded 0.1 cms/km2 fifteen percent (15%) of the time whereas Cupeyes exceeded the same flow rate (0.1 cms/km2) only 2.5% of the time. Also, 1% chance of exceedance for Olimpia at 0.8139 cms/km2 is higher than Cupeyes at 0.4057 cms/km2. These observations indicate a drainage basin with a geology allowing higher permeability at the Cupeyes watershed that in addition to having a similar annual runoff distribution to the Waupaca River, it produces less intermediate values and lower high flows (analogous to the Waupaca River when compared to the Embarass river). The Olimpia watershed duration curve and annual streamflow distribution is similar to the Embarass river with clayey soils and an intermediate hydraulic conductivity.

$$P = \frac{m}{n+1} * 100 \tag{5.2}$$

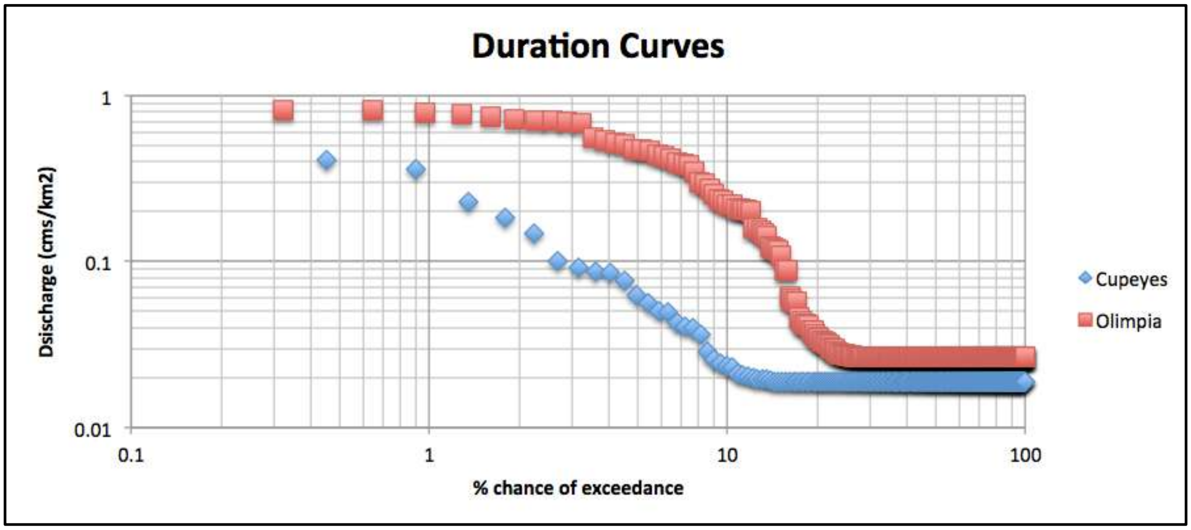

Figure 5. 9 Duration curves showing the annual runoff distribution in the watersheds under study.

5.2.4. Storm Event Recharge (GW) Contribution

In order to estimate the amount of water that enters the sub-surface and enters the river as baseflow as a result of a storm event the Rorabough method was used. This method calculates the volume of recharge as a result of a precipitation event that has caused an upward shift on the baseflow recession curve and is also known as the recession curve displacement method. It states that after D days have elapsed surface runoff has ceased, and discharge is considered the potential baseflow (V_{tp}). D is defined as the amount of days between the peak and the end of overland flow (equation 5.3). Rorabough (1964 as cited from Fetter, 2001) defined a critical time past the peak flow (equation 5.4) in where the total potential baseflow discharge is approximately one half of the water that recharged the ground-water system.

$$D = A^{0.2} \tag{5.3}$$

where A is in the catchment area in square miles, D is days between the peak and the end of overland flow

$$t_c = 0.2144 t_1 \tag{5.4}$$

where t_1 is the amount of time it takes the baseflow recession to decline one log cycle (i.e. Q to 0.1Q)

In order to calculate t_1 the baseflow recession equation (equation 5.5) was applied using two discharge measurements at least D days after the hydrograph peak along the recession curve of the hydrograph to find the recession constant A. Then t_1 was calculated, solving for t in the same equation, using Q=0.1 and Q=1. To calculate the recharge, recession curve A (before the event) and recession curve B where extrapolated to t_c days after the peak of the discharge event under analysis; then equation (5.6) is used to calculate the total recharge of the event. Figures 5.10 and 5.11 shows the construction of this method for two similar precipitation events at the Cupeyes and Bosque Olimpia watersheds, respectively. Stream hydrographs developed from the installed HOBO water levels was used (see Appendix 7 and 8). Table 5.7 shows the calculated parameter values corresponding to each watershed in the construction of this method.

$$Q = Q_0 e^{-at} \tag{5.5}$$

where Q is the flow at some time after the recession started (cms)
Q_0= is the flow at the start of recession (cms)
a = is the recession constant of the basin (1/d)

$$G = \frac{2(Q_B - Q_A)t_1}{2.3026} \tag{5.6}$$

where G is the volume of water that recharged the aquifer as a result of the precipitation event that caused the peak flow.
Q_A is the discharge of recession A at t_c past the peak
Q_B is the discharge of recession B at t_c past the peak
t_1 is the amount of time it takes the baseflow recession to decline one log cycle in seconds

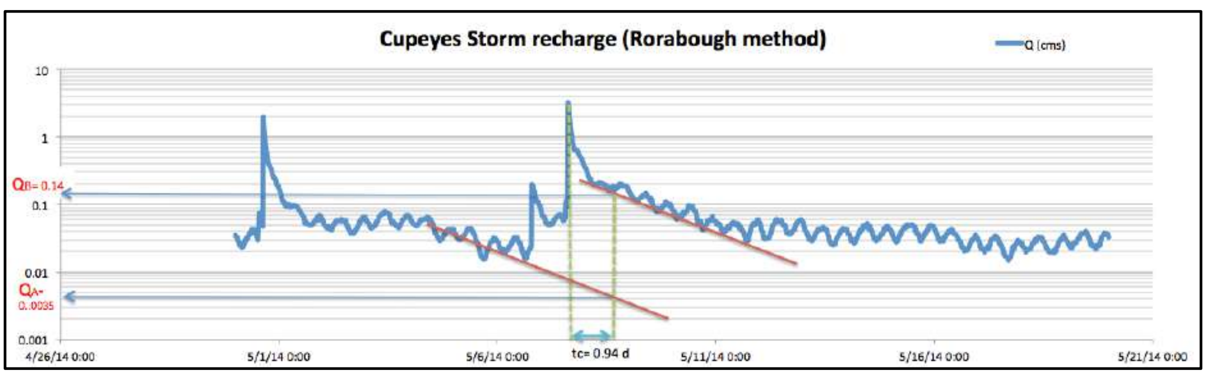

Figure 5. 10 Rorabough method construction used to calculate the recharge corresponding to a storm event on May 6, 2014 in the Cupeyes watershed.

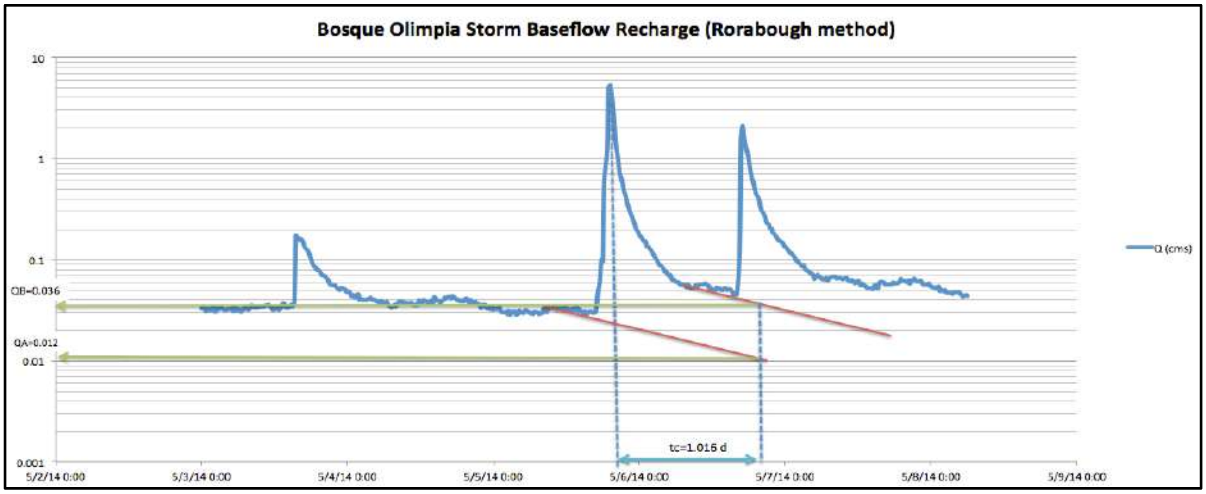

Figure 5. 11 Rorabough method construction used to calculate the recharge corresponding to a storm event on May 5, 2014 in the Bosque Olimpia watershed.

Table 5. 7 Calculated parameter values for recharge volume estimation at each watershed.

Variable	Cupeyes	Olimpia
Q_o (cms)	0.172	0.068
Q (cms)	0.034	0.042
t (days)	3.083	1.000
a	0.524	0.486
t_1 (days)	4.393	4.739
t_c (days)	0.942	1.016
Q_A (cms)	0.004	0.012
Q_B (cms)	0.140	0.036
G (m3)	**45,051.550**	**8,545.032**

5.2.5. Water Balance

The Rorabough storm recharge analysis shows that Cupeyes has higher recharge for similar events since even when in Bosque Olimpia the precipitation event was larger, the recharge depth in the basin was less than Cupeyes (see table 5.7). The recharge depth at Cupeyes is equivalent to 17.2% of the total precipitation event. This was calculated by dividing the depth of recharge in the watershed (9.37 mm) by the total precipitation event (55.37 mm). Hypothetically, if the recharge rate in Cupeyes were as the one in Olimpia (7.83 mm) then an additional 1.54 mm (equivalent to 7,407.4 m^3)would have been overland flow. This is equivalent to 10% of the total event discharge volume in Cupeyes (which was 74,704 m^3) and only 2.3 % of the total precipitation event volume in Cupeyes. Using this the recharge in

Cupeyes could be assumed to be 17% + 2.3% = 20%. Using the highest volume to precipitation % in Figure 5.5 would then result in a maximum of approximately 60% (40%+20%) of the total event precipitation depth. In this hypothetical case still 40% of the storm event will be distributed between evapotranspiration and aquifer storage-recharge. Also the value of 20% in recharge corresponds to the storm event under analysis and not necessarily to the event with the highest volume to precipitation percent in Figure 5.5. Still this exercise shows that even using the highest recorded discharge and assuming the same recharge contribution as in Olimpia, the Cupeyes watershed appears to be infiltrating large volumes of storm water.

Table (5.8) shows the runoff volume, recharge depth, and ET estimation, in both watersheds in order to determine the water balance. ET estimation was obtained from the PR-ET program (Harmsen, E. W. and A. González, 2005), which uses the Penman-Monteith equation to calculate ET rates for PR using remotely sensed weather data. According to the water balance equation (5.7) (Bedient, et al., 2012) delta storage in the Cupeyes watershed is 1.6 times the storage in the Bosque Olimpia watershed. This approach proves that infiltration losses are higher at Cupeyes even when the same soil series predominate and indicate that it could be due to the sub surface geology of the watershed. Longer monitoring of stream discharge at these watersheds is necessary as well as analysis of recharge rates using computerized methods that compute recharge from continuous sets of stream flow records using the Rorabough method (Rutledge, 1998). The method express changes in aquifer storage (ΔS) as follows:

$$P - R - G - E - T = \Delta S \tag{5.7}$$

where: P= precipitation, R=surface runoff, G=ground water flow, E=evaporation, T=transpiration and ΔS=aquifer storage.

Table 5. 8 Water balance for the storm events under analysis at each watershed.

	Cupeyes	Olimpia
Antecedent PCP (mm)	55.37	56.89
Runoff Volume (m3)	74,704	30,739.90
Recharge Volume (m3)	45,051.55	8,545.03
Basin Area (m2)	$4.81\text{x}10^6$	$1.09\text{x}10^6$
Recharge Depth- G (mm)	9.37	7.83
Storm Runoff-R (mm)	15.5	28.2
ET (mm)	5	5
Δ Storage (mm)	25.5	15.86

5.2.6. Statistical Analysis Discussion

Given that, as explained above, infiltration losses and runoff coefficients (R/P ratio) affect directly the soil erosion dynamics of storm TP loadings this finding plays a key role in elucidating the loading dynamics of storm runoff loadings at these watersheds. Yet since the loading dynamics depend on not only storm runoff volume but also the falling raindrop intensity loadings cannot be analyzed in terms of these events, which differ in precipitation intensity. Assuming a 10% higher storm volume on the Cupeyes watershed will not compensate for said dynamics.

A possible explanation to loading differences between watersheds is that higher recharge and storage in the Cupeyes watershed could lead to higher dilution of the groundwater TP concentration. For example if the delta storage (25.5 mm and 15.86 mm) at each watershed is converted into volume by multiplying by the watershed area then the delta storage will be $1.22x10^5$ m^3 and $1.72x10^4$ m^3 on the Cupeyes and Bosque Olimpia watersheds, respectively. If we assume that the volume of storage at Bosque Olimpia produced a TP baseflow concentration of 0.03 mg/L then the volume of storage of Cupeyes being approximately 7 times the volume of storage in Olimpia will dilute the TP soil concentration to 0.004 mg/L. This hypothetical situation could explain the differences between TP baseflow loadings in the watersheds under study which shows 10 fold concentrations in the reference studies (Martinez et al., 2010).

The geologic formations underlying the Cupeyes watershed are shown in Figure 5.12. It can be seen that this watershed lays almost entirely within the TKm formation, which represents metamorphic rock (Serpentinite), sedimentary and igneous rocks. Qa represents quaternary alluvial deposits and TKv volcanic and sedimentary rocks. Figure 5.13 obtained from the USGS Ground Water Atlas 1996 (Veve, et al., 1996) shows the geologic formations on the island and the location of faults along these formations. The location of the Cupeyes watershed is indicated with a red arrow on Figure 5.13, where it is evident that a fault line crosses the Cupeyes watershed under study. Fractured metamorphic rocks can permeate large amounts of water and certainly is one of the main reasons of high infiltration and aquifer storage for the Cupeyes WS in the water balance analysis.

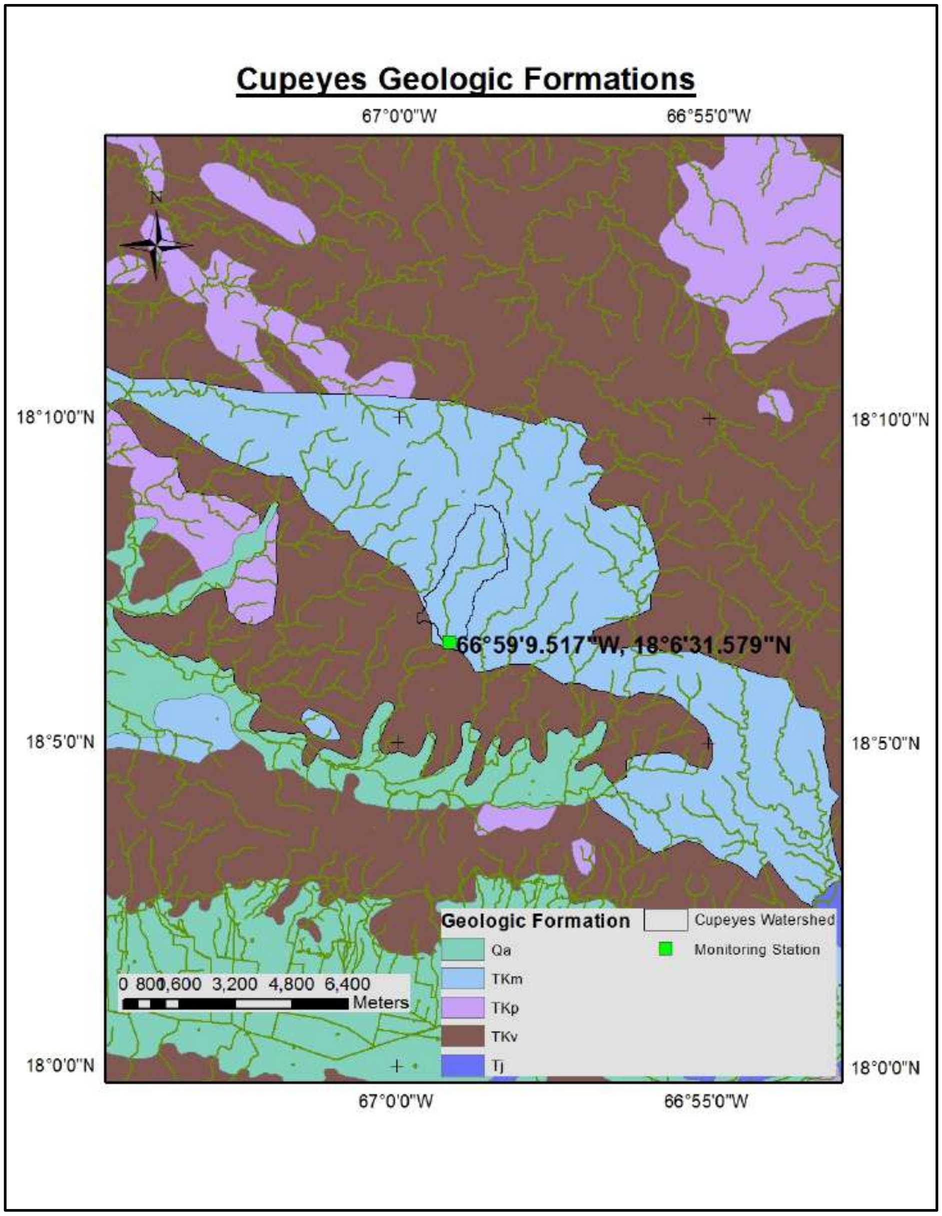

Figure 5. 12 Geologic formations in the San German-Lajas area. The Cupeyes watershed and the coordinates of the monitoring station are shown.

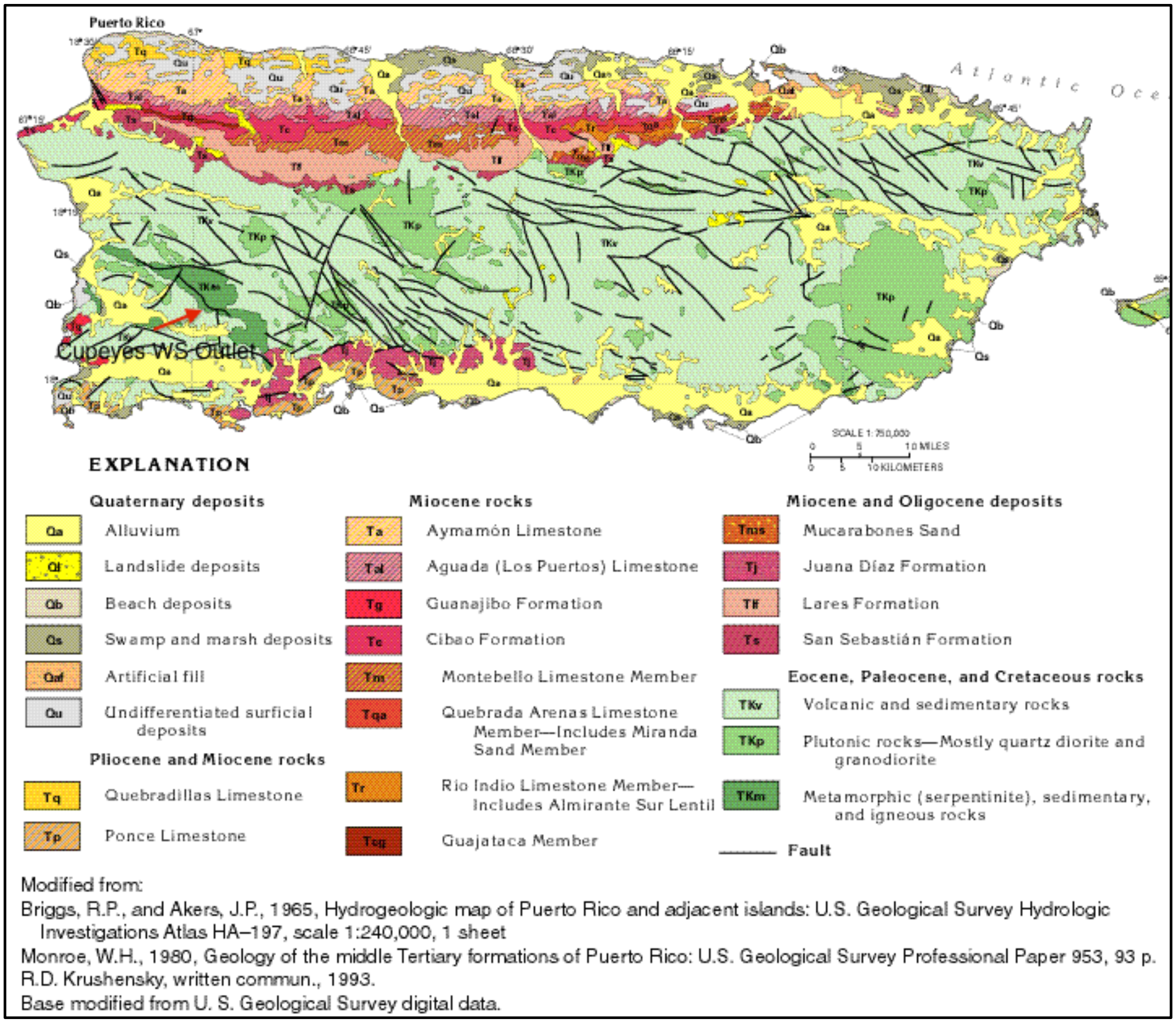

Figure 5. 13 Hydro-geologic formations of Puerto Rico including faults. The Cupeyes WS outlet is indicated with a red arrow.

In order to further prove these findings a watershed models, which allows continuous simulation of water quantity and quality are necessary. This will allow us to quantify the effects that key watershed parameters can have on the TP loading dynamics of these watersheds.

5.3. Discussion of Calibration Results

5.3.1. Effect of Regolith Depth in Baseflow and TP Loadings

Discharge and TP loading seem to be consistently under estimated in the Bosque Olimpia watershed SWAT runs. During soil sampling fieldwork it came to the study group's attention that the soil regolith on Olimpia was apparently deeper than the soil regolith on Cupeyes. The effect of the regolith depth in the baseflow discharge and the TP loadings was assessed using the Bosque Olimpia watershed SWAT model. Given that soil regolith depth was estimated to be 2000 mm for all of the soil series in the watershed; this was changed into 500 mm. Figures 5.14 and 5.15 show the water balance, using the SWAT error checker included within SWAT, of each SWAT model run with a 2000 mm and a 500 mm regolith respectively. It can be seen that when the regolith depth is reduced the percolation to the shallow aquifer is 1.65 times higher (as in the case with Bosque Olimpia and Cupeyes aquifer storage in section 8.5) and that "return flow", the main contributor of base flow, is also higher. This way the effect of the depth of the regolith in the watershed could account for the underestimation of baseflow in the Bosque Olimpia watershed since when monthly baseflow contributions from the watershed were compared to the observed monthly baseflow these were always being under estimated.

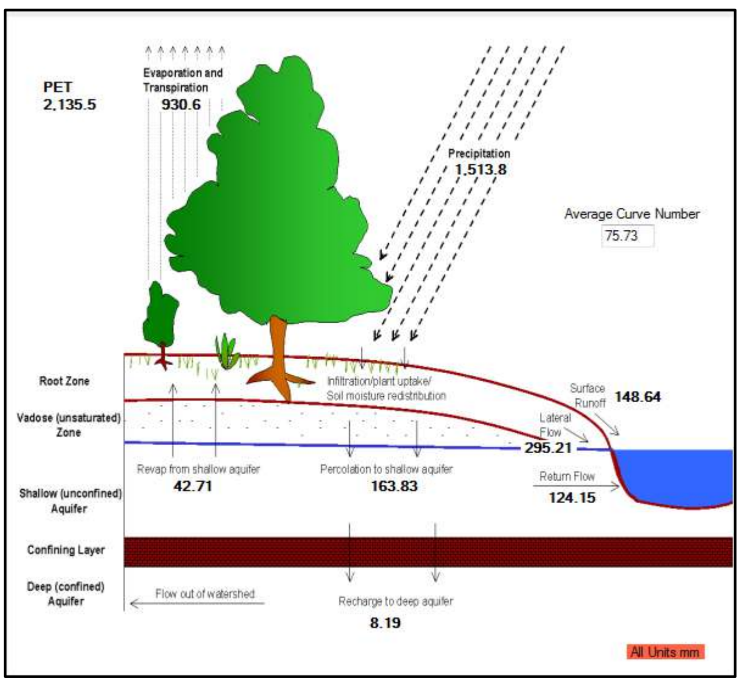

Figure 5. 14 Water balance for the Bosque Olimpia SWAT model using a regolith of 2000 mm.

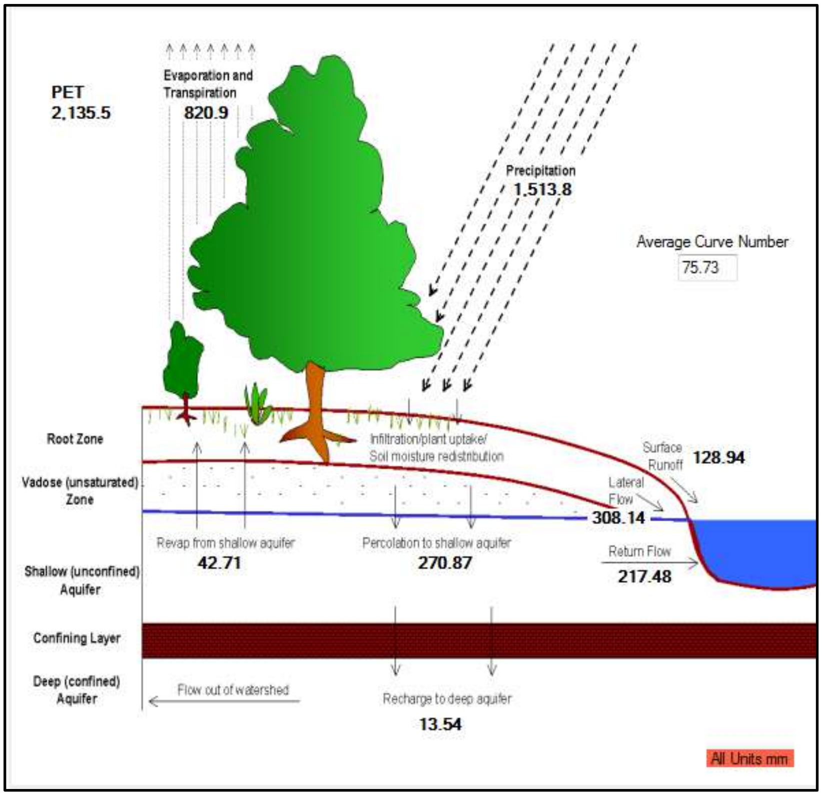

Figure 5. 15 Water balance for the Bosque Olimpia SWAT model using a regolith of 500 mm.

In addition to affecting the baseflow discharge in a watershed the regolith depth will also affect TP loadings since less organic phosphorous will be available and since percolation values are greater the soluble P surface runoff losses will be lower (see Figures 5.16 and 5.17 for the 2000 mm and 500 mm regolith depth landscape nutrient losses). This phenomenon can also account for the TP storm load dynamics seen in the Cupeyes river watershed, where higher percolation rates due to a shallow regolith, results in lower storm discharge and storm TP loading coefficients than in the Bosque Olimpia watershed.

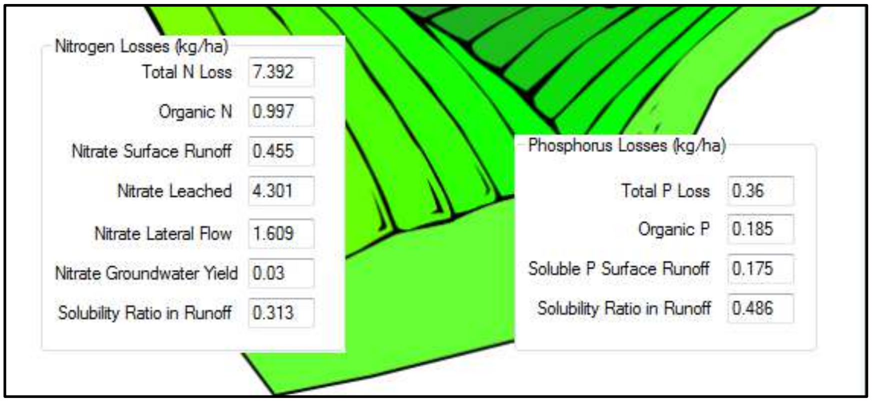

Figure 5. 16 Landscape nutrient losses for the Bosque Olimpia watershed model using a regolith of 2000mm.

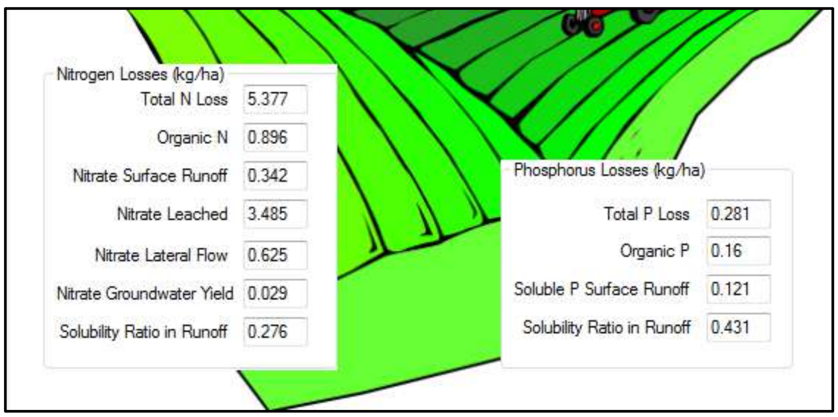

Figure 5. 17 Landscape nutrient losses for the Bosque Olimpia watershed model using a regolith of 500 mm.

After adding full soil profiles from SSURGO to the Bosque Olimpia watershed model the calibration of the model was not possible. Discharge and TP loadings values were always way below no matter what the values of the calibration parameters were. This indicates that a deeper soil profile will not necessarily provide more base flow in the watershed, as stated before, but will result in more realistic runoff simulations. In terms of the Cupeyes watershed the discharge calibration values for the objective function using the SSURGO database provided better results. The regolith depth in this watershed ranges from 20 to 150 mm (see SSURGO values in Appendix 13) so the shallow regolith definitely had a positive effect on the proper simulation of discharge.

5.3.2. Calibrated Parameters Discussion

After calibration and validation, calibrated parameters were introduced into the SWAT model again in order to compare the results in terms of the SWAT check tool. For Bosque Olimpia the SWAT check before calibration is shown in Figure 5.18. After calibration the results shown in Figure 5.19 were obtained. Note that the average CN increased from 75.73 to 85.61 which represents less infiltration (see percolation to shallow aquifer), much higher runoff that increased approximately 300% and less ET. For Cupeyes the original model without calibration is shown in Figure 5.20 while the calibrated simulation is shown on Figure 5.21, where it can be seen that in order to obtain a satisfactory calibration the average CN went from 74.44 to 46.5. This supports that the Cupeyes watershed has higher permeability and for which lower runoff is produced and therefore lower loadings. It is evident that the calibration of these models supports the hypothesis that the lower loadings in the Cupeyes watershed are due to water quantity differences and not to soil TP enrichment due to past agricultural activities in the watershed. Although other parameters were varied in the calibration process the parameter that resulted in better simulation and to which the model outputs were more sensible was the SCS Curve Number. The SCS CN was formulated to estimate discharge under different land uses and soil types with different hydrologic soil groups. The fact that varying this parameter resulted in good TP calibrated values also supports that it is the hydrologic properties of the watershed that causes the loading discrepancies between these two tropical forested watersheds. Soil surveys and therefore soil mapping units are usually not entirely comprehensive due to the complexity of soil sampling accessibility and heterogeneity of our landscapes. Sometimes these mapping units need to be updated to reflect the actual conditions found on field. This is why even when CN data was being drawn directly from the mapping units' changes had to be done to achieve attainable results.

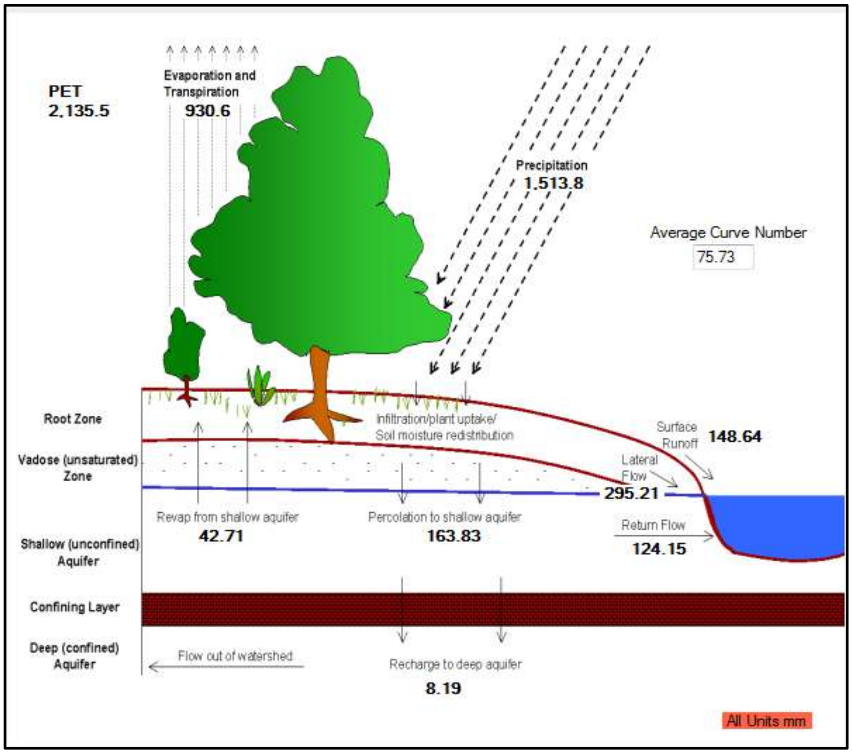

Figure 5. 18 SWAT hydrology check for the Bosque Olimpia WS before calibration.

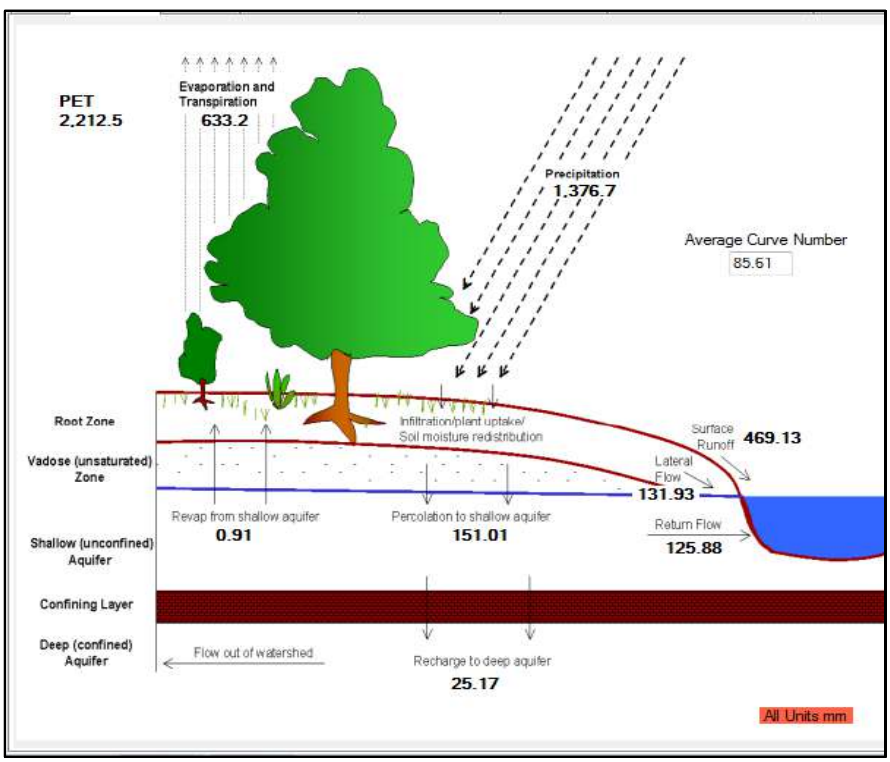

Figure 5. 19 SWAT hydrology check for the Bosque Olimpia WS after calibration.

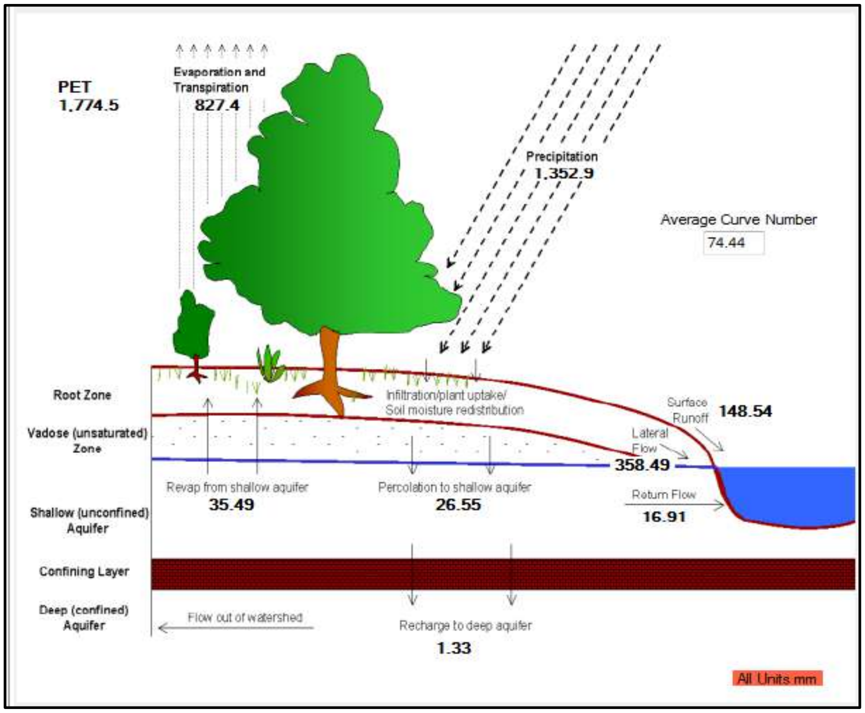

Figure 5. 20 SWAT hydrology check for the Cupeyes WS before calibration.

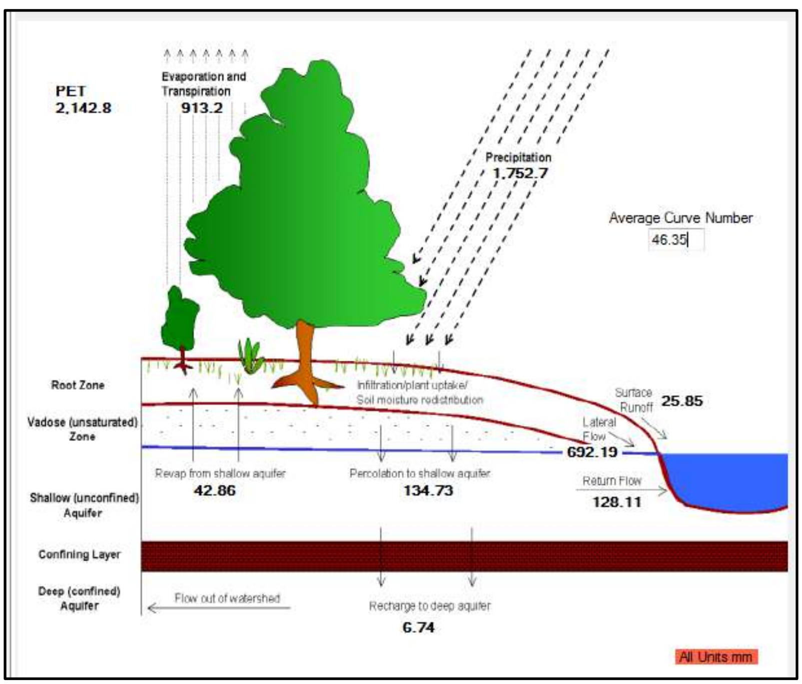

Figure 5. 21 SWAT hydrology check for the Cupeyes WS after calibration.

The calibrated Bosque Olimpia watershed model was used to simulate past agricultural activities in the region and its transition into a secondary forest in chosen sub basins of the watershed while others will remain under native land cover. This will result in a spatial and temporal record of the TP loadings to the river and their relationship with agricultural and forestry land uses. Results of the temporal modeling in Bosque Olimpia will be used to determine if there is a legacy of soil's phosphorous enrichment from past agricultural activities in the watershed that is still responsible to higher TP loadings from this watershed.

5.4. Long term simulations: Results and Analysis

5.4.1. Secondary vs Primary Forest Simulations

The modified SWAT version for the tropics was developed for SWAT 2009 and the weather data, which is the main driving variable, has a different format in SWAT 2012. For this reason SWAT 2009 was used for the long-term simulations although the calibration in section 4.4 was performed in SWAT 2012. In order to use calibrated parameters the "txtin" files for the calibrated version of the BO Model in SWAT 2012 was used to run the simulations in SWAT 2009. Figure 5.22 shows the simulation of the temporal distribution of yearly total soluble phosphorous to streams in kg/ha as a result of the agricultural land to forest transition along with the yearly runoff and total water yield (runoff + lateral flow) in millimeters. When analyzed the years 2012 to 2014 show a sudden drop in discharge and consequently in total phosphorous. This is due to the change from simulated to observed data as discussed below. As it is shown for the majority of years phosphorous loads respond directly to changes in water yield or discharge. However an increase in exported phosphorous is shown after the year 1954 when the kill operation is performed. This appears to respond to the all the "killed" biomass covering the forest floor, thus causing the exported phosphorous to decrease as a response to the cover or mulch which would break the water drop's erosive force. After this and following the simulation, in 1958 the residue has washed off and the soil protection is not there anymore. Instead bare soil and trees (which in this case were assumed to be 25 years old) planted since 1955 are in place. In the year 1960 the forest goes back to a 30 year old forest and returns to its current phosphorous export and enrichment trend. In the 1980s a similar situation seemingly takes place given that trees under the "mixed forest" land use were assumed to have a 50 year old life cycle (1980-1955=25yrs). This life cycle was taken directly from the data base and should have been changed to 100 years or more, but this explains the sudden drop and increase in exported phosphorous with the same dynamics as in 1954. Most importantly this doesn't seem to affect the trend observed from 1929 to 2011 years, which when standardized in terms of unit discharge there is no evident increase in phosphorous exports to stream. If the trend is expanded from 1928 (before agriculture started in the watershed) to 2014 and standardized in terms of discharge, an increase from $3.6x10^{-4}$ to $9.4x10^{-4}$ (kg/ha)/mm was evident. This is equivalent to increase of 2.6 times. At the beginning of the simulation a standing mixed forest was assumed, and no fertilizers had ever been applied to the land, this explains the low values in soluble phosphorous during the first years of simulation.

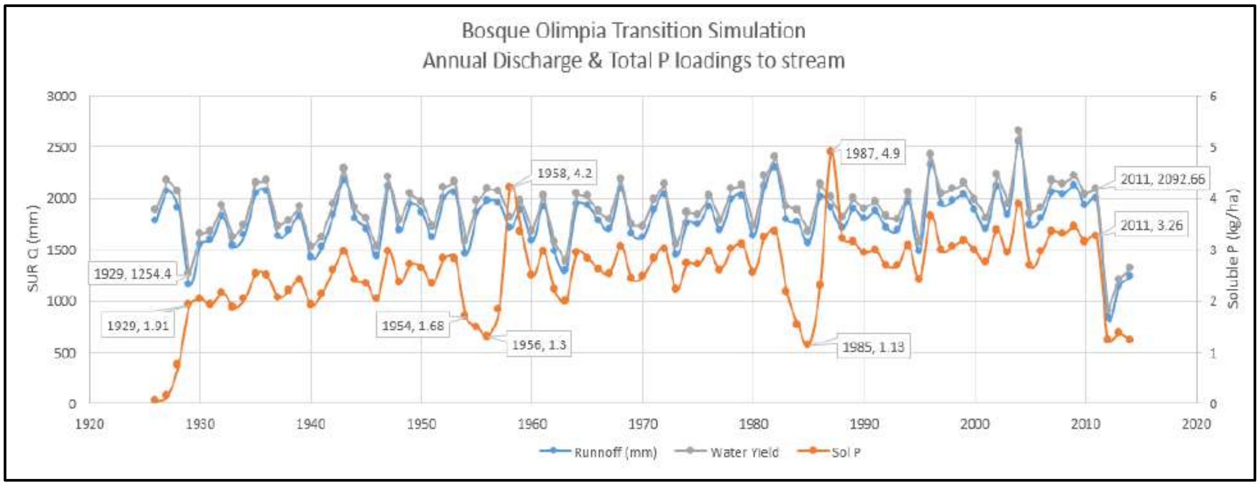

Figure 5. 22 Land use transition simulation: Annual discharge in mm and total soluble P to stream per unit of land in kg/ha.

Figure 5.23 shows the transition simulation temporal results (TRANS2009) and the forest simulation temporal results (FOR2009) for yearly exported mineral phosphorous out of reach in kilograms per year and water yield in millimeters. These values are different from the total phosphorous loadings to streams (figure 5.22) mainly in that in figure 5.22 the instream nutrient dynamics are not being considered. Figure 5.22 shows the soluble phosphorous being exported from the land to the stream in kilograms per hectare and figure 5.23 (MINP_OUTkg) shows the mineral phosphorous load in kilograms at the outlet of the watershed including instream transformation and transport of nutrients out of the watershed. Examining the transition graph we see a direct relation between water yield and phosphorous loadings except for the years where the kill operation took place just as discussed above. If the transition from the year 1928 to 2014 is considered and standardized in terms of discharge as above an increase from 0.08 kg/mm to 0.16 kg/mm and equivalent to double the amount of phosphorous exports. If we look at the period from 1933 to 2010, the mineral phosphorous loading dynamics are different from the one exposed in figure 5.22 in that an increase in the amount of exported phosphorous load is present. If we standardize this value by water yield unit we have an increase in mineral phosphorous concentration of 0.04 mg/L (see table 5.9). In terms of P loadings this is an increase of 213.1 kg in 73 years and as a result of only 25 years of intensive agriculture. Whereas in the forest simulation we have a decrease in concentration of 0.01 mg/L. When the final mineral phosphorous export is compared for the year 2014 in both simulations 120.7 kg were exported in the primary forest simulation and 206.1 kg in the transition to secondary forest simulation. This represents the effect fertilizers being locked into the soil for long periods of time until instream nutrient transformations and an accumulation of mineral phosphorus in the channel bed slowly transformed and exported the dissolved and suspended phosphorous out of the watershed.

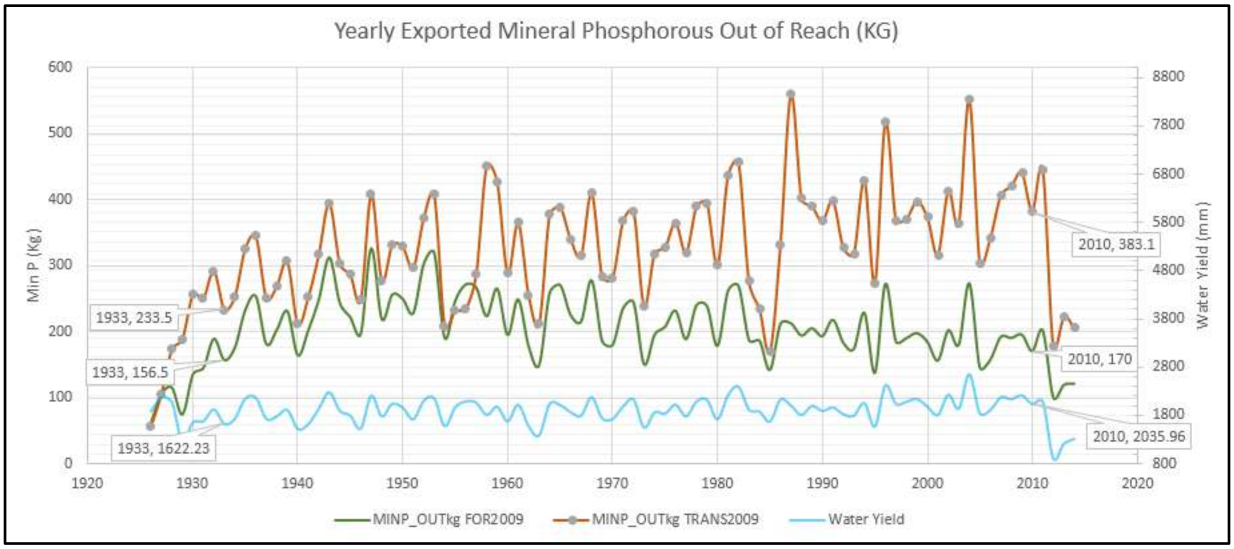

Figure 5. 23 Yearly exported mineral phosphorous out of reach kg/yr. and water yield in mm for transition and forest simulations.

Table 5. 9 Exported mineral phosphorous from watershed per unit of water yield

MINP_OUT (kg/mm)		
YEAR	***TRANS***	***FOR***
1933	0.143938	0.096472
2010	0.188167	0.083499

Figure 5.24 shows the long-term transition simulation results of organic phosphorous transported out of the river reach. As we can see in the simulated transition from agriculture to secondary forest versus the permanent primary forest, the organic phosphorous exported out of the watershed resulted in 4.6 kg higher at the end of the simulation as a result of the antecedent agricultural practices. The dynamics shown in the graphs suggests that mineral phosphorous enrichment in the form of fertilizers resulted in the recalcitrant fertility of soils and thus more vegetation production and organic matter was created in the long term resulting in higher phosphorous exports after the year 1954 for the transition

simulation compared to the forest simulation where apparently organic matter and therefore organic phosphorous exports were less.

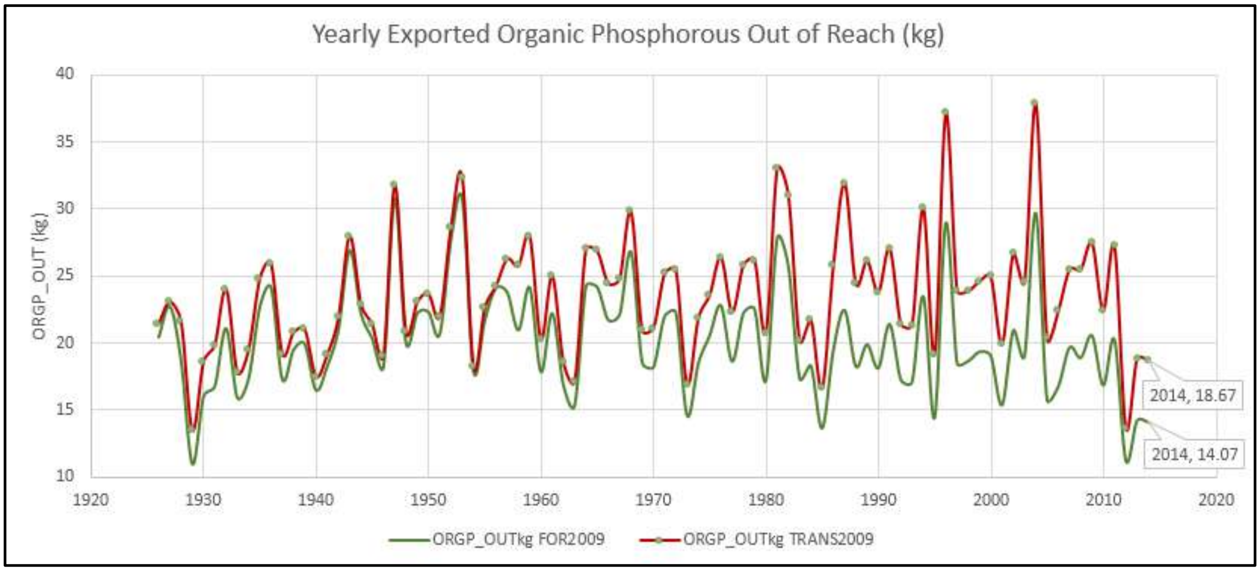

Figure 5. 24 Long term transition and forest simulation results of organic phosphorous transported out of the river reach.

If total phosphorous is considered (mineral + organic) at near the end of the simulation (year 2013) we have that 2.19 kg/ha/year were exported in the transition simulation while 1.20 kg/year/ha were exported for the primary forest simulation (see table 5.10). This suggests according to model results that phosphorous loadings to streams could double in secondary forest with antecedent agricultural activities. As seen in table 5.10 the average of the last three years the transition simulation (TRANS2009) resulted in 1.74 times the loading of the forest (FOR2009) simulation. This is also in accordance to results seen when calculated loadings from Cupeyes were compared with those of Bosque Olimpia.

Table 5. 10 Annual TP loads per unit area exported in transition and forest SWAT simulations.

YEAR	Annual TP Load per unit area (kg/ha)		Rate
	FOR2009	TRANS2009	TRANS/FOR
2012	1.01	1.73	1.72
2013	1.20	2.19	1.82
2014	1.22	2.04	1.67
		Average rate	**1.74**

5.4.2. Simulated vs Observed Precipitation

If we look at the water yield graph in Figures 5.22 and 5.23 in the last years 2012-2014 a sudden drop in discharge and in soluble phosphorous export is evident. This is due to the difference between the precipitation data from the weather generator and the observed data from the installed rain gages. Figure 5.25 shows the mean annual rainfall for the municipalities of Puerto Rico obtained from observed data from 1981 to 2010. If we look at figure 5.25 the municipality of Jayuya has a mean annual rainfall of 2,523 mm (99.3 in). This is in accordance with the mean simulated precipitation by the weather generator for the BO watershed model which is 2,547 mm. This means the weather generator is providing weather data corresponding to Jayuya accurately. Comparingly in figure 5.25 Adjuntas has 1,972 mm of average precipitation while observed average precipitation data from the two installed gages is 1,603 mm. There's a possibility that the forest canopy and wind direction affected the quality of the precipitation data, this has been the experience of the study group in several studies in forests of the island. Leaves and litter clog the receiving plate causing it to overflow and days to weeks of precipitation data gets unaccounted for. However, the values provided from the rain gages installed in BO Olimpia by the study group are much closer than the values simulated by the model. Also, both precipitation datasets are within a realistic range representing actual conditions in the forests of the island. Furthermore, Bosque Olimpia's watershed borders the municipality of Peñuelas that has a mean annual precipitation of 1,480 mm in the mountainous region. If we average Adjunta's and Peñuelas precipitation we have an average annual rainfall of 1,726 mm in the BO watershed, being even closer to the observed values from the rain gages. This can be seen clearly in appendix 6 where the location of the B.O. watershed can be seen along with the watershed ridge and the borders with adjacent municipalities. This analysis gives us a quantitative insight into the uncertainties in the weather data used for the model in calibrations and long-term simulations.

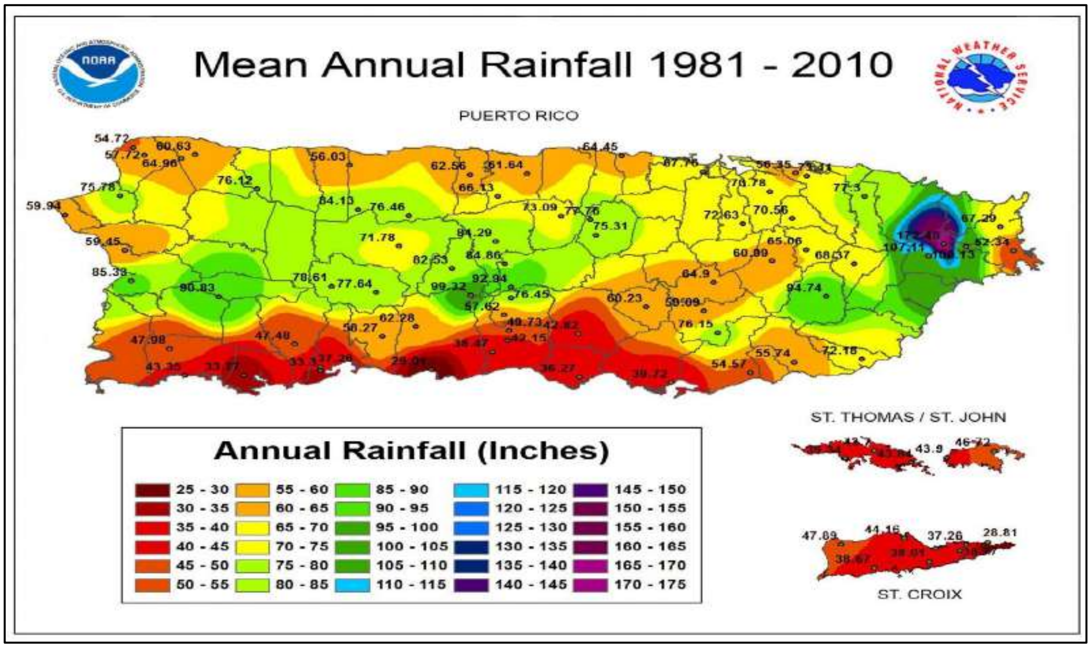

Figure 5. 25 NCDC precipitation normals from 1981 to 2010 (NCDC, 2010)

5.4.3. Modified SWAT vs Regular SWAT Simulation

Using the modified version of SWAT 2009 for the tropics by (Strauch & Volk, 2013a) the same scenarios were simulated with the purpose of comparing the possible differences in phosphorous loading output dynamics with the SWAT 2009. This simulation had the exact same data for both programs in each of the simulations, the only variable was the executable program used and the three additional parameters needed for running the modified SWAT version for the tropics (TROP). Figure 5.26 shows the annually exported mineral phosphorous out of reach for the four runs and the water yield output, which is the same for all 4 cases. The outputs shown for TRANS2009 and FOR2009 are the exact same outputs as in the past section. The new simulations are TRANSTROP and FORTROP where it is evident that the same general trend was found for both land use simulations. However, dynamics and values were higher for the simulations using the modified SWAT version. This higher nutrient export must be due to the continuous simulation of plant growth thus skipping the dormant season in the modified version. Whereas in the unmodified version dormant season created a small gap in the plant growth simulation process.

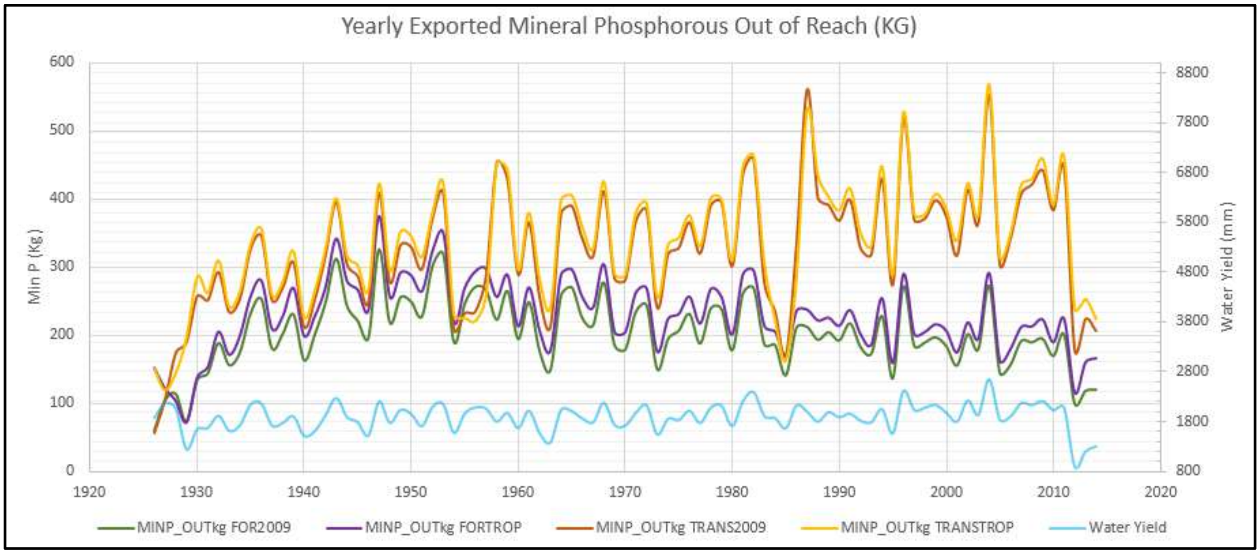

Figure 5. 26 Annually exported mineral phosphorous out of reach and water yield. Both simulations.

Transition simulations for TROP and 2009 versions for mineral and organic phosphorous are shown in Figures 5.27 and 5.28 respectively where if observed closely year by year changes in phosphorous loadings dynamics are reflected and can be justified by the change in canopy. For example, the continuous production of leaf litter maintains a higher amount of nutrients being exported out of the river reach as is the case in 1954 when the transition from farm to forest starts and such is the case in 2012 the first year simulated with observed precipitation data where the modified version exported 239.1 kg while the unmodified SWAT simulation exported 177.8 kg reflecting a difference of 35% between both simulations. Such is also the case for organic phosphorous dynamics between the two SWAT versions.

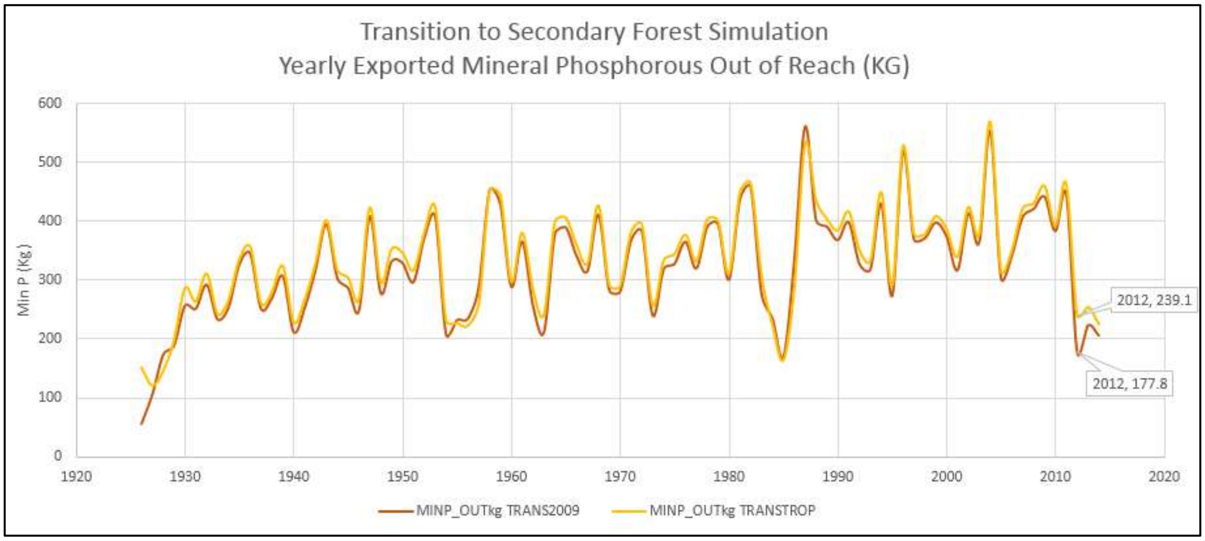

Figure 5. 27 Annually exported mineral phosphorous out of reach and water yield. Transition Simulation.

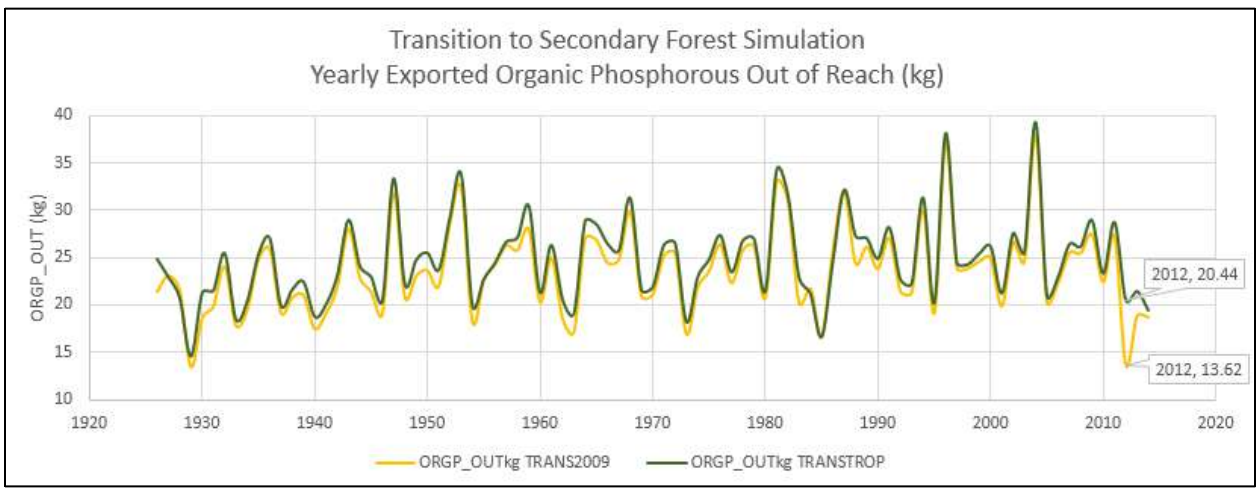

Figure 5. 28 Annually exported organic phosphorous out of reach and water yield. Transition Simulation.

Figure 5.29 shows the simulated annually exported mineral phosphorous out of the river reach for both of the permanent forest simulations. Here we can see that predominantly the modified version resulted in higher values of phosphorous exports. If the last year is analyzed a difference of 37% is found between simulations. As for organic phosphorous simulations in Figure 5.30 the values for the modified version were also higher with the year 2013 showing 21% of difference. These results also reflect the higher litter contribution coming from the modified version for the tropics.

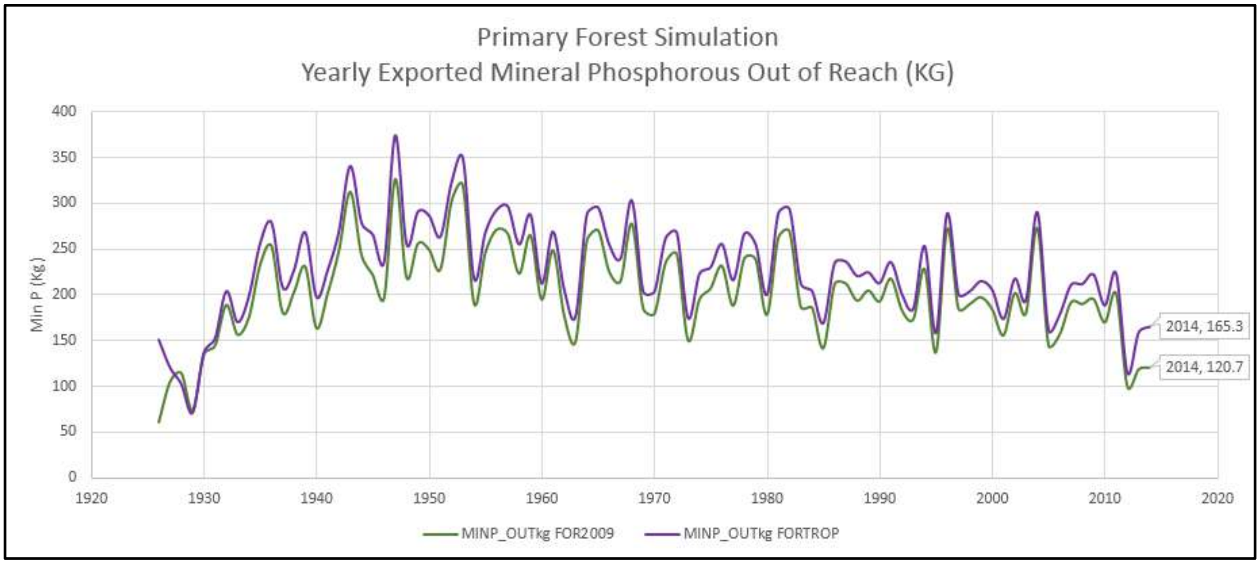

Figure 5. 29 Annually exported mineral phosphorous out of reach and water yield. Forest Simulation.

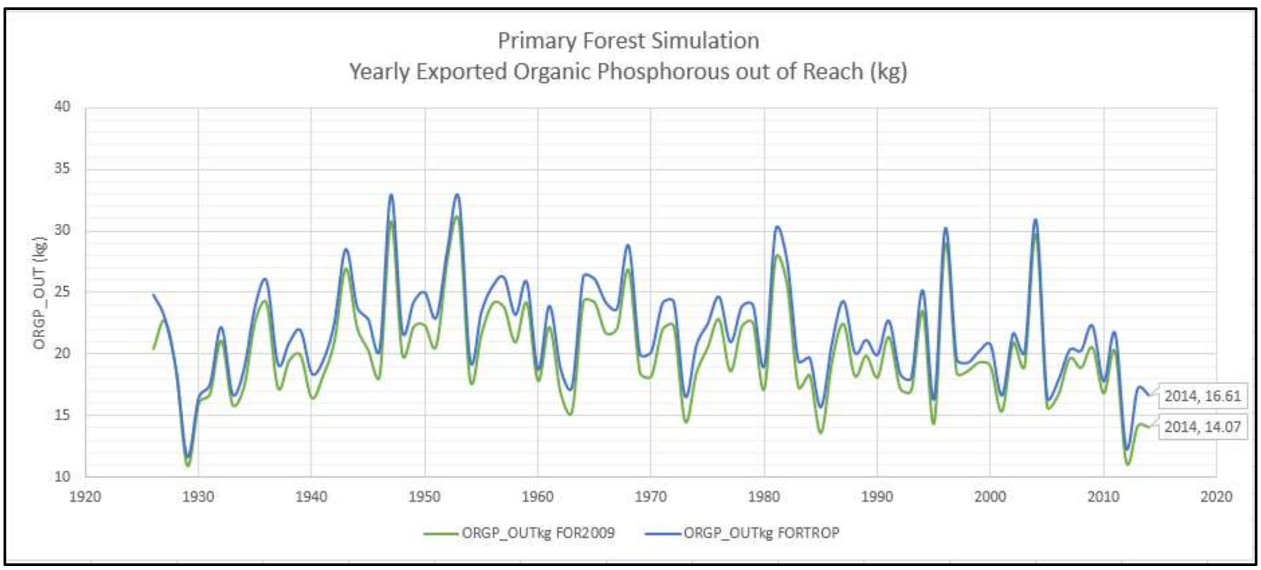

Figure 5. 30 Annually exported organic phosphorous out of reach and water yield. Forest Simulation.

Table 5.11 shows yearly results since the beginning of simulation (year 1926) to the year where farming operations ceased in the watershed (year 1953) and to the present. These results are shown for the 4 simulations the transition simulation with SWAT2009 (TRANS2009) and SWAT modification for the tropics (TRANSTROP) and the forest simulation for SWAT2009 (FOR_2009) and the modified version for the tropics (FOR_TROP). If we analyze this information we can see that precipitation (PREC) and potential evapotranspiration (PET) is the same in the 4 simulations. Yet other parameters such as lateral flow of water (LATQ), surface runoff (SURQ) and water yield vary depending on the simulation. This makes sense given that plant growth will affect water balance in the watershed. Also, we can see the sediment yield and nutrient loadings per unit area for each year. All these values refer to the total amount in a given year. First if we look at dissolved phosphorous we see that there is a notable increase between forest and transition simulations in the years 1953 and 2014. Yet sediment yields are very similar and do not account for this increase in dissolved phosphorous. SWAT does not provide a direct value of phosphorous entering the stream through lateral flow. However, there is also a notable increase in the NO3 contributed in lateral flow.

Table 5. 11 Yearly outputs from BO SWAT model simulations.

Simulation	UNIT	PREC	SURQ	LATQ	ET	PET	WATER	SED	NO3	NO3	P	P
	YEAR						YIELD	YIELD	SURQ	LATQ	SOLUBLE	ORGANIC
		(mm)	(mm)	(mm)	(mm)	(mm)	(mm)	(t/ha)	-------------(kg nutrient/ha)-----------------			
TRANSTROP	1926	2643.01	1989.19	41.06	689.66	1658.6	2030.32	2.93	18.55	0.17	0.43	1.49
	1953	2764.82	2105.75	63.09	588.89	1633.23	2179.26	3.42	116.16	1.1	2.91	1.32
	2014	1788.27	1318.05	41.72	398.35	2028.55	1359.79	1.98	92.89	1.79	1.4	0.71
TRANS2009	1926	2643.01	1776.62	105.7	785.85	1658.6	1882.39	2.64	6.04	0.2	0.05	1.31
	1953	2764.82	2052.61	90.4	676.83	1633.23	2153.57	3.33	96.59	3.49	2.83	1.26
	2014	1788.27	1233.22	78.95	399.59	2028.55	1312.19	1.86	34.52	1.44	1.23	0.71
FOR_TROP	1926	2643.01	1989.3	43.31	695.91	1658.6	2032.61	2.91	18.19	0.18	0.43	1.48
	1953	2764.82	2107.1	97.5	574.17	1633.23	2204.6	3.39	19.22	0.48	2	1.7
	2014	1788.27	1342.66	56.82	363.56	2028.55	1399.48	1.99	20.94	0.59	0.97	0.94
FOR_2009	1926	2643.01	1691.45	122.66	866.41	1658.6	1814.11	2.5	6.05	0.24	0.06	1.24
	1953	2764.82	1971.74	133	685.14	1633.23	2104.74	3.21	16.64	0.95	1.83	1.58
	2014	1788.27	1203.41	90.71	434.74	2028.55	1294.13	1.81	12.61	1.14	0.58	0.87

If we standardize this by volume of water, we have the same results (see table 5.12. These key outputs show an increase from the forest simulation to the transition simulation. Evidently, higher values of soluble phosphorous result from the transition simulation but not necessarily coming from exported sediments. When NO3 LATQ is standardized in terms of LATQ it also shows an increase exported nutrients. Meaning that a higher concentration of nutrients is entering the stream through lateral flow. This means that the increase is coming from leaching of nutrients locked in the soil as a result of the intensive fertilizer applications in the past operations of the watershed. Table 5.13 shows the rate between transition and forest simulation results. If we look at the years 1953 and 2014 in both SWAT versions, we see that dissolved phosphorous enrichment according to SWAT_TROP occurs after the agricultural activities take place in the watershed and basically stays the same until the end of simulation. Yet in the SWAT2009 regular version this rate is even bigger at the end of simulation and represents twice the amount of exported TP per year for the transition simulation. In terms of NO3 table 5.13 shows an increase of exported NO3 in both SWAT versions reinforcing that soluble phosphorous is entering the stream through lateral flow. This also suggest that the modified SWAT model results in improved simulation of phosphorous leaching into stream through lateral flow. This is given to the continuous and cumulative production of biomass that the modified SWAT version allows (see section 2.5). Part of this biomass will be turned into litter which will then be either decomposed or mineralized and finally slowly leached into the streams available as mineral and organic phosphorous.

Table 5. 12 Key outputs standardized by volume of water.

Simulation	Time	Sed Yield	P Soluble	NO3 LATQ
	Year	ton/ha/mm	kg/ha/mm	kg/ha/mm
TRANSTROP	1926	1.44E-03	2.12E-04	8.55E-05
	1953	1.57E-03	1.34E-03	5.22E-04
	2014	1.46E-03	1.03E-03	1.36E-03
TRANS2009	1926	1.40E-03	2.66E-05	1.13E-04
	1953	1.55E-03	1.31E-03	1.70E-03
	2014	1.42E-03	9.37E-04	1.17E-03
FOR_TROP	1926	1.43E-03	2.12E-04	9.05E-05
	1953	1.54E-03	9.07E-04	2.28E-04
	2014	1.42E-03	6.93E-04	4.39E-04
FOR_2009	1926	1.38E-03	3.31E-05	1.42E-04
	1953	1.53E-03	8.69E-04	4.82E-04
	2014	1.40E-03	4.48E-04	9.47E-04

Table 5. 13 Rate of transition vs forest simulation for key outputs.

Model Version	Year	TRANS/FOR Rates	
		P Soluble	NO3 LATQ
SWAT TROP	1926	1.00	0.94
	1953	1.47	2.29
	2014	1.49	3.09
SWAT 2009	1926	0.80	0.79
	1953	1.51	3.53
	2014	2.09	1.23

We also found that these simulations resulted in the most similar to the observed or calculated values. In Table 5.11 results for total phosphorous (mineral + organic) for the years 2012 and 2013 corresponding to the primary forest simulations are shown next to the observed values. Avg. % refers to the fraction of the observed values that these simulations represent or percent of equivalence. As it is evident the values corresponding to the modified version of SWAT were closer to the observed values suggesting that the modified SWAT simulation adjusted better to observed values. Results from the modified version resulted in average to a 91% of equivalence to the observed values while the regular SWAT version resulted in a 74%. This means a 9% error for the modified SWAT version versus a 26% error in the regular SWAT. The fact that the forest simulations resulted in better estimation of the actual values in Bosque Olimpia suggests that the effects of past agricultural activities in the watershed are small or equivalent to a 9% to 26% of what phosphorous loadings would have been in a primary forest. We could also argument that observed loadings were undercalculated given that in the transition simulations 130% and 160% of the observed values were obtained from the regular and modified SWAT versions respectively. However, using the regular SWAT version, a similar amount of percent error (26% and 30% for forests and transition respectively) was found on both simulations while in the modified SWAT version simulations (9% and 60% error for forest and transition respectively) a much more accurate value was obtained for the forest simulation.

Table 5. 14 Yearly total phosphorous loads for SWAT simulations and calculated load values.

Yearly Total Phosphorous Loads (KG)					
YR	**Forest Simulation**		**Transition Simulation**		
	SWAT2009	*TROPSWAT*	*SWAT2009*	*TROPSWAT*	*OBSERVED*
2012	111.21	127.08	191.42	259.54	136.032
2013	132.96	176.07	242.17	275.72	197.54
Avg. %	73%	**91%**	130%	160%	

6. Conclusions

The following conclusions can be drawn from this study:

1. Loading analysis results show that monthly and annual TP loading coefficients are definitely higher in the Bosque Olimpia watershed (the secondary subtropical forest) yet the difference in baseflow loadings is much larger (20 times) than in storm loadings (2 times).

2. Data analysis and modeling results suggest that the Cupeyes river watershed has higher percolation values than the Bosque Olimpia watershed. This seems to be due to a deeper regolith in the Bosque Olimpia watershed, which can successfully account for the percolation ratio; the water balance for the observed storm event and the water balance from the model show that the percolation to shallow aquifer, which is equivalent to delta storage, in Cupeyes (equivalent to the 500 mm regolith depth simulation) was 1.6 times the storage in Bosque Olimpia. The fact that the serpentinite outcrop has a fault before the outlet of the watershed accounts water quantity discrepancies.

3. The differences in storm TP loadings can be due to the hydrologic and hydraulic characteristics of the watershed and not to the soil TP concentrations. In fact, TP concentrations in composite samples taken during storm events were similar, being 0.22 mg/L in Cupeyes and 0.29 mg/L in Olimpia. Yet the storm hydrograph volume by unit area (in inches) in the Cupeyes watershed corresponded to a maximum of 40% of the total precipitation depth whereas in the Bosque Olimpia the storm hydrograph corresponded to almost 100% of the total precipitation. Section 5.3.1 successfully shows that the regolith depth will directly affect overland TP loading coefficients, yet it does not represent the same magnitude as in the annual TP Storm loading coefficient calculations. A possible reason is that other factors such as the watershed slope and soil are not being considered in said analysis.

4. Model performance was satisfactory for both watersheds given the available data, time frame and geomorphological complexity. Better results could've been attained if the observed data (weather and discharge) wasn't so limited and had a lower grade of uncertainty. Also, the difficulty of measuring flows in steep rocky river beds due to turbulence represents a higher grade of uncertainty in observed discharge measurements. Such is the case in Bosque Olimpia where observed discharge values were always above simulated discharge values. Still NS values of 0.07 and 0.63 for discharge and TP respectively were achieved for the Bosque Olimpia watershed. Calibrated parameters respond to the characteristics observed in the hydrologic analyses and observed geomorphological features of each watershed. These calibrated parameters represent characteristic features of these forested watersheds in Puerto Rico which

help improve our understanding of the natural processes occurring in forested tropical watersheds, in the island of Puerto Rico and other places with similar backgrounds.

5. The effect of past agricultural activities could still be present in the soil and could be affecting TP loadings in the watershed only that not at the same extent as expected. The statistical analysis and calibrations showed that storm TP dynamics are being affected by the watershed physical properties, hydraulics and aquifer recharge/storage. Parameters in each of the calibrated models respond to the hypotheses based on the observed hydrologic and water quality data. The higher permeability in the Cupeyes watershed (with a calibrated composite CN of 45) along with the elongated shape of the watershed results in lower TP loadings even when both watersheds have essentially similar weather, land cover, slopes, and soils. Another characteristic of the Cupeyes watershed that results in higher permeability is the depth of the regolith which was integrated into the model and resulted in better simulations. Even when the model results were acceptable in both watersheds the TP loadings in Cupeyes seemed to be overestimated by the model during storm events. This could be due to the condition of the watershed given that the shallow regolith will not provide so much sediment for erosion as the model is estimating. The analyses discussed in section 5.2 resolve a great deal on the discrepancies between these two watersheds.

6. Simulations for the historically forested watershed and the transition to secondary forest clearly show a different export trend especially after the end of agricultural activities in the watershed on 1954 where the historical forest simulation slowly decreases the exported phosphorous out of reach concentration 0.01 mg/L and the transition secondary forest increases the exported phosphorous out of reach concentration 0.04 mg/L during the same time period of 73 years (see Figure 5.23). Also, when compared to the dynamics of the exported soluble phosphorous from land, it shows that apparently soil phosphorous reached a maximum (no increase in exported phosphorous by unit discharge is shown) and that phosphorous exports to receiving waters increased from 1.5 to 2 times. According to results discussed in section 5.4.3 the increase in dissolved phosphorous could be due to lixiviated phosphorous entering the stream as lateral flow. Soil phosphorous enrichment also appears to have happened because when the dynamics of phosphorous exports are compared the transition simulation is always higher than the historical forest simulations. However, the increase in exported phosphorous from land reaches a maximum in 1933 and basically stays there for the rest of the simulation. At the end of the simulation we can clearly evidence the magnitude of the contribution of the antecedent agricultural activities in the watershed. An increase from 1.15 to 2.35 kg/ha/year was shown from the historical forest simulation to the transitional secondary forest. This is in accordance with what we found in the observed data between

the Cupeyes and Bosque Olimpia watersheds where the TP loadings have twice the magnitude in the secondary forest.

7. Results for the modified version of SWAT showed that simulating the plant growth dynamics based on available water instead of using solely heat units will have an effect of up to 35% in the transition simulation and 37% in the forest simulation to the exported phosphorous out of reach and therefore in the results of water quality simulations using the SWAT. These simulations also show that the effects are more evident when natural long-term growth is simulated as in the case of the primary forest simulation. This makes sense given that nutrient dynamics will depend more on the organic matter being produced by the plant growth module in the form of residue. For instance, having higher lateral contribution of phosphorous through lateral flow can will be an effect of accelerated growth and litter contribution. Litter will turn into mineral P through mineralization and then contribute to the active phosphorous pool to be leached into the stream. In section 2.5 authors prove that the modified SWAT version simulates cumulative biomass production and litter contribution better than the regular SWAT in tropical climates. We can also see that the best results in terms of having similar annual loads were achieved using the modified SWAT version with a 91% of equivalence to the observed values. Interestingly the simulations that achieve the closest values to the observed ones are the ones corresponding to the historical forest simulation. However, the difference between the final values of total phosphorous loads for the historical forest and transition simulation suggest the same increase in TP loads as the observed values from Cupeyes and Bosque Olimpia. This evidently is related to the fact that the model was calibrated to provide results as close as possible to the observed values under a mixed forest land use and with the actual soil series that all simulations have with no alterations in their chemical composition, meaning no fertilizer application.

All this implies that the fact that both the simulations and the observed values resulted in double the amount of annual phosphorous loadings when historical and secondary forest with antecedent agricultural activities where compared shows that past agricultural activities most probably have this actual effect of recalcitrant enrichment of exported phosphorous from the river reach. This also means that the argument that simulations with the modified version of SWAT for the tropics provided better results is valid because it basically improved the calibration that had been done using that exact soil series, land use and climate data. Also, being able to obtain similar results with observed values and simulated values means the SWAT model successfully simulates the main driving processes for phosphorous cycling in soils and loadings to waters. That SWAT can be successfully employed to simulate the effect to water quality of changes in land use and/or management activities related to plant growth in forested tropical watersheds.

The work performed on this investigation is key on finding the effects of past agriculture on secondary forested watersheds in Puerto Rico. Also, it provides a methodology for finding the long-term effects using the simulation capabilities of SWAT. This kind of long term simulation using SWAT, to my knowledge, has never been done in the island of Puerto Rico for which it provides a novel investigation. More importantly it provides evidence of the nutrient enrichment effect of past agricultural activities on our secondary forests for which it should be considered to perform further investigations and move forward studies to the establishment of a comprehensive nutrient criteria for the island. Finally knowing that using the modified version for the tropics will impact long term nutrient simulation results is of key importance. Further studies should be performed addressing the specific elements parameters and mechanisms which contribute to the difference in nutrient export dynamics.

Bibliography

Abbaspour, K. C. (2014). *SWAT-CUP 2012 Calibration and Uncertainty Programs - A User Manual.*

Arnold, J.G.,Kiniry, J.R., Srinivasan, R.,Williams, J.R.,Haney, E.B., S. L. N. (2011). *SOIL AND WATER ASSESSMENT TOOL INPUT/OUTPUT FILE DOCUMENTATION*

Arnold, J., & Moriasi, D. (2012). SWAT: MODEL USE, CALIBRATION, AND VALIDATION. *Transactions of the …*, *55*(4), 1491–1508. Retrieved from http://swat.tamu.edu/media/70993/azdez.asp.pdf

Asner, G. P., Scurlock, J. M. O., & Hicke, J. a. (2003). Global synthesis of leaf area index observations : *Global Ecology & Biogeography*, *12*(2003), 191–205. http://doi.org/10.1046/j.1466-822X.2003.00026.x

Bedient, P. B., Huber, W. C., & Vieux, B. E. (2012). *Hydrology and floodplain analysis*. Upper Saddle River. Pearson.

Buss, H. L., Mathur, R., White, A. F., & Brantley, S. L. (2010). Phosphorus and iron cycling in deep saprolite, Luquillo Mountains, Puerto Rico. *Chemical Geology*, *269*(1–2), 52–61. http://doi.org/10.1016/j.chemgeo.2009.08.001

Chow, 1959. Chow, V. T. (1959). Open-channel hydraulics. New York: McGraw-Hill.

Cumming, J.R., Weinstein, L.H., 1990. Utilization of AlPO4 as a phosphorus source by ectomycorrhizal Pinus rigida mill. seedlings. New Phytol. 116, 99–106.

Evans-White, M. a, Haggard, B. E., & Scott, J. T. (2013). A review of stream nutrient criteria development in the United States. *Journal of Environmental Quality*, *42*(4), 1002–14. http://doi.org/10.2134/jeq2012.0491

Farfan, . V. F, & B, U. J. (2007). Descomposición de la hojarasca y liberación de nutrientes de Coffea arabica, Cordia alliodora, Pinus oocarpa y Eucalyptus grandis, en sistemas agroforestales con café. *Cenicafé*, *58(1)*(1), 20–39.

Fetter, C. w. (2001). Applied Hydrogeology - Fetter 4th Edition.pdf.

Fuka, D. R., Walter, M. T., Macalister, C., Degaetano, A. T., Steenhuis, T. S., & Easton, Z. M. (2014). Using the Climate Forecast System Reanalysis as weather input data for watershed models. *Hydrological Processes*, *28*(22), 5613–5623. http://doi.org/10.1002/hyp.10073

Gier, P. De. (2015). The impact of coffee-based agroforestry on the hydrology of the upper Genale River basin, Sidama Zone, Ethiopia., (September).

Gould, W., Alarcón, C., Fevold, B., Jiménez, M., Martinuzzi, S., Potts, G., … Ventosa, E. (2008). The Puerto Rico Gap Analysis Project. Volume 1: Land cover, vertebrate species distributions, and land stewardship. *Gen. Tech. Rep. IITF-GTR-39.*, (March), 165 p.

Harmsen, E.W., Cruz, P.T. and Mecikalski, J.R. (2014) 'Calibration of selected pyranometers and satellite derived solar radiation in Puerto Rico', Int. J. Renewable Energy Technology, Vol. 5, No. 1, pp.43–54.

Jeong, C., Joo, K., Lee, W., Shin, H., & Heo, J.-H. (2013). Estimation of optimal grid size for radar reflectivity using a SWAT model. *Journal of Hydro-Environment Research*, *8*(1), 20–31. http://doi.org/10.1016/j.jher.2013.05.005

Jones, C.A. C.V. Cole, A.N. Sharpley, and J.R. Williams. 1984. A simplified soil and plant phosphorus model. I. Documentation. Soil Sci. Soc. Am. J. 48:800-805.

Kennaway, T. (2007). The Forest Types and Ages Cleared for Land Development in Puerto Rico, *1991*(4), 356–382.

Liersch, Stefan (2003). The Program pcpSTAT. Berlin (stliersh@freenet.de)

Kleinman, P. J. a., Sharpley, A. N., McDowell, R. W., Flaten, D. N., Buda, A. R., Tao, L., … Zhu, Q. (2011). Managing agricultural phosphorus for water quality protection: principles for progress. *Plant and Soil*, *349*(1–2), 169–182. http://doi.org/10.1007/s11104-011-0832-9

Majumdar, D. (2003). The Blue Baby Syndrome. *Resonance*, *8*(10), 20–30. http://doi.org/10.1007/BF02840703

Martinez, G., Sotomayor, D., & Perez, L. (2010). Evaluation of the land-use legacy effect of agricultural practices on the water quality of streams from forest watersheds of Puerto Rico. *Mc Intire Stenis MS-17 Project Proposal*. Retrieved from hc

Moriasi, D., Arnold, J., & Liew, M. Van. (2007). MODEL EVALUATION GUIDELINES FOR SYSTEMATIC QUANTIFICATION OF ACCURACY IN WATERSHED SIMULATIONS. *Transactions of the ASABE. 2007 American Society of Agricultural and Biological Engineers*, *50*(3), 885–900. Retrieved from http://swat.tamu.edu/media/1312/moriasimodeleval.pdf

Nash, J. E. and J. V. Sutcliffe (1970), River flow forecasting through conceptual models part I — A discussion of principles, Journal of Hydrology, 10 (3), 282–290.

Naumov, A. (2005). Multi-Criteria Validation of the SWAT Hydrologic Model in a Small Forested Watershed.

Neitsch, S., Arnold, J., & Kiniry, J. (2011). Soil & Water Assessment Tool Theoretical Documentation Version 2009. *Texas,* Retrieved from http://repository.tamu.edu/handle/1969.1/128050

NOAA. 2012. Atlas 14 Point precipitation Frequency Estimates. hdsc.nws.gov/hdsc/pfds

NCDC (2010) https://www.weather.gov/images/sju/hydrology/2010_ncdc_precip_normals_PR_USVI.jpg

Nolan, B. K. M., & Shields, R. R. (2000). Measurement of Stream Discharge by Wading Water Resources Investigations Report 00-4036.

NRCS. 1986. Urban hydrology for small watersheds. Tech. Release No. 55. USDA. June 1986.

NRCS 2010. www.websoilsurvey.nrcs.usda.gov

Ouyang, W., Skidmore, A. K., Toxopeus, a. G., & Hao, F. (2010). Long-term vegetation landscape pattern with non-point source nutrient pollution in upper stream of Yellow River basin. *Journal of Hydrology*, *389*(3–4), 373–380. http://doi.org/10.1016/j.jhydrol.2010.06.020

Ouyang, W., Wang, X., Hao, F., & Srinivasan, R. (2009). Temporal-spatial dynamics of vegetation variation on non-point source nutrient pollution. *Ecological Modelling*, *220*(20), 2702–2713. http://doi.org/10.1016/j.ecolmodel.2009.06.039

Pereira, A. R., Camargo, M. B. P. de, & Villa Nova, N. A. (2011). Coffee crop coefficient for precision irrigation based on leaf area index. *Bragantia*, *70*(4), 946–951. http://doi.org/10.1590/S0006-87052011000400030

Puerto Rico GAP Analysis Project (PRGAP), 2006, PRGAP Landcover: USDA Forest Service, International Institute of Tropical Forestry, Río Piedras, Puerto Rico.

Richter, D.D., Allen, H., Li, J., Markewitz, D., Raikes, J., 2006. Bioavailability of slowly cycling soil phosphorus: major restructuring of soil P fractions over four decades in an aggrading forest. Oecologia 150 (2), 259–271.

Rorabaugh, M.I. 1964. Estimating changes in bank storage and ground-water contribution to stream flow. International Association of Scientific Hydrology 63:432-41

Shen, J., Yuan, L., Zhang, J., Li, H., Bai, Z., Chen, X., … Zhang, F. (2011). Phosphorus dynamics: from soil to plant. *Plant Physiology*, *156*(3), 997–1005. http://doi.org/10.1104/pp.111.175232

Singh, J., & Knapp, H. (2005). Hydrological modeling of the iroquois river watershed using HSPF and SWAT1. *JAWRA Journal of the.*. Retrieved from http://onlinelibrary.wiley.com/doi/10.1111/j.1752-1688.2005.tb03740.x/abstract

Sloan, P.G., I.D. Morre, G.B. Coltharp, and J.D. Eigel. 1983. Modeling surface and subsurface stormflow on steeply-sloping forested watersheds. Water Resources Inst. Report 142. Univ. Kentucky, Lexington.

Smith, R.A., R.B. Alexander, and G.E. Schwarz. 2003. Natural background concentrations of nutrients in streams and rivers of the conterminous United States. Environ. Sci. Technol. 37:3039–3047. doi:10.1021/es020663b

Sotomayor Ramírez, D., & Pérez Alegría, L. R. (2012). Nutrient Management and Sediment Source Identification in Lajas Valley Agricultural Reserve and Guánica Watershed. Final report of project, perfomed under contract with National Fish and Wildlife Foundation contract number 210-0069-017. 68pp.

Srinivasan, Pierre, G.-M., Veith, T. L., Gburek, W. J., & Steenhuis, T. S. (2005). Watershed scale modeling of critical source areas of runoff generation and ph. *Journal of the American Water Resources Association*, *41*(2), 361–375.

Station, A. R. (1997). Conjunto tecnológico para la producción de café. *University of Puerto Rico Mayaguez*.

Strauch, M., & Volk, M. (2013). SWAT plant growth modification for improved modeling of perennial vegetation in the tropics. *Ecological Modelling*, *269*, 98–112. http://doi.org/10.1016/j.ecolmodel.2013.08.013

USACE. 2010. HEC_HMS, HEC_RAS. United States Army Corps of Engineers. www.hec.usace.army.mil

USEPA. (2007). National Nutrient Strategy Nutrient Policy Data.

Vadas, P.A., Krogstad, T., A. N. S. (2006). Modeling Phosphorus Transfer between Labile and Nonlabile Soil Pools : Updating the EPIC Model.

Veve, T. D., & Taggart, B. E. (1996). Atlas of ground-water resources in Puerto Rico and the U.S. Virgin Islands. Water-Resources Investigations Report 94-4198. US Geological Survey.

Vivoni, E. E. (n.d.). La Olimpia - historia oral de La Olimpia. Oraganizacion Casa Pueblo.

Wischmeier, W. H., & Smith, D. D. (1978). Predicting rainfall erosion losses: A guide to conservation planning. Washington, D. C: United States Department of Agriculture.

Yuan, Y., & Lincoln, W. H. (2016). Evaluation of Soil Erosion and Sediment Yield From Ridge Watersheds Leading to Guánica Bay , Puerto Rico , Using the Soil and Water Assesment Tool. *Soil Science*, *181*(7), 315–325. http://doi.org/10.1097/SS.0000000000000166

Appendix

1. Hydrologic Analysis

Runoff hydrographs for both river systems were developed with computerized mathematical model HEC-HMS (USACE, 2010). The Soil Conservation Service Method was used to estimate peak discharge for storm events with recurrence intervals of 1, 2, 5, 10, 25, 50, and 100 years. This method is widely used for estimating discharge given a certain rain event. HEC-HMS requires a (i) basin model, (ii) meteorological model and (iii) control specification model. The control specification model simply defines the period of time or time frame for the simulation; a lapse of 48 hours was chosen for both simulations.

a. Basin Model

In the basin model the sub-basins, reaches and outlets must be added and combined in a logistical manner. The watersheds were represented by only one sub-basin given that the areas are relatively small and the rainfall within the area will drain into a single outlet at the water quality (WQ) monitoring station. The outlet coordinates of each watershed under study are the same as the ones shown above in section 4.1.1 for the water quality monitoring stations. The area of both watersheds at the point of analysis was obtained from the watershed delineation performed using hydrology tools within the Toolbox provided with ESRI's ArcMap. The Cupeyes watershed has a catchment area of 4.81 km^2 and Bosque Olimpia 1.09 km^2 (Figures 1 and 2). In both models the Soil Conservation Service (SCS) Curve Number (CN) method (NRCS, 1986) was used as the precipitation loss method and the SCS unit hydrograph was used as the transform method.

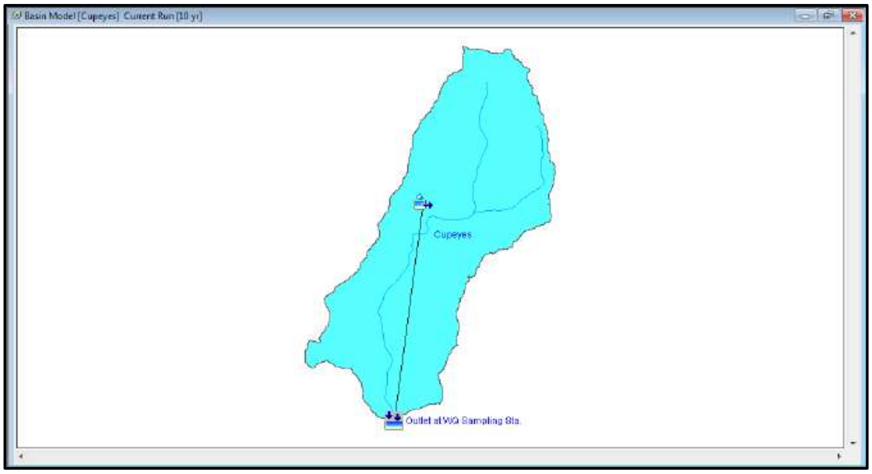

Figure 1. Cupeyes watershed basin model in HEC-HMS (USACE, 2010).

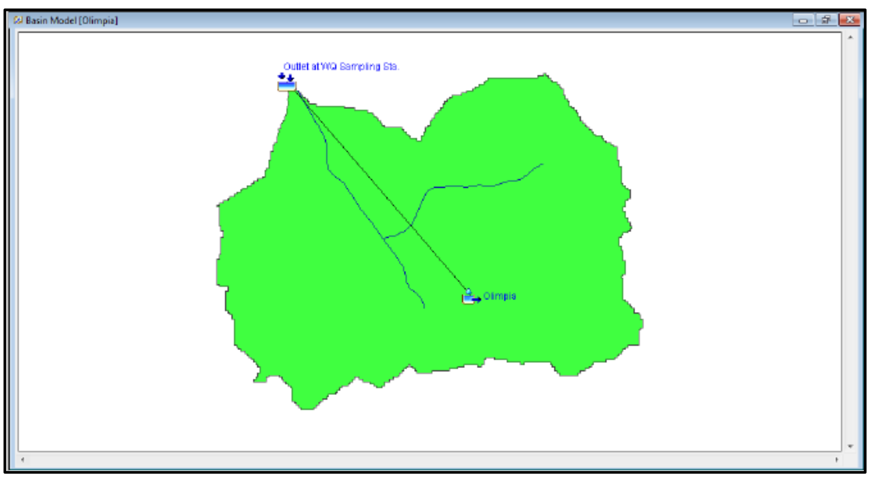

Figure 2. Bosque Olimpia watershed basin model in HEC-HMS (USACE, 2010).

i. Hydrologic Soil Groups (HSG's).

The hydrologic soil groups within the watershed are key parameters in determining the SCS curve number. It describes runoff potential as a function of the soil type, which depends mainly on the soil's texture. Figures 3 and 4 show the HSG's in the Cupeyes and Bosque Olimpia watersheds respectively. A HSG rated A has a low surface runoff potential while a rated D has a high surface runoff potential.

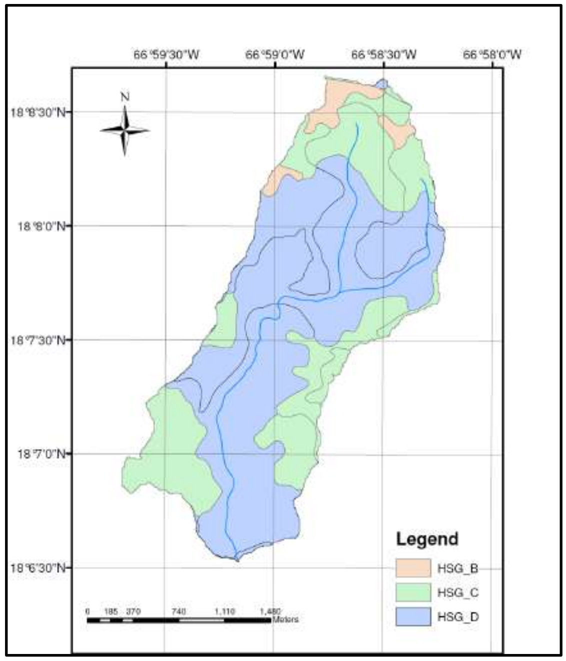

Figure 3 HSG's in the Cupeyes watershed (NRCS, 2010).

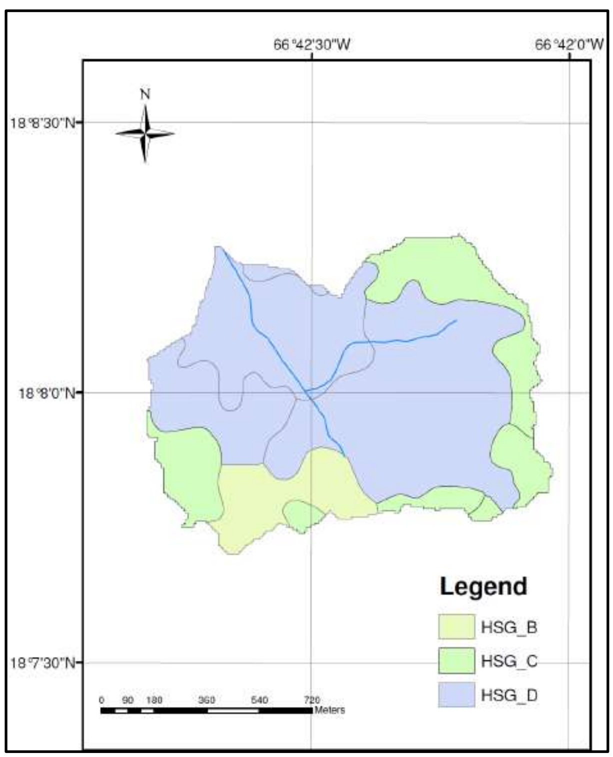

Figure 4 HSG's in the Bosque Olimpia watershed (NRCS, 2010).

ii. Curve Number (CN) assignment.

The curve number is assigned depending on the land use distribution and the HSG of an area. CN was calculated from land use cover cropped from the PRGAP project (PRGAP, 2006), the NRCS soils shapefile for the study area (NRCS, 2010) and their corresponding hydrologic soil groups (HSG). This value was computed for the pervious areas; high and low density urban developments were considered as impervious area. Impervious area percent were 0.59% and 0.031% in the Cupeyes and Bosque Olimpia watersheds, respectively. Weighted CN value for each watershed was calculated using Equation (1). Tables 1 and 2 show the CN calculation for the Cupeyes and Bosque Olimpia watersheds, respectively.

$$\overline{CN} = \frac{\sum CN_i A_i}{\sum A_i} \quad (1)$$

Table 1. Weighted average composite CN calculation for the Cupeyes watershed

Land use	HSG	CN_PR	Area (m^2)	CN*Area
Forest and Groves	B	55	18050.57582	992781.6699
Forest and Groves	C	70	88549.08319	6198435.823
Forest and Groves	D	77	5691.419604	438239.3095
Forest and Groves	B	60	14480.48016	868828.8097
Forest and Groves	C	73	1064260.772	77691036.34
Forest and Groves	D	79	2525341.474	199501976.5
Grasses and Shrubs	B	56	23533.00212	1317848.119
Grasses and Shrubs	C	70	388735.5468	27211488.27
Grasses and Shrubs	D	77	280836.2919	21624394.48
Grasslands	D	84	4768.703866	400571.1248
Low density urban development	B	92	117678.0029	10826376.27
Low density urban development	C	94	101827.1017	9571747.555
Low density urban development	D	95	421.3007386	40023.57016
Weighted average CN --> 76.96				

Table 2. Weighted average composite CN calculation for the Bosque Olimpia watershed

Land use	*HSG*	*CN_PR*	*Area (m2)*	*CN*Area*
River Stream	*D*	*0.00*	*6360.568*	*0.0*
Forest and Groves	*B*	*55.00*	*2599.307*	*142961.9*
Forest and Groves	*B*	*60.00*	*101627.973*	*6097678.4*
Forest and Groves	*C*	*70.00*	*3403.933*	*238275.3*
Forest and Groves	*C*	*70.00*	*2603.094*	*182216.6*
Forest and Groves	*C*	*70.00*	*276.410*	*19348.7*
Forest and Groves	*C*	*73.00*	*56955.998*	*4157787.8*
Forest and Groves	*C*	*73.00*	*183610.364*	*13403556.6*
Forest and Groves	*D*	*77.00*	*18348.770*	*1412855.3*
Forest and Groves	*D*	*77.00*	*105172.144*	*8098255.1*
Grasses and Shrubs	*C*	*79.00*	*11.144*	*880.4*
Forest and Groves	*D*	*79.00*	*600780.573*	*47461665.2*
Low density urban development	*D*	*84.00*	*9600.253*	*806421.3*
			Total permeable area (m2) -> 1084989.961	*Σ 82021902.455*
Weighted average CN --> 75.60				

iii. Time of Concentration and Lag Time.

Time of concentration and lag time for each watershed were developed with the SCS Methods described in USACE 2010. The SCS lag time (t_L) for each sub-basin was calculated with Equation 2 and potential abstraction parameter (S) was calculated with Equation 3.

$$t_L = \frac{(L^{0.8} * (S+1)^{0.7})}{(1900 * y^{0.5})} \quad (2)$$

where, t_L is the lag time in hours, L is the hydraulic length of the watershed in feet and Y is the average land slope in percentage.

$$S=\left(\frac{1000}{CN}\right)-10 \quad (3)$$

where, S is the potential abstraction and CN is the SCS curve number.

The average slope for each watershed was obtained from the corresponding topographic contours downloaded from the PR Planning Board (PRPB, 2011). These values were 0.52 m/m and 0.43 m/m for Cupeyes and Bosque Olimpia respectively and were calculated with Equation 4 (USGS, 2012) using a contour interval of 50 m.

$$y = \frac{(length\ of\ contour\ lines, ft)(contour\ interval) * 100}{(watershed\ area, acres)(43560)} \quad (4)$$

where, y is the average watershed slope.

The hydraulic length of each basin was obtained from ArcGIS by tracing the longest path a drop of water will travel from the highest point to the basin outlet. These were 4.85 km. and 1.56 km. for Cupeyes and Bosque Olimpia, respectively. Figures 5 and 6 show these measurements in ArcGIS.

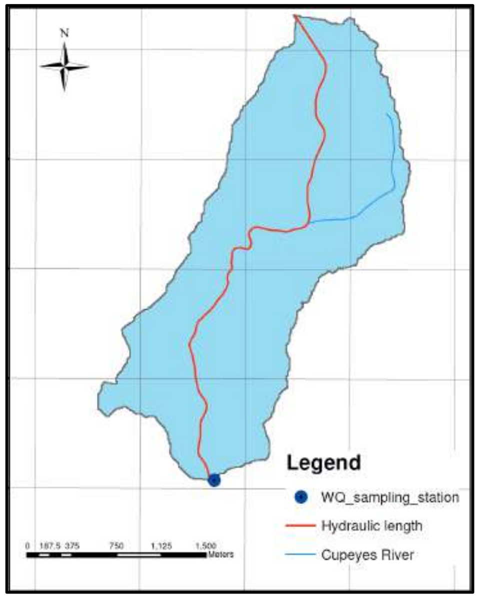

Figure 5 Hydraulic Length measurements for the Cupeyes watershed.

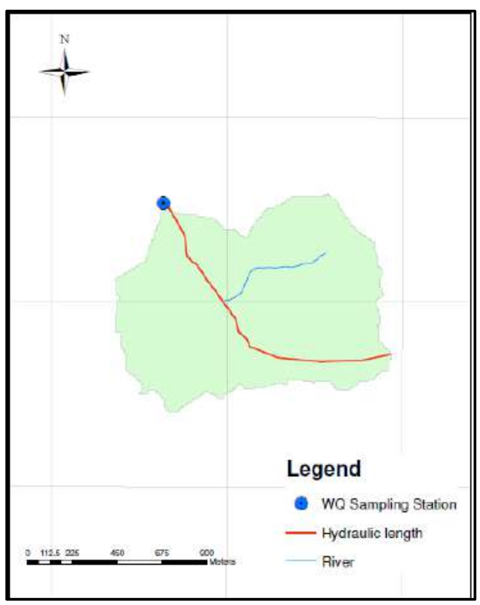

Figure 6 Hydraulic Length measurements for the Bosque Olimpia watershed.

iv. Basin Model Parameters

Using computed variables the lag time (t_L) for each sub basin was computed. In HEC-HMS the Soil Conservation Service loss method requires the curve number and impervious area for each sub basin, additionally the transform method requires the lag time in minutes. Table 4 shows the computed parameters along with the Lag time values; CN values, impervious area and lag time (minutes) for Cupeyes and Bosque Olimpia. These values were introduced into each model; lag time was computed using the computed composite CN values.

Table 3 Basin model parameters for the watersheds under analysis.

Basin	Cupeyes River	Bosque Olimpia
Basin Area (km2)	4.81	1.091
Average Slope (y)	0.52	0.43
Length to Devide (km)	52.15	16.83
Potential Abs. (S) mm	75.95	81.99
Initial abs (mm)	0.01	0.012
Impermeable Area (m2)	2.85	0.03
Impermeable %	0.59	0.59
Lag Time (hr.)	4.46	2.046
Lag time-t_l (min)	267.67	122.78
Weighted average CN	76.97	75.60

b. Meteorological model

In order for the program to compute an outflow "rain" has to be introduced to the program. For this the program provides several methods. The one used for this study is the SCS Storm where a 24-hr. dimensionless hydrograph is assumed. A Type II distribution was used and depths for recurrence intervals were obtained from the NOAA-Atlas 14 for Puerto Rico (NOAA, 2012). The Atlas 14 allows for the user to choose the coordinates for where the precipitation frequency estimates are desired, and it provides a table of point precipitation estimates in inches for different recurrences (from 1 to 1000 years) and durations. These estimates are based on gathered empirical data and statistical methods. In this analysis the duration was taken to be equal to the time of concentration (t_c) which in the SCS lag method is equal to 1.67 times the lag time. For the Cupeyes basin the time of concentration was equal to 7.45 hrs. and for Bosque Olimpia 3.41 hrs. Using these values the precipitation corresponding to recurrences of 1, 2, 5, 10, 25, 50, 100 years were obtained by interpolation. Values in mm are shown in Table 4 in the next section. The coordinates used were 18.1334°N, 66.9781°W for Cupeyes and 18.1338°N, 66.7063°W for Bosque Olimpia aiming to obtain estimates for the center coordinates of each WS. A copy of the Atlas 14 Point Frequency document for both locations is included in the Appendix 3.

c. Model Results

The main purpose of building this model is to obtain the maximum discharge at the watershed's outlet of each basin given various precipitation events at different recurrences. With these values it's possible to estimate the discharge that a certain known rainfall event will cause at the point of analysis. HEC-HMS computes a hydrograph, which is the product of a certain rain event given to the meteorological model and within the limits of the watershed. Figures 7 and 8 shows the computed hydrograph given a rain event with a recurrence of 10 years in the Cupeyes and Bosque Olimpia watersheds, respectively. Table 4 shows the precipitation and peak discharge for each of the corresponding recurrences in the both watersheds. This calculation assumes that all of the precipitation is homogeneously distributed among the whole watershed during each storm event.

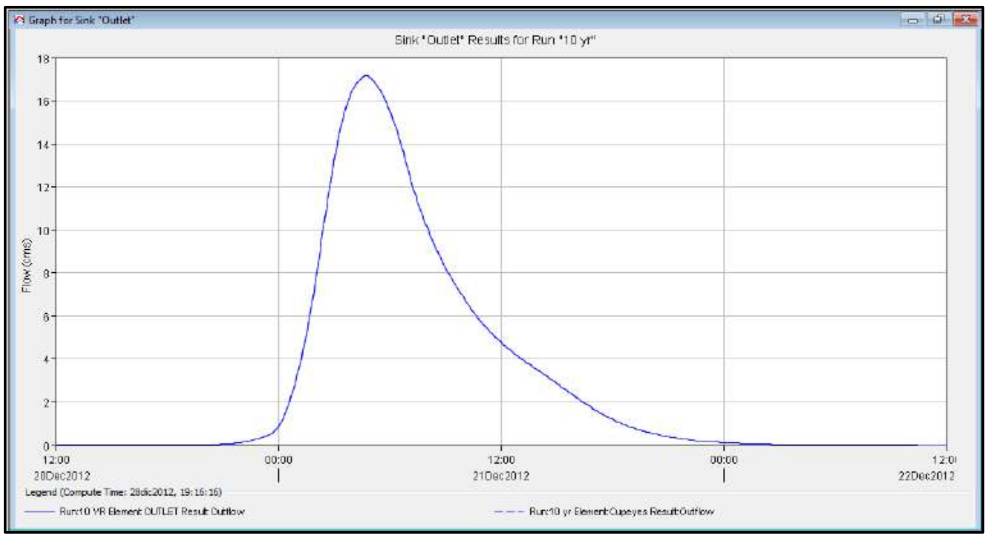

Figure 7 Computed runoff hydrograph at the sink outlet for the Cupeyes watershed (USACE, 2010).

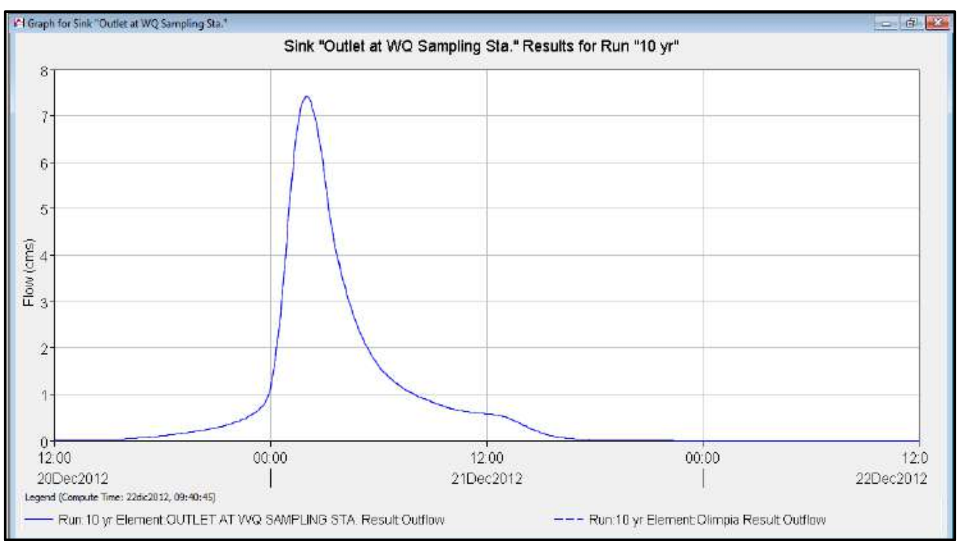

Figure 8 Computed runoff hydrograph at the sink outlet for the Bosque Olimpia watershed (USACE, 2010).

Table 4 Maximum discharges for design precipitation values.

Recurrence	Cupeyes		Bosque Olimpia	
	Precipitation (mm)	Peak Discharge (m3/s)	Precipitation (mm)	Peak Discharge (m3/s)
1	88.1	5.6	87.9	2.9
2	111.5	8.6	110.7	4.1
5	142.5	12.9	140.7	5.8
10	171.5	17.2	168.7	7.4
25	215.1	23.7	210.3	9.9
50	252.2	29.4	245.4	12.1
100	293.4	35.7	284.2	14.5

2. *Hydraulic Analysis*

The rating curve for each watershed was developed using a hydraulic model that routed the runoff hydrograph generated in the hydrologic model. Hydraulic analysis for a transect of approximately 25 m at Cupeyes and 40 m at Bosque Olimpia were assembled with U.S. Army Corps of Engineers model HEC-RAS (USACE, 2010). This model is widely used for flood plain analysis as well as many other applications where the change in water level at a given location is desired given a change in discharge and/or channel geometry.

a. *Geometric Data*

The geometric data of the river system is key in constructing a hydraulic model of any river system. Cross sections of both channels were surveyed using a total station SOKKIA SET 530R/R3. Coordinates used were State Plane projected in the North American Datum 1983, Puerto Rico 5200 and vertical datum GRS84. All the measurements were performed using surveyed data and AutoCAD 2013. Distances between the main channel and the left and right overbanks were measured between each cross section for both river reaches. For Cupeyes a plan view of the surveyed area is shown in Figure 9 along with the downstream reach, right overbank (RO) and left overbank (LO) measurements. Table 5 shows the measured values, which were introduced into the hydraulic model. An example of surveyed cross sections used for building the Cupeyes River reach in the model and data entered into the hydraulic model is available upon request. Cross-section data was entered looking downstream from left to right beginning at the downstream cross section.

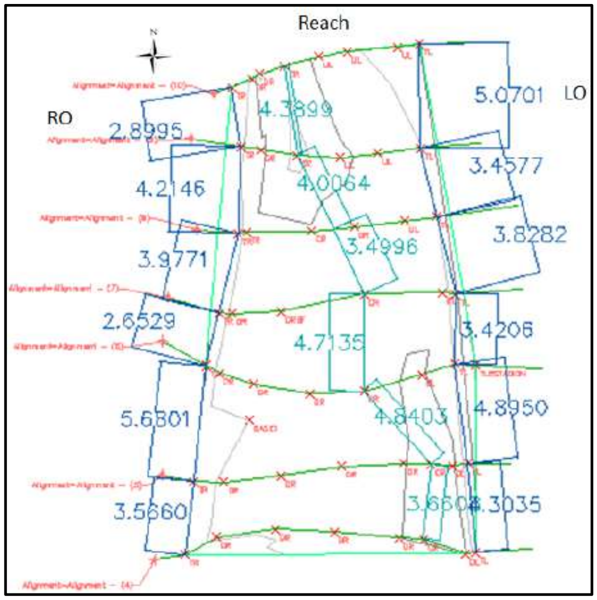

Figure 9. Surveyed area for the Cupeyes river reach along with measured downstream cross-section lengths. The WQ monitoring station is located in the third cross section counting from the lower cross section. The Cupeyes River drains south.

Table 5 Total length to downstream cross sections for the Cupeyes river reach.

Downstream Reach Lengths (m)			
River Station	**LOB**	**Reach**	**ROB**
7	5.07	4.39	2.9
6	3.46	4.01	4.22
5	3.83	3.5	3.98
4	3.42	4.72	2.66
3	4.89	4.84	5.68
2	4.3	3.66	3.56
1	0	0	0

Figure 10 shows a plan view of the geometry data in HEC-RAS for the Cupeyes river reach, cross sections were interpolated using a tool provided in HEC-RAS to a maximum interval of one meter (1 m).

Additionally the extensions for the floodplains can be appreciated and the red dots mark the extents of the channel reach. Figure 11 shows the profile view of the Cupeyes river section under analysis for a discharge with a recurrence of 2 yrs. The monitoring station is located in cross section # 3 and is highlighted in Figure 11.

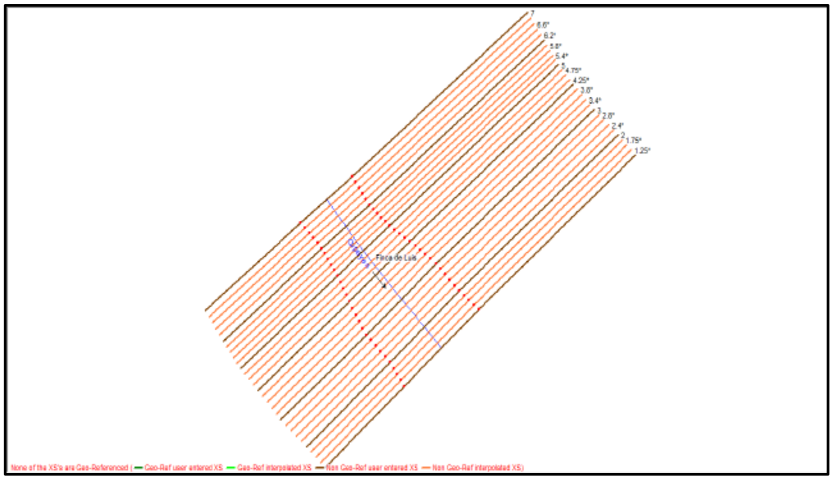

Figure 10 HEC-RAS reach for Cupeyes river reach with flood plain extensions (USACE 2010).

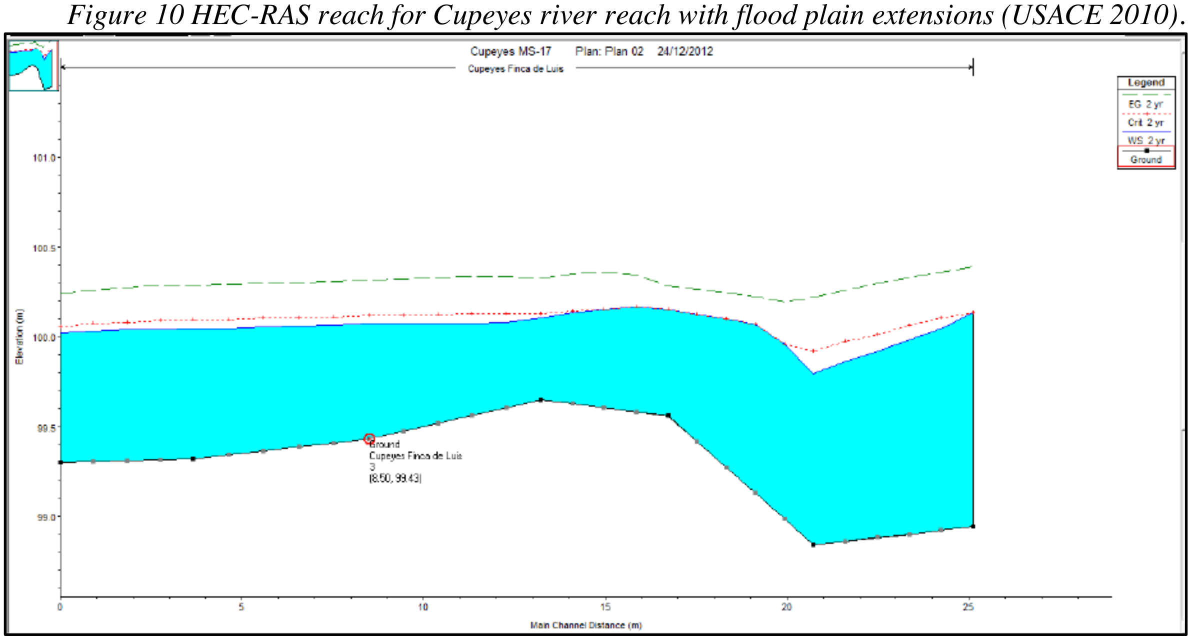

Figure 11 Profile view of the Cupeyes river section under analysis for a discharge with a recurrence of 2 yrs. The WQ monitoring station is highlighted and the downstream end is at the left side of the figure (USACE, 2010).

For Bosque Olimpia, the plan view of the surveyed area is shown in Figure 12 along with the downstream reach, right over bank and left overbank measurements. Table 6 shows the measured values, which were introduced into the hydraulic model. The surveyed cross sections used for building the Bosque Olimpia reach under analysis in the model and the geometric data entered to the hydraulic model are available upon request.

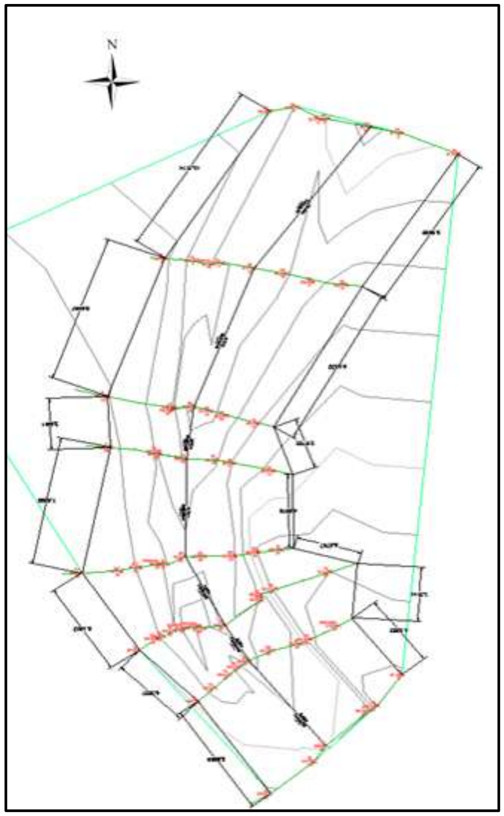

Figure 12 Plan view of the Bosque Olimpia river reach under analysis. This river flows towards the north side of the island.

Table 6 Downstream cross section lengths for the Bosque Olimpia river reach.

Downstream Reach Lengths (m)			
River Station	**LOB**	**Reach**	**ROB**
8	6.6565	6.49	4.2322
7	4.3537	2.48	3.2144
6	5.4803	4.54	3.5767
5	7.5298	5.78	4.2675
4	2.9811	3.07	2.9722
3	8.6557	8.74	9.533
2	10.3174	10.4	9.2926
1	0	0	0

Figure 13 shows a plan view of the geometry data in HEC-RAS for the Bosque Olimpia river reach. Cross sections were interpolated using a tool provided in HEC-RAS to a maximum interval of one meter (1 m). Additionally the extensions for the floodplains can be appreciated and the red dots mark the extents of the channel reach. These extensions were given based on available topographic maps. Figure 14 shows the profile view of the Bosque Olimpia river section under analysis for a discharge with a recurrence of 2 yrs. The monitoring station is located in cross section # 7 and is highlighted in Figure 14.

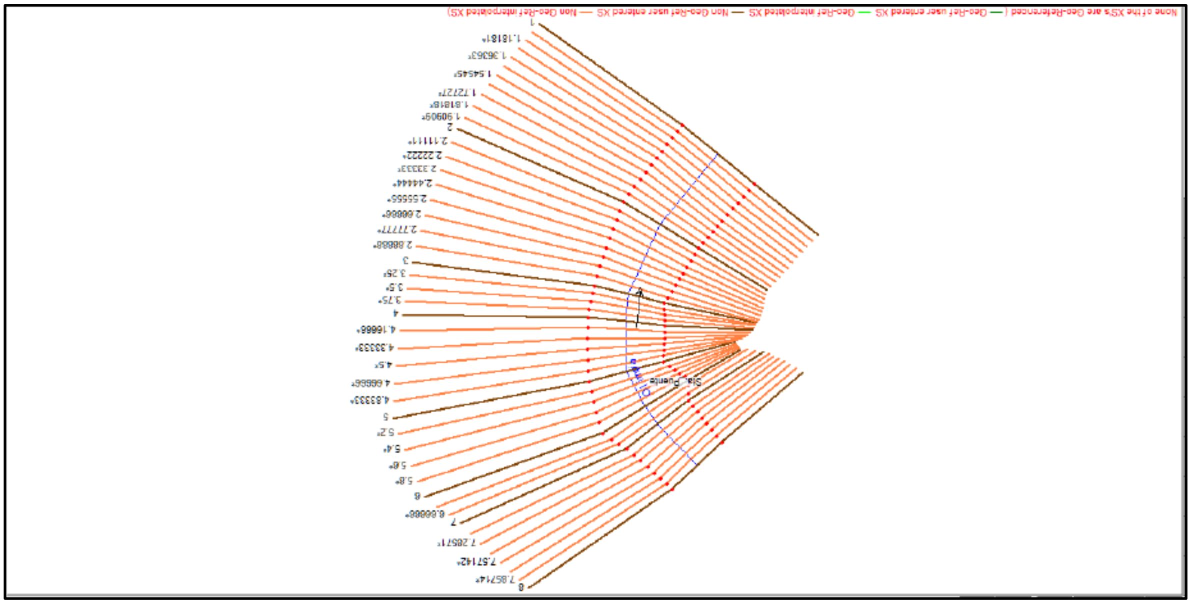

Figure 13 HEC-RAS reach for Bosque Olimpia river reach with flood plain extensions (USACE 2010). Note that figure is inverted to show the same orientation draining towards north.

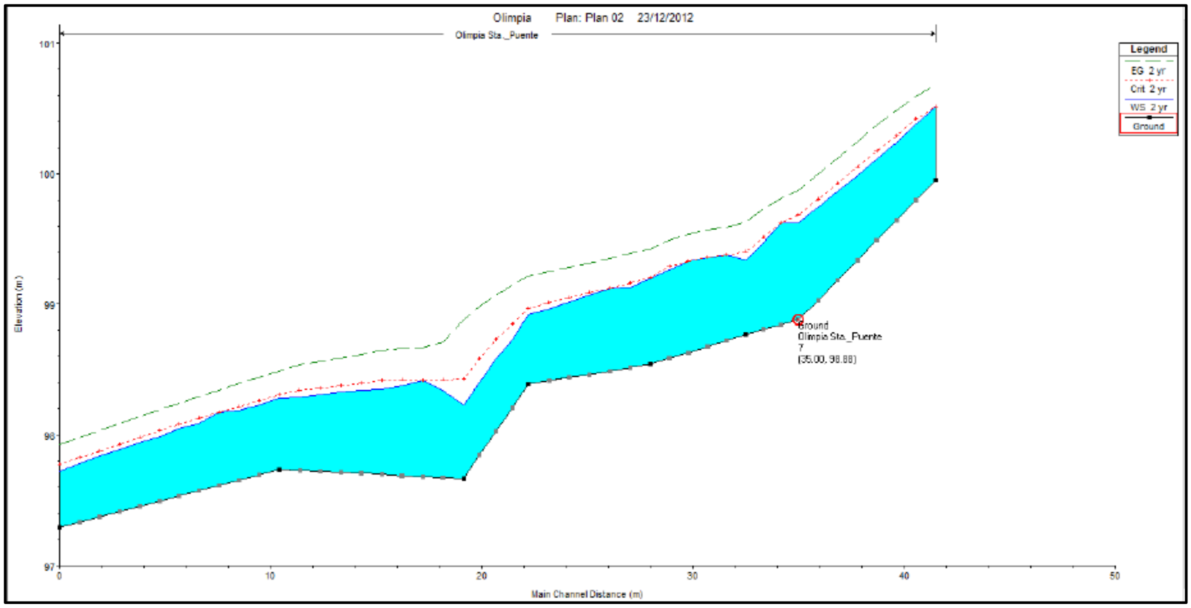

Figure 14 Profile view of the Bosque Olimpia river section under analysis for a discharge with a recurrence of 2 yrs. The WQ monitoring station is highlighted (USACE, 2010).

b. Manning's roughness coefficient

The Manning roughness coefficient is a measure of the friction or resistance that certain characteristics of a given material or in this case of the river reach or channel will impose on flowing waters. These values are chosen by field observation of the river's main reach and overbanks. Figures 15 to 18 show Cupeyes' and Bosque Olimpia's upstream and downstream reaches respectively. Reference tables for Manning's n values were obtained from Open Channel Hydraulics (Chow, 1959). In both reaches the description chosen for the river reach was "Mountain streams, no vegetation in channel banks usually steep, trees and brush along banks submerged at high stages with gravel, cobbles and a few boulders in the bottom". In Cupeyes "heavy stand of timber, a few down trees, little undergrowth with flood stage reaching branches" was chosen for the right overbank (RO) and "scattered brush with heavy weeds" for the left overbank (LO). In Bosque Olimpia from cross-sections 1 to 4 normal conditions n values were chosen for the main reach, "normal pasture with no brush" was chosen for the LO and for the RO a minimum condition of the same characteristics as Cupeyes' RO was chosen. For cross-sections 5 to 8 in Olimpia a maximum condition of the main reach was chosen and the same conditions as Cupeyes' RO was chosen for both sides of the overbanks. Table 7 shows the n values chosen for each reach.

Figure 15 Picture of the Cupeyes river reach under analysis, upstream from WQ and monitoring station.

Figure 16: Picture of the Cupeyes river reach under analysis, downstream from the WQ monitoring station.

Figure 17 Upstream section of the surveyed area of the BO river reach under analysis.

Figure 18 Downstream section of the surveyed area of the BO river reach under analysis.

Table 7 Manning roughness coefficient values introduced in HEC-RAS for the BO watershed.

River	Section	ROB	Main Reach	LOB
Cupeyes	All	0.1	0.04	0.07
Olimpia	1 to 4	0.08	0.05	0.03
	5 to 8	0.1	0.07	0.1

c. Steady flow analysis data and parameters

After the geometric data was added in each model the peak discharges for each of the recurrences established were introduced to their corresponding models. For Cupeyes, subcritical flow regime was used for recurrences of 1 to 25 years and supercritical flow regime was used for recurrences of 50 to 100 years. Reach boundary conditions were assumed as if the normal depth was reached at the downstream end with a slope of 0.0055 and at the upstream end with a slope of 0.022. For Bosque Olimpia supercritical flow regime was used for all recurrences and it was assumed that critical depth was reached in the upstream end. These assumptions were made based on the hydraulic characteristics of the river under analysis, observation, understanding of river dynamics and the results and warnings provided by the HEC-RAS. Tables 9 and 10 in the next section include the flow regime used for each of the recurrences in the last column.

3. Rating curves

Using results from the hydraulic model and the peak outflows generated from the hydrologic models, rating curves or elevation-discharge curves were developed for the Cupeyes and Bosque Olimpia watersheds. These graphs define the equation that will relate a specific water depth at a given cross section to the runoff generated from the precipitation corresponding to each recurrence in each watershed. This equation will be used to convert observed water depth hydrographs at the WQ sampling station into discharge hydrographs for any recorded event. These observed runoff hydrographs will be used for model calibration/validation and storm volume calculation. Tables 8 and 9 show the storm runoff and the corresponding water depth generated from the H-H analyses using point precipitation frequency estimates from Atlas 14 (NOAA, 2012) at different recurrences for both sampling stations. These values were used to construct the rating curves for Cupeyes and Bosque Olimpia showed in Figures 19 and 20, respectively.

Table 8. Peak runoff and corresponding maximum water depth for the Cupeyes sampling station.

Recurrence	Cupeyes

(yrs)	Precipitation (in)	Peak Discharge (m3/s)	Water Depth (m)	Regime
1	88.1	5.6	0.74	Sub Critical
2	111.5	8.6	0.87	
5	142.5	12.9	0.99	
10	171.5	17.2	1.06	
25	215.1	23.7	1.14	
50	252.2	29.4	1.23	Super Critical
100	293.4	35.7	1.34	

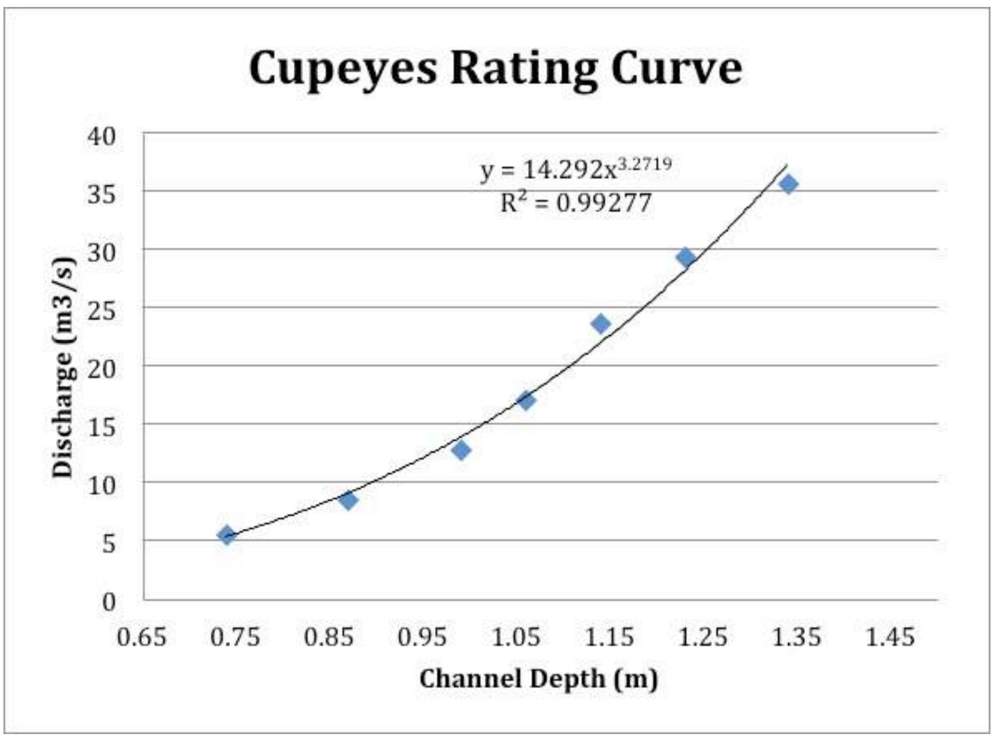

Figure 19. Elevation-discharge curve for the Cupeyes watershed at the water quality sampling station.

Table 9. Peak runoff and corresponding maximum water depth for the Bosque Olimpia sampling station.

Recurrence (yrs)	**Bosque Olimpia**			
	Precipitation (in)	**Peak Discharge (m³/s)**	**Channel Depth (m)**	**Regime**
1	87.9	2.9	0.67	Super Critical
2	110.7	4.1	0.74	
5	140.7	5.8	0.82	
10	168.7	7.4	0.88	
25	210.3	9.9	0.96	
50	245.4	12.1	1	
100	284.2	14.5	1.04	

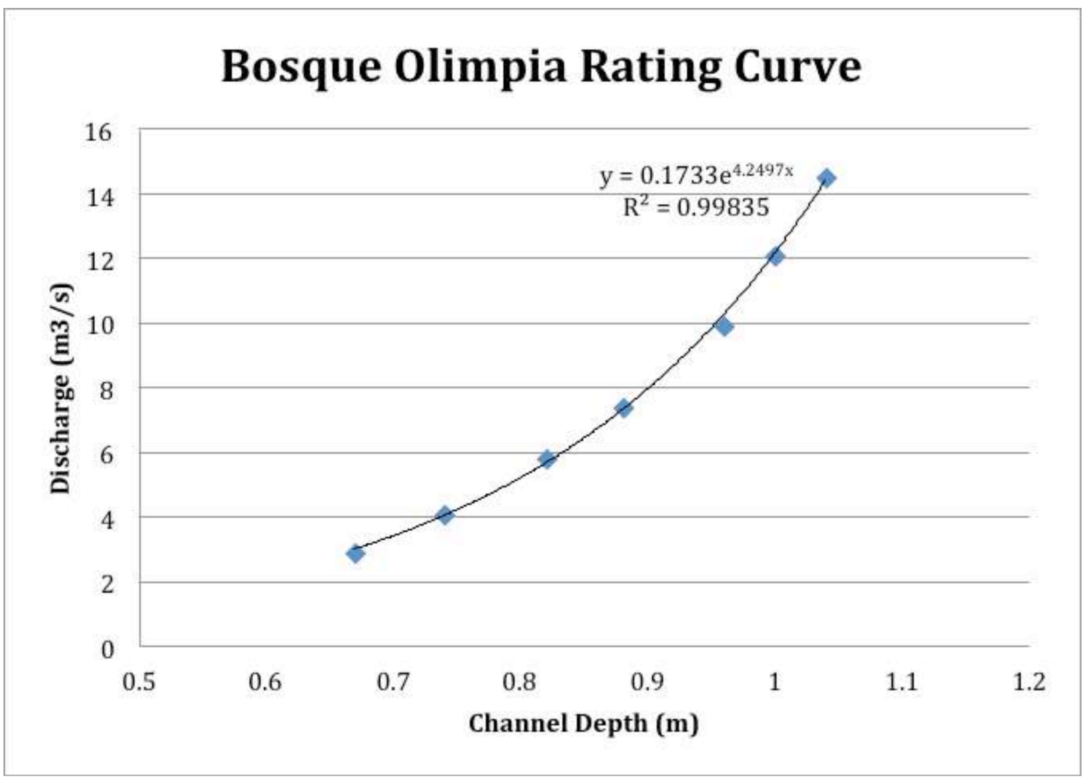

Figure 20. Elevation-discharge curve for the Bosque Olimpia watershed at the water quality sampling station.

Equations 5 (Cupeyes) and 6 (Bosque Olimpia) were used to estimate discharge (m^3/s) using river stage (water elevation in m) at the location of the water quality monitoring stations in each watershed.

These equations were obtained from the exponential and power fit equations (using Microsoft Excel 2010) of the rating curves in Figures 19 and 20, respectively.

$$Q = 14.292D^{3.2719} \quad (5)$$

$$Q = 0.1733e^{4.2497D} \quad (6)$$

where D is water depth measured at the water quality monitoring station and is expressed in meters (m)

4. Loading Calculations and Results

a. Water Quality Analysis

Water quality analysis of samples taken at the Cupeyes River and Bosque Olimpia automatic samplers were sent to Water Quality laboratory of the Agricultural Research Station of the University of Puerto Rico on order to perform TP, NO3 and TKN_N analyses. These were then matched to their corresponding storm event in order to calculate the total nutrient load per storm event. Analysis results can be seen in tables 10 and 11 along with their corresponding event date.

b. Event Load Calculation

The nutrient load per storm event in each watershed was calculated by integrating the product of the event runoff hydrograph and the concentration of the nutrient species and suspended sediments over the length of the storm event. Water depth hydrographs were transformed into actual discharge hydrographs using the constructed rating curves. The volume generated by the storm event was calculated integrating the transformed runoff hydrograph by using the trapezoidal rule as in equation 7. An example of the calculations for a storm event is shown in Appendix 5 data and calculations regarding other storm events used are available upon request. The total load generated by a storm event monitored by composite samples was calculated as the product of the total volume generated by the storm and the average concentration obtained from the laboratory analysis of the composite sample. Tables10 and 11 show the total load calculation values along with water quantity (total volume in liters) and the dates the samples were taken during storm events. A total of nine (9) events were analyzed for Bosque Olimpia and ten (10) for Cupeyes.

$$V(t)_{event} = \int_{t_i}^{t_f} Q(t)dt \approx \frac{1}{2}\sum_{k=1}^{N}(t_{k+1} - t_k)(Q(t_{k+1}) + Q(t_k)) \quad (7)$$

Table 10 Event Nutrient Load Calculation for Bosque Olimpia.

Storm Event Date	Set #	Mean TP (mg/L)	Mean NO3-N (mg/L)	Mean TKN_N (mg/L)	Total N (mg/L)	Mean Q (m3/s)	TOTAL V (L)	Load TP (kg)	Load Total N (kg)
24-Aug-12	808	0.100	0.28	0.44	0.72	6.11	5.12E+07	**5.12**	**36.87**
15-Apr-13	874	0.39	0.30	2.04	2.35	3.15	2.83E+07	**11.10**	**66.40**
17-Apr-13	874	0.39	0.30	2.04	2.35	5.55	4.30E+06	**1.69**	**10.09**
29-Apr-13	881	0.36	0.30	2.21	2.51	2.65	2.47E+07	**8.99**	**61.89**
30-Apr-13	881	0.36	0.30	2.21	2.51	3.24	1.94E+07	**7.08**	**48.78**
15-May-13	907	0.25	0.20	1.60	1.80	1.73	7.15E+07	**17.67**	**128.70**
8-Jun-13	907	0.240	0.55	1.90	2.44	1.98	6.94E+07	**16.68**	**169.56**
12-Jun-13	907	0.240	0.55	1.90	2.44	1.85	3.99E+07	**9.59**	**97.49**
29-Jun-13	907	0.08	0.20	0.82	1.02	1.63	4.37E+07	**3.61**	**44.34**

Table 11 Event Nutrient Load Calculation for Cupeyes

Storm Event Date	Set #	Mean TP (mg/L)	Mean NO3-N (mg/L)	Mean TKN_N (mg/L)	Total N (mg/L)	Mean Q (m3/s)	TOTAL V (L)	Load Total P (kg)	Load Total N (kg)
24-Aug-12	808	0.24	0.20	1.10	1.30	1.45	1.39E+08	**33.29**	**180.31**
25-Dec-12	866	0.16	0.59	1.28	1.86	1.91	2.69E+07	**4.37**	**50.13**
26-Dec-12	866	0.16	0.59	1.28	1.86	1.20	1.73E+07	**2.81**	**32.24**
16-Apr-13	874	0.62	0.35	6.34	6.70	0.96	2.95E+07	**18.28**	**197.57**
29-Apr-13	877	0.10	0.24	0.71	0.94	1.26	4.30E+07	**4.32**	**40.61**
7-May-13	881	0.20	0.45	1.05	1.50	0.62	1.12E+07	**2.19**	**16.75**
10-May-13	881	0.20	0.45	1.05	1.50	3.65	1.27E+08	**24.84**	**190.17**
17-Jul-13	923	0.501	0.747	2.576	3.32	0.77	3.07E+07	**15.36**	**101.95**
20-Jul-13	923	0.501	0.747	2.576	3.32	0.12	2.96E+06	**1.48**	**9.84**
8-Aug-13	923	0.131	0.284	1.471	1.76	0.29	2.01E+07	**2.62**	**35.24**

c. *Nutrient export precipitation coefficients*

Nutrient export precipitation coefficients (expressed in kg of the species per inch of antecedent precipitation) were calculated standardizing the calculated storm load per species with the antecedent "relevant" precipitation. Antecedent relevant precipitation was determined taking into account storm events that occurred either during three to five hours before the time that sampling stations indicated taking samples, note that this is not the same as the day the samples were retrieved from the station. Tables 12 and 13 show the date of the event in relation to the day they were retrieved. The antecedent precipitation event was obtained from the set of rain gages installed in each watershed (two rain gages were installed in each monitored watershed). Tables 12 and 13 show the antecedent precipitation along with their corresponding nutrient export precipitation coefficients for each of the events in the Bosque Olimpia and Cupeyes watersheds, respectively.

Table 12 Bosque Olimpia nutrient export precipitation coefficients.

Location	Event Date	Antecedent Precipitation (mm)	Load (kg)		Nutrient Coefficient (kg/mm)	
			Total P	Total N	Total P	Total N
Olimpia	24-Aug-12	40.64	5.12	36.87	0.1260	0.9072
	15-Apr-13	56.9	11.1	66.4	0.1951	1.1670
	17-Apr-13	19.81	1.69	10.09	0.0853	0.5093
	29-Apr-13	44.7	8.99	61.89	0.2011	1.3846
	30-Apr-13	44.45	7.08	48.78	0.1593	1.0974
	15-May-13	76.45	17.67	128.7	0.2311	1.6835
	8-Jun-13	69.09	16.68	169.56	0.2414	2.4542
	12-Jun-13	50.8	9.59	97.49	0.1888	1.9191
	29-Jun-13	32.51	3.61	44.34	0.1110	1.3639

Table 13 Cupeyes river nutrient export precipitation coefficients.

Location	Date	Antecedent Precipitation (mm)	Load (kg)		Nutrient Coefficient (kg/in)	
			Total P	Total N	Total P	Total N
Cupeyes	24-Aug-12	74.93	33.29	180.31	0.444281329	5.416341244
	16-Apr-13	53.85	18.28	197.57	0.24396103	5.93481526
	29-Apr-13	31.50	4.32	40.61	0.05765381	1.219885852
	7-May-13	20.07	2.19	16.75	0.029227279	0.5031541
	10-May-13	72.64	24.84	190.17	0.331509409	5.712526284
	17-Jul-13	44.45	15.36	101.95	0.204991325	3.062481226
	20-Jul-13	18.16	1.48	9.84	0.019751768	0.29558426
	8-Aug-13	33.02	2.62	35.24	0.034965968	1.058576149

5. Storm Volume Calculation at ISCO Water Quality Monitoring Stations

Bosque Olimpia Watershed

Set 808 (water level from paper rolls)									
Fecha de recogido	Fecha del evento	Hour	Reading	Level (ft)	Level adjusted (m)	Q (L/s)	Mean (L/s)	Δt (s)	V (L)
28-Aug-12	24-Aug-12	11:00	0.8	0.56	0.628049	2499.9927			
28-Aug-12	24-Aug-12	6:00	0.8	0.56	0.628049	2499.9927	2499.992721	3600	9.00E+06
28-Aug-12	24-Aug-12	7:00	0.8	0.56	0.628049	2499.9927	2499.992721	3600	9.00E+06
28-Aug-12	24-Aug-12	8:00	0.8	0.56	0.628049	2499.9927	2499.992721	3600	9.00E+06
28-Aug-12	24-Aug-12	9:00	0.8	0.56	0.628049	2499.9927	2499.992721	3600	9.00E+06
28-Aug-12	24-Aug-12	10:00	0.8	0.56	0.628049	2499.9927	2499.992721	3600	9.00E+06
28-Aug-12	24-Aug-12	11:00	0.8	0.56	0.628049	2499.9927	2499.992721	3600	9.00E+06
28-Aug-12	24-Aug-12	11:30	0.8	0.56	0.628049	2499.9927	2499.992721	1800	4.50E+06
28-Aug-12	24-Aug-12	12:00	0.8	0.56	0.628049	2499.9927	2499.992721	1800	4.50E+06
28-Aug-12	24-Aug-12	13:00	0.8	0.56	0.628049	2499.9927	2499.992721	3600	9.00E+06
28-Aug-12	24-Aug-12	14:00	0.8	0.56	0.628049	2499.9927	2499.992721	3600	9.00E+06
28-Aug-12	24-Aug-12	15:00	0.8	0.56	0.628049	2499.9927	2499.992721	3600	9.00E+06
28-Aug-12	24-Aug-12	16:00	0.8	0.56	0.628049	2499.9927	2499.992721	3600	9.00E+06
28-Aug-12	24-Aug-12	17:00	0.8	0.56	0.628049	2499.9927	2499.992721	3600	9.00E+06
28-Aug-12	24-Aug-12	18:00	0.8	0.56	0.628049	2499.9927	2499.992721	3600	9.00E+06
28-Aug-12	24-Aug-12	19:00	0.8	0.56	0.628049	2499.9927	2499.992721	3600	9.00E+06
28-Aug-12	24-Aug-12	20:00	0.8	0.56	0.628049	2499.9927	2499.992721	3600	9.00E+06
28-Aug-12	24-Aug-12	21:00	0.8	0.56	0.628049	2499.9927	2499.992721	3600	9.00E+06
28-Aug-12	24-Aug-12	22:00	0.8	0.56	0.628049	2499.9927	2499.992721	3600	9.00E+06
28-Aug-12	24-Aug-12	22:30	1	0.7	0.670732	2997.1968	2748.594764	1800	4.95E+06
28-Aug-12	24-Aug-12	23:00	0.9	0.63	0.64939	2737.3290	2867.262917	1800	5.16E+06
28-Aug-12	24-Aug-12	23:30	0.8	0.56	0.628049	2499.9927	2618.660874	1800	4.71E+06
28-Aug-12	25-Aug-12	0:00	1.5	1.05	0.777439	4716.8988	3608.445737	1800	6.50E+06
28-Aug-12	25-Aug-12	0:30	1	0.7	0.670732	2997.1968	3857.04778	1800	6.94E+06
28-Aug-12	25-Aug-12	1:00	0.8	0.56	0.628049	2499.9927	2748.594764	1800	4.95E+06
28-Aug-12	25-Aug-12	1:30	0.8	0.56	0.628049	2499.9927	2499.992721	1800	4.50E+06
28-Aug-12	25-Aug-12	2:00	0.8	0.56	0.628049	2499.9927	2499.992721	1800	4.50E+06
								Total Vol. (L)	5.12E+07

Set 907 (RTD)								
Fecha de recogido	Fecha del evento	Hour	Level (m)	Level adjusted (m)	Q (L/s)	Mean (L/s)	Δt (s)	V (L)
27-Jun-13	12-Jun-13	12:45	0	0.457317	1210.1318			
27-Jun-13	12-Jun-13	13:00	0.053	0.510317	1515.8304	1362.9811	900	1226682.976
27-Jun-13	12-Jun-13	13:15	0.121	0.578317	2023.7313	1769.7808	900	1592802.747
27-Jun-13	12-Jun-13	13:30	0.23	0.687317	3216.0705	2619.9009	900	2357910.824
27-Jun-13	12-Jun-13	13:45	0.225	0.682317	3148.4548	3182.2627	900	2864036.388
27-Jun-13	12-Jun-13	14:00	0.201	0.658317	2843.1682	2995.8115	900	2696230.324
27-Jun-13	12-Jun-13	14:15	0.189	0.646317	2701.8118	2772.4900	900	2495240.985
27-Jun-13	12-Jun-13	14:30	0.175	0.632317	2545.7538	2623.7828	900	2361404.506
27-Jun-13	12-Jun-13	14:45	0.157	0.614317	2358.2792	2452.0165	900	2206814.819
27-Jun-13	12-Jun-13	15:00	0.135	0.592317	2147.7887	2253.0339	900	2027730.52
27-Jun-13	12-Jun-13	15:15	0.115	0.572317	1972.7821	2060.2854	900	1854256.846
27-Jun-13	12-Jun-13	15:30	0.097	0.554317	1827.5023	1900.1422	900	1710127.993
27-Jun-13	12-Jun-13	15:45	0.082	0.539317	1714.6426	1771.0725	900	1593965.232
27-Jun-13	12-Jun-13	16:00	0.07	0.527317	1629.3942	1672.0184	900	1504816.572
27-Jun-13	12-Jun-13	16:15	0.055	0.512317	1528.7689	1579.0816	900	1421173.399
27-Jun-13	12-Jun-13	16:30	0.045	0.502317	1465.1620	1496.9654	900	1347268.892
27-Jun-13	12-Jun-13	16:45	0.037	0.494317	1416.1872	1440.6746	900	1296607.114
27-Jun-13	12-Jun-13	17:00	0.03	0.487317	1374.6790	1395.4331	900	1255889.807
27-Jun-13	12-Jun-13	17:15	0.025	0.482317	1345.7773	1360.2282	900	1224205.368
27-Jun-13	12-Jun-13	17:30	0.019	0.476317	1311.8962	1328.8368	900	1195953.094
27-Jun-13	12-Jun-13	17:45	0.015	0.472317	1289.7840	1300.8401	900	1170756.109
27-Jun-13	12-Jun-13	18:00	0.01	0.467317	1262.6672	1276.2256	900	1148603.038
27-Jun-13	12-Jun-13	18:15	0.007	0.464317	1246.6715	1254.6693	900	1129202.391
27-Jun-13	12-Jun-13	18:30	0.003	0.460317	1225.6587	1236.1651	900	1112548.564
27-Jun-13	12-Jun-13	18:45	0	0.457317	1210.1318	1217.8952	900	1096105.711
							21600	3.99E+07

Cupeyes

Set 877									
Fecha de recogido	Fecha del evento	Hour	Reading	Level (ft)	Level adjusted (m)	Q (L/s)	Mean (L/s)	Δt (s)	V (L)
03-may-13	30-abr-13	14:00	0.8	0.64	0.37296748	567.0786			
03-may-13	30-abr-13	14:30	2	1.6	0.66565041	3773.7424	2170.410501	1800	3906738.903
03-may-13	30-abr-13	15:00	1.5	1.2	0.54369919	1946.3148	2860.028612	1800	5148051.501
03-may-13	30-abr-13	15:30	1.3	1.04	0.4949187	1430.9958	1688.655289	1800	3039579.520
03-may-13	30-abr-13	16:00	1.1	0.88	0.44613821	1019.0418	1225.018802	1800	2205033.844
03-may-13	30-abr-13	16:30	1	0.8	0.42174797	847.8205	933.431161	1800	1680176.090
03-may-13	30-abr-13	17:00	1	0.8	0.42174797	847.8205	847.8204984	1800	1526076.897
03-may-13	30-abr-13	17:30	0.9	0.72	0.39735772	697.6787	772.7496098	1800	1390949.298
03-may-13	30-abr-13	18:00	0.8	0.64	0.37296748	567.0786	632.3786489	1800	1138281.568
03-may-13	30-abr-13	18:30	0.75	0.6	0.36077236	508.6330	537.8557647	1800	968140.376
03-may-13	30-abr-13	19:00	0.65	0.52	0.33638211	404.5177	456.5753397	1800	821835.611
03-may-13	30-abr-13	19:30	1.8	1.44	0.61686992	2941.8967	1673.207228	1800	3011773.010
03-may-13	30-abr-13	20:00	1.7	1.36	0.59247967	2578.1210	2760.008843	1800	4968015.918
03-may-13	30-abr-13	20:30	1.3	1.04	0.4949187	1430.9958	2004.558369	1800	3608205.064
03-may-13	30-abr-13	21:00	1.2	0.96	0.47052846	1212.9050	1321.950395	1800	2379510.710
03-may-13	30-abr-13	21:30	1	0.8	0.42174797	847.8205	1030.362754	1800	1854652.956
03-may-13	30-abr-13	22:00	1	0.8	0.42174797	847.8205	847.8204984	1800	1526076.897
03-may-13	30-abr-13	22:30	0.9	0.72	0.39735772	697.6787	772.7496098	1800	1390949.298
03-may-13	30-abr-13	23:00	0.9	0.72	0.39735772	697.6787	697.6787213	1800	1255821.698
03-may-13	30-abr-13	23:30	0.85	0.68	0.3851626	630.0311	663.8549021	1800	1194938.824
								Total Volume	43014807.982

Additional storm volume calculations used available upon request.

6. Supplementary Rain Gage Locations

a. Lago Garzas and Lago Adjuntas USGS Rain Gages used for Bosque Olimpia

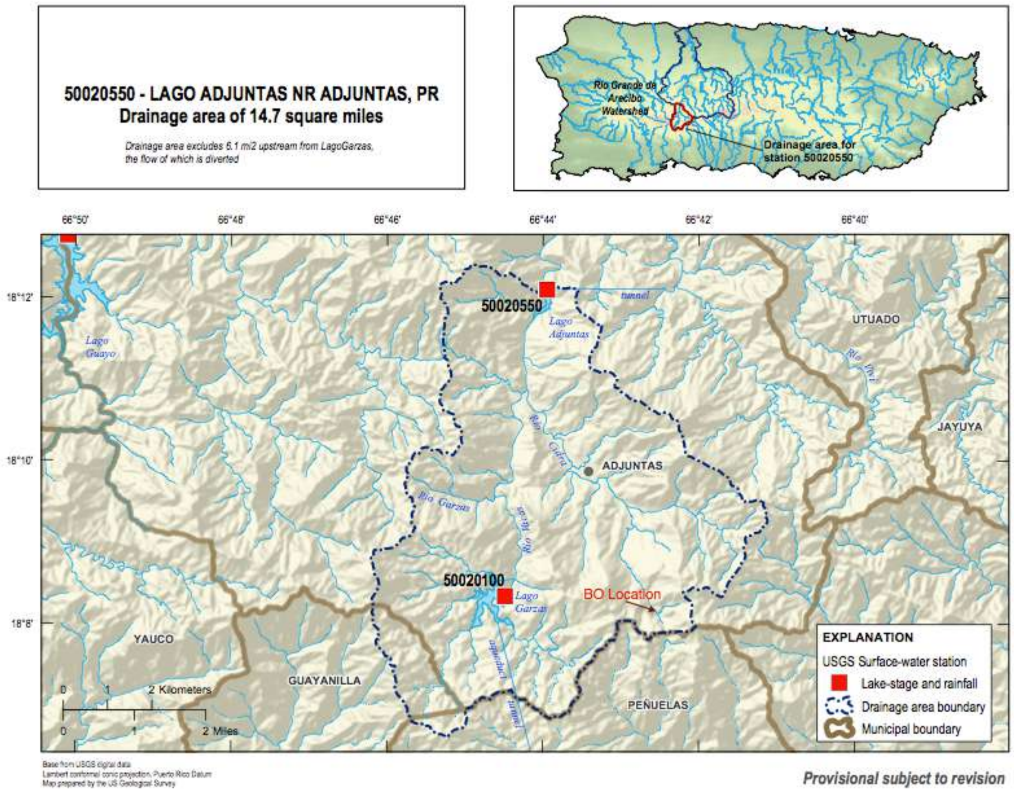

b. Maricao fish hatchery rain gage (NOAA, 2014)

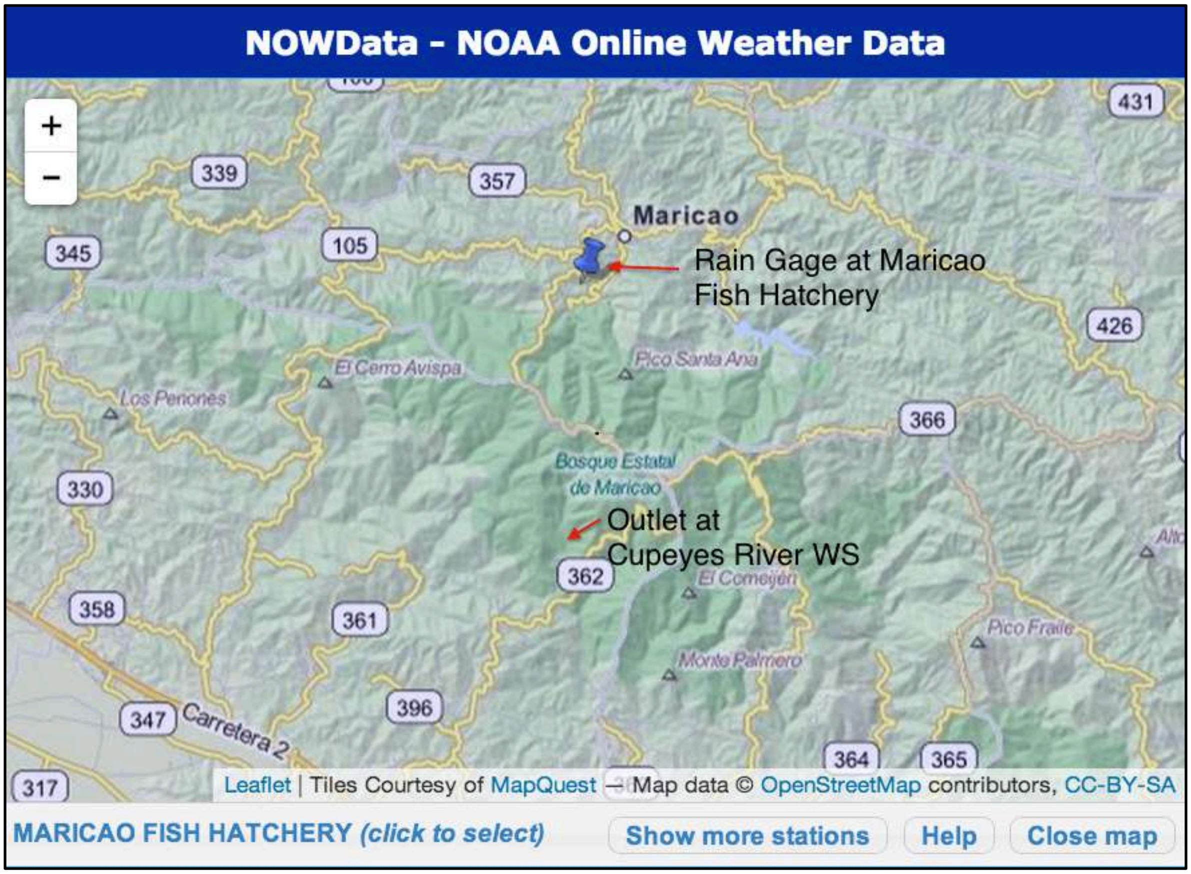

Latitude: 18°10'21N   Longitude: 066°59'14W   Elevation: 1500'

7. *Base Flow Nutrient Concentration Analyses from Grab Samples*

Reference Streams, Final Data											
Updated 12-14-09											
River	Riverid	Date	Replicate	Set#	Sample#	Chl-a	NO3-N	TKN	TN	TP	DP
Cupeyes	3	8/19/09	1	901	1	0.153	0.267	0.230	0.498	0.009	0.006
Cupeyes	3	8/19/09	2	901	2	0.150	0.263	0.101	0.364	0.004	0.003
Cupeyes	3	9/2/09	1	903	1	0.176	0.243	0.116	0.359	0.002	0.002
Cupeyes	3	9/2/09	2	903	2	0.185	0.246	0.115	0.361	0.002	0.001
Cupeyes	3	9/9/09	1	907	2	0.282	0.271	0.000	0.271	0.001	0.002
Cupeyes	3	9/9/09	2	907	3	0.257	0.268	0.000	0.268	0.002	0.001
Cupeyes	3	9/16/09	1	909	2	0.249	0.303	0.013	0.316	0.005	0.000
Cupeyes	3	9/16/09	2	909	3	0.247	0.305	0.023	0.328	0.003	0.001
Cupeyes	3	9/29/09	1	912	2	0.076	0.273	0.078	0.351	0.003	.
Cupeyes	3	9/29/09	2	912	3	0.070	0.246	0.041	0.287	0.002	.
Cupeyes	3	10/19/09	1	916	2	0.173	0.275	0.105	0.380	0.003	.
Cupeyes	3	10/19/09	2	916	3	0.186	0.285	0.143	0.428	0.004	.
Cupeyes	3	11/3/09	1	919	2	2.564	0.285	0.061	0.346	0.006	.
Cupeyes	3	11/3/09	2	919	3	2.624	0.273	0.111	0.384	0.002	.
Cupeyes	3	11/25/09	1	921	2	0.100	0.316	0.027	0.343	0.000	
Cupeyes	3	11/25/09	2	921	3	0.111	0.313	0.063	0.376	0.004	
Cupeyes	3	12/1/09	1	923	2	0.136	0.316	0.110	0.426	0.006	
Cupeyes	3	12/1/09	2	923	3	0.121	0.315	0.117	0.432	0.003	
Cupeyes	3	12/9/09	1	925	2	0.192	0.312	0.118	0.430	0.003	

								Avg.	0.366	**0.003**	**mg/L**

Reference Streams, Final Data											
Updated 12-14-09											
River	Riverid	Date	Replicate	Set#	Sample#	Chl-a	NO3-N	TKN	TN	TP	DP
Olimpia	1	8/20/09	1	902	3	.	0.252	0.168	0.421	0.033	0.030
Olimpia	1	8/25/09	1	905	3	0.054	0.241	0.101	0.341	0.033	0.026
Olimpia	1	8/25/09	2	905	4	0.056	0.238	0.148	0.386	0.032	0.026
Olimpia	1	9/3/09	1	904	4	0.024	0.230	0.000	0.230	0.034	0.032
Olimpia	1	9/11/09	1	908	3	0.043	0.274	0.000	0.274	0.038	0.037
Olimpia	1	9/11/09	2	908	4	0.042	0.275	0.010	0.285	0.031	0.032
Olimpia	1	9/17/09	1	910	4	0.082	0.287	0.011	0.298	0.037	0.032
Olimpia	1	9/30/09	1	913	3	0.034	0.244	0.000	0.244	0.035	.
Olimpia	1	9/30/09	2	913	4	0.028	0.251	0.054	0.305	0.034	.
Olimpia	1	10/6/09	1	914	4	0.046	0.248	0.000	0.248	0.037	.
Olimpia	1	10/21/09	1	917	3	0.092	0.317	0.647	0.964	0.039	.
Olimpia	1	10/21/09	2	917	4	0.094	0.326	0.881	1.207	0.034	.
Olimpia	1	11/2/09	1	918	4	0.065	0.257	0.165	0.422	0.038	.
Olimpia	1	11/24/09	1	920	2	0.125	0.288	0.039	0.327	0.037	
Olimpia	1	11/24/09	2	920	3	0.155	0.287	0.055	0.342	0.035	
Olimpia	1	11/30/09	1	922	2	0.074	0.308	0.038	0.346	0.035	
Olimpia	1	12/8/09	1	924	2	0.036	0.269	0.191	0.460	0.037	
Olimpia	1	12/8/09	2	924	3	0.036	0.274	0.200	0.474	0.038	
								Avg.	0.421	0.035	mg/L

8. Monthly Loading Coefficient Statistics

Yr-Month	Monthly Loading coeff. (kg/ha)		
	Olimpia	Cupeyes	Count
2012-01	0.11280564	0.012795716	1
2012-02	0.05021871	0.000625098	1
2012-03	0.17802265	0.117674952	1
2012-04	0.13993176	0.225649718	0
2012-05	0.162737749	0.191764754	0
2012-06	0.040303255	0.010051117	1
2012-07	0.097597802	0.038980316	1
2012-08	0.245748539	0.152811161	1
2012-11	0.0240945	0.02525458	0
2012-12	0.097172401	0.101951685	0
2013-01	0.02489765	0.001662721	1
2013-02	0.027155653	0.001501813	1
2013-03	0.188127982	0.001662721	1
2013-04	0.284212089	0.001609085	1
2013-05	0.356232168	0.051306843	1
2013-06	0.233656333	0.102531399	1
2013-07	0.219651555	0.046893025	1
2013-08	0.194556651	0.0332472	1

2013-09	0.175263949	0.107757904	1
2013-10	0.047753132	0.021142503	1
2013-11	0.032664688	0.054861626	0
2013-12	0.026527583	0.01258727	1
2014-01	0.040192008	0.057130228	0
2014-02	0.0416235	0.005872163	1
2014-03	0.131174413	0.039243077	1
2014-04	0.068601407	0.083955615	0
2014-05	0.188323752	0.020684042	1
2014-06	0.038851229	0.009528469	1
2014-07	0.046206314	0.113532401	0
% of time that Olimpia exceeded the Cupeyes monthly TP loading coefficient → 72.41%			21

Yr-Month	Storm Loading coeff. (kg/ha)		
	Olimpia	Cupeyes	Count (BO>Cup)
2012-01	0.09031744	1.21E-02	1
2012-02	0.03094311	0.00E+00	1
2012-03	0.1595502	1.17E-01	1
2012-04	0.12306561	2.25E-01	0
2012-05	0.145871599	1.91E-01	0
2012-06	0.017011905	9.43E-03	1

2012-07	0.076715902	3.85E-02	1
2012-08	0.230488689	1.52E-01	1
2012-11	0	2.39E-02	0
2012-12	0.073881051	1.01E-01	0
2013-01	0	0.00E+00	0
2013-02	0.006273753	0.00E+00	1
2013-03	0.167246082	0.00E+00	1
2013-04	0.270558539	0.00E+00	1
2013-05	0.351586292	5.00E-02	1
2013-06	0.218396483	1.01E-01	1
2013-07	0.202785405	4.58E-02	1
2013-08	0.180099951	3.19E-02	1
2013-09	0.160004099	1.07E-01	1
2013-10	0.028477532	1.99E-02	1
2013-11	0.011782788	5.37E-02	0
2013-12	0.002433083	1.10E-02	0
2014-01	0.016097508	5.56E-02	0
2014-02	0.0207416	4.53E-03	1
2014-03	0.107883063	3.78E-02	1
2014-04	0.050128957	8.26E-02	0
2014-05	0.169851302	1.92E-02	1

2014-06	0.015559879	8.03E-03	1
2014-07	0.024521264	1.12E-01	0
% of time that Olimpia exceeded the Cupeyes monthly TP loading coefficient →65.51%			19

Yr-Month	Baseflow Loading coeff. (kg/ha)		
	Olimpia	Cupeyes	Count (BO>Cup)
2012-01	0.0224882	6.47E-04	1
2012-02	0.0192756	6.25E-04	1
2012-03	0.01847245	5.39E-04	1
2012-04	0.01686615	5.82E-04	1
2012-05	0.01686615	6.25E-04	1
2012-06	0.02329135	6.25E-04	1
2012-07	0.0208819	4.96E-04	1
2012-08	0.01525985	4.31E-04	1
2012-11	0.0240945	1.34E-03	1
2012-12	0.02329135	1.45E-03	1
2013-01	0.02489765	1.66E-03	1
2013-02	0.0208819	1.50E-03	1
2013-03	0.0208819	1.66E-03	1
2013-04	0.01365355	1.61E-03	1
2013-05	0.00401575	1.34E-03	1

2013-06	0.01525985	1.29E-03	1
2013-07	0.01686615	1.07E-03	1
2013-08	0.0144567	1.34E-03	1
2013-09	0.01525985	1.18E-03	1
2013-10	0.0192756	1.29E-03	1
2013-11	0.0208819	1.18E-03	1
2013-12	0.0240945	1.56E-03	1
2014-01	0.0240945	1.56E-03	1
2014-02	0.0208819	1.34E-03	1
2014-03	0.02329135	1.39E-03	1
2014-04	0.01847245	1.39E-03	1
2014-05	0.01847245	1.50E-03	1
2014-06	0.02329135	1.50E-03	1
2014-07	0.02168505	1.34E-03	1
% of time that Olimpia exceeded the Cupeyes monthly TP loading coefficient in BF →100%			29

9. Baseflow Measurements

Bosque Olimpia

Bosque Olimpia base flow measurement 1 was taken downstream of the monitoring and sampling stations, baseflow measurement 2 was taken at the water level cross section in the river reach located approximately 3 meters upstream of the sampling station.

B.O. Baseflow measurement 1									
Sec.	V1 (ft/s)	D1 (cm)	D1 (ft)	Q1 (cfs)	V2	D2	D2	Q2 (cfs)	Qmean
0.5	0.57	13	0.4264	0.243048	0.59	12	0.3936	0.232224	0.237636
1.5	0.75	15	0.492	0.369	0.82	19	0.6232	0.511024	0.440012
2.5	0.25	10	0.328	0.082	0.24	10.5	0.3444	0.082656	0.082328
3.5	0.07	6	0.1968	0.013776	0.1	6	0.1968	0.01968	0.016728
4.5	0.07	5	0.164	0.01148	0.17	5	0.164	0.02788	0.01968
5.5	0.29	20	0.656	0.19024	0.28	21	0.6888	0.192864	0.191552
								Total Avg. Q (cfs)	0.987936

B.O. Base flow measurement 2				
Sec. (1ft W)	V1 (ft/s)	D1 (in)	D1 (ft)	Q1 ft3/s
1	0.6	2	0.166666667	0.100
2	1.155	1.75	0.145833333	0.168
3	0.295	3	0.25	0.074
4	0.295	1	0.083333333	0.025
5	0.36	2.75	0.229166667	0.083
6	0.36	3	0.25	0.090
7	0.775	4	0.333333333	0.258
8	0.47	4.25	0.354166667	0.166
9	0.3	2.5	0.208333333	0.063
10	0.05	1.75	0.145833333	0.007
Total Q (cfs)				1.034

Cupeyes

Both baseflow measurements were taken in the same cross section which corresponded to the location of the water sampling and monitoring station at the Cupeyes watershed.

Cupeyes BF Measurement Day 1				
Sec.	**V1 (ft/s)**	**D1 (cm)**	**D1 (ft)**	**Q1 ft3/s**
0.5	1.87	20	0.656	1.22672
1.5	1.66	30	0.984	1.63344
2.5	1.08	24	0.7872	0.850176
3.5	1.6	20	0.656	1.0496
4.5	1.28	17	0.5576	0.713728
5.5	0.77	7	0.2296	0.176792
6.5	0.15	7	0.2296	0.03444
7.5	0.02	6	0.1968	0.003936
Total Q (cfs)				5.688832

Cupeyes BF Measurement Day 2				
Sec.	**V1 (ft/s)**	**D1 (in)**	**D1 (ft)**	**Q1 ft3/s**
1	0.15	1.25	0.104	0.015
2	0.38	2.5	0.208	0.079
3	0.8	4.25	0.354	0.283
4	0.9	4	0.333	0.3
5	0.73	4.5	0.375	0.273

6	0.63	4.5	0.375	0.236
7	0.5	3	0.25	0.125
8	0.12	2.25	0.1875	0.0225
Total Q (cfs)				1.335625

*10. **Water Level Rating Curves***

Bosque Olimpia

The following table shows the depth and discharge values used for construction of the rating curve corresponding to the cross section where the HOBO pressure transducer was located. The first value in the table corresponds to the BO baseflow measurement shown above and the rest corresponds to the upper cross section of the Bosque Olimpia watershed hydraulic model discussed in section 4.2.

Peak Discharge (m3/s)	Channel Depth (m)
0.029	0.106
2.9	0.48
4.1	0.56
5.8	0.71
7.4	0.76
9.9	0.82
12.1	0.86
14.5	0.9

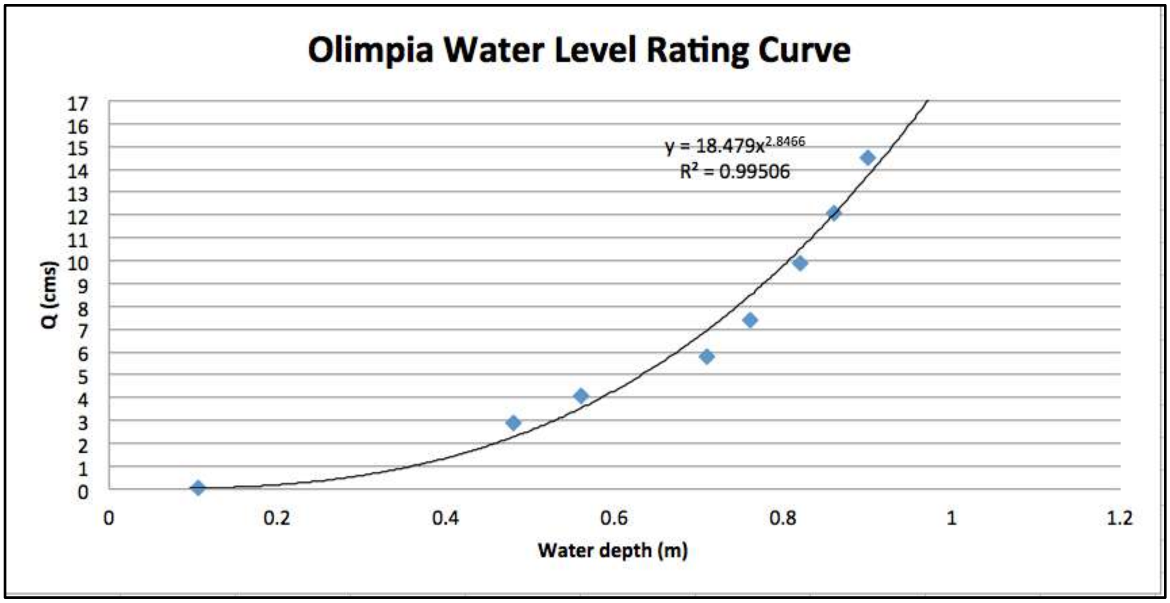

Rating curve corresponding to the cross section of the installed HOBO water level (pressure transducer) in Bosque Olimpia for continuous discharge measurements.

Cupeyes

Depth and discharge values used for construction of the rating curves where the first two values correspond to the Cupeyes baseflow measurements 1 and 2 shown above and the rest corresponds to the rating curve developed for Cupeyes using the hydraulic model discussed in section 4.

Cupeyes	
Peak Discharge (m3/s)	Channel Depth (m)
0.03	0.11
0.1612	0.27
5.6	0.74
8.6	0.87
12.9	0.99
17.2	1.06

23.7	1.14
29.4	1.23
35.7	1.34

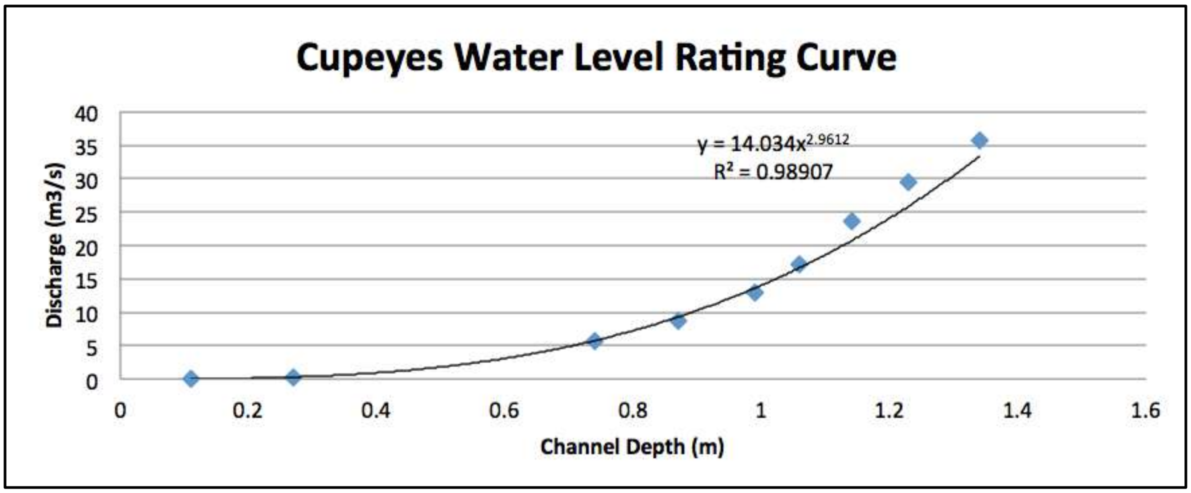

11. Stream Hydrographs

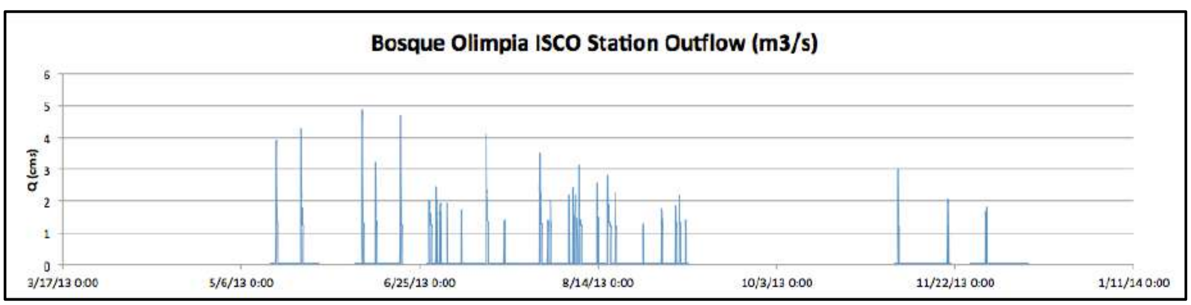

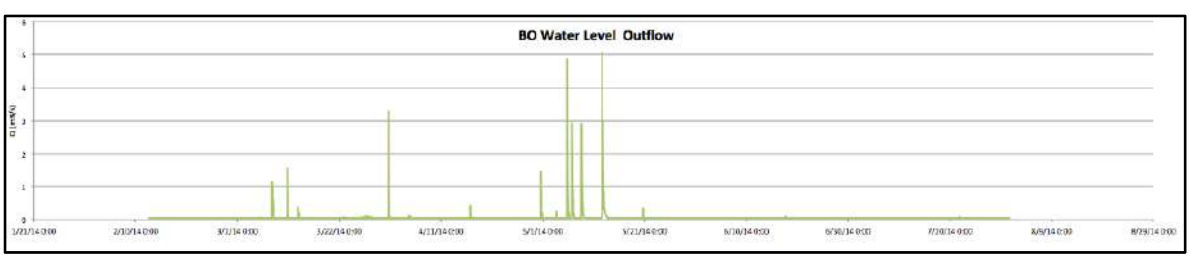

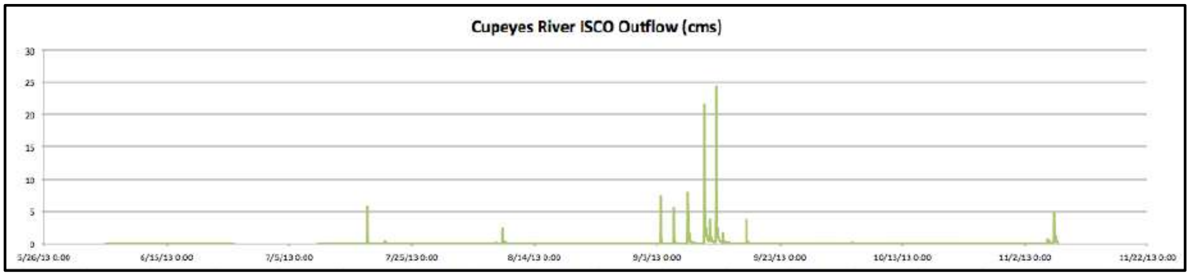
Cupeyes River ISCO Outflow (cms)
30
25
20
15
10
5
0
5/26/13 0:00
6/15/13 0:00
7/5/13 0:00
7/25/13 0:00
8/14/13 0:00
9/1/13 0:00
9/23/13 0:00
10/13/13 0:00
11/2/13 0:00
11/22/13 0:00

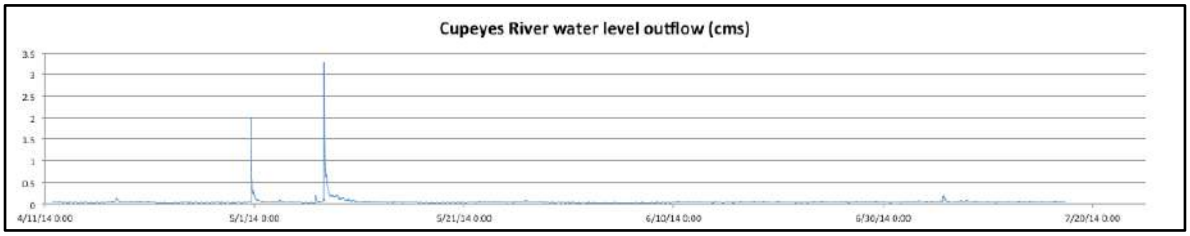
Cupeyes River water level outflow (cms)
3.5
3
2.5
2
1.5
1
0.5
0
4/11/14 0:00
5/1/14 0:00
5/21/14 0:00
6/10/14 0:00
6/30/14 0:00
7/20/14 0:00

12. ET estimation using PRET

This is the Data of Project MS-17

Crop - Generic
Location - Mayaguez
Latitude - 18.33
Elevation - 60 m
Planting Date - 5/5/2014
Type Irrigation - Flood
Length of Initial Crop Stage - 1 days
Length of Development Crop Stage - 365 days
Length of Mid (Mature) Crop Stage - 365 days
Length of End Crop Stage - 365 days
Interval Between Irrigation - 7 days
Depth of irrigation - 55 mm
Type of soil - Fine
Climate Zone - 6
Wind speed at 2 m
Unadjusted Mid Stage Kc - 120
Unadjusted End Stage Kc - 95
Maximum Crop Height - 50 m

Month	Tmin(∞C)	Tmax(∞C)	SR(MJ/m≤d)	U2(m/s)	TDew(∞C)	ETo(mm/day)
January	18.3	28.8	15.4	1.3	18.3	3.2
February	18.0	28.9	17.8	1.5	18.0	3.7
March	18.4	29.7	20.7	1.5	18.4	4.3
April	19.5	30.2	22.6	1.5	19.5	4.7
May	20.9	30.7	23.4	1.6	20.9	4.9
June	21.6	31.3	23.4	1.8	21.6	5.1
July	21.8	31.6	23.3	1.8	21.8	5.1
August	21.9	31.7	22.8	1.5	21.9	4.9
September	22.6	31.7	21.4	1.2	22.6	4.5
October	21.1	31.4	18.9	1.1	21.1	4.0
November	20.3	30.5	16.2	1.0	20.3	3.3
December	19.2	29.4	14.7	1.0	19.2	2.9

13. Web Soil Survey (NRCS) Soil Parameters for the Bosque Olimpia and Cupeyes SWAT Models

Bosque Olimpia Watershed

SNAME	HYDGRP	USLE_k	SOL_Z (mm)	Bulk Density	SOL_AWC (cm/cm)	Ksat (mm/hr)	SOL_ ORG %	CLAY %	SAND %	SILT %
AnF2	B	0.021	2000	1.18	0.15	32.4	1.71	64.1	11.9	23.7
CbF2	D	0.17	2000	1.33	0.06	19.10808	1.29	31	35.4	33.6
HmF2	D	0.28	2000	1.31	0.16	2.41092	0.97	60.4	5.5	34.1
LuE	C	0.1	2000	1.28	0.16	32.4	2.94	52.5	18.2	29.3
LuF	C	0.1	2000	1.28	0.16	32.4	2.88	52.5	18.2	29.3
MkF2	D	0.37	2000	1.2	0.11	2.367	1.93	49.4	13.6	37

Cupeyes Watershed

MUID	SNAM	S5ID	CMPPCT	NLAYERS	HYDGRP	SOL_ZMX	ANION_EXCL	SOL_CRK	SOL_Z1	SOL_BD1
1407041	Maresua	PR787	80	6	C	1185	0.5	0.5	20	1.57
1356080	Caguabo	PR787	85	4	D	505	0.5	0.5	150	1.05
1386420	Mucara	PR787	80	3	D	810	0.5	0.5	130	1.48
1386546	Quebrada	PR787	95	3	C	1520	0.5	0.5	50	1.35
1386661	El Cacique	PR787	60	4	D	2180	0.5	0.5	150	1.35
1386551	Rosario	PR787	80	5	C	1145	0.5	0.5	50	0.49
1884632	Cerro	PR787	90	3	B	2060	0.5	0.5	80	0.69
1386422	Nipe	PR787	95	4	C	1520	0.5	0.5	50	0.49
1386662	El Cacique	PR787	60	4	D	2180	0.5	0.5	150	1.35
1884723	El Descanso	PR787	50	4	C	2030	0.5	0.5	80	0.69
1884721	El Descanso	PR787	50	4	C	2030	0.5	0.5	80	0.69
1907042	El Descanso	PR787	50	4	C	2030	0.5	0.5	80	0.69

MUID	SNAM	SOL_AWC1	SOL_K1	SOL_CBN1	CLAY1	SILT1	SAND1	ROCK1	SOL_ALB1	USLE_K1
1407041	Maresua	0.2	32.4	31.9606	34.2	40.6	25.2	18	0.09	0
1356080	Caguabo	0.13	32.4	2.59861	30.3	26.9	42.8	6	0.16	0.24
1386420	Mucara	0.13	1.8	2.79582	25.8	32.9	41.3	4	0.06	0.1
1386546	Quebrada	0.18	32.4	1.16009	30	30	40	5	0.16	0.2
1386661	El Cacique	0.2	18	3.48028	32	38	30	17	0.09	0.1
1386551	Rosario	0.01	4.32	36.5429	0	0	0	0	0.09	0
1884632	Gordo	0.15	360	46.4037	0	0	0	0	0.09	0
1386422	Nipe	0.13	32.4	7.30858	0	0	0	12	0.09	0
1386662	El Cacique	0.2	18	3.48028	32	38	30	17	0.09	0.1
1884723	El Descanso	0.17	363.6	40.6032	0	0	0	12	0.09	0
1884721	El Descanso	0.17	363.6	40.6032	0	0	0	12	0.09	0
1907042	El Descanso	0.17	363.6	40.6032	0	0	0	12	0.09	0

14. Historia Oral de La Olimpia gathered by E.E Vivoni

Conversación con Guillermo Mattei y su esposa Doña Boni

Don Guillermo cuenta que hace cerca de 50 años su padre, Don Francisco Mattei de Lucca, descendiente del ducado de De Lucca en Italia, adquirió la finca de sus anteriores propietarios, Sucesión Parra. Don Francisco Mattei de Lucca vino a Puerto Rico cerca del año 1890 a los 17 años de edad en compañía de su tío Don Domingo de Luccas. Fueron a vivir a la Hacienda Jauca de Domingo Franceschi, otro tío de Don Francisco, en el barrio Jauca de Jayuya. En el 1925 es adquirida La Olimpia, por Don francisco, habiéndose este ya casado con Doña Vicenta Baerga Millán, joven natural del Barrio Collores en las proximidades de Juana Díaz.

La mayor parte de la familia permaneció en Ponce hasta el año 1928, año en el que el Huracán San Felipe hace estragos en la finca. Dice Don Guillo que a raíz del paso del huracán por la finca, la familia se trasladó completa a La Olimpia “porque papá decía que dos estufas gastaban mucho”. Don francisco y Doña Vicenta partieron desde Ponce hasta La Olimpia con sus nueve hijos: Juanito, Eugenia, Francisco (François), Carlos (Charlie), Ana María, Domingo (Mingo), Emilia, Ángel Guillermo (Guillo) y Joaquín (Quín).

Con una extensión territorial de 644 cuerdas La Olimpia llegó a producir bajo la atención de François 1,500 quintales de café en 1945 y se llegaron a cortar de 20,000 a 25,000 plátanos semanales. Contó Don Guillo que en aquellos tiempos trabajaban en la recogida del café entre cien y ciento cincuenta personas. Recogian el grano tanto hombres como mujeres y los niños.

Don François atendió la finca personalmente desde el 1926 hasta el 1953, año en el que murió su padre. La hacienda fue adquirida por la Sucesión Parra de Don Casimiro Torres. Don François, el único de los hermanos Mattei que pasó el huracán San Felipe en La Olimpia nos cuenta que el año posterior al huracán ordenó la siembra de 80,000 palos de café, habiendo sido necesario antes ahoyar y limpiar de piedras el terreno.

15. Land Cover/Plant Growth Database

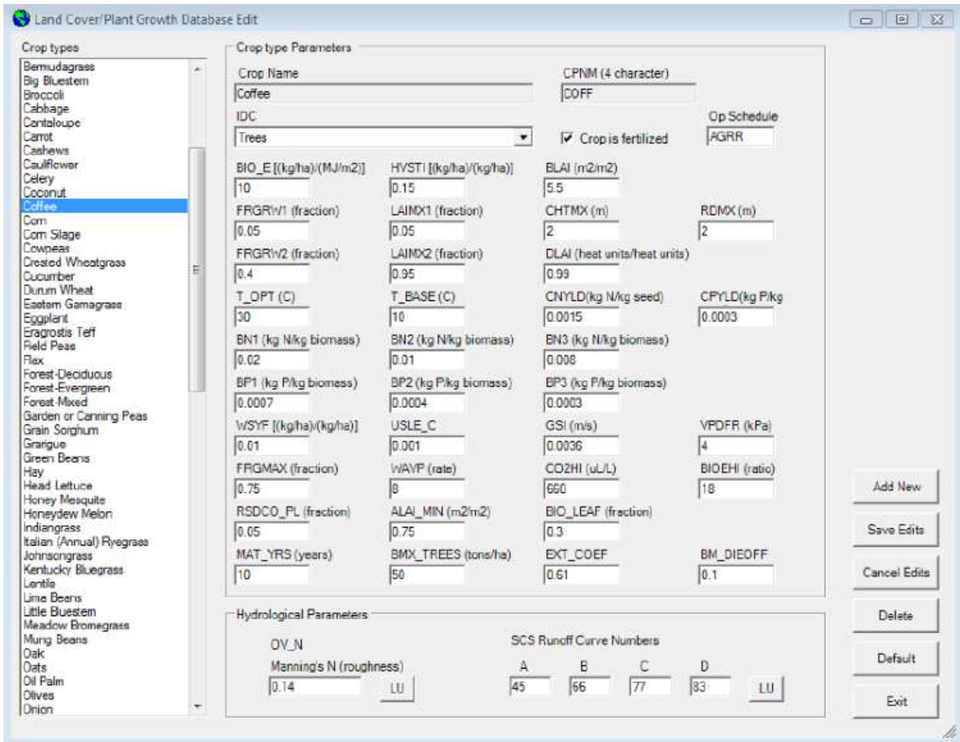

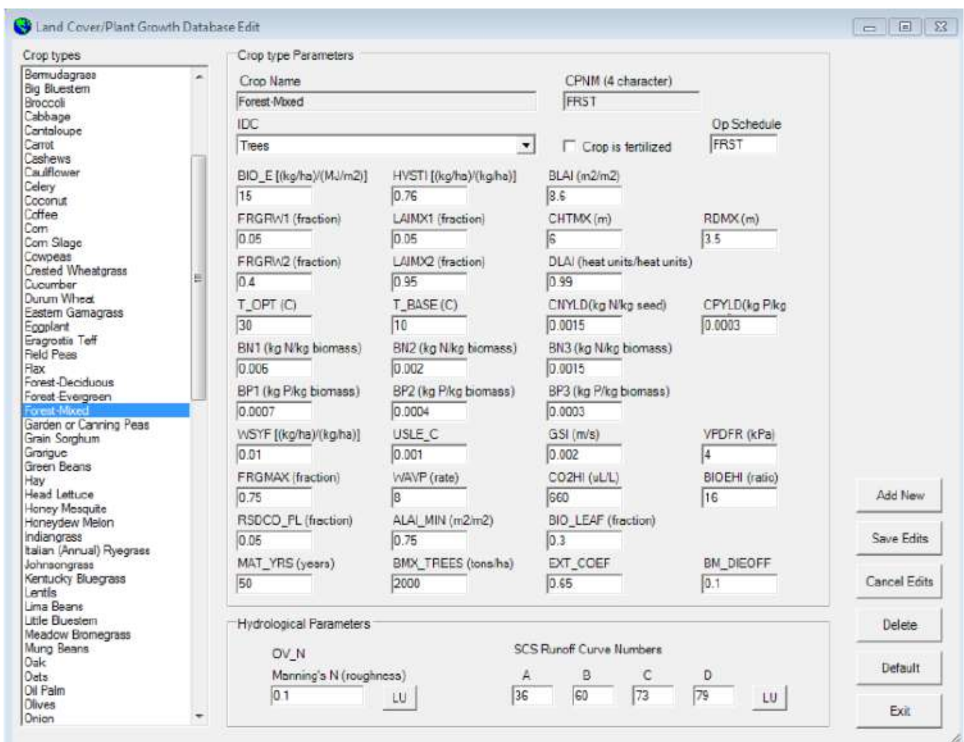

16. Management Parameters Assigned to Model

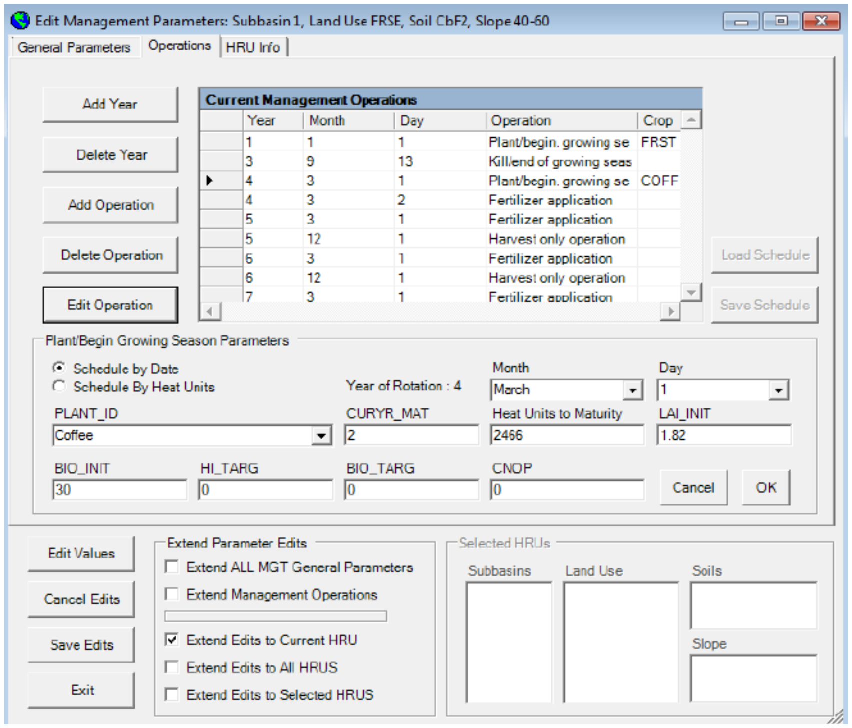

Plant/Begin Growing Season Operation for Coffee

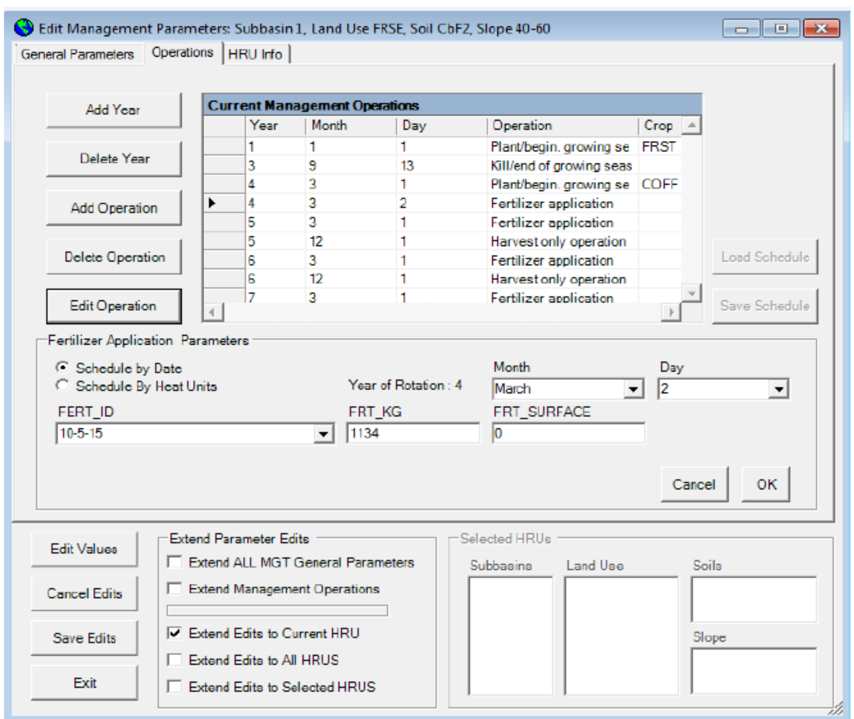

Fertilizer application operation

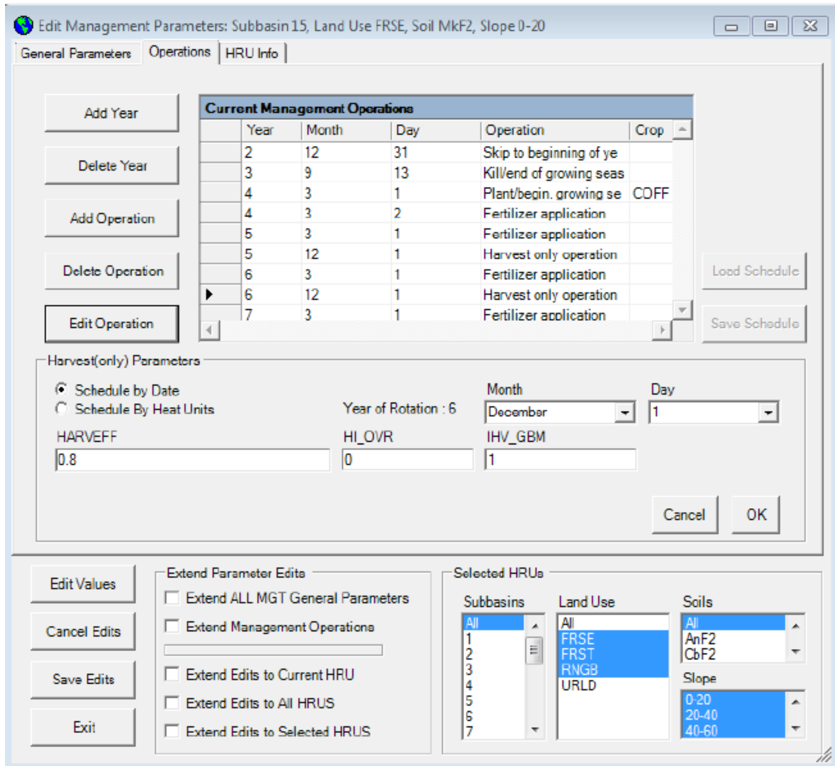

Harvest only for Coffee

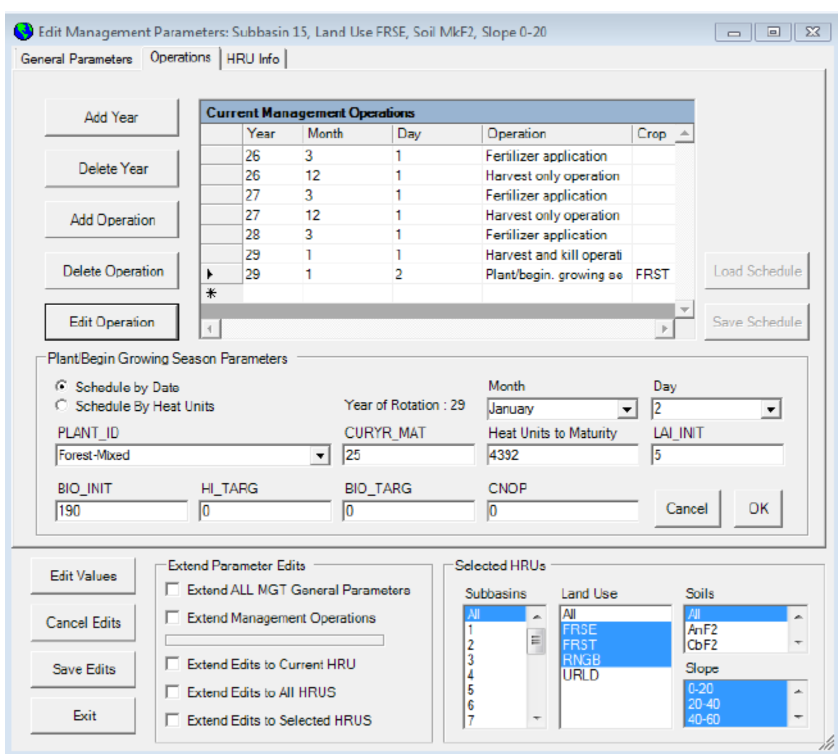

Plant /Begin growing season for Mixed forest

17. Management Operations as Entered to the Model

Year	Month	Day	Op Code	Operation Description	LU
1	1	1	1	Plant/begin. growing season	FRST
3	9	13	8	Kill/end of growing season	
4	3	1	1	Plant/begin. growing season	COFF
4	3	2	3	Fertilizer application	
5	3	1	3	Fertilizer application	
5	12	1	7	Harvest only operation	
6	3	1	3	Fertilizer application	
6	12	1	7	Harvest only operation	
7	3	1	3	Fertilizer application	
7	12	1	7	Harvest only operation	
8	3	1	3	Fertilizer application	
8	12	1	7	Harvest only operation	
9	3	1	3	Fertilizer application	
9	12	1	7	Harvest only operation	
10	3	1	3	Fertilizer application	
10	12	1	7	Harvest only operation	
11	3	1	3	Fertilizer application	
11	12	1	7	Harvest only operation	
12	3	1	3	Fertilizer application	
12	12	1	7	Harvest only operation	
13	3	1	3	Fertilizer application	
13	12	1	7	Harvest only operation	
14	3	1	3	Fertilizer application	
14	12	1	7	Harvest only operation	
15	3	1	3	Fertilizer application	
15	12	1	7	Harvest only operation	
16	3	1	3	Fertilizer application	
16	12	1	7	Harvest only operation	
17	3	1	3	Fertilizer application	
17	12	1	7	Harvest only operation	
18	3	1	3	Fertilizer application	
18	12	1	7	Harvest only operation	
19	3	1	3	Fertilizer application	
19	12	1	7	Harvest only operation	
20	3	1	3	Fertilizer application	
20	12	1	7	Harvest only operation	
21	3	1	3	Fertilizer application	
21	12	1	7	Harvest only operation	
22	3	1	3	Fertilizer application	
22	12	1	7	Harvest only operation	

23	3	1	3	Fertilizer application	
23	12	1	7	Harvest only operation	
24	3	1	3	Fertilizer application	
24	12	1	7	Harvest only operation	
25	3	1	3	Fertilizer application	
25	12	1	7	Harvest only operation	
26	3	1	3	Fertilizer application	
26	12	1	7	Harvest only operation	
27	3	1	3	Fertilizer application	
27	12	1	7	Harvest only operation	
28	3	1	3	Fertilizer application	
29	1	1	5	Harvest and kill operation	
29	1	2	1	Plant/begin. growing season	FRST